This is to certify that the

dissertation entitled

A Model for Antiplasticization
in Polystyrene

presented by

Sandie Anderson Hlatshwayo

has been accepted towards fulfillment
of the requirements for

Ph.D. degree in CHE

Major professor

Date 4-2-93

A MODEL FOR ANTIPLASTICIZATION IN POLYSTYRENE

By

Sandie Anderson Hlatshwayo

A DISSERTATION

Submitted to
Michigan State University
in partial fulfillment of the requirements
for the degree of

DOCTOR OF PHILOSOPHY

Department of Chemical Engineering

1993

ABSTRACT

A MODEL FOR ANTIPLASTICIZATION IN POLYSTYRENE

By

Sandie Anderson Hlatshwayo

Antiplasticization can occur when small quantities of a known "plasticizer" have been blended into a glassy polymer. Commonly, the Tg of the polymer and its free volume decrease. However, the mechanical properties of the antiplasticized polymer are altered significantly, causing the polymer to become stiffer and more brittle. Experimental results from flexural tests of polystyrene/mineral oil blends conducted at room temperature showed that antiplasticization is molecular weight dependent, thus supporting a hypothesis that the phenomenon can be attributed to a chain-end effect. A high molecular weight polystyrene (Mw = 270,000 Daltons) exhibited plasticization only, whereas a low molecular weight (Mw = 40,000 Daltons) exhibited both antiplasticization and plasticization effects. The 40,000 MW sample showed a 2X

increase in flexural moduli and flexural strengths as mineral oil concentration increased up to 6 volume percent. These moduli and strengths decreased rapidly at higher concentrations of mineral oil. Positron Annihilation Spectroscopy (PAS) data showed a 10% decrease in fractional free volume up to 6% mineral oil. ^{13}C NMR experiments showed that there was no change in the polymer backbone dynamics during antiplasticization. ^{1}H NMR Goldman-Shen experiments showed that antiplasticization occurs when the average diameter of the mineral oil domains is less than the average size of the free volume voids. One mineral oil molecule was associated with each polystyrene chain end during antiplasticization. These results are consistent with the hypothesis that antiplasticization is due to a decrease in fractional free volume at the chain ends.

Many peop

an extrem

Thermopla

The Dow C

Mother, F

Brian May

Brook and

Dr. Phil

their te

and had

indebted

mother, I

offered

Not in W

ACKNOWLEDGEMENTS

Many people contributed to the success of this project and I am extremely grateful. I thank the members of the Designed Thermoplastics Laboratory and the Analytical Laboratory of The Dow Chemical Company, especially, Patrick Smith, William Kocher, Brian Landes, Karen Quinn, Phil Kuch, Julie Smith and Brian Maurer, for their generous support. I also thank Gary Krook and Kerry Kelly. To my advisors, Dr. Eric Grulke and Dr. Phillip DeLassus, I extend my sincerest gratitude for their technical assistance and guidance. They believed in me and had the utmost confidence in my abilities. Finally, I am indebted to my wonderful husband, Simphiwe Hlatshwayo, my mother, Marie Anderson, and children, Mfundo and Sandile, who offered much encouragement and sacrifice. Their efforts were not in vain and I thank them very much.

LIST OF T

LIST OF F

LIST OF A

CHAPTER I

CHAPTER 2

CHAPTER 3

TABLE OF CONTENTS

LIST OF TABLES xi

LIST OF FIGURES xii

LIST OF ABBREVIATIONS xiv

CHAPTER 1: INTRODUCTION 1

1-1. Introduction 1

1-2. References 7

CHAPTER 2: SURVEY OF RELEVANT LITERATURE 11

2-1. Plasticizers and Plasticization 11

2-1.1 Mechanisms of Plasticization 12
2-1.2 Free Volume and Plasticization 12

2-2. Antiplasticization 13

2-2.1 Review of Previous Work Done 14
2-2.2 Summary of Past Reasearch 27

2-3. References 29

CHAPTER 3: MECHANICAL BEHAVIOR DURING ANTIPLASTICIZATION 34

3-1. Introduction 34

3-2. Flexural Properties 34

3-3. Experimental Section 35
3-3.1 Materials and Blending 35
3-3.2 Gel Permeation Chromatography 36
3-3.3 Gas Chromatography 36
3-3.4 Compression Molding 36
3-3.5 Mineral Oil Concentrations 37
3-3.6 Differential Scanning Calorimetry 37
3-3.7 Flexural Properties 38

3-4. Results and Discussion 38

3-4.1 Molecular Weight Distribution 38
3-4.2 Gas Chromatogram of Mineral Oil 38
3-4.3 Solubility of Mineral Oil 40
3-4.4 Glass Transition Temperatures 40
3-4.5 Flexural Properties of Polystyrene/ Mineral Oil Blends 43

3-5. Conclusions 49

3-6. References 49

CHAPTER 4: INVESTIGATION OF THE HOLE FILLING MECHANISM 51

4-1. Introduction 51

4-2. Positron Annihilation Spectroscopy 52

4-2.1 Background 52
4-2.2 Determination of Average Hole Size from PAS Lifetimes 54
4-2.3 Fractional Free Volume and Number Densities of Holes 54

4-3. Experimental Section 56

4-3.1 Positron Annihilation Spectroscopy 56

4-4. Results and Discussion 57

4-4.1 Determination of Fractional Free Volume 57
4-4.2 Free Volume Hole Sizes 59
4-4.4 Effect of Mineral Oil on Hole Number Densities 59
4-4.5 Effect of Mineral Oil on Fractional Free Volume 64

4-5. Hole Filling Mechanism 64

4-6. Conclusions 67

4-7. References 68

CHAPTER 5: SOLID STATE NMR INVESTIGATION OF POLYMER AND DILUENT DYNAMICS DURING ANTIPLASTICIZATION 70

5-1. Introduction 70

5-2. Nuclear Magnetic Resonance 70

5-3. Experimental Section 73

5-3.1 Polymer Dynamics 73
5-3.2 Mineral Oil Domains 75

5-4. Results and Discussion 75

5-4.1 Polymer Chain Dynamics 76
5-4.2 ^{1}H NMR and Mobility of Mineral Oil 79
5-4.3 Mineral Oil Domain Sizes 81
5-4.4 Comparison of Mineral Oil Domains with Hole Sizes 83

5-5. Conclusions 85

5-6. References 85

CHAPTER 6: MODEL FOR ANTIPLASTICIZATION IN POLYSTYRENE 87

6-1. Introduction 87

6-2. Development of Antiplasticization Model 87

6-2.1 Comparison of Chain End Holes 87
6-2.2 Comparison of Hole Sizes with Mineral Oil Domains 91
6-2.3 Interaction of Mineral Oil Molecules with Polymer Chain Ends 94

6-3. Model For Antiplasticization 96

6-4. Conclusions 100

6-5. References 100

CHAPTER 7:

CHAPTER 8:

Appendix A:

Appendix B

CHAPTER 7: CONCLUSIONS AND PROPOSALS FOR FUTURE RESEARCH 102

7-1. Conclusions 102

7-2. Proposals for Future Research 103

CHAPTER 8: ADDENDUM: BEHAVIOR OF BLENDS ABOVE Tg 105

8-1. Introduction 105

8-2. Experimental Section 105

8-3. Results 105

8-4. Conclusions 111

8-5. References 112

Appendix A: Molecular Weight Distributions 113

A-1. Molecular Weight Distribution of 40,000 MW Polystyrene 114
A-2. Molecular Weight Distribution of 128,000 MW Polystyrene 118
A-3. Molecular Weight Distribution of 270,000 MW Polystyrene 120

Appendix B: GC Determination of Mineral Oil Concentrations 122

B-1. Nominal and Actual Mineral Oil Concentrations in 40,000 MW PS 123
B-2. GC Analysis of Mineral Oil in 40,000 MW Blends 124
B-3. Nominal and Actual Mineral Oil Concentrations in 40,000 MW PAS Samples 130
B-4. GC Analysis of Mineral Oil in 40,000 MW PAS Blends 131
B-5. Nominal and Actual Mineral Oil Concentrations in 128,000 MW Blends 138
B-6. GC Analysis of Mineral Oil in 128,000 MW Blends 139
B-7. Nominal and Actual Mineral Oil Concentrations in 270,000 MW Blends 145
B-8. GC Analysis of Mineral Oil in 270,000 MW Blends 146

Appendix C

Appendix D

Appendix E

Appendix F

Appendix G

Appendix C: Glass Transition Temperatures 154

C-1. Glass Transition Temperatures of 40,000 MW Blends 155
C-2. Glass Transition Temperatures of 128,000 MW Blends 161
C-3. Glass Transition Temperatures of 270,000 MW Blends 167

Appendix D: Flexural Properties 174

D-1. Flexural Properties of 40,000 MW Blends 175
D-2. Flexural Properties of 270,000 MW Blends 181

Appendix E: Torque Data 187

E-1. Torque Data for 40,000 MW Blends 188
E-2. Torque Data for 128,000 MW Blends 189
E-3. Torque Data for 270,000 MW Blends 190

Appendix F: Positron Annihilation Spectroscopy 191

F-1. 0% Mineral Oil PAS Spectrum for 40,000 MW PS 192
F-2. PAS Data for 40,000 MW Blends 193
F-3. PAS Data for 128,000 MW Blends 199
F-4. PAS Data for 270,000 MW Blends 205

Appendix G: Nuclear Magnetic Resonance 211

G-1. Data and Decay Curves for $T_{1\rho C}$ Analysis 212
G-2. Data and Decay Curves for $T_{1\rho H}$ and T_{CH} Analysis 218
G-3. ^{1}H NMR Spectra of 40,000 MW Blends 227

LIST OF TABLES

Table		Page
1-1.	Abbreviated List of Antiplasticization Research	3
3-1.	Molecular Weight Distribution of Polystyrenes	39
5-1.	NMR Spin-Lattice Relaxation Times (msec)	78
5-2.	Recovery Factors as a Function of Diffusion Time	82
5-3.	Comparison of Mineral Oil Domains with Hole Sizes	84
6-1.	Comparison of Relative Chain End Densities	88
6-2.	Free Volume Holes Associated with Chain Ends	90
6-3.	Effect of Mineral Oil Concentration on Mineral Oil Domain Sizes in 40,000 MW Polystyrene Blends	93
8-1.	Activation Energies for the Polystyrene Blends	110

Figures

3-1. Gas

3-2. Effe

3-3a. Effe
Flex

3-3b. Effe
Flex

3-4a. Effe
Flex

3-4b. Effe
Flex

4-1a. Effe
O-Ps

4-1b. Effe
Hole

4-2a. Effe
O-Ps

4-2b. Effe
Hole

LIST OF FIGURES

Figure		Page
3-1.	Gas Chromatogram of Mineral Oil	41
3-2.	Effect of Mineral Oil Concentration on Tg	42
3-3a.	Effect of Mineral Oil Concentration on Flexural Modulus of 270,000 MW Polystyrene	44
3-3b.	Effect of Mineral Oil Concentration on Flexural Strength of 270,000 MW Polystyrene	45
3-4a.	Effect of Mineral Oil Concentration on Flexural Modulus of 40,000 MW Polystyrene	46
3-4b.	Effect of Mineral Oil Concentration on Flexural Strength of 40,000 MW Polystyrene	47
4-1a.	Effect of Mineral Oil Concentration on o-Ps Lifetimes	60
4-1b.	Effect of Mineral Oil Concentration on Hole Size	61
4-2a.	Effect of Mineral Oil Concentration on o-Ps Intensities	62
4-2b.	Effect of Mineral Oil Concentration on Hole Densities	63

4-3. Effec
Volu

5-1. ^{13}C I
Blen

5-2. ^{1}H M
Blen

6-1a. Sche
Weig

6-1b. Sche
Amid
Low M

8-1. Effe
270,0

8-2. Effe
128,0

8-3. Effe
40,0

4-3. Effect of Mineral Oil on Fractional Free Volume 65

5-1. ^{13}C NMR Spectrum of 40,000 MW Polystyrene Blend 77

5-2. ^{1}H NMR Spectra of 40,000 MW Polystyrene Blends 80

6-1a. Schematic of an Amorphous High Molecular Weight Polymer/Diluent Blend 98

6-1b. Schematic of a Proposed Model For Antiplasticization in an Amorphous Low Molecular Weight Polymer/Diluent Blend 99

8-1. Effect of Mineral Oil Concentration on 270,000 MW Blends Above Tg 106

8-2. Effect of Mineral Oil Concentration on 128,000 MW Blends Above Tg 107

8-3. Effect of Mineral Oil Concentration on 40,000 MW Blends Above Tg 108

AV	Ac
ASM	Ac
BA	Bi
BP	Bu
CP	Ca
DBS	Di
DCPS	Di
DOS	Di
DPA	Di
DPS	Di
DTBP	Di
DTP	Di
DTS	Di
EHM	Gl

LIST OF ABBREVIATIONS

AN	Acrylonitrile
ASTM	American Standard Test Method
BPA	Bis-phenol A
BBP	Butyl Benzyl Phthalate
CP	Cross-Polarization
DBS	Dibutyl Sebacate
DCDPS	Dichlorodiphenyl Sulfone
DCS	Differential Scanning Calorimetry
DMA	Dynamic Mechanical Analysis
DMS	Dynamic Mechanical Spectroscopy
DNBP	Dinitrobiphenol
DOP	Dioctyl Phthalate
DOS	Dioctyl Sebacate
EPDM	Graft Copolymer of Ethylenepropylene-1:4 Hexadiene

EHHA 4

EH E

EH F

G

EH H

M

M

M

W

A

M

C

P

P

P

P

P

EPPHAA	4-(2-hydroxy-3-phenoxy-propyloxy) acetanilide
EVOH	Ethylene Vinyl Alcohol Copolymer
FTIR	Fourier Transform Infrared Spectroscopy
GC	Gas Chromatography
HPLC	High Performance Liquid Chromatography
MAS	Magic Angle Spinning
Mn	Number Average Molecular Weight
MW	Molecular Weight
Mw	Weight Average Molecular Weight
NBR	Acrylonitrile Butadiene Rubber
NMR	Nuclear Magnetic Resonance
o-Ps	Ortho-positronium
PAS	Positron Annihilation Spectroscopy
PC	Polycarbonate
PCL	Poly-e-caprolactone
PMMA	Poly(methyl methacrylate)
PPO	Poly(phenylene oxide)

p-Ps	Para-Positronium
PS	Polystyrene
PVAC	Poly(vinyl acetate)
PVC	Poly(vinyl chloride)
TCP	Tricresyl Phosphate
Tg	Glass Transition Temperature
THF	Tetrahydofuran
TSD	Thermally Stimulated Depolarization

CHAPTER 1

INTRODUCTION

1-1. Introduction

In the last twenty-five years or so, there has been documented evidence of antiplasticization, an unusual phenomenon that occurs when small quantities of a known "plasticizer" have been blended into a glassy polymer [1,2]. Although the glass transition temperature (Tg) of a polymer may be lowered upon addition of these plasticizers, the modulus and tensile strength increase significantly, and ultimate elongation decreases, causing the polymer to become stiffer and more brittle. This behavior is opposite to that expected of a plasticized material - rather the material behaves as though motions in the polymer chains are restricted. In addition, the transport properties are affected [3].

Antiplasticization has been observed in many polymer-diluent systems e.g. polycarbonate and dibutyl phthalate, polyvinyl chloride and tricresyl phosphate, polystyrene and mineral oil. Mechanical property tests, differential scanning calorimetry (DSC), dynamic mechanical spectroscopy (DMS), dielectric loss studies, nuclear magnetic resonance (NMR),

and dens

antiplas

a) a
d
d
i
d
[

b) s
t

c) p
h
p

d) r
d
t
t

Table 1
antipla
polymer
analytic
Majorit

and density measurements collectively infer that antiplasticization results from one or more of the following:

(a) a decrease in free volume upon the addition of the diluent - perhaps the polymer chains have some small degree of mobility that allows them to align themselves in a more ordered, densely packed state or that the diluents fill the excess volume of the polymer glass [3,4].

(b) suppression of the secondary relaxation transitions at the temperature of interest [5].

(c) polymer-diluent interactions which create steric hindrance and decrease segmental mobility of the polymer [6,7].

(d) reduced mobility of the diluent - perhaps solid diluents with higher glass transition temperatures near the temperature of mechanical testing, have a greater tendency of promoting antiplasticization [4].

Table 1-1 lists, in detail, researchers that have observed antiplasticization in polymers. The table shows the polymer/diluent system studied, the types of mechanical or analytical tests performed, and major observations. The majority of these authors relied solely on either a

Table 1-1

Polymer	
Polycarbonate PC	
Polystyrene PS	
PC	
Polysulfone	
PS	
PC	
PC	
PC	
Polyvinyl chloride PVC	
PC	

Table 1-1. Abbreviated List of Antiplasticization Research

Polymer	Diluent	Mechanical Tool	Analytical Tool	Conclusion	Reference
Polycarbonate (PC)	Chlorinated Biphenyls and Terphenols	Tensile	----	Higher Modulus. Interaction	Jackson[1,2]
Polystyrene (PS)	Benzophenone	Tensile	----	Higher Modulus	Litt[8]
PC Polysulfone	Arochlor, dichlorodiphenyl sulfone	Torsion Pendulum	----	Elimination of secondary loss peaks. Decrease in water vapor diffusion rates.	Robeson[5,9]
PS PC	Aroclor and Phthlates	Dynamic Mechanical Studies (DMS)	----	Antiplasticization is temperature dependent	Petrie[10]
PC	Arochlor	Tensile	----	Free changes for antiplasticization differ from that of annealing	Robertson[11]
PC	Arochlor & Dibutyl Phthalate	Tensile and DMS	----	Higher Modulus and Suppression of ß	Wyzgoski[12]
Poly(vinyl chloride (PVC)	Tricresyl Phosphate (TCP)	Tensile Dynamic Mech. Spectroscopy (DMS)	----	Higher Modulus Suppression of ß	Kinjo[13,14]
PC	Ester Derivative of Bisphenol A	Tensile Free Volume Calculations	----	Influenced by polar groups. Tight filling of free volume	Makaruk[15,16]

Table 1-1 (cont'd). List of Antiplasticization Research

Polymer	Diluent	Mechanical Tool	Analytical Tool	Conclusion	Reference
PVC	Acrylonitrile butadiene rubber (NBR)	Creep	----	Interaction	Bergman[17,18]
PVC graft copolymer	Dioctyl phthalate	DMS	----	Antiplasticization temperature dependent	Chang[19,20]
PC	Charge transfer complex	Tensile	Thermally stimulated depolarization	Interactions	Kryszewski 21,22
Poly(methy methacrylate)	Phthalates	Tensile	----	Interactions	Olayemi[23]
PC	Diphenyl Phthalate	----	Nuclear Magnetic Spectroscopy (NMR)	Interactions	Belfiore[24-27]
PVC	TCP	Permeability	NMR	Lower Diffusion. Reduced chain motion	Sefcik[28]
PC	Dinitrobiphenyl	Stress-strain	NMR Fourier Transform Infrared Spectroscopy (FTIR)	Interaction	Gupta[29]
PVA	Cholesterylls	Dielectric	----	Increase in Tg	Deshpande[30]
Polystyrene Polysulfone Poly(phenyl-ene oxide)	Mineral OIl TCP,Dichloro-diphenyl sulfone, phthalates	Permeability	----	Lower Permeability	Maeda[31-34]
Poly(arylene ether sulfones)	4,4-dichlorodiphenyl sulfone	----	NMR	Suppression of ß Reduction in phenyl flips	Dumais[35]

Table 1-1 (cont'd). List of Antiplasticization Research

Polymer	Diluent	Mechanical Tool	Analytical Tool	Conclusion	Reference
Phenoxy	Hydroxy-phenoxy-propyloxy acetani-lide (EPPHAA)	----	Infrared Spectroscopy (IR)	Hydrogen bonding	Stevenson[36]
PC	DBP	----	NMR	Interaction	Roy[6]
PC	Dibutyl Phthalate (DBP)	----	NMR	Interaction Decreased mobility of PC	Liu and Roy[7]
Polystyrene Polysulfone Poly(phenyl -ene oxide)	TCP, Dichlo ro-diphenyl sulfone, phthalates , dioctyl sebacate	Free volume calculations	----	High Tg diluents cause a decrease in hole free volume	Vrentas[4]
PVC	TCP	Tensile	WAXS	Crystallin-ity enhances antiplastici zation	Guerrero[37]
Polyimides	EPPHAA	Tensile, Water absorption	----	Decrease in free volume	Shockey[38]
PC	Diphenyl-hydrazones	Density Tensile DMS Abrasion	----	Brittleness Suppression of ß. Increase in abrasion resistance	Cais[39]

mech

and

one

dil

ther

beha

give

fill

the

anti

unti

calc

fill

The p

mecha

Polys

these

invol

the c

numbe

and t

obtai

Poten

Photog

mechanical or an analytical test to verify antiplasticization and then speculated on a mechanism for antiplasticization. No one has related the microscopic physical behavior of the diluent to the local molecular motions of the polymer, and then extend that information to explain the bulk mechanical behavior of the polymer. The most predominant hypothesis given for antiplasticization is that it is due to hole-filling by the diluent, and hence results in a decrease in the free volume of the polymer. Attributing antiplasticization to a decrease in free volume was based, until now, solely on density measurements and theoretical calculations. No prior published report describes the hole-filling mechanism of the diluent.

The purpose of this research is to study the hole-filling mechanism and propose a model for antiplasticization. Polystyrene/mineral oil blends were studied. The selection of these blends is based on the simple nature of the polymer involved. The experimental approach is to measure directly the changes in free volume, including hole sizes and hole number densities, using Positron Annihilation Spectroscopy, and then relate those results to polymer chain dynamics data obtained via solid state NMR techniques.

Potential applications for antiplasticization include thin photographic plates where rigidity is important, durable

charge-transport layers for organic photoconductors made from polymer binders blended with antiplasticizers to reduce wear in electrophotographic copiers, and packaging plastics or separation membranes for moderate improvement of the barrier properties. Research in this area could also be used to describe conditions where addition of a liquid additive is not likely to yield the expected monotonic change in physical properties.

1-2. References

1. W.J. Jackson Jr., and J.R. Caldwell, J. Applied Polymer Science, 11(2), 211-226, 1967.

2. W.J. Jackson Jr., and J.R. Caldwell, J. Applied Polymer Science, 11(2), 227-44, 1967.

3. Y. Maeda and D.R. Paul, J. Polymer Science Part B: Polymer Physics Edition, 25, 1005, 1987.

4. J.S. Vrentas, J.L. Duda, and H.C. Ling, Macromolecules, 21, 1470-1475, 1988.

5. L.M. Robeson and J.A. Faucher, J. Polymer Science:Part B: Polymer Letters, 7(1), 35-40, 1969.

6. A.K. Roy, P.T. Inglefield, J.H. Shibata, and A.A. Jones, Macromolecules, 20, 1434, 1984.

7. Y. Liu, A.K. Roy, A.A. Jones, P.T. Inglefield, and P. Ogden, Macromolecules, 23, 968-977, 1990.

8. M.H. Litt and A.V. Tobolsky, J. Macromolecular Science - Physics, B193, 433-443, 1967.

9. L.M. Robeson, Polymer Engineering and Science, 9(4), 277-281, 1969.

10. S.E.B. Petrie, R.S. Moore, and J.R. Flick, J. Applied Polymer Science, 43(11), 4318-4326, 1972.

11. R.E. Robertson and C.W. Joynson, J. Applied Polymer Science, 16, 733-738, 1972.

12. M.G. Wyzgoski and G.S.Y. Yeh, Polymer J., 4(1), 29-34, 1973.

13. N. Kinjo and T. Nakagawa, Polymer J., 4(2), 143-153, 1973.

14. N. Kinjo, Japan Plastics, 6, 6-28, 1973.

15. L. Makaruk, H. Polanska, and E. Staros, J. Applied Polymer Science, 20, 60-70, 1976.

16. L. Makaruk, H. Polanska, and T. Mizerski, J. Applied Polymer Science, 23(7),1935-42.

17. G. Bergman, H. Bertilsson, and Y. Shur, J. Applied Polymer Science, 21, 2953-2961.

18. N. Sundgren, G. Bergman, and Y. Shur, J. Applied Polymer Science, 22, 1255-1265, 1978.

19. E.P
Pol

20. E.P
Pol

21. M.
Po

22. M.
So

23. J.
So

24. L
Po

25. L
Z
M

26. I
P

27. I
J

28. M
S

19. E.P. Chang, R. Kirsten, and R. Salovey, J. Applied Polymer Science, 24, 827-836, 1979.

20. E.P. Chang, R. Kirsten and E.L. Slagowski, J. Applied Polymer Science, 21, 2167-2180, 1977.

21. M. Kryszewski, J. Ulanski, and A. Galeski, J. Applied Polymer Science, 23, 1271-1278, 1979.

22. M. Kryszewski and J. Ulanski, J. Applied Polymer Science: Applied Polymer Symposium, 35, 553-562, 1979.

23. J.Y. Olayemi and N.A. Oniyangi, J. Applied Polymer Science, 26, 4059-4067, 1981.

24. L. Belfiore and S.L. Cooper, J. Polymer Science: Polymer Physics Edition, 21, 2135-2157, 1983.

25. L.A. Belfiore, P.M. Henrichs, D.J. Massa, N. Zumbulyadis, W.P. rothwell, and S.L. Cooper, Macromolecules, 16, 1744-1753, 1983.

26. L.A. Belfiore, P.M. Henrichs, and S.L. Cooper, Polymer, 25, 452-458,1984.

27. L. Belfiore, J. Elastomers and Plastics, 19, 238-251, 1987.

28. M.D. Sefcik, J. Schaefer, and F.L. May, J. Polymer Science: Polymer Physics Edition, 21, 1041-1054, 1983.

29. M.K. Gupta, J.A. Ripmeester, D.J. Carlsson, and D.M. Wiles, J. Polymer Science: Polymer Letters Edition, 21, 211-215, 1983.

30. D.D. Deshpande, N.R. Kandaswamy, and V.K. Tiwari, J. Applied Polymer Science, 30, 2869-2882, 1985.

31. Y. Maeda and D.R. Paul, Polymer, 26, 2055-2063, 1985.

32. Y. Maeda and D.R. Paul, J. Polymer Science:Part B: Polymer Physics, 25, 957-1016, 1987.

33. Y. Maeda and D.R. Paul, J. Membrane Science, 30, 1-9, 1987.

34. P.T. DeLassus, in Styrene Polymers, Encyclopedia of Polymer Science and Engineering, 2nd Ed., 16, 1989.

35. J.J. Dumais, A.L. Cholli, L.W. Jelinski, J.L. Hedrick, and J.E. McGrath, Macromolecules, 19, 1884-1889, 1986.

36. W.T.K. Stevenson, A. Garton, and D.M. Wiles, J. Polymer Science: Part B: Polymer Physics, 24, 717-722, 1986.

37. S.J. Guerrero, Macromolecules, 22, 3480-3485, 1989.

38. E. Shockey and A. Garton, American Chemical Society, Polymeric Materials Science and Engineering, 65, 257-258, 1991.

39. R.E. Cais, M. Nozomi, M. Kawai, and A. Miyake Macromolecules, 25, 4588-4596, 1992.

2.1. Plas

Plasticize

usually ad

polymer an

aids, plas

also lowe

the end-us

the glass

modulus a

elongatio

addition,

molecules

example,

plasticiz

ethylene

become pl

basically

First, th

be added

of a seco

CHAPTER 2

COMPARISON OF ANTIPLASTICIZATION STUDIES

2-1. Plasticizers and Plasticization

Plasticizers, low molecular weight miscible substances, are usually added to polymers to improve processibility of the polymer and/or to modify the final product [1]. As processing aids, plasticizers may lower the processing temperature and also lower the hot melt viscosity. Regarding the effect on the end-use properties, plasticizers soften the resin, lower the glass transition temperature (Tg), lower the tensile modulus and tensile strength, increase the ultimate elongation and flexibility, increase toughness, and, in addition, raise the diffusion coefficient of penetrant molecules. Plasticization can occur unintentionally. For example, a liquid stabilizer when added to a polymer may plasticize that polymer; some hydrophilic polymers like ethylene vinyl alcohol (EVOH) copolymer and certain nylons become plasticized by water in humid environments. There are basically two modes of adding a plasticizer to a polymer. First, there is the internal mode, where the plasticizer may be added during polymerization; for example, copolymerization of a second monomer. Second, there is the external addition,

polymer. S

depends on

2.1.1 Mech

Several th

plasticiza

Theory, th

lubricatio

as a lubri

over each

three-dime

between th

According

disrupt s

less rigi

the Gel t

considere

aspects o

Volume Th

free volu

mobility,

2.1.2 Fre

In the si

differenc

temperatu

polymer. Sometimes both modes of additions are used - this depends on the end-use properties of the product desired.

2-1.1 Mechanisms of Plasticization

Several theories have been proposed for the mechanisms of plasticization [1,2,3]. These are notably the Lubrication Theory, the Gel Theory, and the Free Volume Theory. The Lubrication Theory basically claims that the plasticizer acts as a lubricant to facilitate movement of the polymer chains over each other. The Gel Theory assumes that the polymer is a three-dimensional network, with 'loose points of attachment' between the polymer chains closely resembling that of a gel. According to the Gel Theory, plasticizers will selectively disrupt some points of attachment. The structure then becomes less rigid and thus more flexible. Both the Lubrication and the Gel theories were developed in the early 1900's and are considered to be inadequate in terms of explaining all aspects of plasticization. Many researchers rely on the Free Volume Theory, which asserts that plasticizers increase the free volume of the polymer, thereby increasing chain mobility, and ultimately decreasing Tg.

2-1.2 Free Volume and Plasticization

In the simplest terms, free volume is often defined as the difference between the specific volume of the polymer at any temperature T and the specific volume of the equilibrium

liquid at

xation of

side group

the motion

of the pol

increasing

increasing

plasticiza

hindrance

aterial w

plasticiz

2-2. Ant

As mentio

behaviors

Antiplast

exhibit n

Specific

in the fr

Plasticiz

Antiplast

additive.

liquid at 0 K [4]. Free volume is a direct consequence of motion of the polymer including the polymer backbone, the side groups, and the chain ends. In other words by increasing the motion of the polymer, one can increase the free volume of the polymer. This may be accomplished in several ways: increasing the number of end groups (lower molecular weight); increasing the number or length of side chains (internal plasticization); inclusion of groups with lower steric hindrance (internal plasticization); inclusion of compatible material with lower molecular weight (external plasticization); increasing temperature (plastication) [1].

2-2. Antiplasticization

As mentioned earlier antiplasticization has some opposite behaviors to those observed with plasticization. Antiplasticized blends are stiffer than expected; the blends exhibit negative deviation from the additivity rule in the specific volume of the blend components i.e. show a decrease in the free volume. Furthermore, antiplasticization and plasticization can be observed in the same system, with antiplasticization occurring at low concentrations of aditive.

[illegible]

[illegible]

Jackson ar

to report

of bisphe

concluded

additive

proposed

a decreas

antiplast

polymer b

the flexi

Jackson a

of effec

were com

atoms li

should c

than -50

dimensio

the mole

since th

polymer.

tended t

antiplas

2-2.1 Chronological Review of Previous Work Done to Investigate the Mechanisms of Antiplasticization.

Jackson and Caldwell [5,6] were among the first researchers to report evidence of antiplasticization. They studied blends of bisphenol polycarbonates with various additives and concluded that rigidity and polarity in both the polymer and additive were necessary to effect antiplasticization. They proposed that the mechanism of antiplasticization may involve a decrease in the free volume of the polymer, polymer-antiplasticizer interactions, and physical stiffening of the polymer by the rigid antiplasticizer molecules, which reduce the flexibility of the polymer.

Jackson and Caldwell [5,6] also described the characteristics of effective antiplasticizers - these were additives that were compatible with the polymer, were polar i.e. contain atoms like a halogen, oxygen, nitrogen, and sulfur, they should contain at least two nonbridged rings, had Tgs greater than -50^{o}C, and were relatively flat molecules i.e. had one dimension less than 5.5 A^{o} in at least 65% of the length of the molecules. Rigidity of the polar additive was stressed, since this reduced flexibility and imparted stiffness to the polymer. These authors also found that low Tg compounds tended to act as plasticizers while higher Tg ones were antiplasticizers.

Litt et al

benzophenc

attributed

crystallir

the dilue

efficient

volume.

Robeson a

antiplast

reasoning

ultimate

transitic

eliminate

polysulfc

observed

rates, wh

They spec

occupied

antiplast

polymer

and Fauch

antiplast

loss tra

transiti

low temp

Litt et al. [7] saw a 5% increase in modulus when 3 and 6% of benzophenone was blended into polystyrene (PS). They attributed the observed 0.6% increase in density to the crystalline nature of benzophenone. They believed that since the diluent contained no excess free volume, it packed efficiently in the polymer and caused a loss in polymer free volume.

Robeson and Faucher [8,9] were the first to report that antiplasticization affects secondary loss transitions. Their reasoning was based on the fact that impact strength and ultimate elongation are associated with secondary loss transitions. These authors found that antiplasticizers eliminated the secondary loss peaks in polycarbonate (PC), polysulfone, and poly(vinyl chloride) (PVC). In addition they observed an accompanying decrease in water vapor diffusion rates, which they attributed to a decrease in free volume. They speculated that the potential sites for water were occupied by the antiplasticizer molecules. In so doing, the antiplasticizer molecules also hindered the mobility of the polymer chains and eliminated the loss transitions. Robeson and Faucher also claimed that a polymer's potential for antiplasticization depended on the magnitude of its secondary loss transitions and the ability for elimination of the transitions. For example, polystyrene, which has a very small low temperature transitions, would not be a good candidate

for antipla

as support

Petrie et

that a dec

mobility a

They found

sub-Tg tra

[...] who s

and found

free volur

antiplast

elimination

Plasticize

sub-Tg re

polymer m

over a wi

Mechanica

polystyre

concluded

antiplast

antiplast

Plasticiz

Robertson

and antip

for antiplasticization. They cited the work of Jackson et al. as supporting evidence.

Petrie et al. [10] disagreed with the findings of Robeson that a decrease in polymer free volume restricts polymer mobility and hence affects the low temperature β transition. They found that the loss in free volume had little effect on sub-Tg transitions. Petrie et al. cited the work of Pezzin [11] who studied the dynamical mechanical properties of PVC and found that the β peak was not affected by changes in free volume. Petrie et al. did not believe that antiplasticization was a result of the suppression and/or elimination of the β peak. In fact they found that so-called plasticizers and antiplasticizers had a similar effect on the sub-Tg relaxation processes. They investigated all modes of polymer motion and studied the effects of diluent mobility over a wide temperature range. They conducted dynamic mechanical and dielectric loss studies of polycarbonate and polystyrene blended with various diluents. Petrie et al. then concluded that the temperature ranges for plasticization and antiplasticization are distinct; in other words an antiplasticizer at one temperature may behave as a plasticizer at another temperature.

Robertson and Joynson [12] studied the effects of annealing and antiplasticization on free volume. They found that the

effects wer

in a glass

is affecte

Wypgoski a

dibutyl ph

polycarbon

suppressio

the elimin

Minjo et a

diluents:

BBP), di

dioctyl s

ariplast

of the di

reverse c

DCS>DBS>p

suppress

They also

independ

observat

or therm

molecula

decrease

decrease

Order as

effects were additive, which suggested that the free volume in a glass consisted of two separate entities, one of which is affected by antiplasticization and the other by annealing. Wyzgoski and Yeh [13] found that 30% Arochlor 5442 and 10% dibutyl phthalate decreased the fractional free volume of polycarbonate glass by 0.015. They also observed a suppression of the β peak, which they suggested was due to the elimination of the WLF free volume.

Kinjo et al. [14, 15] studied PVC blended with various diluents: tricresyl phosphate (TCP), butyl benzyl phthalate (BBP), dioctyl phthalate (DOP), dibutyl sebacate (DBS), and dioctyl sebacate (DOS). They reported that the antiplasticizing ability (increasing stiffness and rigidity) of the diluents TCP>BBP>DOP>DBS>DOS in PVC were in the reverse order of their plasticizing ability (decrease in Tg) DOS>DBS>DOP>BBP>TCP. They observed a decrease in Tg and a suppression and subsequent disappearance of the β peak. They also found that the suppression of the β peak was independent of the diluent species. Another interesting observation was that the coefficient of the specific volume or thermal expansion coefficient, which is related to the molecular interaction or the cohesive energy density, decreased in antiplasticized blends. The magnitude of the decrease was in the order TCP>BBP>DOP>DBS>DOS, the exact order as the antiplasticizing ability. Kinjo et al. proposed

that antip

disappeara

Haucher.

Makaruk et

antiplasti

deviations

heats of s

interactio

polycarbo

et al. tha

groups in

free volu

Antiplast

systems.

Acryloni

antiplast

samples)

antiplast

proposed

linearity

effects

high AN

enhanced

antiplas

that antiplasticization of PC and PVC is primarily due to a disappearance of the β peak, thus supporting Robeson and Faucher.

Makaruk et al. [16] used calorimetric techniques to study antiplasticization in polycarbonate. They suggested that deviations from the volume additivity and differences of heats of solutions pointed to the existence of strong interactions between the antiplasticizer molecules and polycarbonate. In a later paper [17] they agreed with Jackson et al. that antiplasticization depends on the number of polar groups in the diluent, and also on the ability to fill the free volume of the polymer.

Antiplasticization was also observed with high polymer blend systems. Bergman et al. [18], in a study of PVC/NBR (acrylonitrile butadiene rubber) blends, found that antiplasticization by NBR (in high acrylonitrile content samples) resulted in non-linear viscoelastic behavior. Since antiplasticization suppressed the β transition, they proposed that the stress-activated mechanism causing non-linearity has a highly cooperative nature, due to coupling effects between the α- and β-transition mechanisms. The high AN levels improved PVC/NBR blend compatibility, which enhanced antiplasticization. Later experiments with the antiplasticizer poly-e-caprolactone (PCL) confirmed the

mportance
nd support
ntiplastic

Chang et al
temperature
ethyleneprc
% weight p
DP increas
while decre
antiplastic
dipolar in
segments.
that antim
phase in h
inert fill
transition

Kryszewski
polycarbon
[22]. Mec
teracyanoe
the temper
stimulated
polymer di
the polyme

importance of the β relaxation in stress activated processes and support the pseudo cross-linking hypothesis for antiplasticization [19].

Chang et al. [20] found that antiplasticization was temperature dependent. They blended a graft copolymer of ethylenepropylene-1:4 hexadiene (EPDM) and PVC with 0, 5, and 10 weight percent dioctyl(di-2-ethylhexyl)phthalate (DOP). DOP increased the storage modulus between -20°C and 70°C, while decreasing the storage modulus above 100°C. The antiplasticization behavior was attributed to an increase in dipolar interaction between the DOP molecules and PVC chain segments. In earlier experiments Chang et al. [21] also found that antimony oxide additives can antiplasticize the rubber phase in high impact polystyrene (HIPS) while acting as an inert filler in the PS phase at a temperature above the glass transition temperature of the rubber.

Kryszewski et al. studied the mechanical properties of polycarbonate antiplasticized with a charge-transfer complex [22]. Mechanical tests indicated that the diluent, teracyanoethylene-t-stilbene complex, raised the modulus in the temperature range -60 to +60°C. Using thermally stimulated depolarization (TSD) techniques they proposed that polymer diluent interactions cause "physical crosslinks" in the polymer blend, which was manifested as

antiplasti

60°C, thes

The additi

Kyszewsk

the blend

function

increased

constant.

When smal

cause the

interacti

temperat

after st

mobili.

In a sep

low temp

antiplas

These ar

showed

pure po

possibl

complex

chain.

antiplasticization. As the temperature was increased above 60°C, these relatively weak physical crosslinks were broken. The additive then behaved like a plasticizer and lowered the Tg.

Kryszewski et al. [22] also studied the mechanical modulus of the blends containing the complex and its components as a function of cycle number and temperature. At 30°C the moduli increased up to 3 cycles. At 60°C the moduli remained constant. The authors explained that at low temperatures, when small chain segment movements occurred, stretching can cause them to rearrange their positions to favor increased interactions, which resulted in increased moduli. At higher temperatures, the large chain segments often relaxed quickly after stretching. As a result, there was no increase in the moduli.

In a separate study Kryszewski et al. [23] confirmed that at low temperatures the polar complex acts as an antiplasticizer, due to interactions with the chain segments. These authors found that the most antiplasticized blends showed higher activation energies for relaxation than the pure polymer, which again suggested some interaction, possibly dipole-dipole type bonding, between the charge complex molecules and the carbonyl groups on the polymer chain. They proposed that the interaction inhibited the

xibility o

oncentrat

oward a l

and the co

behavior w

Clayeni e

dimeyl p

with poly

plasticiz

followed

strength

elongatio

the first

thus the

increase

secondar

interact

PMMA mol

larger m

They exp

effect w

the PMMA

without

movement

mobility of the carbonyl groups. At high complex concentrations, the equilibrium bonding formation shifted toward a lowering of the concentration of bond crosslinks, and the complex acted as a plasticizer. This plasticizing behavior was also observed at elevated temperatures.

Olayemi et al. [24] observed a three-stage interaction of dimetyl phthalate, dibutyl phthalate, and poly(vinyl acetate) with poly(methyl methacrylate) (PMMA). They saw an initial plasticization i.e. decrease in tensile strength and modulus, followed by antiplasticization, an increase in tensile strength and modulus with an anomalous increase in elongation, and finally plasticization. They proposed that in the first stage, very few additive molecules were present thus the interaction was nonspecific. As the concentration increased, polymer-additive interaction increased forming secondary bonds like hydrogen bonds and van der Waals interactions. Olayemi et al. suggested cross-linking of the PMMA molecules by additive molecules. They believed that larger molecules would be more effective antiplasticizers. They explained the anomalous elongation as a form of spacer effect where the additive molecules are positioned between the PMMA molecules. They described it as simple cross-linking without the extensive network, which would permit limited movement within the system. They attributed the final

plasticiza

MW.

Mubarak an

stiff back

polymer-ad

additive a

Before e

higher Tg

which anti

the mid-ki

chain, but

the β-rel

intermolec

antiplasti

relaxation

were most

Sefcik et

H_2 and CO

coefficie

15% TCP.

decreased

theory of

diluent i

resulting

plasticization to a lubrication action of the additives on PMMA.

Mubarak and Polanska [25] have suggested that polymers with stiff backbones can exhibit antiplasticization when strong polymer-additive interactions are greater than additive-additive and polymer-polymer interactions.
Belfiore et al. [26 to 29] found via NMR techniques that the higher Tg diluents dinitrobiphenyl and diphenylphthalate, which antiplasticized polycarbonate, had negligible effect on the mid-kilohertz micro-Brownian motions in the polymer chain, but significantly affected the mega-hertz mobility of the β-relaxation processes. They proposed that the intermolecular interactions that gave rise to antiplasticization can only occur in the solid state. The relaxation rates of the aromatic groups on the polymer chain were most sensitive to the antiplasticization phenomenon.

Sefcik et al. [30] measured permeabilities and time-lag for H_2 and CO in PVC-TCP blends and saw that the diffusion coefficients decreased initially and then increased beyond 15% TCP. C-13 NMR data showed that the polymer mobility decreased during antiplasticization. Using the diffusion theory of Pace and Datyner [31], they proposed that the diluent increased interaction between the polymer chains, resulting in increased interchain cohesion, which

subsequent

higher inte

for diffus

Gupta et a

polycarbon

variety of

maximum wa

DSC and MM

with the p

and nuclea

presence o

An increas

acetate) (

additives

glassy reg

Dielectric

analysis r

authors al

Williams-

antiplasti

Tg was hig

Plasticize

In additio

dielectric

subsequently caused an increase in tensile strength. The higher interchain cohesion also raised the activation energy for diffusion.

Gupta et al. [32] studied antiplasticization in bisphenol A polycarbonate/ 2,2 dinitrobiphenol (DNBP) blends via a variety of mechanical and analytical techniques. A modulus maximum was observed at about 30% DNBP. They concluded from DSC and NMR experiments that the DNBP was intimately mixed with the PC. Fourier transform infrared spectroscopy (FTIR) and nuclear magnetic resonance (NMR) data implied the presence of a strong PC-DNBP interaction.

An increase in the α-relaxation temperature for poly(vinyl acetate) (PVAC) blended with low quantities of cholesteryl additives was observed by Deshpande et al. [33]. Thus the glassy region was extended over a wider temperature interval. Dielectric depolarization spectroscopy and dynamic mechanical analysis results suggested antiplasticization behavior. These authors also analysed the thermal data based on the WLF (Williams-Landel-Ferry) equation [34] and found that with antiplasticized blends, the WLF reference temperature, T_o, or Tg was higher than that of the pure polymer PVAC. For a plasticizer, the Tg was lower than that of the pure polymer. In addition, the apparent enthalpy of activation for the dielectric relaxation, ΔH_a, was higher for antiplasticized

blends. Sp

molecules

antiplasti

Maeda and

decreased

poly(pheny

selectivi

depending

volume an

free volu

penetrant

Dumais et

antiplas

at 40 we

phenyl r

aromatic

responsi

distribu

ethers).

Stevenso

that an

polar di

(PPPHLP

blends. Specific dipolar interaction between the additive molecules and the PVAC chain was the suggested cause for the antiplasticization phenomenon.

Maeda and Paul [35 to 38] found that antiplasticizers decreased the permeability of polysulfone, polystyrene, and poly(phenylene oxide), but either decreased or increased the selectivity of the gas pairs through these membranes depending on the relative molecular sizes of the gases. Free volume analysis showed that the diluents caused a decrease in free volume of the blends, which led to a decrease in penetrant gas mobility.

Dumais et al. [39] found via deuterium NMR studies that the antiplasticizer, 4,4-dichlorodiphenyl sulfone (DCDPS), added at 40 weight percent decreased the rate and magnitude of 180^{o} phenyl ring flips in poly(arlene ether sulfones). The aromatic ring flips are the primary mode of motion responsible for β relaxations and represent a broad distribution of frequencies (10^{2} - 10^{7} s^{-1}) in poly(aryl ethers).

Stevenson et al. [40] found via Infrared (IR) spectroscopy that antiplasticization in phenoxy blends containing the polar diluent, 4-(2-hydroxy-3-phenoxy-propyloxy) acetanilide (EPPHAA), was due to hydrogen bonding interactions between

the phenoxy

diluent. Su

Ky et al.

between bi

antiplasti

solid-stat

labelled s

in the BPA

antiplasti

existed be

groups on

closer to

aliphatic

increased

phenylene

spatial s

spatial p

interact

led to pl

those of

diluent i

A mathema

explain t

antiplast

the phenoxy hydroxyl groups and the amide groups on the diluent. Suppression of the β peak was also observed.

Roy et al. [41-42] set out to look for a specific interaction between bisphenol A polycarbonate (BPA-PC) and the antiplasticizer di-n-butyl phthalate (DBP). They conducted solid-state C-13 NMR spin diffusion experiments between a labelled site on the DBP and various natural abundant sites in the BPA-PC repeat unit. They proposed that during antiplasticization (< 10% DBP) a specific interaction existed between the carbonyl ester of DBP and the phenylene groups on the polymer chain; the carbonyl ester of DBP was closer to the phenylene groups relative to the quaternary aliphatic carbons at 10% DBP. As the DBP concentration increased, the labelled carbonyl was close to both the phenylene and the quaternary sites, and the intermolecular spatial specificity was minimized. This non-specific relative spatial positioning meant that the DBP molecules did not interact with special sites on the PC repeat units and thus led to plasticization. The conclusions of Roy et al. support those of Olayemi et al., who suggested that a non-specific diluent interaction was responsible for plasticization.

A mathematical model was developed by Vrentas et al. [43] to explain the volumetric changes that occur during antiplasticization. These authors derived a concentration

dependent e

and propose

increase in

plasticizir

specific ho

antiplastic

The effect

blends was

to rule ou

antiplasti

manifest a

which were

elevated t

crystalliz

containing

temperatu

manifested

to be pre

crystalli

was that

polymer c

into a mo

increase

dependent equation describing the specific hole free volume and proposed that low Tg diluents will initially cause an increase in specific hole free volume and hence a plasticizing effect. High Tg diluents will decrease the specific hole free volume initially, and hence behave like antiplasticizers.

The effect of crystallinity on antiplasticization in PVC/TCP blends was investigated by Guerrero [44] An effort was made to rule out aging as the primary cause for antiplasticization. Completely amorphous samples did not manifest antiplasticization. The same was true of samples, which were blended at room temperature rather than at elevated temperatures. These latter samples did not crystallize when blended at room temperature. Instead samples containing low levels of TCP that were blended at elevated temperatures showed some degree of crystallinity and manifested antiplasticization. Apparently, the additive had to be present during a critical cooling stage to cause crystallization and effect antiplasticization. One argument was that the additive may have imparted mobility to the polymer chains, such that the polymer could rearrange itself into a more densely packed crystalline state, yielding an increase in modulus.

Stockey et

MMAA, in

relaxation

in densiti

to a decre

Cais et al

polycarbo

in organic

diphenylh

the polyca

wear. The

from a du

analysis

sub-Tg mo

artiplast

to strong

resin.

2.2.2 Su

In summa

polymer-c

artiplast

artiplast

occurred

dilient s

Shockey et al. [45] studied the role of the antiplasticizer, EPPHAA, in polyimides and found a suppression of sub-Tg relaxations, a decrease in water absorption, and an increase in densities, which led them to attribute antiplasticization to a decrease in free volume.

Cais et al. [46] studied the abrasion resistance of polycarbonate binder resins blended with diphenylhydrazones in organic photoconductors. They found that the diphenylhydrazones charge transport molecules antiplasticized the polycarbonate layer, stiffened the polymer, and decreased wear. The antiplasticization was manifested by a transition from a ductile to a brittle failure mode. Dynamic mechanical analysis (DMA) and density measurements indicated decreased sub-Tg molecular mobility and a decrease in free volume upon antiplasticization. The authors attributed antiplasticization to strong charge-transfer interaction with the polycarbonate resin.

2-2.2 Summary of Past Research on Antiplasticization

In summary, antiplasticization has been observed in diverse polymer-diluent systems. The major observations were that antiplasticization was observed at low diluent levels, antiplasticization is temperature dependent, it usually occurred in the glassy state, and antiplasticization is diluent specific. Mechanical property tests, differential

scanning calorimetry (DSC), dynamic mechanical spectroscopy (DMS), dielectric loss studies, nuclear magnetic resonance (NMR), and density measurements collectively infer that antiplasticization results from one or more of the following:

(a) a decrease in free volume upon the addition of the diluent - perhaps the polymer chains have some limited degree of mobility, which allows them to align themselves in a more ordered densely packed state or that the diluents fill the excess volume of the polymer glass.

(b) suppression of the secondary relaxation transitions at the temperature of interest, which reduces polymer flexibility.

(c) specific polymer-diluent interactions which create steric hindrance and decrease segmental mobility of the polymer Often the higher frequency motions are most affected.

(d) reduced mobility of the diluent - it has been suggested that diluents with relatively high Tgs (or Tgs very near the temperature of interest) have a greater tendency of promoting antiplasticization.

The majority

mechanical

and then sp

one has rel

diluent to

then extend

behavior of

2-4. Refe

1. J.K.
Plast

2. J.T.
Theor

3. J.D.
New Y

4. R.M.
Macro

5. W.J.
Scie

6. W.J.
Scie

7. M.H.
Phy

The majority of these authors relied solely on either a mechanical or an analytical test to verify antiplasticization and then speculated on a mechanism for antiplasticization. No one has related the microscopic physical behavior of the diluent to the local molecular motions of the polymer, and then extended that information to explain the bulk mechanical behavior of the polymer.

2-4. References

1. J.K. Sears, and R.J. Darby, The Technology of Plasticizers, Wiley, New York, 1982.

2. J.T. Lutz Jr., ed., Thermplastic Polymer Additives - Theory and Practice, Dekker, New York, 1989.

3. J.D. Ferry, Viscoelastic Properties of Polymers, Wiley, New York, 1980.

4. R.N. Haward, J. Macromolecular Science - Reviews of Macromolecular Chemistry, C4(2), 191-242, 1970.

5. W.J. Jackson Jr., and J.R. Caldwell, J. Applied Polymer Science, 11(2), 211-226, 1967.

6. W.J. Jackson Jr., and J.R. Caldwell, J. Applied Polymer Science, 11(2), 227-44, 1967.

7. M.H. Litt and A.V. Tobolsky, J. Macromolecular Science - Physics, B193, 433-443, 1967.

8. L.M. R
B: Pol

9. L.M. R
277-28

10. S.E.B.
Polym

11. G. Pe
Polym

12. R.E.
Scien

13. M.G.
1973.

14. N. Ki
1973.

15. N. K

16. L. Ma
Polym

17. L. Ma
Polym

18. G. Be
Polym

8. L.M. Robeson and J.A. Faucher, J. Polymer Science:Part B: Polymer Letters, 7(1), 35-40, 1969.

9. L.M. Robeson, Polymer Engineering and Science, 9(4), 277-281, 1969.

10. S.E.B. Petrie, R.S. Moore, and J.R. Flick, J. Applied Polymer Science, 43(11), 4318-4326, 1972.

11. G. Pezzin, G. Ajroldi, and C. Garbuglio, J. Applied Polymer Science, 11, 2553-2566, 1967.

12. R.E. Robertson and C.W. Joynson, J. Applied Polymer Science, 16, 733-738, 1972.

13. M.G. Wyzgoski and G.S.Y. Yeh, Polymer J., 4(1), 29-34, 1973.

14. N. Kinjo and T. Nakagawa, Polymer J., 4(2), 143-153, 1973.

15. N. Kinjo, Japan Plastics, 6, 6-28, 1973.

16. L. Makaruk, H. Polanska, and E. Staros, J. Applied Polymer Science, 20, 60-70, 1976.

17. L. Makaruk, H. Polanska, and T. Mizerski, J. Applied Polymer Science, 23(7),1935-42.

18. G. Bergman, H. Bertilsson, and Y. Shur, J. Applied Polymer Science, 21, 2953-2961.

19. N. Sun
Polyme

20. E.P. C
Polyme

21. E.P. C
Polyme

22. M. Kr
Polyme

23. M. Kr
Scien

24. J.Y.
Scien

25. L. Mu
1981.

26. L. Be
Physi

27. L.A.
W.P.
1744

28. L.A.
25, 4

19. N. Sundgren, G. Bergman, and Y. Shur, J. Applied Polymer Science, 22, 1255-1265, 1978.

20. E.P. Chang, R. Kirsten, and R. Salovey, J. Applied Polymer Science, 24, 827-836, 1979.

21. E.P. Chang, R. Kirsten and E.L. Slagowski, J. Applied Polymer Science, 21, 2167-2180, 1977.

22. M. Kryszewski, J. Ulanski, and A. Galeski, J. Applied Polymer Science, 23, 1271-1278, 1979.

23. M. Kryszewski and J. Ulanski, J. Applied Polymer Science: Applied Polymer Symposium, 35, 553-562, 1979.

24. J.Y. Olayemi and N.A. Oniyangi, J. Applied Polymer Science, 26, 4059-4067, 1981.

25. L. Mubarak and H. Polanska, Polymer Bulletin, 4, 127, 1981.

26. L. Belfiore and S.L. Cooper, J. Polymer Science: Polymer Physics Edition, 21, 2135-2157, 1983.

27. L.A. Belfiore, P.M. Henrichs, D.J. Massa, N.Zumbulyadis, W.P. Rothwell, and S.L. Cooper, Macromolecules, 16, 1744-1753, 1983.

28. L.A. Belfiore, P.M. Henrichs, and S.L. Cooper, Polymer, 25, 452-458,1984.

29. L. Be
1987.

30. M.D.
Scie

31. R.J.
Phys

32. M.K.
Wile
211-

33. D.D.
Appl

34. M.L.
Chem

35. Y. M

36. Y.
Poly

37. Y.
198

38. P.T
Pol

29. L. Belfiore, J. Elastomers and Plastics, 19, 238-251, 1987.

30. M.D. Sefcik, J. Schaefer, and F.L. May, J. Polymer Science: Polymer Physics Edition, 21, 1041-1054, 1983.

31. R.J. Pace and A. Datyner, J. Polymer Science: Polymer Physics Edition, 17, 437-465, 1979.

32. M.K. Gupta, J.A. Ripmeester, D.J. Carlsson, and D.M. Wiles, J. Polymer Science: Polymer Letters Edition, 21, 211-215, 1983.

33. D.D. Deshpande, N.R. Kandaswamy, and V.K. Tiwari, J. Applied Polymer Science, 30, 2869-2882, 1985.

34. M.L. Williams, R.F. Landel, and J.D. Ferry, J. American Chemical Society, 77, 3701-3707, 1955.

35. Y. Maeda and D.R. Paul, Polymer, 26, 2055-2063, 1985.

36. Y. Maeda and D.R. Paul, J. Polymer Science:Part B: Polymer Physics, 25, 957-1016, 1987.

37. Y. Maeda and D.R. Paul, J. Membrane Science, 30, 1-9, 1987.

38. P.T. DeLassus, in Styrene Polymers, Encyclopedia of Polymer Science and Engineering, 2nd Ed., 16, 1989.

39. J.J. Dumais, A.L. Cholli, L.W. Jelinski, J.L. Hedrick, and J.E. McGrath, Macromolecules, 19, 1884-1889, 1986.

40. W.T.K. Stevenson, A. Garton, and D.M. Wiles, J. Polymer Science: Part B: Polymer Physics, 24, 717-722, 1986.

41. A.K. Roy, P.T. Inglefield, J.H. Shibata, and A.A. Jones, Macromolecules, 20, 1434-1437, 1987.

42. Y. Liu, A.K. Roy, A.A. Jones, P.T. Inglefield, and P. Ogden, Macromolecules, 23, 968-977, 1990.

43. J.S. Vrentas, J.L. Duda, and H.C. Ling, Macromolecules, 21, 1470-1475, 1988.

44. S.J. Guerrero, Macromolecules, 22, 3480-3485, 1989.

45. E. Shockey and A. Garton, American Chemical Society, Polymeric Materials Science and Engineering, 65, 257-258, 1991.

46. R.E. Cais, M. Nozomi, M. Kawai, and A. Miyake Macromolecules, 25, 4588-4596, 1992.

ME

3.1. Intr

This chapt

antiplasti

becomes st

study the

antiplasti

as the mod

of the pol

3.2. Fle

rectangula

due to the

blends. Th

accordance

flexural

each end,

the mid-p

which is

from the

flexural

CHAPTER 3

MECHANICAL BEHAVIOR DURING ANTIPLASTICIZATION

3-1. Introduction

This chapter deals with the mechanical effects of antiplasticization. During antiplasticization the polymer becomes stiffer and more brittle [1,2]. Work was done to study the effect of chain end concentration on antiplasticization. Polystyrene/mineral oil blends were used as the model. Emphasis is placed on the flexural properties of the polystyrene/mineral oil blends.

3-2. Flexural Properties Flexural mechanical tests of rectangular bars were conducted, instead of tensile tests, due to the brittle nature of the polystyrene/mineral oil blends. The three-point bending technique was used in accordance with ASTM Method D-790 procedures [3]. During the flexural test, the test bar rests on two supports, one on each end, and a load is applied via a loading nose located at the mid-point between the supports. The flexural modulus, which is a measure of the degree of stiffness, is determined from the initial slope of the stress-strain curve. The flexural strength, which is the ability of the material to

withstand bending forces, is equivalent to the maximum stress in the outer fibers at the moment of break. In the case of materials that do not break upon bending, the flexural strength is calculated using the maximum load at which there is no longer an increase in load with increasing deflection [4,5].

3-3. Experimental Section

3-3.1 Materials and Blending

Three different types of atactic polystyrene (MW = 270,000 and 40,000 Daltons, obtained from Scientific Polymer Products, Inc. and MW = 128,000, obtained from The Dow Chemical Company), were blended separately with different concentrations of Penreco Drakeol Supreme High Viscosity mineral oil in a Haake Buchler Rheocord System 40 mixing bowl set at 50 rpm and 200^{o}C. Nominal mineral oil concentrations of 0 to 10 parts per hundred resin (0 to 9.09 weight percent or 0 to 10.9 volume percent) were studied.

3-3.2 Gel Permeation Chromatography (GPC)

Molecular weight distributions of the pure polystyrene samples, dissolved in high performance liquid chromatography (HPLC) grade tetrahydrofuran (THF) with 500 ppm di-t-butyl benzene as an internal standard, were determined using a Hewlett-Packard GPC. The instrument was calibrated using

twelve narrow anionic polystyrene standards (MW = 2.95 X 10^6 to 2.2 X 10 ^{3}) obtained from Polymer Laboratories, Inc. Two PLgel Sum mixed columns (each 7.5 mm X 300 mm), obtained from Polymer Labs., were used in series at 40°C to obtain separation. The injection sample volume was 50 ml of 0.25% polymer solution in THF eluent. The flow rate of the THF eluent was 1 ml/min. The samples were filtered prior to injection. A Filter Photometric Detector tuned to 254 nm was used. The support apparatus consisted of a Hewlett-Packard 1090 Liquid Chromatograph with autosampler, an HP 85-B Computer, and a 9153A Controller.

3-3.3 Gas Chromatography

High temperature gas chromatography (GC) with flame ionization detection and a Quadrex aluminum clad capillary column (25 m x 0.25 mm I.D., 0.1 mm) with split injection was used to determine the qualitative nature of the mineral oil. The temperature ramp was from 100°C to 400°C. The chromatogram of the mineral oil was compared to a chromatogram of a mixture of C-7 to C-40 straight chain hydrocarbons obtained from Polyscience Corp. (Analytical Standard Kit #21c and #26cx).

3-3.4 Compression Molding

Compression bars (approximately 0.076 X 0.012 X 0.0016 m or 3 X 1/2 X 1/16 inch) were molded in an electrically heated

hydraulic press set at 200°C and 100 to 5000 psi for 3 minutes.

3-3.5 Mineral Oil Concentrations.

The mineral oil concentration in the molded bars was determined by gas chromatography (GC) using polystyrene samples dissolved in methylene chloride. The analyses were performed with a Waters 510 HPLC Pump, a Spectrum 1021A Filter and Amplifier, an ACS Mass Detector Model 750/14, and a Hewlett Packard 3396A Integrator. A DuPont ZORBAX SIL 4.6 mm x 25 cm column with a Brownlee Labs Silica 4.6 mm x 3 cm guard column was used. HPLC Grade hexane was the mobile phase. The injection size was 20 microliters. The flow rate was 1.5 ml per minute. The analyses were conducted at room temperature. Calibration was accomplished using standards containing 0.5 weight % to 10 weight % mineral oil dissolved in methylene chloride.

3-3.6 Differential Scanning Calorimetry

Glass transition temperatures of the blends (after molding) were determined by differential scanning calorimetry using DuPont 9900 Computer/ Thermal Analyser calibrated with indium. Scanning rates were 10°C/min from room temperature to 200°C. All samples were run in air.

3-3.7 Flexural Properties

Flexural moduli and flexural strengths of the compression molded bars were determined at room temperature using an Instron Universal Testing Instrument Model 4201. The test were done at room temperature a few days after molding according to the ASTM Method #D790 for a 3-point bend test. Tensile property testing could not be performed due to the extremely brittle nature of most of the bars. All of the bars broke during the flexural tests except the 270,000 MW blends containing 8% mineral oil.

3-4 Results and Discussion

3-4.1 Molecular Weight Distribution of the Polystyrenes

The molecular weight distributions for the polystyrene samples are shown in Table 3-1. The 40,000 MW sample was bimodal. All of these materials were synthesized by free-radical polymerization.

3-4.2 Gas Chromatogram of the Mineral Oil

Figure 3-1 shows the high temperature gas chromatogram, which indicated that the mineral oil sample was comprised of primarily C-28 to C-46 hydrocarbons.

Table 3-1. Molecular Weight Distribution of Polystyrenes

	270,000 MW	128,000 MW	Bi- Modal 40,000 MW	
Mn	111, 700	58, 420	56,970	850
Mw	274, 400	127, 900	103, 900	1, 058
Mz	448, 100	216, 400	164, 700	1, 343
Mp	244, 200	87, 930	109, 300	751
PD*	2.455	2.190	1.824	2.190

PD - Polydispersity

3-4.3 Solubility of Mineral Oil in Polystyrene

GC analysis of the 270,000 MW, 128,000 MW, and 40,000 MW polystyrene test bars indicated a maximum concentration of approximately 8, 9, and 10 volume percent of absorbed mineral oil respectively, compared to the nominal 11 % concentration that was added to the polystyrene in the HAAKE mixing bowl. Blends containing greater than 8% mineral oil were opaque at room temperature i.e. phase separation occured as temperature was decreased. This was indicative of Upper Critical Solution Temperature (UCST) behavior.

3-4.4 Glass Transition Temperatures

Figure 3-2 shows that the glass transition temperatures decreased with mineral oil concentration. There was a 21^{o}C, a 33^{o}C and a 15^{o}C decrease in glass transition temperatures for the 270,000, 128,000 and 40,000 molecular weight blends respectively, at the highest mineral oil concentrations. While the Tg of the 270,000 MW and 128,000 blends decreased linearly, there was a change in slope or discontinuity in the Tg of the 40,000 MW blends at 6% mineral oil. At concentrations less than 6% mineral oil the Tg decreased linearly, whereas above 6% mineral oil the Tg of the 40,000 MW blends remained constant. This change in slope at 6% Corresponds to the work of Braun et al. and Pezzin et al., where they describe a singularity in the Tg versus

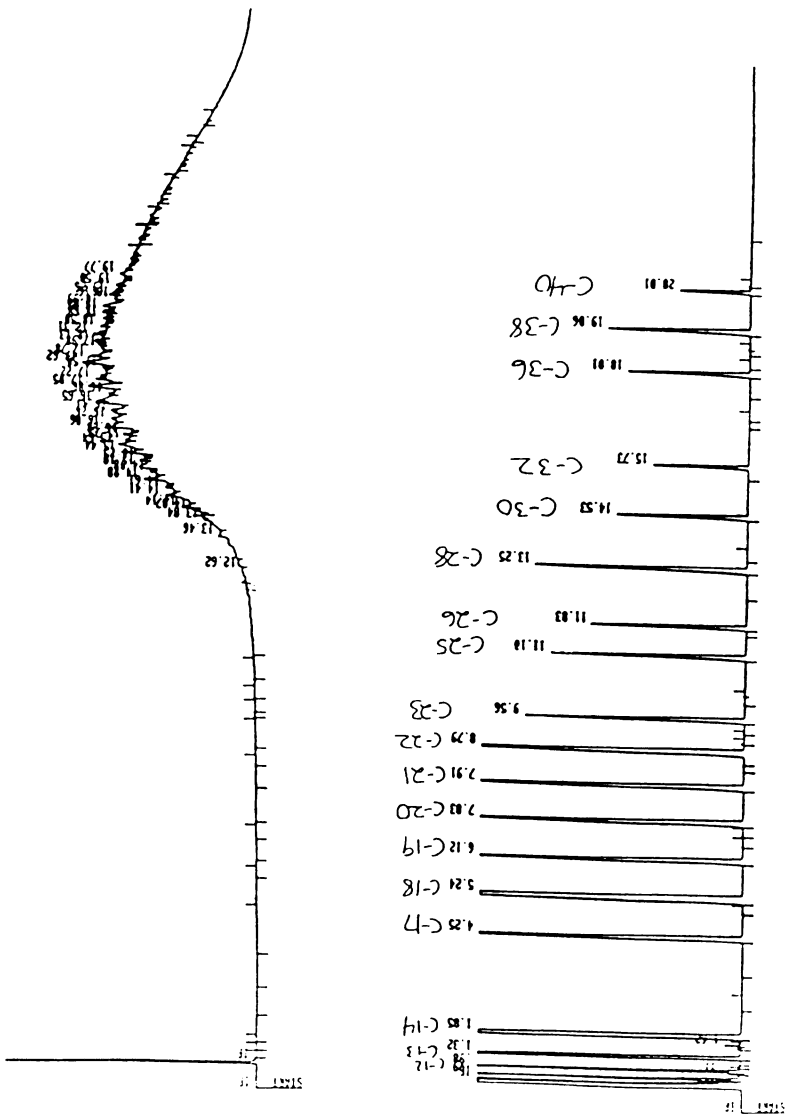

Figure 3-1. Gas Chromatogram of Mineral Oil

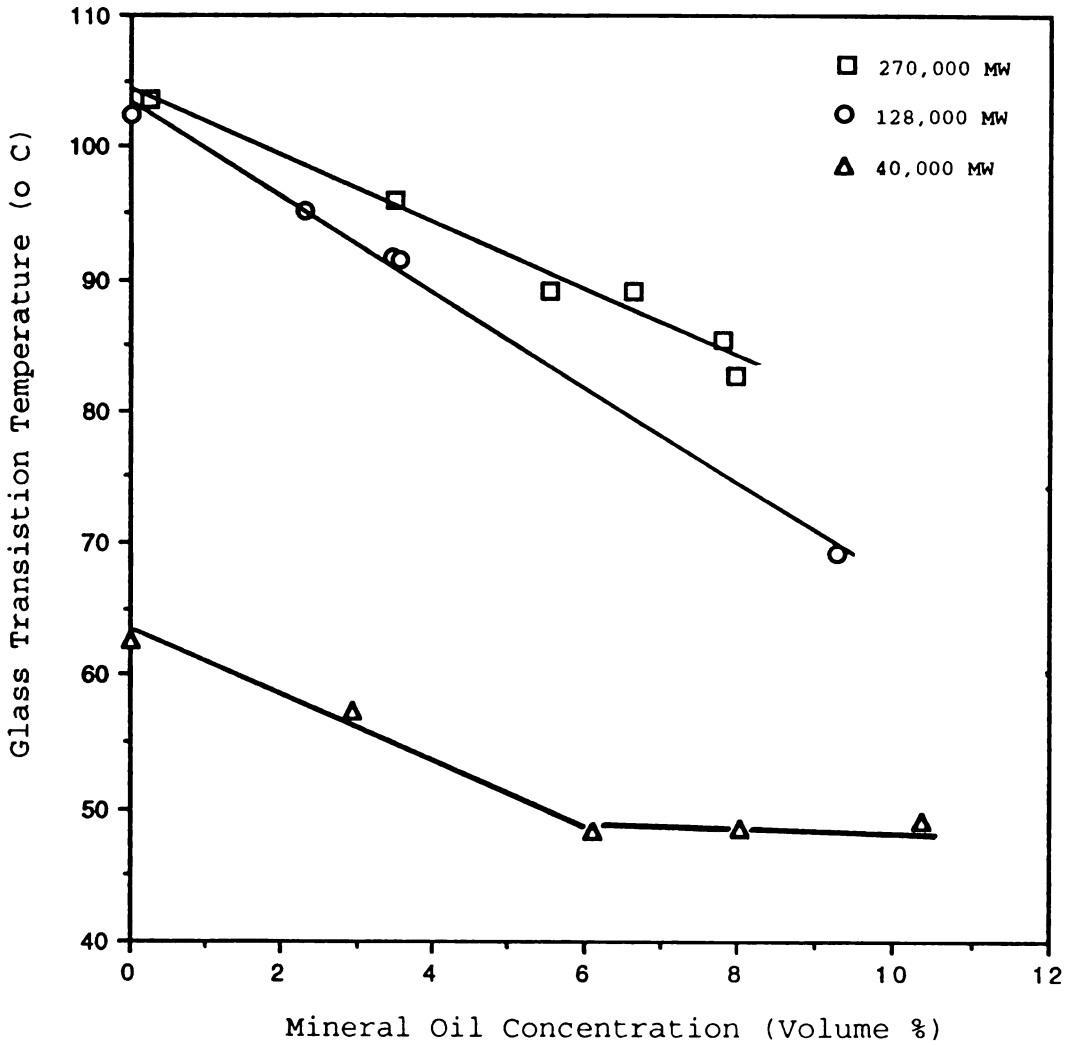

Figure 3-2. Effect of Mineral Oil Concentration on Tg

concentration data of poly(vinyl chloride) with dibutyl phthalate and dicyclohexyl phthalate [6,7]. This singularity occurs when the diluent eliminates the WLF free volume. According to Boyer the plasticizer is more efficient at lowering the free volume once this singularity is achieved [8]. A similar deviation in Tg from linearity was observed by Cais et al. with polycarbonate diluent blends [9].

3-4.5 Flexural Properties of Polystyrene/Mineral Oil Blends

Figures 3-3a and 3-3b illustrate the effect of mineral oil concentration on the flexural properties of the 270,000 MW polystyrene blends. As mineral oil was added to the 270,000 MW system, the flexural modulus remained constant and then decreased significantly at concentrations greater than 5%; whereas, there was an immediate decrease in flexural strength. This was indicative of plasticization of the high molecular weight polystyrene by the mineral oil. The error bars on the graphs represent a 95% confidence interval.

Figures 3-4a and 3-4b show the effect of the mineral oil concentration on the flexural properties of the 40,000 MW polystyrene blends. Here one observed about a 2X increase in flexural modulus up to about 6% mineral concentration, followed by a rapid decrease in flexural modulus with higher concentrations of mineral oil. The same behavior was seen with the flexural strength. There was a 1.7X increase in

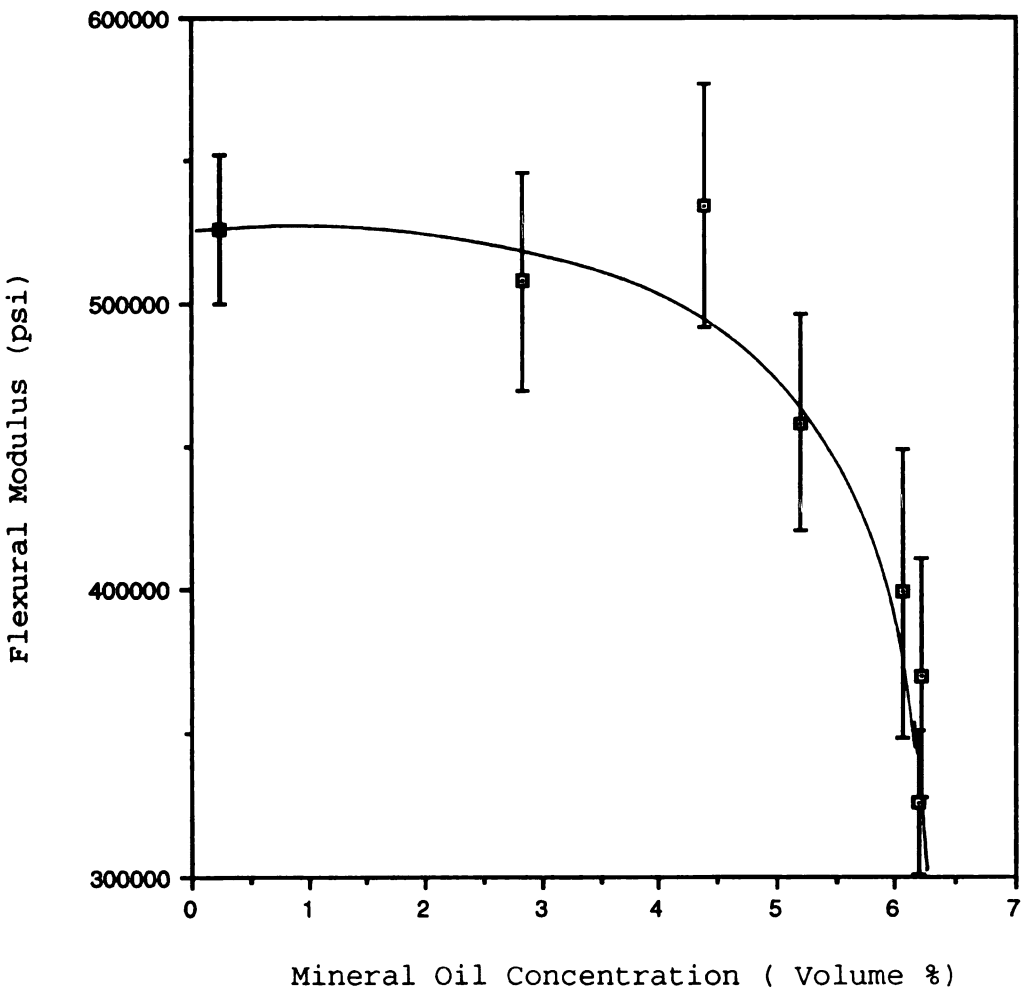

Figure 3-3a. Effect of Mineral Oil Concentration on Flexural Modulus of 270,000 MW Polystyrene

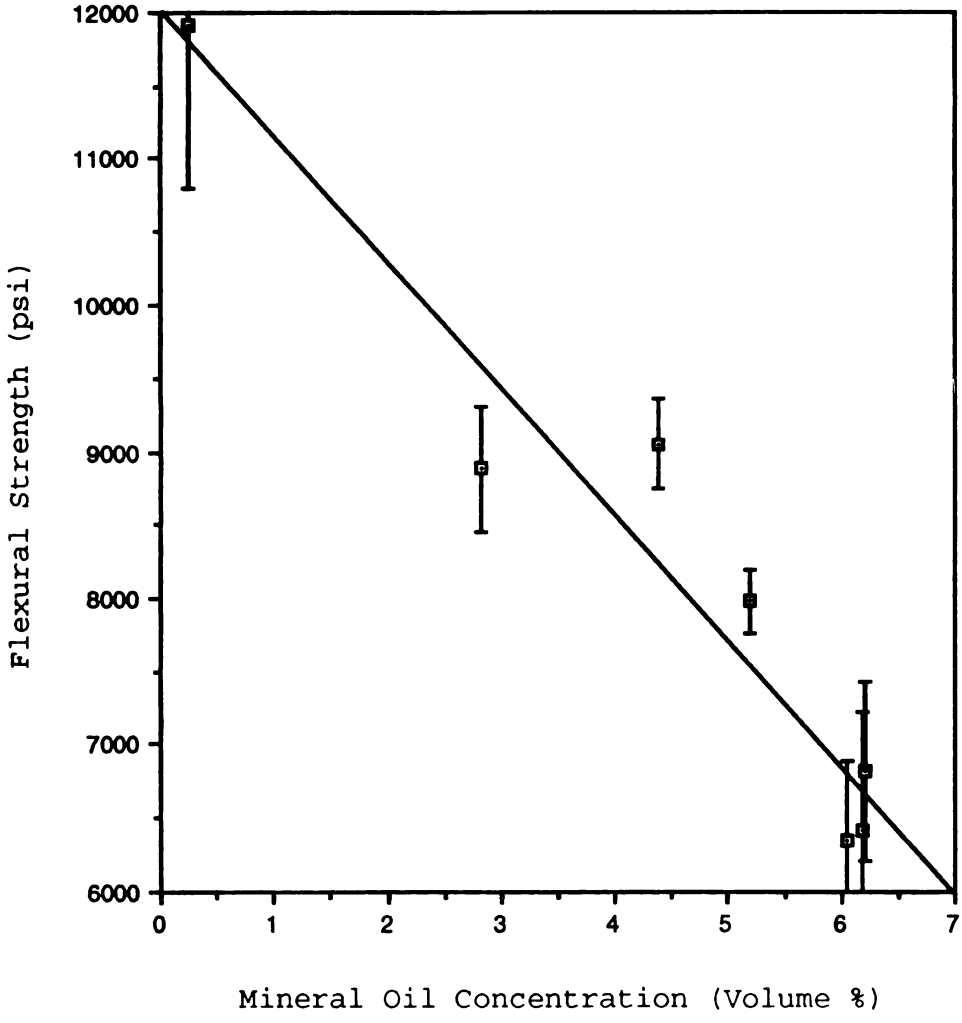

Figure 3-3b. Effect of Mineral Oil Concentration on Flexural Strength of 270,000 MW Polystyrene

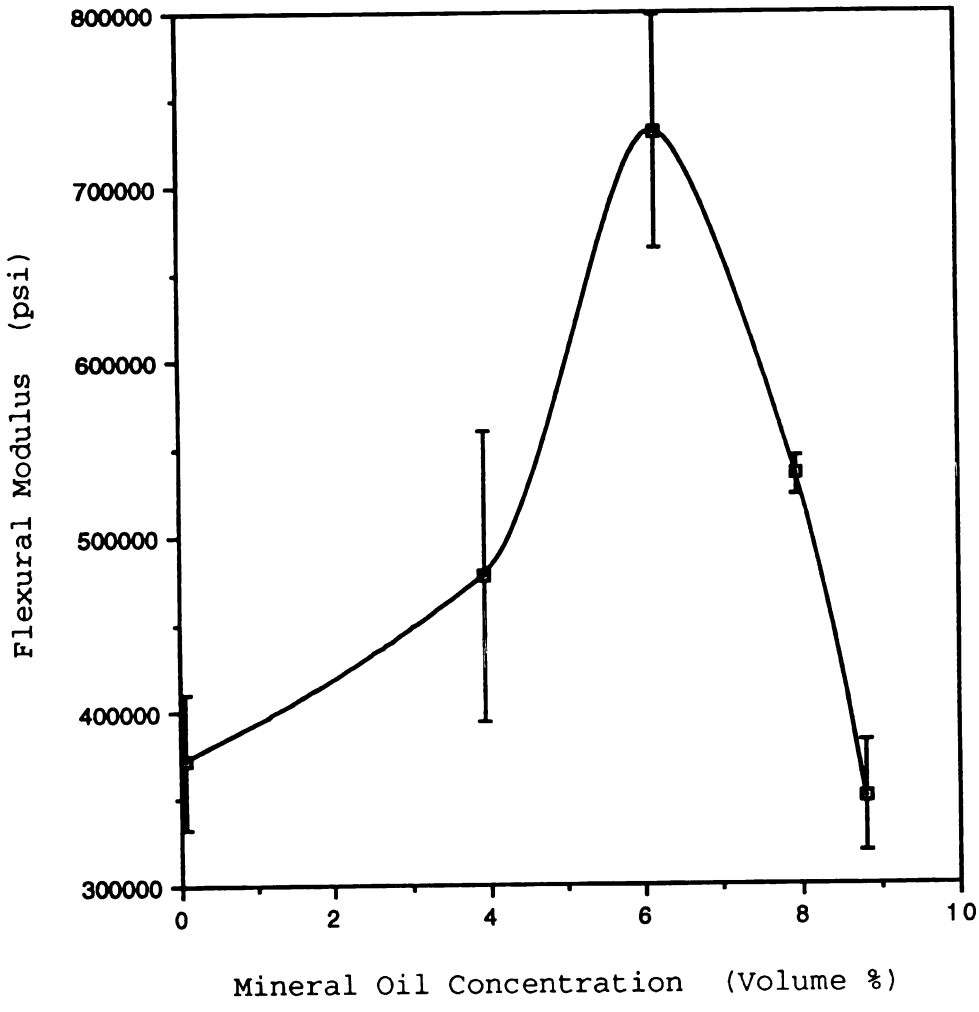

Figure 3-4a. Effect of Mineral Oil Concentration on Flexural Modulus of 40,000 MW Polystyrene

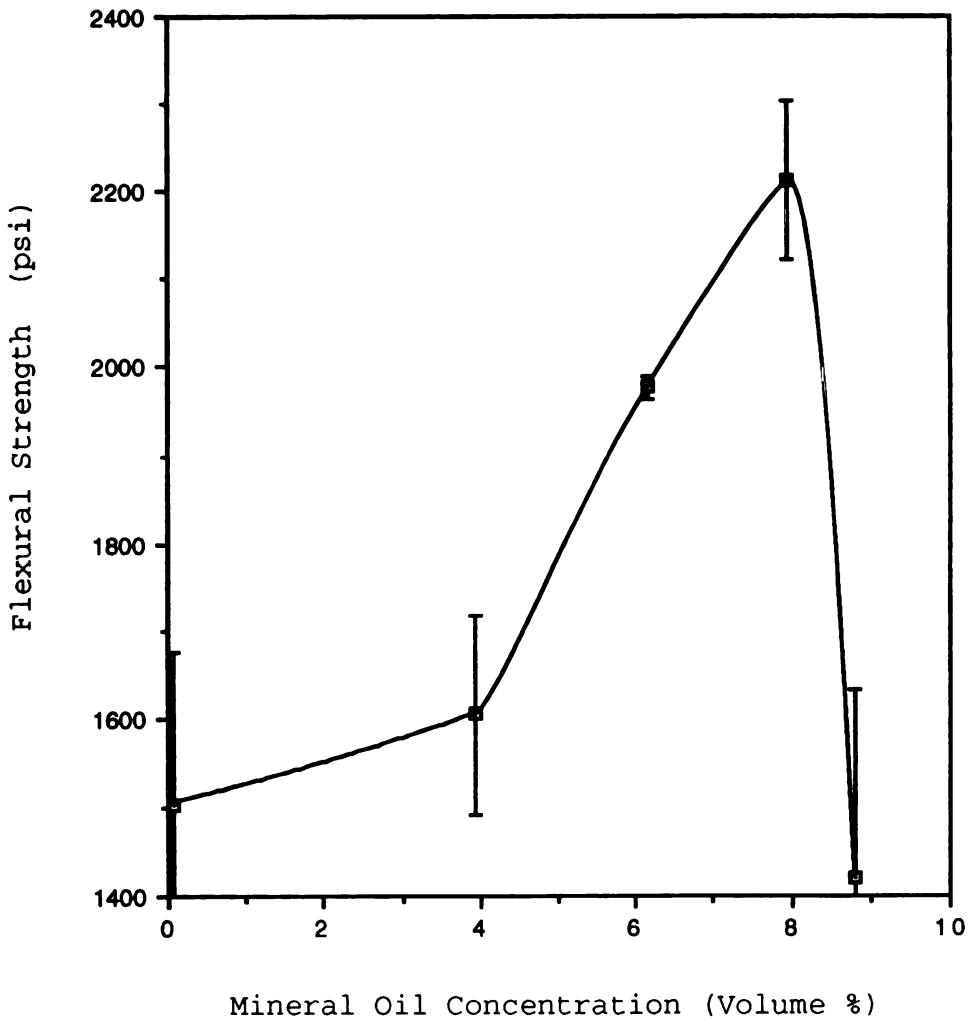

Figure 3-4b. Effect of Mineral Oil Concentration on Flexural Strength of 40,000 MW Polystyrene

flexural strength up to about 8% mineral oil concentration followed by a rapid drop in flexural strength at higher mineral oil concentrations. The increase in flexural modulus and strength is indicative of antiplasticization. This apparent stiffening of the blend below Tg resulted when small quantities of mineral oil (less than 6%) were blended into 40,000 MW atactic polystyrene. This behavior was not observed in the 270,000 MW polystyrene blends. Possibly antiplasticization occurs only below a critical molecular weight. These results are consistent with the hypothesis that antiplasticization is primarily attributed to a chain end effect.

The 40,000 MW bimodal sample had a significantly greater concentration of chain ends than the 270,000 MW material. Using a basis of 1,000,000 grams, one determines that the 270,000 MW sample had approximately 18 moles of chains ends, whereas the 40,000 MW bimodal sample had 1,426 moles (14 and 1,412 moles for the high and low molecular weight fractions respectively). There are two orders of magnitude more "voids" available at the chain ends in the low molecular weight material for the mineral oil to occupy and hinder the mobility and realignment of the polymer chain.

3-5 Conclusions

Antiplasticization, as evidenced by a stiffening of the blends below Tg, resulted when small quantities of mineral oil (less than 6%) were blended into the 40,000 MW polystyrene samples. It is speculated that measureable antiplasticization occurs only above a critical concentration of chain ends.

These observations also support our hypothesis that antiplasticizaton is primarily due to a chain end effect. The 40,000 MW bimodal sample had a significantly greater concentration of chain ends, than the 270,000 MW polystyrene sample, approximately a 83:1 ratio. This means that there were more chain end voids available for the mineral oil to occupy in the 40,000 MW sample. In polystyrene, the chain ends are the most mobile units. Thus by filling the voids, mobility of the chain ends is hindered, and antiplasticization is manifested.

3-6 References

1. W.J. Jackson Jr. and J.R. Caldwell, J. Applied Polymer Science, 11, 211-226, 1967.

2. W.J. Jackson, Jr. and J.R. Caldwell, J. Applied Polymer Science, 11, 227- 244, 1967.

3. American Standard Test Method for Flexural Properties of Plastics and Electrical Insulating Materials, ASTM D790-71, Annual Book of ASTM Standards, 1987.

4. V. Shah, Handbook of Plastics Testing Technology, John Wiley and Sons, New York, p 23, 1984.

5. M.D. Baijal, Plastics Polymer Science and Technology, John Wiley and Sons, New York, p 809, 1982.

6. G. Braun, and A.J. Kovacs, C.R. Acad. Sci., 260, 2217, 1965.

7. G. Pezzin, A. Omacini, and F. Zilio-Grandi, La Chimica E. L'Industria, 50, 309, 1968.

8. R. Boyer, Transitions and Relaxations in Amorphous and Semicrystalline Organic Polymers and Copolymers, in Encyclopedia of Polymer Science and Technology Supplement, John Wiley and Sons, Inc, New York, Vol II, p 797, 1977.

9. R.E. Cais, M. Nozomi, M. Kawai, and A. Miyaki, Macromolecules, 25, 4588, 1992.

CHAPTER 4

AN INVESTIGATION OF THE HOLE FILLING MECHANISM VIA POSITRON ANNIHILATION SPECTROSCOPY

4-1 Introduction

Antiplasticization [1,2] has been attributed to a decrease in free volume upon addition of the diluent. Several researchers have inferred that the diluents fill the excess free volume of the polymer glass or that the polymer chains have some small degree of mobility, which allows them to align themselves into a more ordered densely packed state [3,4]. These inferences have been made indirectly through theoretical calculations and density measurements.

Positron Annihilation Spectroscopy (PAS) was used to determine changes in free volume. The results of this research will be related to a hole-filling mechanism of the diluent during antiplasticization. PAS is a valuable tool for studying defects/holes in solids. It relies on the affinity of ortho-positronium (o-Ps) for domains with low electron densities. From information about their lifetimes and intensities, one can determine independently the hole size and hole densities [5].

4-2. Positron Annihilation Spectroscopy

4-2.1 Background

Positrons, which are the conjugate antimatter of electrons, are emitted with high energy (≈ 0.54 Mev) from a radioactive isotope such as ^{22}Na and thermalize quickly (picoseconds) upon entering a condensed sample. They can exist in several states, each having a characteristic lifetime τ_i and intensity I_i. Typically, PAS spectra are resolved into three exponentially decaying components corresponding to the specific state of the positron.

The spectrum is expressed as a series of negative exponential functions of time t:

$$N(t) = \sum_{i=1}^{n} I_i \, e^{-\lambda i t} + B \qquad (4\text{-}1)$$

where N (t) is the count at time t, n is the number of exponential terms, I_i is the number of positrons (intensity), λ_i is the positron annihilation rate for the ith state, and B is the background count.

The positron lifetime , τ_i, is the reciprocal of the annihilation rate, λ_i, which is the overlap integral of the positron density, ρ_+, and the electron density, ρ_- , at the site of annihilation.

$$\lambda = k \int \rho^{-}(r)\, \rho^{+}(r)\, dr \qquad (4\text{-}2)$$

The parameter k is a normalization constant related to the number of electrons. Thus the annihilation rate is dependent on the electron density experienced by the positron species. The electron density is inversely proportional to the free volume hole sizes.

Positrons may annihilate with free electrons in condensed media resulting in photon emission. A positron may also combine with an electron to form a positronium (Ps), which can exist in either the singlet i.e. para state, or triplet i.e. ortho state, depending on the spin state of the bound electron. Para-positronium (p-Ps) has the shortest lifetime of about 0.1 ns, corresponding to τ_1. In condensed media free positrons and positron-molecular complexes have intermediate lifetimes of about 0.4 to 0.8 ns, corresponding to τ_2. The longest lifetime component, τ_3 of 1 to 10 ns, attributed to ortho-positronium (o-Ps) "pick-off decay" by electrons, is used to study free volume changes, since the o-Ps lifetimes are more sensitive to the changes in free volume. The o-PS lifetime, τ_3, is proportional to the average hole size, while the intensity, I_3, of the o-Ps component of the lifetime spectra is proportional to the number density of holes. An approximate measure of the relative free volume can

be obtained from the product of the lifetime and the relative intensity.

4-2.2 Determination of Average Hole Size From PAS Lifetimes

Tao and Nakanishi, using the particle-in-a-spherical-box theory, have shown that that the o-Ps lifetime, τ_3, in nanoseconds, can be related to the average hole radius, r, in nanometers, in the following way [6,7].

$$\tau_3 = 0.5[1-r/(r+0.166)+(2\ \pi)^{-1}(\sin(2\ \pi r/(r+0.166))]^{-1}$$

Several researchers have observed excellent agreement between measured o-Ps lifetimes and average hole radii for materials with known hole sizes. The model is valid for radii of less than 0.2 nm to greater than 0.6 nm [7].

The average hole volume, <V>, is then derived from:

$$\langle V \rangle = 4\ \pi r^3/3$$

4-2.3 Fractional Free Volume and Number Density of Holes

Brandt et al. have shown that the o-Ps intensity, I, is a measure of the number density of holes or free volume sites [8]. Given that n(v)dv is the number density of holes having volumes between v and (v+dv), then the number of holes per unit volume, N, is the integral $\int n(v)dv$.

The fractional free volume, f_v, is given as

$$f_v = \int n(v)\ v\ dv = \langle V \rangle\ N \qquad (4\text{-}5)$$

$$f_v = c\ \langle V \rangle\ I, \text{ where } N = c\ I \qquad (4\text{-}6)$$

The parameter c is a proportionality constant relating o-Ps intensity , I, to the total number density of holes, N.

The constant c, which depends on the type of polymer, can be determined from a calculated or known value of the fractional free volume of pure polystyrene, as will be shown now.

The free volume, V_f, of a polymer at any temperature T is typically explained as the difference between the specific volume of the polymer, V_T, and the specific volume of the equilibrium liquid or occupied volume, V_0, at 0 K.

$$V_f = V_T - V_0 \qquad (4\text{-}7)$$

According to Bondi [9],

$$V_0 \approx 1.3\ V_w \qquad (4\text{-}8)$$

where V_w is the van der Waals specific volume determined from group contributions.

$$f_V = V_f / V_T = (V_T - V_0) / V_T \qquad (4\text{-}9)$$

$$V_T = V_{273K} \exp [\alpha_g (T-273)] \qquad (4\text{-}10)$$

where α_g = d ln V/dT is the coefficient of thermal expansion of the glass at constant pressure.

4-3 Experimental Section

4-3.1 Positron Annihilation Spectroscopy

PAS experiments were conducted at 23°C in air using a ^{22}Na source (50 mCi) deposited on a 0.1 mil thick Mylar film and sandwiched between two layers (each approximately 1 mm thick) of compression molded nearly identical 1 inch diameter polymer discs. PAS spectra were acquired using a standard fast-fast coincidence spectrometer from EG&G Ortec. The birth gamma and annihilation gamma rays were detected by two detectors, one set at 1.28 MeV and the other set at 0.511 MeV radiation respectively. Each detector consisted of a photomultiplier (RCA 8835) and a fast plastic scintillator (Pilot U). Approximately 3 million counts were accummulated during a three-hour to eight-hour period. The lifetime spectra were resolved into three exponentially decaying components using PCPFIT, which is a PC version of POSITRONFIT EXTENDED [10].

4-4. Results and Discussion

4-4.1 Determination of Fractional Free Volume

Zoller et al. found that the specific volume of the polystyrene glass at 273 K was 0.9508 cm^3/g or 98.97 cm^3/mol [11]. According to Ougizawa et al. the equation of state parameters for polystyrene were independent of molecular weight above 34,000 Daltons [12]. This behavior was confirmed by comparing pressure-volume-temperature (PVT) data obtained by Zoller using a 120,000 MW polystyrene with those obtained by researchers at The Dow Chemical Company using a 300,000 MW and 200,000 MW polystyrene; there was good agreement between the Zoller and Dow data within experimental error [13]. The Fox and Loshoek relationship also shows that the fractional free volume of polystyrene (a value of 0.116) is independent of the number average molecular weight above 10,000 Daltons [14]. It is difficult to determine an overall representative number average molecular weight for the bi-modal 40,000 MW sample. However, a comparison of ΔT_g values i.e. (Tg_∞ - Tg) with Boyer's ΔT_g plots of V-T data for thermal polystyrene fractions, shows that a Tg of 63°C for the 40,000 MW bimodal sample, hence a ΔT_g of 40°C, corresponds to a "nominal" fractional free volume of about 0.112 [15].

Using Equation 4-10, a value for α_g of 2.86×10^{-4} ($^oC^{-1}$), and a value for V_{273K} of 98.97 cm^3/mol, the specific volume of polystyrene at 23°C (296 K) was calculated to be 99.6 cm^3/mol

[11]. V_0, obtained from the literature, is 88.4 cm^3/mol [9]. Therefore the fractional free volume, f_v, is 0.112. This value is in agreement with the Simha and Boyer value of 0.113 derived from their empirical relationship for the fractional free volume of a polymer glass [16],

$$(\alpha_l - \alpha_g)\, T_g \approx 0.113 \qquad (4\text{-}11)$$

where α_l is the thermal expansion coefficient for the polymer above Tg.

For the pure 40,000 MW polystyrene, τ_3 is 1.97 ns, which corresponds to an average hole diameter of 0.566 nm and an average hole volume, <V>, of 0.095 nm^3 (Equations 4-3 and 4-4). The o-Ps intensity, I_3, is 0.453. Therefore the proportionality constant c as defined in Equation 4-6 is 2.60 nm^{-3}. The number density of holes, N, is calculated to be 1.18 nm^{-3} or one hole every 0.85 nm^3.
The number density of holes and fractional free volume of the blends were then determined using:

$$N = 2.60\ I \qquad (4\text{-}12)$$

$$f_v = 2.60\ I\ \langle V \rangle \qquad (4\text{-}13)$$

4-4.2 Free Volume Hole Sizes

Figures 4-1a and 4-1b show the effect of mineral oil concentration on the o-Ps lifetimes and average hole sizes for the polystyrene blends respectively. Mineral oil had no effect on the average hole size of the 270,000 MW blends. There was a slight increase in the average hole size of the 128,000 MW blends from 0.107 nm^3 to 0.110 nm^3 with mineral oil addition. The lifetimes of the 40,000 MW blends increased steadily with increasing mineral oil concentration. This corresponds to an increase in the average hole volume from 0.095 nm^3 to 0.101 nm^3. Apparently, in the case of the 128,000 MW and 40,000 MW blends, the mineral oil filled the smaller holes first. The remaining larger holes contributed to the increased average o-Ps lifetimes.

4-4.4 Effect of Mineral Oil on Hole Densities

Figures 4-2a and 4-2b show the effect of mineral oil concentration on the ortho-Positronium intensities and number densities of holes for the polystyrene blends respectively. The o-Ps intensities of the 270,000 MW blends remained constant. There was a 7% decrease in number density of holes for the 128,000 MW blend. With the 40,000 MW sample, the

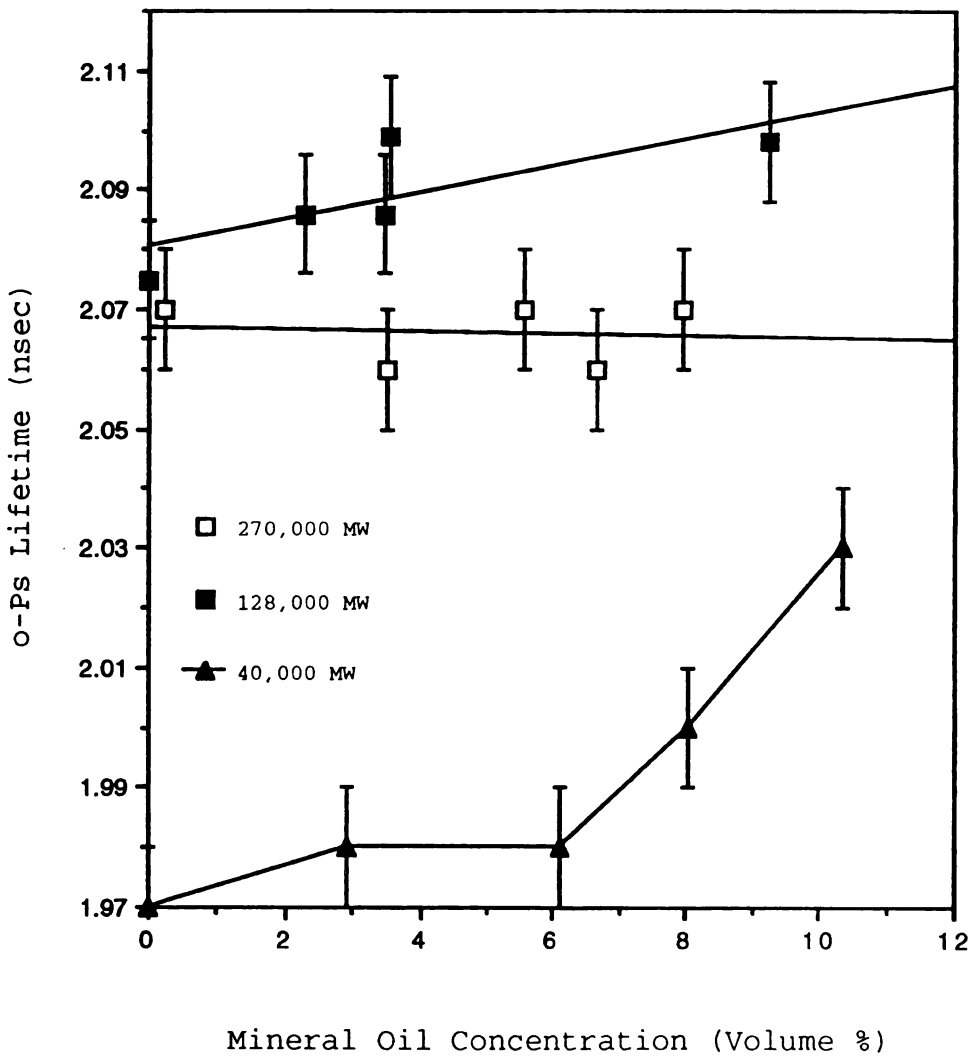

Figure 4-1a. Effect of Mineral Oil Concentration on o-Ps Lifetimes

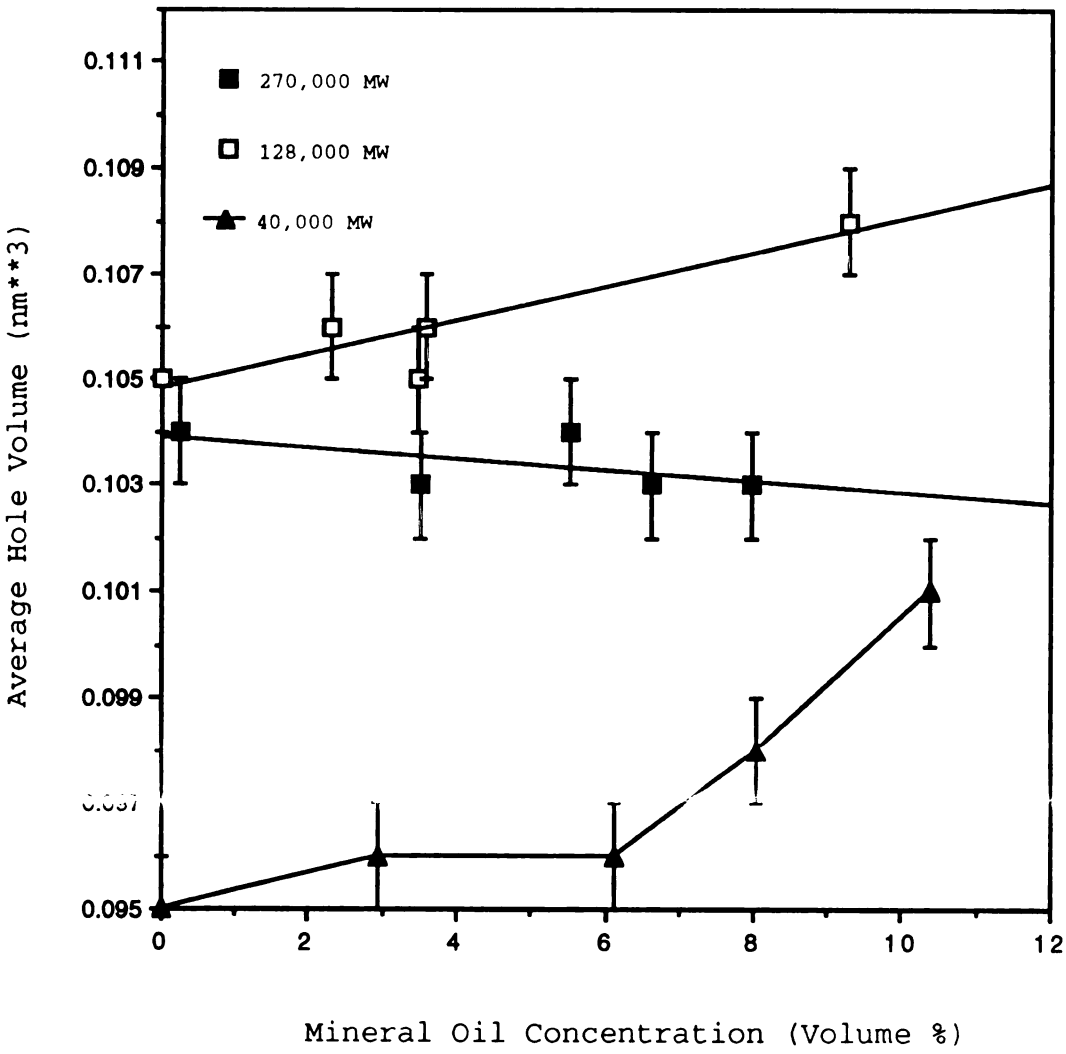

Figure 4-1b. Effect of Mineral Oil Concentration on Hole Size

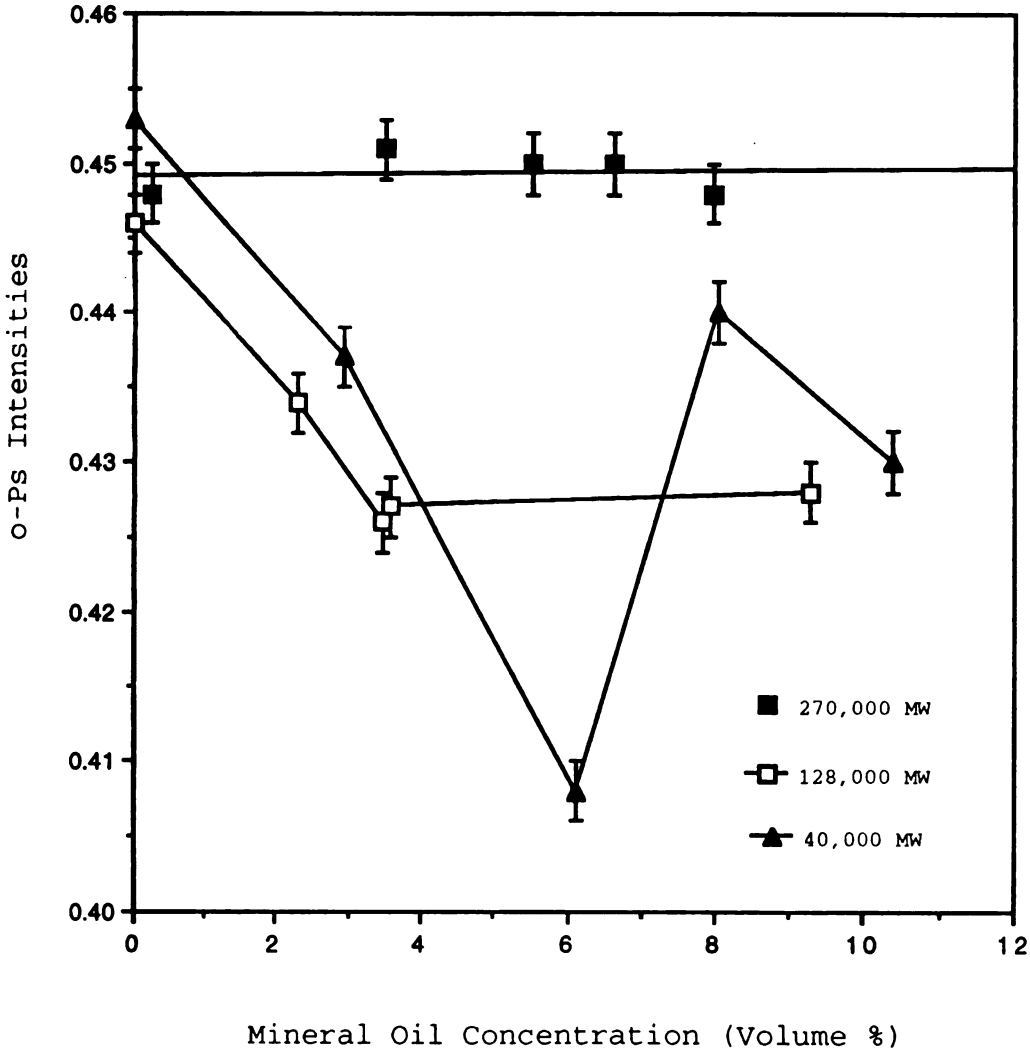

Figure 4-2a. Effect of Mineral Oil Concentration on o-Ps Intensities

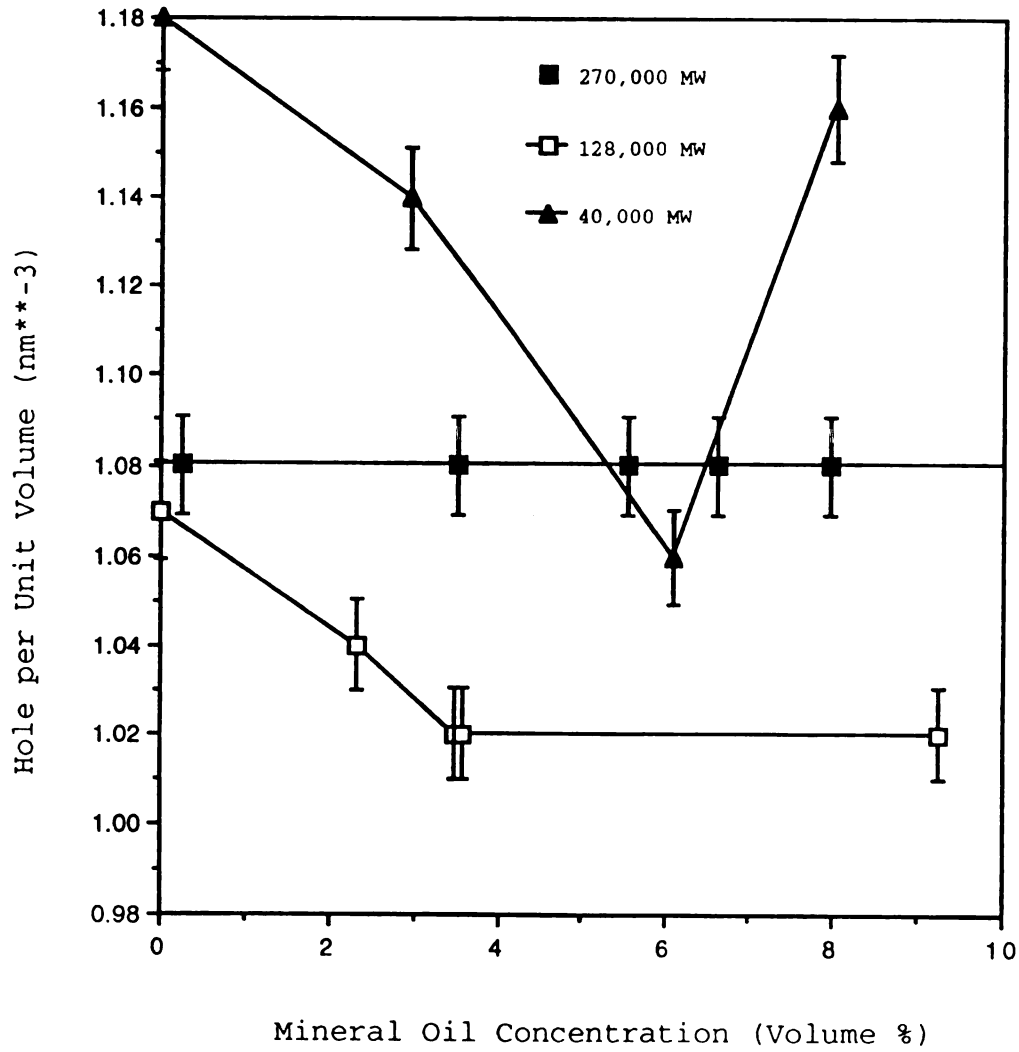

Figure 4-2b. Effect of Mineral Oil Concentration on Hole Densities

number of holes per unit volume decreased by 10% at the maximum degree of antiplasticization (6% mineral oil) and increased with higher levels of mineral oil.

4-4.5 Effect of Mineral Oil on Fractional Free Volume

Figure 4-3 shows that addition of 3.5% mineral oil caused a 3.6% decrease in fractional free volume in the 128,000 MW sample. There was a 9% decrease in fractional free volume at 6% mineral oil for the antiplasticized 40,000 MW polystyrene. There was no change in the free volume of the 270,000 MW sample, which was plasticized.

4-5. Hole Filling Mechanism During Antiplasticization

PAS elucidates the hole-filling mechanism of the mineral oil. The data suggest that in the 40,000 MW and 128,000 MW polystyrene, initially most of the mineral oil filled the smaller holes at the chain ends, leaving the larger holes along the polymer backbone relatively deficient in mineral oil. At a certain critical mineral oil concentration, where phase separation of the mineral oil occurs, these larger holes become sufficiently filled to allow easier slippage between longer chain lengths and effect plasticization.

There is other evidence that the smaller holes are filled first. Researchers have observed a suppression and then disappearance of the β peak in antiplasticized materials

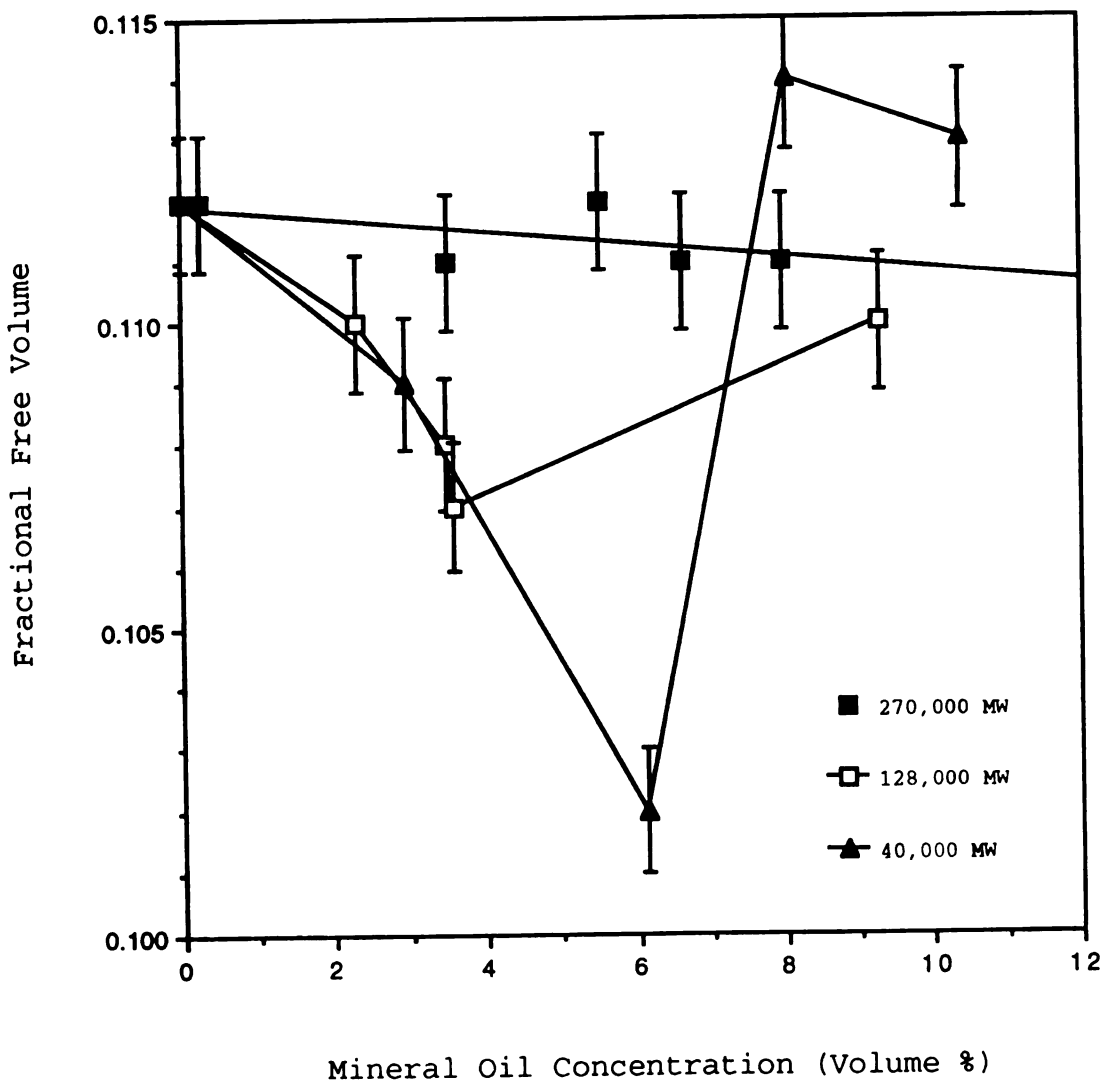

Figure 4-3. Effect of Mineral Oil on Fractional Free Volume

[17]. According to Boyer, the β transition involves torsional or rotational motion of 1 to 3 monomer repeat units or 1 to 10 consecutive atoms. Our argument is consistent with that of Boyer [18]. The β peak is suppressed and shifted to lower temperatures because the smaller holes are filled first.

Evidently, the mineral oil occupying voids at the chain ends contributed directly to antiplasticization, while the mineral oil residing along the polymer backbone was responsible for the accompanying plasticization behavior. In polystyrene the chain ends are the most mobile units on the polymer chain, and hence the mobility of the chain ends would be hindered upon antiplasticization. In the 270,000 MW very few chain ends exist compared to the 128,000 MW and the 40,000 MW polystyrene (a ratio of 1:2:83). Thus a large proportion of the mineral oil will occupy voids along the polymer backbone in the 270,000 MW sample. Those voids along the backbone are larger in volume than voids at the chain ends, and hence never become sufficiently filled with mineral oil to effect antiplasticization.

The phenonenon of antiplasticization therefore is directly related to a decrease in free volume, in that the diluent fills the excess free volume of the glass. In cases where there may be a significantly large concentration of chain

ends e.g. bi-modal systems, a greater decrease in free volume can occur. The PAS data suggest that the decrease in free volume in the 128,000 MW antiplasticized polystyrene was solely due to hole-filling by the mineral oil - blending 3.5 volume % mineral oil resulted in a 3.6% decrease in fractional free volume. However, in the case of the 40,000 MW sample, a 9% decrease in free volume was observed after blending with only 6% mineral oil. Perhaps, in addition to hole-filling by the mineral oil, the 40,000 MW polymer may be realigning itself into a more densely packed state thus causing a greater decrease in free volume than expected. Possibly, in blends that manifest antiplasticization, antiplasticization is dominant below a certain critical diluent level, whereas above that critical concentration, plasticization dominates. In addition a polymer may manifest antiplasticization depending on its concentration of chain ends.

4-6. Conclusions

PAS elucidates the hole-filling mechanism of the mineral oil during antiplasticization. The data show that initially most of the mineral oil filled the smaller holes at the chain ends, leaving the larger holes along the polymer backbone relatively deficient in mineral oil. At concentrations greater than 6% mineral oil, these larger holes become sufficiently filled to effect plasticization.

4-7.

1.

2.

3.

4.

5.

6.

7.

8.

9.

10.

4-7. References

1. W.J. Jackson Jr.and J.R. Caldwell, J. Appl. Polym. Sci., 11, 211, 1967.

2. W.J. Jackson Jr. and J.R. Caldwell, J. Appl. Polym. Sci., 11, 227, 1967.

3. Y. Maeda and D.R. Paul, J. Polym. Sci. Part B: Polym. Phys., 25, 1005, 1987.

4. J.S. Vrentas, H.C. Ling, J.L. Duda, Macromolecules, 21, 1470, 1988.

5. Y.C. Jean, and D.M. Schrader, Experimental Techniques in Positron and Positronium Chemistry, in Positron and Positronium Chemistry, Elsevier, New York, Ch 3, 1988.

6. S.J. Tao, J. Chem. Phys., 56, 5499, 1972.

7. H. Nakanishi, S.J. Wang, and Y.C. Jean, Proceedings of the International Conference on Positron Annihilation in Fluids, Arlington, TX; ed. S.C. Sharma; World Scientific Publishing: Singapore, p 292, 1987.

8. W. Brandt,S. Berko, and W.W. Walker, Phys. Rev., 120, 1289, 1980.

9. A.J. Bondi, J. Polym. Sci., A2, 3159, 1964.

10. P. Kirkegard, and M. Eldrup, Comp. Phys. Commun., 7, 401, 1984.

11. P. Zoller, and H.H. Hoehn, J. Polym. Sci., Polym. Phys. Ed., 20, 1385, 1982.

12. T. Ougizawa, G.T. Dee, and D.J. Walsh, Polymer, 30, 1675, 1989.

13. L.F. Whiting, The Dow Chemical Company Personal Communication, 1991.

14. T.G. Fox Jr., S.J. Loeshek, Polym. Sci., 15, 371, 1955.

15. R. Boyer, Transitions and Relaxations in Amorphous and Semicrystalline Organic Polymers and Copolymers, in Encyclopedia of Polymer Science and Technology Supplement; John Wiley and Sons, Inc: New York, Vol II, p 775, 1977.

16. R. Simha and R.F. Boyer, J. Chem .Phys. 37, 1003, 1962.

17. J.J. Dumais, A.L. Cholli, L.W. Jelinski, J.L. Hedrick, and J.E. McGrath, Macromolecules, 19, 1884, 1986.

18. R. Boyer, Transitions and Relaxations in Amorphous and Semicrystalline Organic Polymers and Copolymers, in Encyclopedia of Polymer Science and Technology Supplement, John Wiley and Sons, Inc: New York, Vol II, p 761, 1977.

CHAPTER 5

A SOLID STATE NMR INVESTIGATION OF POLYMER AND DILUENT DYNAMICS DURING ANTIPLASTICIZATION

5-1. Introduction

In many polymer systems antiplasticization suppresses the rate and amplitude of the chain dynamics [1,2]. This chapter summarizes the results of a solid state NMR study of the 40,000 MW polystyrene blends, and addresses the issue of how the mineral oil is interacting with the polymer chain.

5-2. Nuclear Magnetic Resonance

Three relaxation times are used to characterize the relaxation of nuclear spins in NMR experiments [3,4,5]. These are T_1, the spin-lattice relaxation time, T_2, the spin-spin relaxation time, and $T_{1\rho}$, the spin-lattice relaxation time in the rotating frame. T_1 describes molecular dynamics on the megahertz frequency scale, which is usually observed in mobile systems like low viscosity fluids. Relaxation processes are slow in polymers, typically mid-kilohertz range. Thus polymer dynamics are characterized by $T_{1\rho}$, which describes molecular dynamics on the kilohertz scale. Since these polymer motions are slower than the NMR frequency or Larmor frequency, an increase in $T_{1\rho}$ indicates a decrease in the relaxation rate. In more mobile systems such as low

viscosity liquids, an increase in T_1, or $T_{1\rho}$ indicates faster molecular motions.

$$\frac{1}{T_1} = \frac{h\gamma_I^2\gamma_S^2}{40\pi^2 r^6}\left(J(\omega_S-\omega_I)+3J(\omega_S)+6J(\omega_S+\omega_I)\right) \qquad (5\text{-}1)$$

where,

h is Planck's constant

γ_I is the magnetogyric ratio for the abundant spins I

γ_S is the magnetogyric ratio for the rare spins S

J is the spectral density function

ω is the nuclear precession frequency

r is the radius of gyration

$J(\omega)$ is determined from:

$$J(\omega) = \frac{\tau_c}{1+\omega^2\tau_c^2} \qquad (5\text{-}2)$$

where τ_c is the correlation time.

$$\frac{1}{T_{1\rho}} = \frac{h\gamma_I^2\gamma_S^2}{80\pi^2 r^6}\left(4J(\omega_{SI})+J(\omega_S-\omega_I)+3J(\omega_S)+6J(\omega_S+\omega_I)+6J(\omega_I)\right) \qquad (5\text{-}3)$$

$$\frac{1}{T_2} = \frac{h\gamma_I^2\gamma_S^2}{80\pi^2 r^6}\left(4\tau_c+J(\omega_S-\omega_I)+3J(\omega_S)+6J(\omega_S+\omega_I)+6J(\omega_I)\right) \qquad (5\text{-}4)$$

Magic angle spinning (MAS) and cross-polarization (CP) make it possible to overcome the resolution and sensitivity enhancement problems of the signal in solid state NMR experiments [6]. With MAS the sample is spun at 54.7^{o} with respect to the direction of the applied magnetic field. This averages all anisotropic interactions such as dipole-dipole couplings, which would otherwise cause significant NMR line broadening [7]. In CP experiments, 90^{o} pulses are applied separately to the ^{1}H and ^{13}C spins along the Y-axis, with spin-locking, allowing them to precess in the XY plane, for a given contact time, T_C. The polarization of the ^{13}C spins is increased, which increases their sensitivity. Magnetization is transferred from the ^{1}H coupled to the ^{13}C at a time constant, T_{C-H}, which is the time constant for the build-up of the ^{13}C signal [8].

The intensity, I, of the ^{13}C signal depends on T_{C-H} and ^{1}H $T_1\rho$ according to the following equation:

$$I(t) = I_0 \left[\left(1-\frac{T_{C-H}}{T_{1\rho}(H)}\right) \left(\exp\left(\frac{T_c}{T_{1\rho}(H)}\right) - \exp -\left(\frac{T_c}{T_{C-H}}\right)\right) \right] - 1 \qquad (5-5)$$

Studies of domain sizes in polymers can be conducted via ^{1}H NMR experiments since mobile domains exhibit significantly different T_2 relaxation times when compared to rigid domains. A Goldman-Shen pulse sequence:

$$[\ (\pi/2)_x - t_o - (\pi/2)_x - t - (\pi/2)_x\ ]$$

is applied to destroy selectively the magnetization of the rigid domains [9,10]. This then facilitates the transfer of magnetization from the mobile to the rigid domains. By monitoring the recovery of magnetization in the rigid domains, one can determine the size and shape of the mobile domains from the following equations.

$$R(t) = M(t) / M(t \rightarrow \infty) \qquad (5\text{-}6)$$

$$R(t) = 1\text{-}1/\exp(D\ t\ /\ b^2) \qquad (5\text{-}7)$$

$$D = 0.13\ a^2\ /\ T_2 \qquad (5\text{-}8)$$

where :

M(t) is the magnetization in the rigid phase

R(t) is the recovery factor

D is the spin diffusion coefficent in the rigid domain

b is the mobile domain size

a is the H-H bond distance = 0.2 nm

T_2 is the spin-spin relaxation time

5-3. Experimental Section

5-3.1 Polymer Dynamics

The blend samples were ground in a mortar and loaded into 4mm zirconium rotors. The analysis was done using a Bruker MSL-200 NMR spectrometer. Cross-polarization, magic angle

spinning ^{13}C NMR spectroscopy was performed at 50.3 MHz. The rotor was spun at about 7 KHz. The relaxation delay was 8 seconds, the proton 90^{o} pulse width was 6 msec, the contact time was 1 msec, the acquisition time was 80 msec, the sweep width was 20 KHz, the data size was 8K, and the apodisation was exponential with 10 Hz line broadening.

^{13}C NMR $T_1\rho$ values were determined in the conventional way [10]. The CP pulse sequence was as follows. A 90^{o} pulse was applied to the ^{1}H spins, and the Hartmann-Hahn technique used to cause spin-locking along the X-axis. Another 90^{o} pulse was applied on-resonance to the ^{13}C spins. Both spins then precessed at the same frequency in the XY plane, allowing polarization of the ^{13}C spins. The contact time, T_C, was the time during which polarization transfer occurred. The ^{1}H radio-frequency field was turned off and the free induction decay of the ^{13}C magnetization was measured to determine $T_{1\rho}$. The whole process was repeated after a time of approximately 5 $T_1(H)$. $T_{1\rho}$ values were determined by fitting the data to the following equation:

$$I(t) = A\, e^{-(t/T_{1\rho}^{C})} + B \qquad (5-9)$$

where A and B are constants.

T_{CH} and ^1H $T_1\rho$ values were determined from contact time experiments and Equation 5-5.

$$I(t) = I_0 \left[(1-\frac{T_{C-H}}{T_{1\rho}(H)}) (\exp(\frac{T_c}{T_{1\rho}(H)}) - \exp -(\frac{T_c}{T_{C-H}})) \right]^{-1} \qquad (5-5)$$

5-3.2 Mineral Oil Domains

Goldman-Shen spin diffusion experiments were conducted to determine the domain sizes of the mineral oil [9,10] The experiments were performed using the same spectrometer at 200.14 MHz for ^1H NMR. The relaxation delay was 8 seconds, the proton 90° pulse width was 6 msec, the acquisition time was 80 msec, the sweep width was 200 KHz, the data size was 4K, and the apodisation was exponential with 10 Hz line broadening. The delay between the first two 90° pulses to allow the T_2 relaxation of the rigid phase was 200 sec.

^1H T_1 values were determined from:

$$I(t) = I_0 \left(1-2e^{(\frac{-\tau}{T_1})}\right) \qquad (5-10)$$

where τ is the delay time.

5-4. Results and Discussion

5-4.1 Polymer Chain Dynamics

Figure 5-1 shows the ^{13}C NMR spectrum of the 40,000 MW 6% mineral oil blend with peak assignments. The resonance positions are reported in terms of chemical shifts (ppm) with respect to tetramethylsilane (TMS). The backbone carbons were observed at 40 ppm. The methylene carbons on the backbone are sometimes distinguished as a shoulder at approximately 42 ppm. The quaternary carbon on the aromatic ring was observed at 145 ppm. The other five carbons on the aromatic ring show up as the intense signal at 127 ppm.

As aforementioned, three relaxation times are used to characterize the relaxation of nuclear spins in NMR experiments. These are T_1, the spin-lattice relaxation time, T_2, the spin-spin relaxation time, and $T_{1\rho}$, the spin-lattice relaxation time in the rotating frame. T_1 describes molecular dynamics on the megahertz frequency scale, whereas $T_{1\rho}$ describes molecular dynamics on the kilohertz scale. The frequency of molecular motions in polymers is often observed on the kilohertz scale. Typically, because relaxation processes are slow in polymers, i.e. slower than the NMR frequency or Larmor frequency, an increase in $T_{1\rho}$ would indicate a decrease in the relaxation rate.

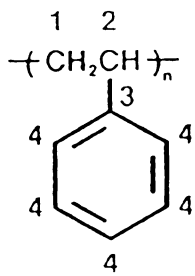

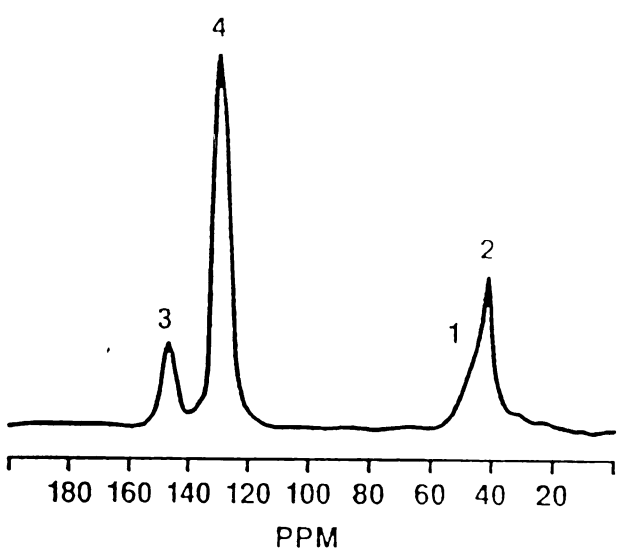

Figure 5-1. ^{13}C NMR Spectrum of 40,000 MW Polystyrene Blend

Table 5-1. NMR Spin-Lattice Relaxation Times (msec) for the 40,000 MW Polystyrene Blends

% MO	145 ppm			127 ppm			40 ppm		
	T_{CH}	$T_{1\rho}H$	$T_{1\rho}C$	T_{CH}	$T_{1\rho}H$	$T_{1\rho}C$	T_{CH}	$T_{1\rho}H$	$T_{1\rho}C$
0%	0.4	10.3	9.6	0.07	10.8	8.5	0.08	8.4	8.3
4%	0.3	8.0	8.5 9.1	0.08	9.6	5.0 5.9	0.08	7.8	2.9 3.6
6%	0.3	11.5	9.6 11.0	0.08	10.7	8.6 8.7	0.09	8.8	7.1 7.9
8%	0.6	11.5	26.0 36.0	0.09	11.6	9.9 10.6	0.10	9.4	5.2 5.2

Tab
the
roc
rer
reg
pla
tha
pol
en:
aff

5-

Th
Fi
mi
th
at
no
th
po

Th
be
mi
Oc

Table 5-1 shows the results of the relaxation experiments of the polystyrene/mineral oil blends in the rotating frame at room temperature. The relaxation times (msec) for the blends remain approximately the same as those of the virgin polymer regardless of whether the sample was antiplasticized or plasticized (greater than 6% mineral oil). These data imply that the mineral oil did not change the mobility of the polymer backbone, which supports our hypothesis of a chain end effect. It is believed that antiplasticization would affect the rate and/or amplitude of the chain end dynamics.

5-4.2 ^{1}H NMR and Mobility of Mineral Oil Domains

The ^{1}H NMR spectra of the mineral oil blends are shown in Figure 5-2. The sharp resonance peak at 1.6 ppm is due to mineral oil. As expected no mineral oil peak was observed in the pure polystyrene sample. Although there was a sharp peak, attributable to mineral oil, in both the 6% and 8% blends, none was observed in the 4% blend. This indicates that at 4%, the mineral oil was microscopically dissolved in the polystyrene.

The NMR data provide additional evidence that plasticization becomes dominant only at concentrations of greater than 6% mineral oil - where phase separation of the mineral oil occurs.

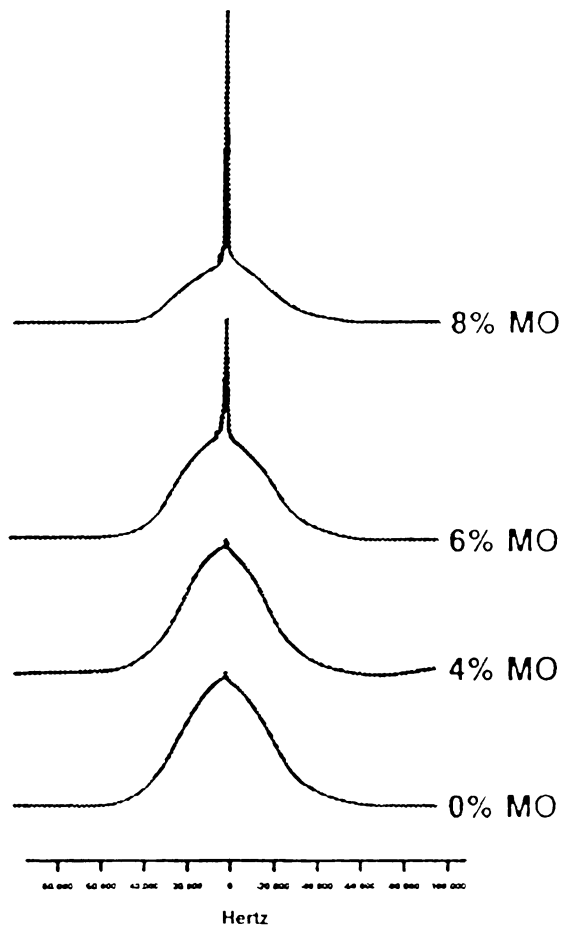

Figure 5-2. ^{1}H NMR Spectra of 40,000 MW Polystyrene Blends

Analysis of the ^1H NMR relaxation curves of the mineral oil peaks gave T_1 values of 0.5 sec and 1.5 sec respectively for the 6% and 8% blends. Since in more mobile systems such as low viscosity liquids, an increase in T_1 indicates faster molecular motions, the higher T_1 values at 8% mineral oil indicated increased mobility of the mineral oil at higher concentrations as expected.

5-4.3 Determination of Mineral Oil Domain Sizes

Table 5-2 shows the recovery factors as a function of spin-diffusion time for the 6% and 8% blends. The data are plotted in Figure 5-3 and fitted to Equation (5-7).

The domain size will now be calculated using the 6% blend as an example. T_2 can be determined from:

$$T_2 = 1/(\pi \Delta_{\frac{1}{2}}) \qquad (5\text{-}11)$$

where $\Delta_{\frac{1}{2}}$ is the line width. The polystyrene line width was 34 kHz, thus T_2 was 9.4×10^{-6} seconds. D calculated from Equation 5-8 was 5.6×10^{-12} cm^2/sec. The value for D/b^2 determined by fitting the recovery factors to Equation 5-7 was 12.17 $msec^{-1}$ or 1.22×10^4 sec^{-1}. Thus b was calculated to be 2.16×10^{-8} cm or 0.2 nm.

Ta

Ti
0.
0.
0.
0.
0.
0.
0.
0.
0.
0.
0.
1.0
5.0
10.
15.
20.
25.
30.
35.
40.

Table 5-2. Recovery Factors as a Function of Diffusion Time

Time (msec)	Recovery Factor (6% Mineral Oil)	Recovery Factor (8% Mineral Oil)
0.01	0.09	
0.02	0.18	
0.03	0.26	
0.04	0.33	
0.05	0.44	
0.06	0.48	
0.07	0.61	
0.08	0.67	
0.09	0.70	
0.10	0.74	
1.00		0.02
5.00		0.06
10.00		0.11
15.00		0.15
20.00		0.17
25.00		0.17
30.00		0.19
35.00		0.20
40.00		0.22

Fitting the 8% recovery factors in Table 5-2 to Equation 5-7 yielded a value for D/b^2 of 0.00728 $msec^{-1}$. The domain size of the mineral oil in the 8% blends was calculated to be approximately 8.8 nm.

The ^1H NMR data confirmed that during the process of antiplasticization (6% mineral oil and less) the mineral oil was intimately mixed with the polystyrene matrix i.e. there was no phase separation of the mineral oil. At concentrations above the solubility limit of the mineral oil, where phase separation occurred, plasticization was dominant.

5-4.4 Comparison of Mineral Domains and Free Volume Holes

Table 5-3 compares the average hole sizes obtained via PAS experiments in the 40,000 MW blends with the mineral oil domain sizes determined by NMR. At the critical domain size of about 9 nm (8% mineral oil) where significant phase separation occurred, plasticization was dominant. The data showed that at concentrations greater than 6% mineral oil, the size of mineral oil domains was 1 order of magnitude larger than the average size of the holes. Thus it can be deduced that antiplasticization is manifested only when the mineral domains approximate the average hole sizes.

The data imply that at concentrations greater than 6% mineral oil, the mineral domains become much larger than the size of

Table 5-3. Comparison of Mineral Oil Domains with Hole Sizes

% Mineral Oil	Hole Diameter from PAS (nm)	Mineral Domain from NMR (nm)
0	0.566	0
4	0.567	< 0.2
6	0.568	0.2
8	0.572	8.8

a mineral oil molecule (approximately 1 nm). This indicates that instead of being microscopically mixed in the polystyrene matrix, pooling of the mineral oil molecules occurred and plasticization was dominant.

5-5. Conclusions

The fact that the ^{13}C NMR relaxation times of the polymer backbone were unaffected by the presence of mineral oil directly supports our hypothesis that antiplasticization in polystyrene is primarily attributable to a chain end effect. The data suggested that during antiplasticization the mineral oil was intimately mixed with the polystyrene matrix. At concentrations above the solubility limit of the mineral oil, pooling of the mineral oil occured. This led to phase separation of the mineral oil and plasticization became dominant.

5-6. References

1. A.K. Roy, P.T. Inglefield, J.H. Shibata, and A.A. Jones, Macromolecules, 20, 1434, 1984.

2. Y. Liu, A.K. Roy, A.A. Jones, P.T. Inglefield, and P. Ogden, Macromolecules, 23, 968-977, 1990.

3. E.D. Becker, High Resolution NMR Theory and Chemical Applications, Academic Press, Inc., New York, 1984.

4. I. Solomon, Physical Reviews, 99, 559, 1955.

5. C.A. Fyfe, Solid State NMR for Chemists, C.F.C. Press, Ontario, 1983.

6. B.C. Gerstein and C. R. Dybrowki, Transient Techniques in NMR of Solids, Academic Press, London, 1985.

7. J. Schaefer and E. Stejskal, in Topics in Carbon-13 NMR Spectroscopy, 3, Chapter 4, 1979.

8. S.W. Homans, A Dictionary of Concepts in NMR. Oxford Science Publications, Oxford Press, New York, 1989.

9. M. Goldman and L. Shen, Phys. Rev., 144, 321, 1966.

10. T.T.P. Cheung and B.C. Gerstein, J. of Appl. Phys., 52, 5517, 1981.

11. J. Schaefer, E.O. Stejskal, T.R. Steger, M.D. Sefcik, and R.A. McKay, Macromolecules, 13, 1121, 1980.

CHAPTER 6

MODEL FOR ANTIPLASTICIZATION IN POLYSTYRENE

6-1. Introduction

This section deals with development of a model for antiplasticization. In the preceding chapters, it was determined that antiplasticization is dependent on the concentration of chain ends. During antiplasticization, the mineral oil is intimately mixed with the polystyrene matrix, filling the smaller holes at the chain ends first, thus restricting mobility of the chain ends. The decrease in mobility of the chain ends is manifested in increased stiffness and brittleness. NMR results showed that beyond the solubility limit (6 %) of the mineral oil in polystyrene, pooling or clustering of the mineral oil occurs, which effects plasticization.

This chapter integrates the above information into a model using balances on holes and mineral molecules.

6-2. Development of Antiplasticization Model

6-2.1 Comparison of Chain End Holes

Table 6-1 compares the relative chain end densities (number of chain ends per nm^3) for the various polystyrene samples.

Table 6-1. Comparison of Relative Chain End Densities

MW	Mn	Chain End Concentration from PAS (moles/g)	Bulk Density (g/cm^3)	Chain End Density (number per nm^3)	*Ratio of Chain End Densities
40,000	650 56,970	1.43×10^{-3}	1.058	0.911	83
128,000	58,420	3.42×10^{-5}	1.047	0.022	2
270,000	117,000	1.79×10^{-5}	1.047	0.011	1

* Ratio of chain end concentration in sample to that in 270,000 MW polystyrene.

The chain end concentration was calculated using the following equation:

$$C.E. = (2/Mn)\ N_A\ \rho\ 10^{-21}\ cm^3/nm^3 \qquad (6\text{-}1)$$

where C.E. = Chain end concentration (molecules/nm^3)

Mn = Number average molecular weight (g)

N_A = Avogadro's number 6.023 X 10^{23} molecules/mole

ρ = density of polystyrene g/cm^3

Table 6-1 shows that there was a significantly greater concentration of chain ends in the 40,000 MW sample than in the 270,000 MW sample - the ratio of chain end concentration was 83:1 .

Table 6-2 compares the relative number densities of holes associated with the chain ends and backbone. As molecular weight was increased, the total number densities of holes decreased. However, if one associates each chain end with a hole, then one can determine the number of holes not associated with the chain ends (backbone holes) from the

Table 6-2. Free Volume Holes Associated with Chain Ends

MW	Chain End Density (number per nm^3)	Total Hole Density (number per nm3)	Backbone Hole Density (number per nm^3)	Percent Chain Ends Holes (%)
40,000	0.911	1.18	0.269	77.2
128,000	0.022	1.07	1.048	2.1
270,000	0.011	1.08	1.069	1.0

difference between the total number density of holes and the concentration of chain ends. The table shows that as molecular weight increases, the number of backbone holes increases significantly. In other words, the percentage of the holes associated with the chain ends decreases as the molecular weight is increased. In the case of the 40,000 MW sample, 77% of the holes are associated with the chain ends. In the case of the 128,000 MW and 270,000 MW samples, 2% and 1% of the holes are associated with the chain ends respectively.

6-2.2 Comparison of Average Hole Sizes with Mineral Oil Domain Sizes

Table 6-3 shows how the size and number of mineral oil molecules vary with the mineral oil concentration in the 40,000 MW blends. The mineral oil domains were calculated from Goldman-Shen NMR experiments as discussed earlier. GC experiments showed that the mineral oil consisted primarily of C-28 to C-46 straight chain alkanes, with a nominal average of C-36. The volume of a C-36 alkane calculated using group contribution values is 605 cm^3/mol or 1 nm^3/molecule [1]. If one assumes spherical mineral oil domains, then the average diameter of a mineral oil molecule is 1.2 nm.

The Goldman-Shen technique measures the mobile mineral oil domain sizes. No mineral oil was detected at 4% mineral oil concentration. Thus it can be deduced that at 4% concentration, during antiplasticization, in addition to being intimately mixed with the polystyrene matrix, the mineral oil was immobile in the chain end holes. Table 6-3 shows that the average size of mobile mineral domain at 6% detemined by NMR was 0.2 nm. This represents the average of a distribution of domain sizes. At 6% mineral oil concentration, each mobile domain site represented less than 1% of a mineral oil molecule. As more mineral oil was blended into the polystyrene, phase separation, due to pooling of the mineral oil, occurred outside of the chain end resulting in a larger average domain size. This larger domain size is consistent with the earlier observations of higher T_1 values for the mineral oil, which reflected increased mobility of the mineral oil molecules at 8% concentration.

Arnould's and Laurence's work suggest that the effective volume of mineral oil may be less than calculated [2]. At 6 % mineral concentration no more than one mineral oil molecule was associated with each chain end.

Table 6-3. Effect of Mineral Oil Concentration on Mineral Oil Domain Sizes in 40,000 MW Polystyrene Blends

% Mineral Oil	Hole Diameter (nm)	Mineral Oil Domain (nm)	Number of MO Molecules
0	0.566	0	0
4	0.567	< 0.2	< 1
6	0.568	0.2	1
8	0.572	8.8	357

6-2.3 Interaction of Mineral Oil Molecules with Polymer Chain Ends

The question then becomes - How does the mineral oil molecule interact with the chain end hole? Obviously, the volume of the mineral oil molecule (1 nm^3) is much larger than the average size of the holes (0.095 nm^3) in the 40,000 MW sample. Bendler claimed that the average free volume of polystyrene chain ends is 0.08 nm^3 [3]. This is approximately 80% of the average size of the holes (0.095 nm^3) as determined from PAS experiments in this study. Earlier in this chapter, it was shown that 77% of the holes in the 40,000 MW sample are associated with the chain ends. It is reasonable to assume that the mineral oil molecule will enter the hole head first i.e. with the CH_3 end. The volume of a CH_3 unit is 22.8 cm^3/mole or 0.038 nm^3/ molecule, which results in a diameter of 0.42 nm [1]. Using the value of 80% of the average free volume of the holes (based on agreement with Bendler's data) gives a value of 0.076 nm^3, which corresponds to a diameter of 0.52 nm.

A comparison of the hole diameter of 0.52 nm with the diameter of a CH_3 unit (0.42 nm) suggests that each hole can accomodate the CH_3 end of a mineral oil chain . This supports the earlier deduction that each polymer chain end has one mineral oil molecule associated with it during antiplasticization (i.e. at concentrations of 6% mineral oil

and less). Arnould's and Laurence's work suggest that the effective volume of mineral oil may be less than calculated [2]. Conceivably, the chain end hole may be able to accomodate an additional mineral oil end through expansion. Since the polymer chain ends are relatively mobile compared to the polymer backbones, the chain end voids may fluctuate to fit additional mineral oil segments. The chain ends are then compressed into a smaller volume, which can result in greater densification of the polymer than expected. For example, it was reported previously, Figure 4-3, that the free volume decreased by 9% when 6% of mineral oil was added to the 40,000 MW polymer. The increased densification further restricts the mobility of the PS chain end, increases stiffness, and causes embrittlement.

The value of 0.42 nm for the diameter of the mineral oil head is also in agreement with Jackson's and Caldwell's conclusions [4,5]. They stated that one necessary characteristic of an antiplasticizer is that it should have one dimension less than 0.55 nm.

In the 270,000 MW sample only 1% percent of the holes are associated with the chain ends. This means that 99% of the holes are along the polymer backbone, which is relatively rigid compared to the mobile chain ends. The small concentration of holes at the chain ends is not enough to

effect any detectable or measurable antiplasticization. At low concentrations, any mineral oil entering the larger holes does not quite fill the holes. Blending additional mineral oil into the 270,000 MW sample results in pooling or clustering of the mineral oil, which is then observed as haziness or phase separation in the PS blend. In fact, this phase separation of the mineral oil has been observed to be as low as 1% by other researchers using NMR techniques with 300,000 MW polystyrene blends containing mineral oil [6].

6-3. Model for Antiplasticization

Figures 6-1a and 6-1b are schematics of amorphous polymers having very low and very high chain end concentrations respectively. These figures are adaptations of the Flory random coil model [7].

When a diluent is blended into a polymer, if the average size of the dispersed domains is less than or equal to the average diameter of the free volume voids, the diluent occupies position 1, that is, the diluent fills the smaller holes at the chain ends first. When larger quantities of diluent are added, the average domain size increases, and depending on the domain size, the diluent will occupy position 2 along the polymer backbone.

In a high molecular weight polystyrene sample (approximate Mn of 100,000 Daltons) as shown in Figure 6-1a, about 1% of the free volume holes are associated with the chain ends compared to a low molecular weight sample (Mn ≈ 1000 Daltons), shown in Figure 6-1b, where approximately 80% of the free volume holes are associated with the chain ends. Thus in the high molecular weight sample the effects of antiplasticization would not be measured. In the low molecular weight after the chain end holes are filled the effects of antiplasticization would be significant.

With a diluent such as mineral oil, the CH_3 head fills the hole at position 1. After the chain end holes are filled, as more mineral oil is added, clustering or pooling of the mineral oil occurs. The large difference (greater than 0.9 $(cal/cm^3)^{0.5}$) in solubility parameters, 7.6 $(cal/cm^3)^{0.5}$ versus 9.1 $(cal/cm^3)^{0.5}$ for mineral oil and polystyrene respectively, suggests stronger diluent-diluent attractive forces than polymer-diluent forces, leading to phase separation of the mineral oil [8]. Position 2 represents clustering of the diluent at high concentraions, where phase separation occurs.

In some polymers, such as polycarbonate, where there is significant main chain mobility, diluent occupation of position 2 may lead to antiplasticization. In fact,

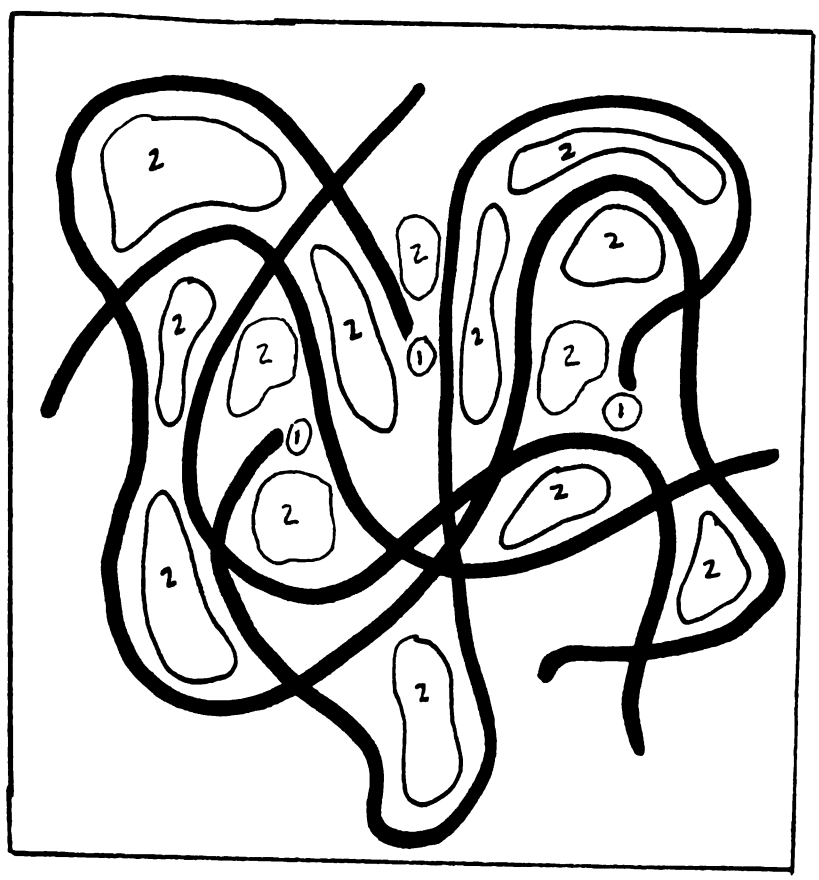

Figure 6-1a. Schematic of an Amorphous High Molecular Weight **Polymer/Diluent Blend**

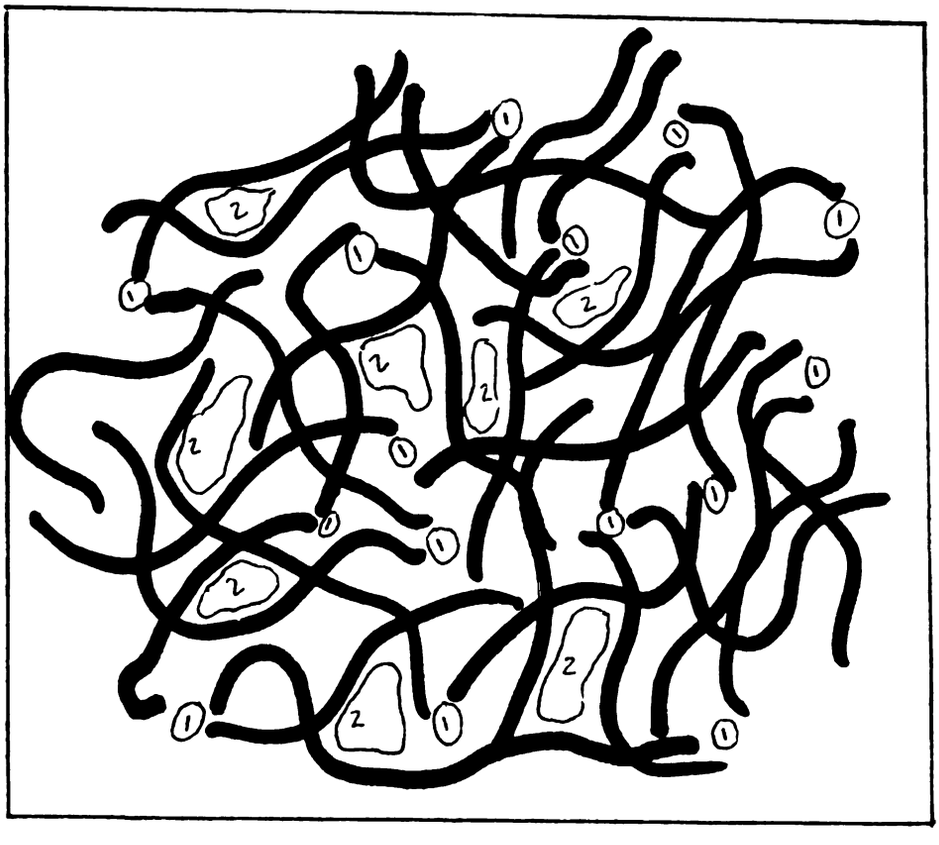

Figure 6-1b. Schematic of an Amorphous Low Molecular Weight Polymer/Diluent Blend

Cais et al. have observed antiplasticization in polycarbonate blends containing as much as 40 weight percent diluent [9]. They speculated that antiplasticization at these high diluent concentrations may be due to interaction between the diluent molecules and the polymer backbone. This interaction would in turn restrict mobility of the main chain segments.

6-4. Conclusions

A model has been proposed for antiplasticization in polystyrene. At low concentrations of mineral oil, when the mineral oil domains approximate the average polystyrene free volume hole diameters, antiplasticization is dominant. One mineral oil molecule is associated with each chain end during antiplasticization. At mineral oil concentrations above the solubility limit 6 %, the average mineral oil domain is 1 order of magnitude greater than the average hole size in polystyrene. This is due to clustering or pooling of the mineral oil, which leads to phase separation and eventual plasticization.

6-5. References

1. D.W. Van Krevelen and P.J. Hoftyzer, Properties of Polymers, Chapter 4, Elsevier, New York, 1976.

2. D. Arnould and R.L. Laurence, Industrial Engineering and Chemistry Research, 31, 218, 1992.

3. J.T. Bendler, Transitions and Relaxations, in Encyclopedia of Polymer Science and Engineering, Vol 17, Wiley, New York, 1989.

4. W.J. Jackson Jr., and J.R. Caldwell, J. Applied Polymer Science, 11, 211, 1967.

5. W.J. Jackson Jr. and J.R. Caldwell, J. Applied Polymer Science, 11, 227, 1967.

6. P.J. Smith and A.S. Ellaboudy, The Dow Chemical Company Personal Communication, 1992.

7. F.W. Billmeyer, Jr., Textbook of Polymer Chemistry, Interscience Publishers Ltd., New York, 1957.

8. E.A. Grulke, Solubility Parameter Values, in Polymer Handbook, Wiley, New York, 1989.

9. R.E. Cais, M. Nozomi, M. Kawai,and A. Miyaki, Macromolecules, 25, 4588, 1992.

CHAPTER 7

CONCLUSIONS AND PROPOSALS FOR FUTURE RESEARCH

7-1. Conclusions

Antiplasticization in polystyrene is molecular weight and diluent concentration dependent. The results support a hypothesis that the phenomenon can be attributed to a chain end effect. The PAS data showed a decrease in fractional free volume in antiplasticized blends. ^{13}C NMR experiments indicated that there was no change in the polymer backbone dynamics during antiplasticization. As seen from the ^{1}H NMR Goldman-Shen experiments, antiplasticization occurs when the average diameter of the mineral oil domains approximates the average size of the free volume voids. One mineral oil molecule was associated with each chain end during antiplasticization. At concentrations above the solubility limit of the mineral oil, where the mineral oil domain sizes are significantly larger than the average free volume hole diameter, phase separation occurs, and plasticization is dominant. The PAS and NMR results are consistent with the hypothesis that antiplasticization is due to a decrease in fractional free volume at the chain ends. This paper discussed the hole-filling mechanism of the diluent and proposed a model for antiplasticization. The diluent initially fills the smaller holes at the chain ends.

Mobility of the chain ends is restricted and thus result in higher moduli and strength, which is usually accompanied by embrittlement of the polymer.

The antiplasticization model could be used to specify and design appropriate plasticizers and/or antiplasticizers for polystyrene if the average free volume hole size relative to the size of the diluent molecule is known apriori. In other words, the behavior of polystyrene blend systems could be predicted. As aforementioned, if the average domain size of the dispersed diluent phase approximates the average free volume hole size, antiplasticization would be dominant. A good plasticizer would have domain sizes significantly larger than the average polystyrene hole size.

7-2. Proposals for Future Research

Additional research should be conducted to further study the chain end dynamics of polystyrene during antiplasticization. Low molecular weight (aproximately Mn = 1,000 to 10,000) polystyrene with a high concentration of chain ends could be synthesized with labelled chain ends using labelled initiators. The chain end dynamics could be then be studied via NMR techniques.

The effects of chain end chemical functionality should also be studied since this would affect the degree of interaction between the mineral oil molecule and the polystyrene chain end.

Finally, the effect of varying the chemical functionality along the polystyrene backbone e.g. use of copolymers such as styrene-acrylonitrile (SAN) or styrene-alkylstyrene copolymers should be studied.

CHAPTER 8

ADDENDUM: BEHAVIOR OF POLYSTYRENE BLENDS ABOVE Tg

8-1. Introduction

According to De Gennes, reptation of polymer chains above Tg is inversely proportional to the square of molecular weight. Theoretical analysis suggests that lower molecular weight polymers should relax at a faster rate than higher molecular weight polymers. It was wondered whether antiplasticization would have any effect on rheological properties above Tg. This chapter summarizes the rheological behavior of the blends above Tg.

8-2. Experimental Section

Torque data at different temperatures were collected for these materials after homogeneity was achieved in the HAAKE mixing bowl set at 50 rpm.

8-3. Results

Figures 8-1 to 8-3 show the Arrhenius plot of Ln torque versus reciprocal temperature for the different blends. As expected the 270,000 MW blends showed a decrease in torque with increasing mineral oil concentrations. However, it was rather surprising to discover what appeared to be antiplasticization of the 128,000 and the 40,000 MW

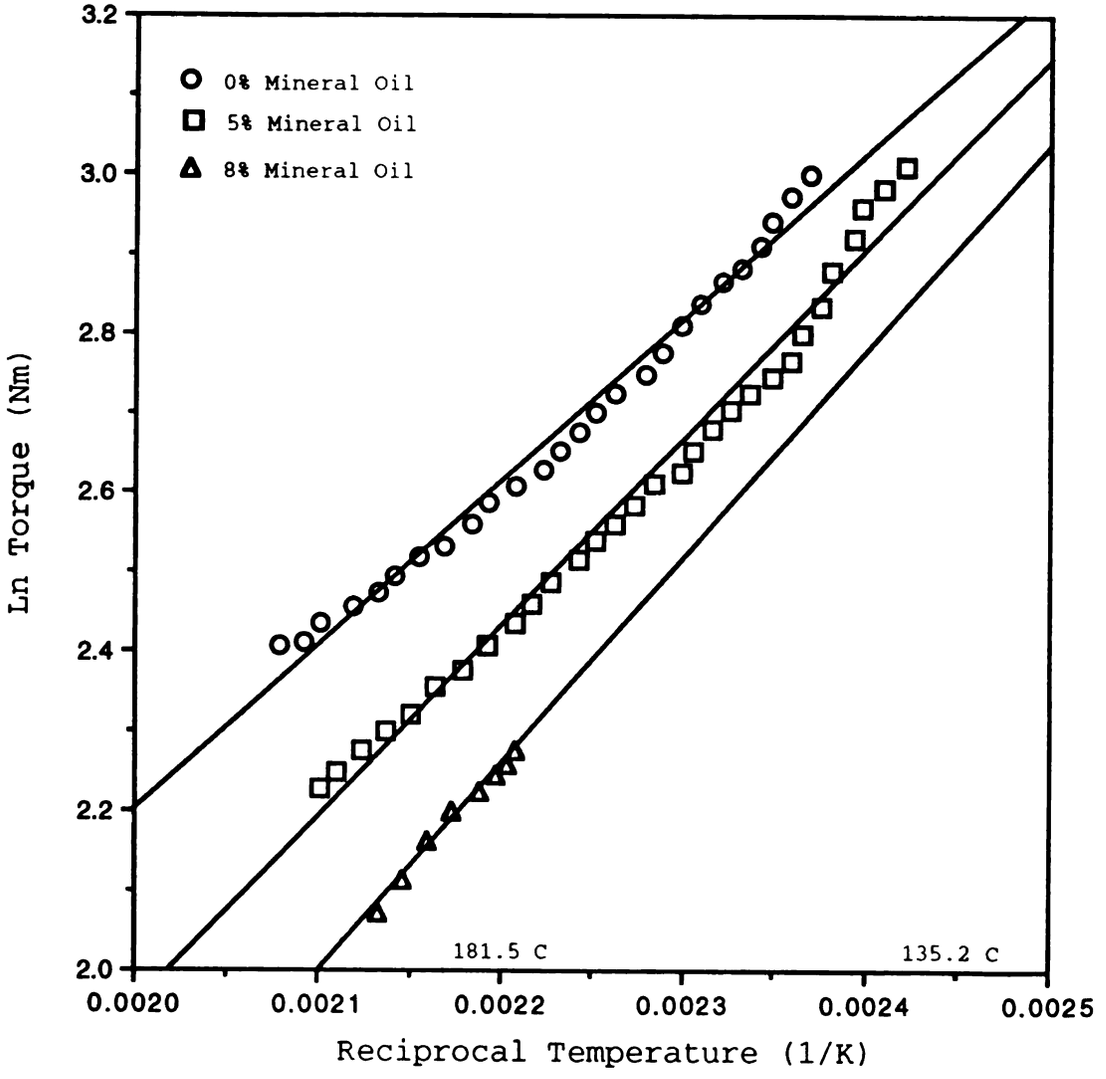

Figure 8-1. Effect of Mineral Oil Concentration on 270,000 MW Blends Above Tg

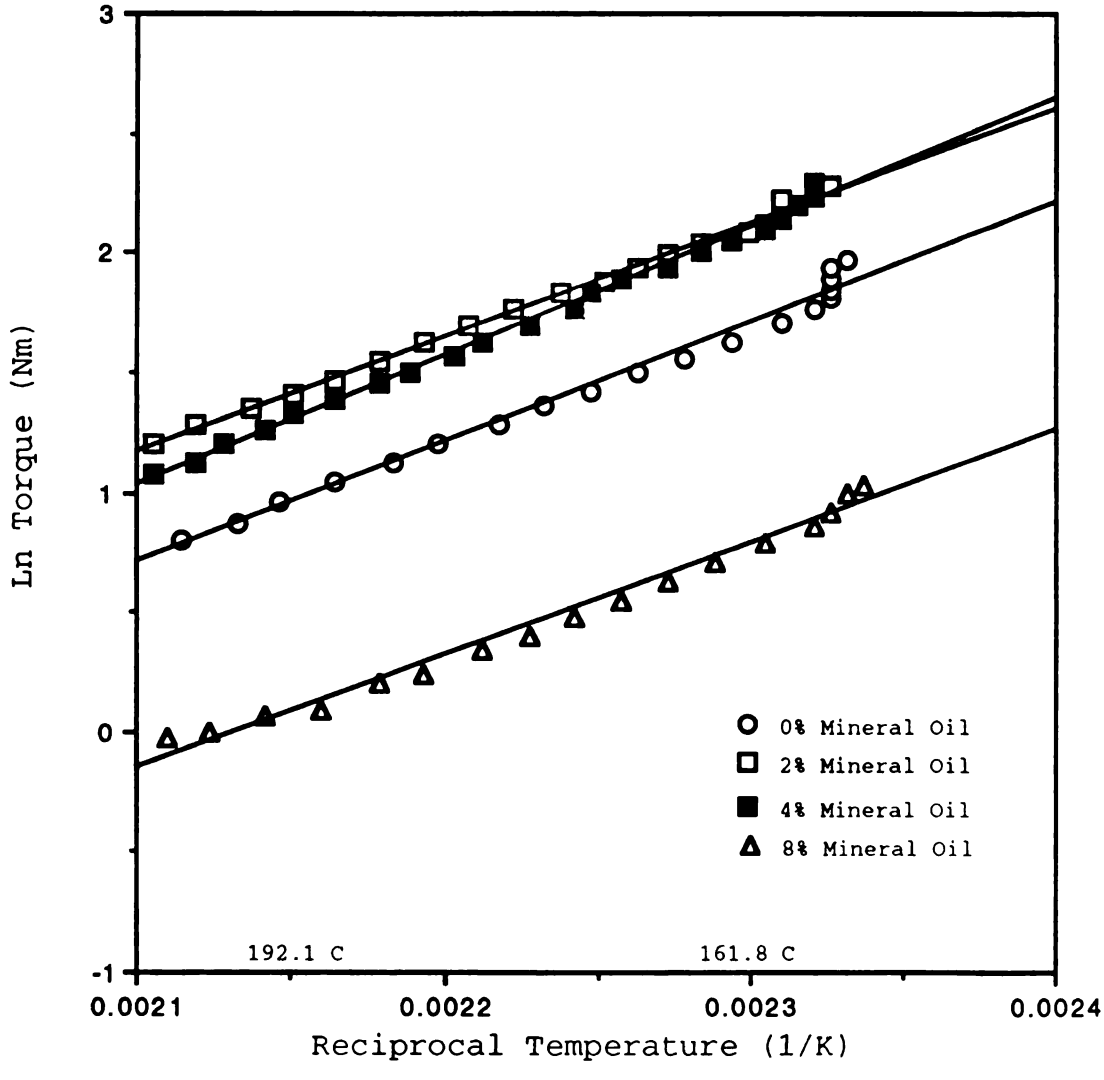

Figure 8-2. Effect of Mineral Oil Concentration on 128,000 MW Blends Above Tg

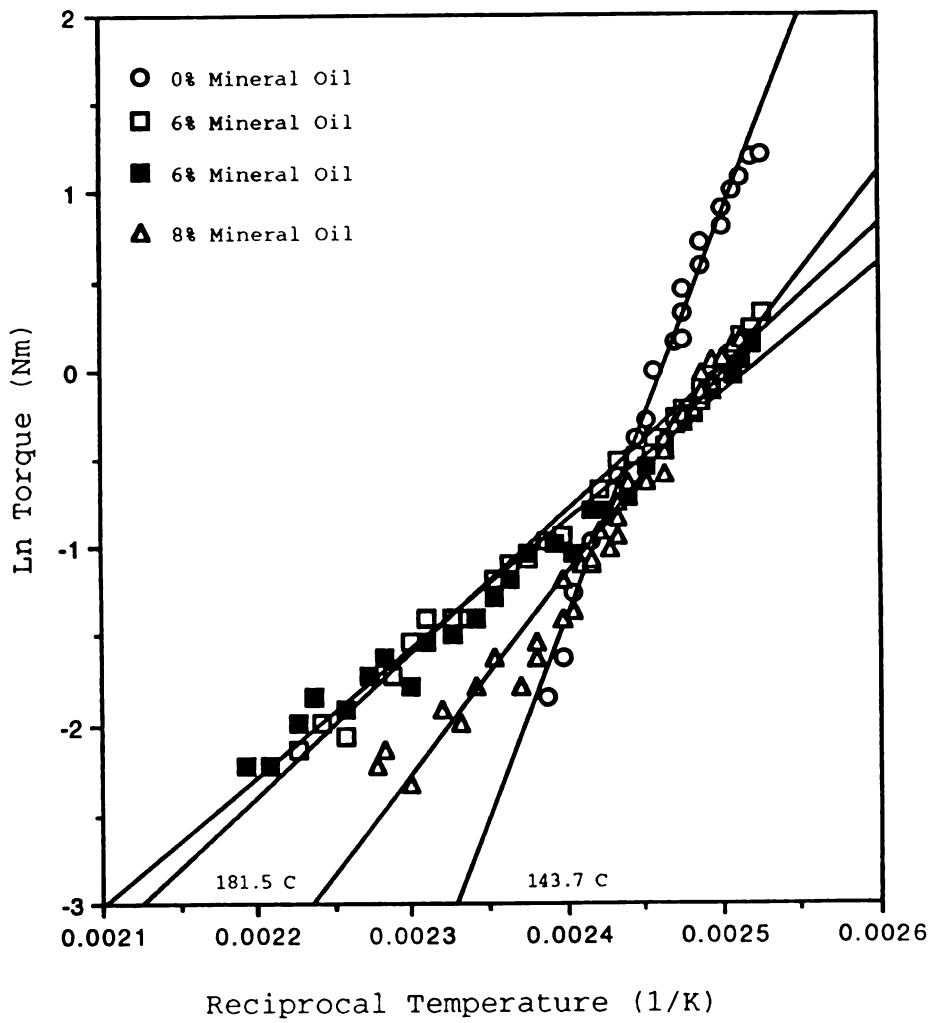

Figure 8-3. Effect of Mineral Oil Concentration on 40,000 MW Blends Above Tg

polystyrene blends even above Tg. With the 128,000 MW blends the torque increased up to 4% mineral oil and then decreased at higher concentrations. In the case of the 40,000 MW blends, between 140°C and 180°C the torque increased from 0% to 6% mineral oil and then decreased at 8%. Below 140°C, the phenomenon was reversed. This behavior was confirmed in duplicate experiments. Furthermore, Table 8-1 shows that the activation energies for the 128,000 MW and 40,000 MW molecular weight polystyrene samples were much higher than those typically observed for high molecular weight general purpose polystyrenes (Ea = 12 to 22 kJ/mole).

In studying the reptation of polymer chains above Tg, De Gennes found that the diffusion coefficient of a chain, D, is inversely proportional to the square of the molecular weight, M [1]:

$$D \alpha M^{-2} \qquad (8\text{-}1)$$

while the relaxation time, τ, is proportional to the cube of the molecular weight, M.

$$\tau \alpha M^{3} \qquad (8\text{-}2)$$

Doi and Edwards extended this theoretical work to study the mechanical properties of reptating chains and related viscosity, η, to molecular weight as follows [2].

Table 8-1. Activation Energies for the Polystyrene Blends

Molecular Weight	Mineral Oil (Vol %)	Activation Energy (KJ/mole)
270,000	0	17
	6	20
	8	22
128,000	0	42
	2	40
	4	45
	8	39
40,000	0	188
	6	60
	6	67
	8	94

$$\eta \alpha M^3 \qquad (8\text{-}3)$$

De Gennes described reptation using the tube model in the following way - as the polymer reptates, the chain ends are the first to leave the tube-like confinement and assumes new confirmations, while the rest of the polymer backbone remains in a confined state. As the chain moves, the other parts of the chain become unrestricted. This suggests that lower molecular weight polymers should relax at a faster rate than higher molecular weight polymers. Perhaps, the same argument could be used to explain antiplasticization of the 40,000 and 128,000 MW above and below Tg. In both temperature regimes, shorter chain lengths would exhibit higher frequency motions. It is hypothesized that antiplasticization is manifested therefore by a slowing down of these faster motions above Tg.

8-3. Conclusions

Antiplasticization above Tg, manifested by an increase in torque, was evident in the 128,000 MW and 40,000 MW blends containing less than 6% mineral oil. This is the first published report of antiplasticization in polymer blends above Tg.

As mentioned earlier, research has shown that antiplasticization affects the higher frequency motions in glassy polymers. Possibly, the same argument applies in

polymers above Tg. In both temperature regimes, shorter chain lengths would exhibit higher frequency motions. Antiplasticization is manifested by a slowing down of these faster motions. Like the glassy state, measurable antiplasticization possibly occurs only above a critical concentration of chain ends.

8-4. References

1. P.J. De Gennes, J. Chem. Phys., 55, 572, 1971.

2. M. Doi and S.F. Edwards, The Theory of Polymer Dynamics, International Series of Monographs on Physics - 73, Oxford University Press, New York, 1989.

APPENDICES

APPENDIX A

MOLECULAR WEIGHT DISTRIBUTIONS

Appendix A-1. Molecular Weight Distribution of 40,000 MW Polystyrene

HP 1090A GPC SYSTEM
438 BLDG MIDLAND
LAB 104 HP85B #1

SAMPLE : ANDERSON PS45K
CONCENTRATION = 0.25%
SOLVENT = THF
DATE = MAR/26/1991
TIME = 11:48:56
GPCDATA FILE = GPC1101001:D701
VIAL# = 11
INJECTION# = 1

CALIBRATION

CALIB.DATE	=	03-18-91
STANDARD NAME	=	1683
CURVE TYPE	=	a*x^3+b*x^2+c*x+d
COEFFICIENT a	=	0.00000E+000
COEFFICIENT b	=	0.00000E+000
COEFFICIENT c	=	-.49067E+000
COEFFICIENT d	=	1.10089E+001
LOG(ALPHA)	=	3.02038E-001
BETA	=	9.41406E-001
RT-ISTD/CAL	=	17.896

NUMERIC PARAMETERS

PNTS SELECTED		AUTOMATICALLY	
NOISE WINDOW	=	3.00 TO=	6.00 min
POLYMER WINDOW	=	9.20 TO=	17.60 min
BASELINE FROM	=	10.63 TO=	17.63 min
SUMMATION WIND.	=	10.68 TO=	17.61 min
RT-ISTD	=	17.775	

****
WARNING(S)! SEE CRI SMP 86-60
STOP PT: 10,11,12
OTHERS: 21
CHROMATOGRAPHY: 33
****

RESULTS

Mn	=	652	
Mw	=	42980	
Mz	=	169600	
Mp	=	88980	745
POLYDISPERSITY	=	65.898	
SUBRATIO 1	=	0.000E+000	(Mwt: 0:0)
SUBRATIO 2	=	7.886E+001	(Mwt: 99920;STOPMWT)
SUBRATIO 3	=	6.254E+001	(Mwt: 24840;STOPMWT)

CHROMATOGRAM
full scale = 53.103 [mV]

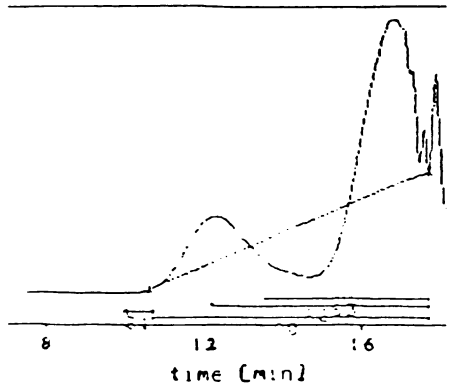

SAMPLE : ANDERSON PS4SK

CONCENTRATION	=	0.25%
SOLVENT	=	THF
DATE	=	MAR/26/1991
TIME	=	13:10:50
GPCDATA FILE	=	GPC1101002:D701
VIAL#	=	11
INJECTION#	=	1

CALIBRATION

CALIB.DATE	=	03-18-91
STANDARD NAME	=	1683
CURVE TYPE	=	a*x^3+b*x^2+c*x+d
COEFFICIENT a	=	0.00000E+000
COEFFICIENT b	=	0.00000E+000
COEFFICIENT c	=	-.49067E+000
COEFFICIENT d	=	1.10089E+001
LOG(ALPHA)	=	3.02038E-001
BETA	=	9.41406E-001
RT-ISTD/CAL	=	17.896

NUMERIC PARAMETERS

PNTS SELECTED		AUTOMATICALLY	
NOISE WINDOW	=	3.00 TO=	6.00 min
POLYMER WINDOW	=	8.20 TO=	15.60 min
BASELINE FROM	=	10.28 TO=	14.78 min
SUMMATION WIND.	=	10.33 TO=	14.76 min
RT-ISTD	=	17.783	

****

WARNING(S)! SEE CRI SMP 86-60

CHROMATOGRAPHY: 33

****

RESULTS

Mn	=	56970	
Mw	=	103900	
Mz	=	164700	
Mp	=	87930	
POLYDISPERSITY	=	1.824	
SUBRATIO 1	=	0.000E+000	(Mwt: 0;0)
SUBRATIO 2	=	6.002E+001	(Mwt: 100500;STOPMWT)
SUBRATIO 3	=	8.328E+000	(Mwt: 25000;STOPMWT)

CHROMATOGRAM

full scale = 52.896 [mV]

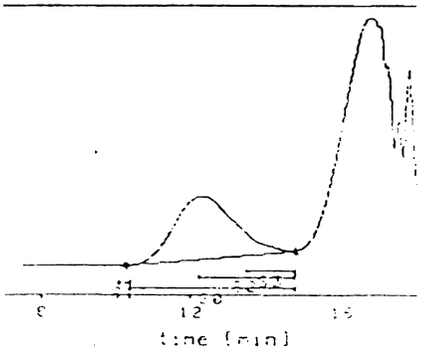

HP 1090A GPC SYSTEM
438 BLDG MIDLAND
LAB 104 HP85B #1

SAMPLE : ANDERSON PS4SK
CONCENTRATION = 0.25%
SOLVENT = THF
DATE = MAR/26/1991
TIME = 13:10:50
GPCDATA FILE = GPC1101002:D701
VIAL# = 11
INJECTION# = 1

CALIBRATION
CALIB.DATE = 03-18-91
STANDARD NAME = 1683
CURVE TYPE = a*x^3+b*x^2+c*x+d
COEFFICIENT a = 0.00000E+000
COEFFICIENT b = 0.00000E+000
COEFFICIENT c = -.49067E+000
COEFFICIENT d = 1.10089E+001
LOG(ALPHA) = 3.02038E-001
BETA = 9.41406E-001
RT-ISTD/CAL = 17.896

NUMERIC PARAMETERS
PNTS SELECTED AUTOMATICALLY
NOISE WINDOW = 3.00 TO= 6.00 min
POLYMER WINDOW = 14.75 TO= 17.55 min
BASELINE FROM = 15.05 TO= 17.42 min
SUMMATION WIND. = 15.09 TO= 17.39 min
RT-ISTD = 17.783
WARNING(S)! SEE CRI SMP 86-60
START PT: 3
STOP PT: 10,12
CHROMATOGRAPHY: 33

RESULTS
Mn = 850
Mw = 1058
Mz = 1343
Mp = 751
POLYDISPERSITY = 1.245
SUBRATIO 1 = 0.000E+000 (Mwt: 0;0)
SUBRATIO 2 = 2.105E+002 (Mwt: 100500;STOPMWT)
SUBRATIO 3 = 1.254E+002 (Mwt: 25000;STOPMWT)

CHROMATOGRAM
full scale = 52.896 [mV]

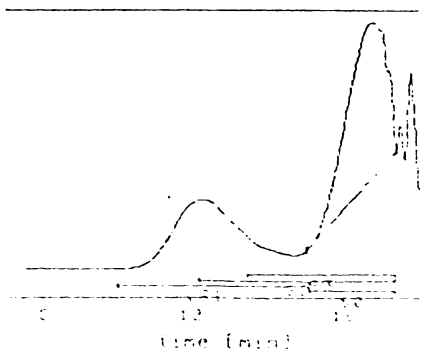

Appendix A-2. Molecular Weight Distribution of 128,000 MW Polystyrene

SAMPLE : DALKE 135K

CONCENTRATION	=	0.25%
SOLVENT	=	THF
DATE	=	OCT/24/1991
TIME	=	14:53:35
GPCDATA FILE	=	GPC1701000:D701
VIAL#	=	17
INJECTION#	=	1

CALIBRATION

CALIB.DATE	=	10-09-91
STANDARD NAME	=	1683
CURVE TYPE	=	a*x^3+b*x^2+c*x+d
COEFFICIENT a	=	0.00000E+000
COEFFICIENT b	=	0.00000E+000
COEFFICIENT c	=	-.49062E+000
COEFFICIENT d	=	1.10253E+001
LOG(ALPHA)	=	2.23056E-001
BETA	=	9.49219E-001
RT-ISTD/CAL	=	17.781

NUMERIC PARAMETERS

PNTS SELECTED		AUTOMATICALLY		
NOISE WINDOW	=	3.00	TO=	6.00 min
POLYMER WINDOW	=	8.20	TO=	17.50 min
BASELINE FROM	=	9.82	TO=	16.53 min
SUMMATION WIND.	=	9.86	TO=	16.51 min
RT-ISTD	=	17.799		

RESULTS

Mn	=	58420	
Mw	=	127900	
Mz	=	216400	
Mp	=	109300	
POLYDISPERSITY	=	2.190	
SUBRATIO 1	=	8.865E-003	(Mwt: STARTMWT;1006000)
SUBRATIO 2	=	5.097E+001	(Mwt: 100800;STOPMWT)
SUBRATIO 3	=	7.279E+000	(Mwt: 25090;STOPMWT)

CHROMATOGRAM

full scale = 35.717 [mV]

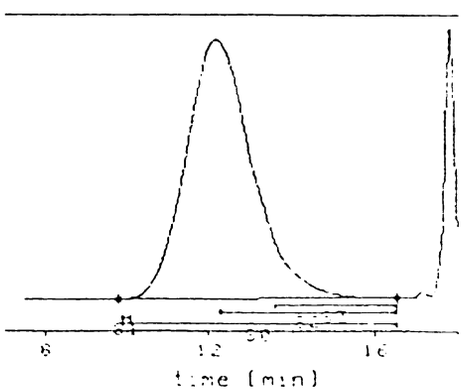

Appendix A-3. Molecular Weight Distribution of 270,000 MW Polystyrene

G P C R E P O R T

HP 1090A GPC SYSTEM
438 BLDG MIDLAND
LAB 104 HP85B #1

SAMPLE : ANDERSON PS 270K

CONCENTRATION	=	0.25%
SOLVENT	=	THF
DATE	=	MAR/26/1991
TIME	=	11:17:57
GPCDATA FILE	=	GPC1001001:D701
VIAL#	=	10
INJECTION#	=	1

CALIBRATION

CALIB.DATE	=	03-18-91
STANDARD NAME	=	1683
CURVE TYPE	=	a*x^3+b*x^2+c*x+d
COEFFICIENT a	=	0.00000E+000
COEFFICIENT b	=	0.00000E+000
COEFFICIENT c	=	-.49067E+000
COEFFICIENT d	=	1.10089E+001
LOG(ALPHA)	=	3.02038E-001
BETA	=	9.41406E-001
RT-ISTD/CAL	=	17.896

NUMERIC PARAMETERS

PNTS SELECTED		AUTOMATICALLY		
NOISE WINDOW	=	3.00	TO=	6.00 min
POLYMER WINDOW	=	8.20	TO=	17.60 min
BASELINE FROM	=	9.38	TO=	16.57 min
SUMMATION WIND.	=	9.43	TO=	16.54 min
RT-ISTD	=	17.763		

RESULTS

Mn	=	111700	
Mw	=	274400	
Mz	=	448100	
Mp	=	244200	
POLYDISPERSITY	=	2.455	
SUBRATIO 1	=	1.097E+000	(Mwt: STARTMWT;992400)
SUBRATIO 2	=	2.092E+001	(Mwt: 100900;STOPMWT)
SUBRATIO 3	=	2.595E+000	(Mwt: 25050;STOPMWT)

CHROMATOGRAM

full scale = 38.135 [mV]

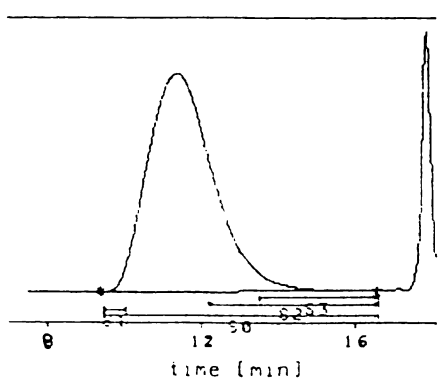

APPENDIX B

GC DETERMINATION OF MINERAL OIL CONCENTRATIONS

Appendix B-1. Nominal and Actual Mineral Oil Concentrations

Nominal wt%	Actual wt%	Actual vol%
0	0.05	0.06
2.5	3.11	3.93
5.0	4.8	6.17
7.5	6.1	7.95
10.0	6.72	8.81

Appendix B-2. GC Analysis of Mineral Oil in 40,000 MW Blends

```
SAMPLE NAME?11

START PENDING
RUN #  488      AUG 14, 1991  12:35:22
START
```

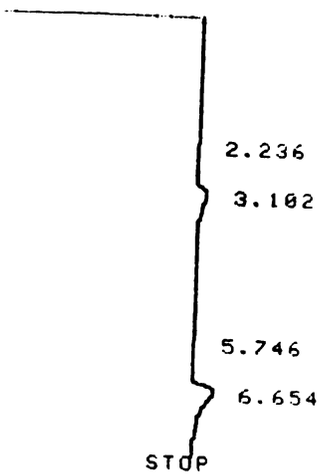


```
RUN#   488              AUG 14, 1991  12:35:22

METHOD NAME: M:MINOIL.MET

AREA%
      RT       AREA TYPE  WIDTH      AREA%
   2.236      38964   PV    .257    4.63656
   3.102     233342   PV    .378   27.76674
   5.746      42503   PV    .249    5.05768
   6.654     525556   VV    .443   62.53902

TOTAL AREA= 840365
MUL FACTOR=1.0000E+00


SAMPLE:11
PEAK NUMBERS?1,3
  WT POLYMER IN MG?200.0
MINERAL OIL= 0.05
MINERAL OIL= 0.05 %
MO1= 0.05 RT1+ 2.236
MO2= 0.05 RT2=
MO2= 0.05 RT2= 5.746
```

```
SAMPLE NAME?20

START PENDING
RUN #  492      AUG 14, 1991  13:12:56
START
```

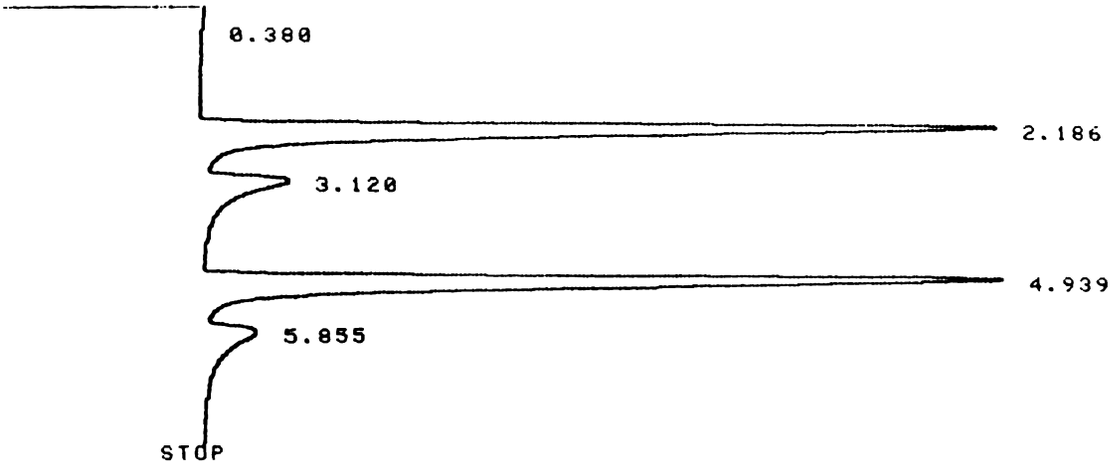


```
RUN#   492          AUG 14, 1991  13:12:56

METHOD NAME: M:MINOIL.MET

AREA%
      RT       AREA TYPE  WIDTH      AREA%
    .380      51574   PV   .328      .21701
   2.186   10407384   PB   .248    43.79094
   3.120    1725513   BP   .405     7.26041
   4.939   10383976   PB   .246    43.69245
   5.855    1197627   BP   .471     5.03923

TOTAL AREA=2.3766E+07
MUL FACTOR=1.0000E+00


SAMPLE:20
PEAK NUMBERS?2,4
  WT POLYMER IN MG?200.7
MINERAL OIL= 3.11
MINERAL OIL= 3.11 %
MO1= 3.11 RT1+ 2.186
MO2= 3.11 RT2=
MO2= 3.11 RT2= 4.939


SAMPLE NAME?STOP

DONE       AUG 14, 1991  13:21:51
```

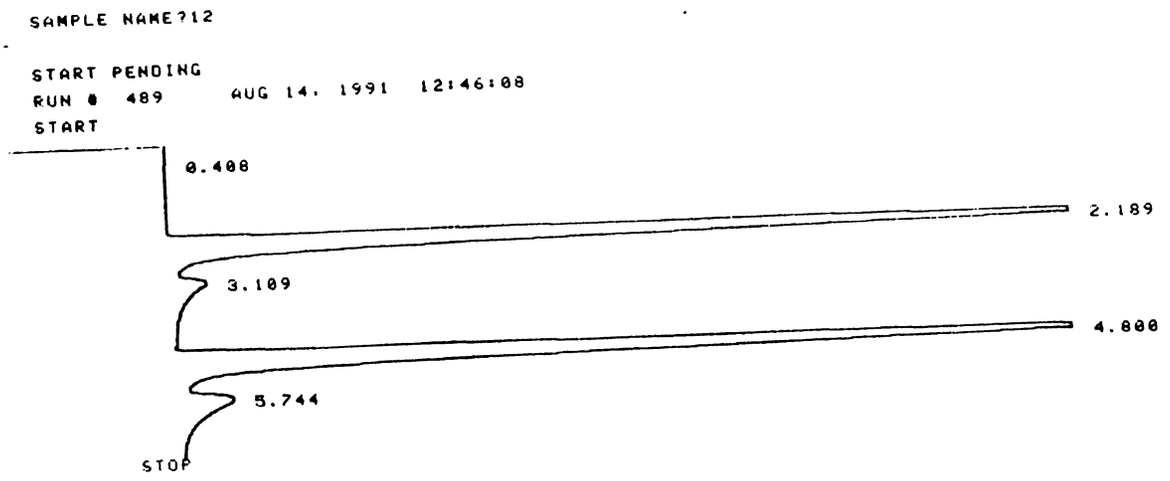

RUN# 489 AUG 14, 1991 12:46:08

METHOD NAME: M:MINOIL.MET

AREA%

RT	AREA	TYPE	WIDTH	AREA%
.408	24052	BV	.254	.06052
2.189	18310832	SHB	.280	46.07603
3.109	810558	TBB	.414	2.03963
4.800	19022528	ISBH	.291	47.86690
5.744	1572496	TBV	.489	3.95692

TOTAL AREA=3.9740E+07
MUL FACTOR=1.0000E+00

SAMPLE:12
PEAK NUMBERS?2,4
WT POLYMER IN MG?199.7
MINERAL OIL= 4.8
MINERAL OIL= 4.8 %
MO1= 4.74 RT1= 2.189
MO2= 4.87 RT2=
MO2= 4.87 RT2= 4.8

```
SAMPLE NAME?19

START PENDING
RUN #  491      AUG 14, 1991  13:04:57
START
```

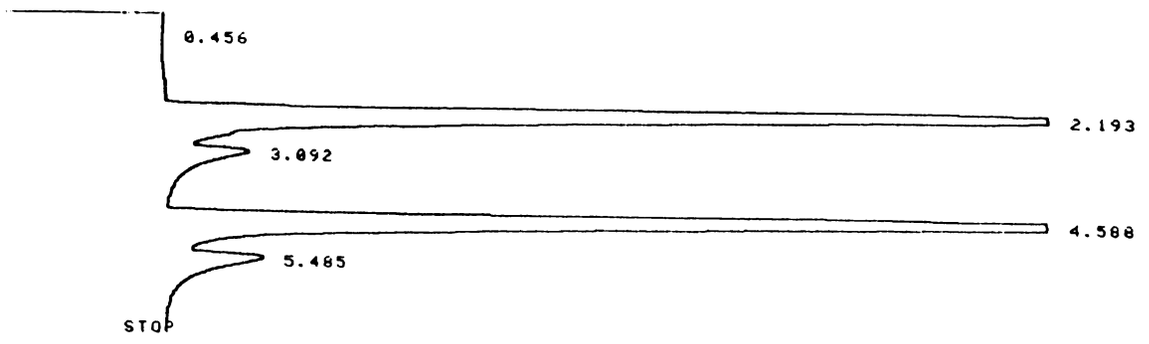


```
RUN#   491          AUG 14, 1991  13:04:57

METHOD NAME: M:MINOIL.MET

AREA%
      RT       AREA TYPE  WIDTH      AREA%
    .456      30361   PV   .198      .05527
   2.193   26033520  SHH   .335    47.39093
   3.092    1313661  TBP   .330     2.39136
   4.588   25659248 ISHH   .322    46.70962
   5.485    1896769  TBB   .364     3.45284

TOTAL AREA=5.4934E+07
MUL FACTOR=1.0000E+00


SAMPLE:19
PEAK NUMBERS?2,4
  WT POLYMER IN MG?199.8
MINERAL OIL= 6.1
MINERAL OIL= 6.1 %
MO1= 6.13 RT1= 2.193
MO2= 6.07 RT2=
MO2= 6.07 RT2= 4.588
```

```
SAMPLE NAME?5

START PENDING
RUN #  481      AUG 14, 1991  11:24:53
START
```

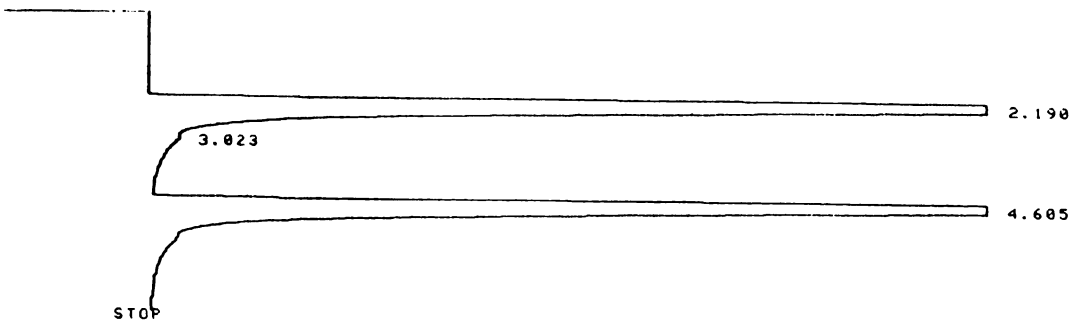


```
RUN#   481          AUG 14, 1991  11:24:53

METHOD NAME: M:MINOIL.MET

AREA%
      RT       AREA TYPE  WIDTH      AREA%
   2.190   29488320  SPH    .327   49.86403
   3.023      40062  TBB    .200     .06774
   4.605   29609088 ISHH    .324   50.06824

TOTAL AREA=5.9137E+07
MUL FACTOR=1.0000E+00


SAMPLE:5
PEAK NUMBERS?1,3
  WT POLYMER IN MG?200.0
MINERAL OIL= 6.72
MINERAL OIL= 6.72 %
MO1= 6.71 RT1= 2.19
MO2= 6.73 RT2=
MO2= 6.73 RT2= 4.605
```

Appendix B-3. Nominal and Actual Mineral Oil Concentrations in 40,000 PAS Samples

Nominal wt%	Actual wt%	Actual vol%
0	0	0
2.5	2.41	2.93
5	5.05	6.11
7.5	7.67	8.04
10	8.63	10.36

Appendix B-4. GC Analysis of Mineral Oil in 40,000 MW PAS Blends

Graft Analysis Sat Nov 23 08:51:57 1991 Page -1-

External Standard Report

Data File Name : C:\HPCHEM\1\DATA\003-0101.D
Operator : PHIL KUCH
Acquired on : Sat Nov 23 08:47:40 1991
Sample Name : 0% MO
Run Time Bar Code:
Instrument Method: MINOIL.M
Analysis Method : MINOIL.M
Multiplier : 1
Last Recalib : 03 Oct 91 11:08 AM
ANDERSON

Instrument : HP35900C
Vial Number : 3
Injection Number: 1
Sequence Line : 1
Sample Amount : 0

ADC CHANNEL A

Ret Time	Area	Type	Width	Ref#	PERCENT	Name
2.149	* not found *			1-R		MINERAL OIL

Time Reference Peak	Expected RT	Actual RT	Difference
1	2.149	* not found *	

Could not find time reference peak:
No peak of Number 1's description at 2.149 + 0.107 - 0.107 min.
Not all time reference peaks were found

Area Percent Report

ADC CHANNEL A

Pk#	Ret Time	Area	Height	Type	Width	Area %

Total amount = 0

Graft Analysis Sat Nov 23 08:51:57 1991 Page -2-

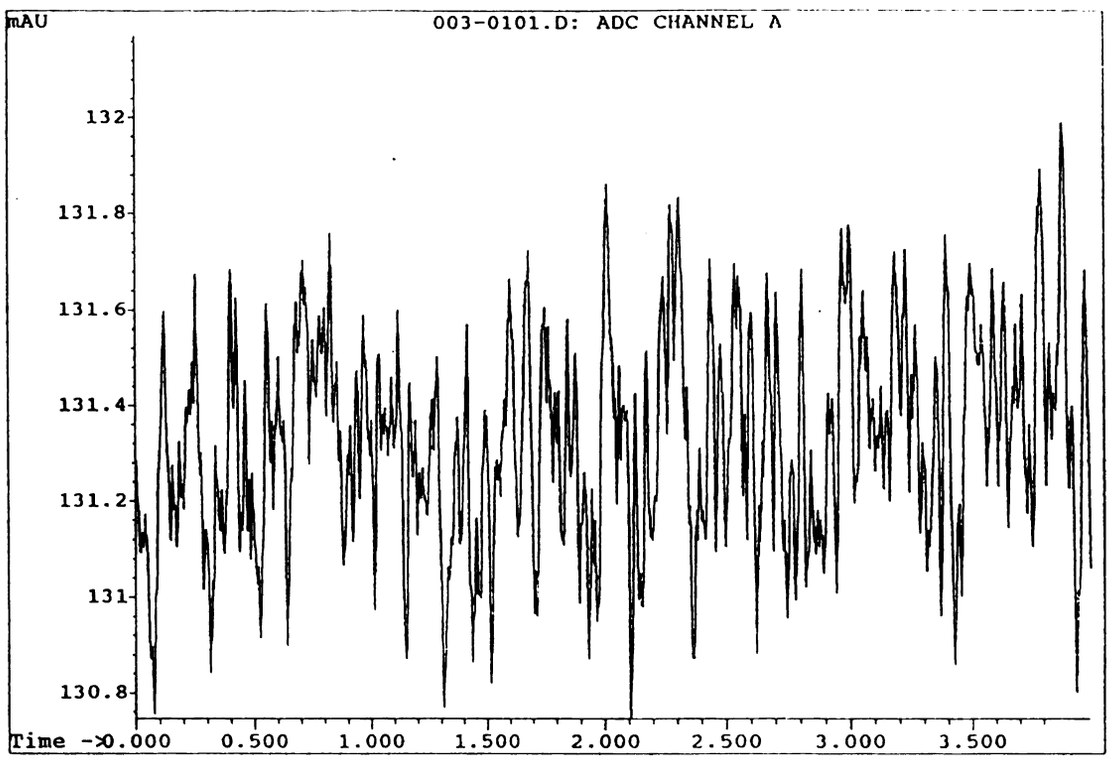

External Standard Report

Data File Name : C:\HPCHEM\1\DATA\005-0101.D
Operator : PHIL KUCH
Acquired on : Sat Nov 23 08:58:43 1991
Sample Name : 2.5% MO
Run Time Bar Code:
Instrument Method: MINOIL.M
Analysis Method : MINOIL.M
Multiplier : 1
Last Recalib : 03 Oct 91 11:08 AM
ANDERSON

Instrument : HP35900C
Vial Number : 5
Injection Number: 1
Sequence Line : 1
Sample Amount : 0

ADC CHANNEL A

Ret Time	Area	Type	Width	Ref#	PERCENT	Name
2.207	5986.388	BB	0.198	1-R	2.405	MINERAL OIL

Time Reference Peak	Expected RT	Actual RT	Difference
1	2.149	2.207	2.7%

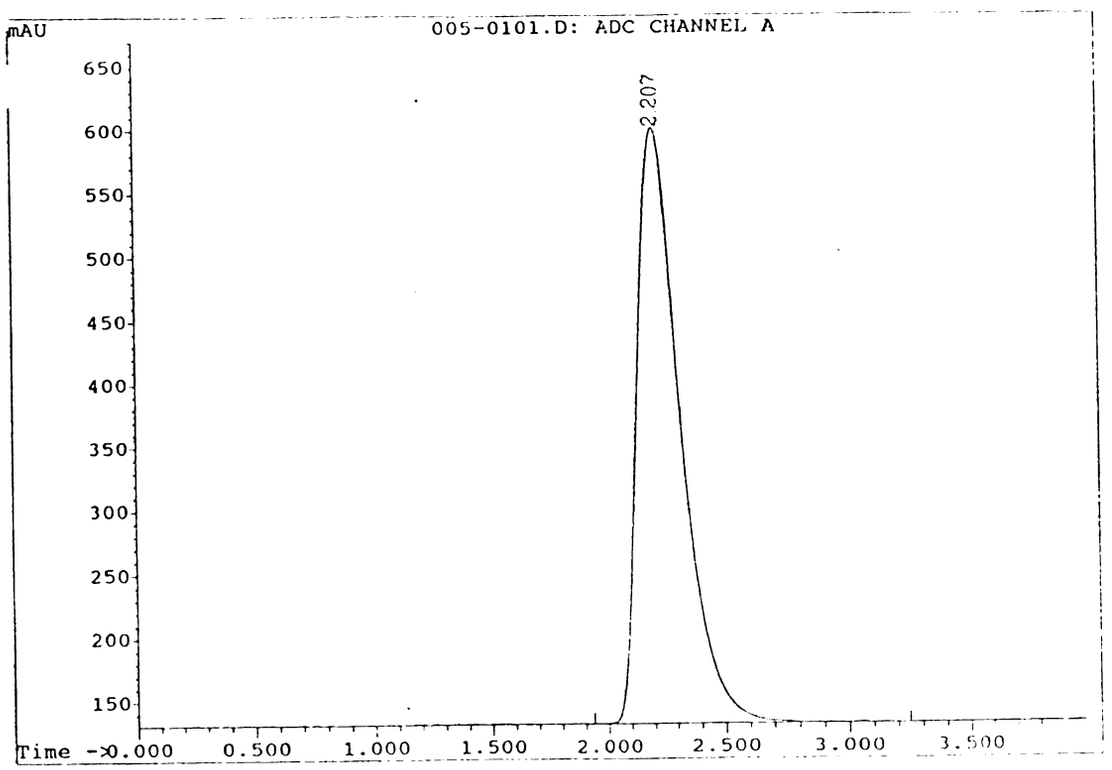

Graft Analysis Sat Nov 23 09:14:04 1991 Page -1-

External Standard Report

Data File Name : C:\HPCHEM\1\DATA\007-0101.D
Operator : PHIL KUCH
Acquired on : Sat Nov 23 09:09:46 1991
Sample Name : 5% MO
Run Time Bar Code:
Instrument Method: MINOIL.M
Analysis Method : MINOIL.M
Multiplier : 1
Last Recalib : 03 Oct 91 11:08 AM
ANDERSON

Instrument : HP35900C
Vial Number : 7
Injection Number: 1
Sequence Line : 1
Sample Amount : 0

ADC CHANNEL A

Ret Time	Area	Type	Width	Ref#	PERCENT	Name
2.211	13640.359	BB	0.227	1-R	5.053	MINERAL OIL

Time Reference Peak	Expected RT	Actual RT	Difference
1	2.149	2.211	2.9%

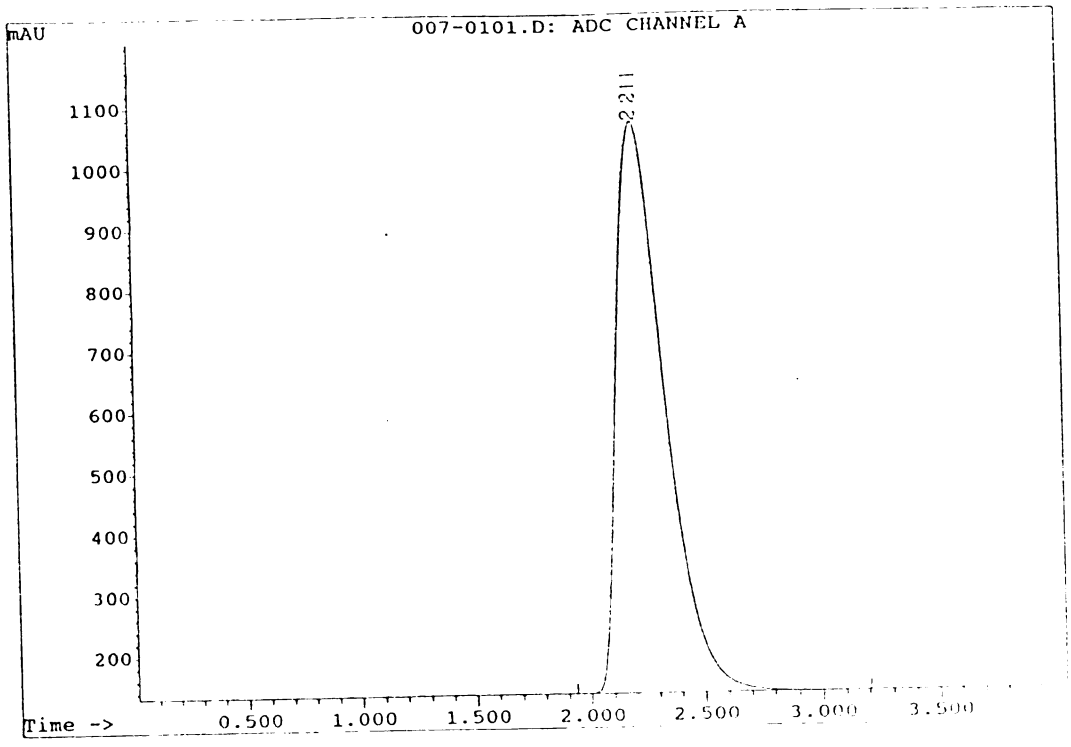

Graft Analysis Sat Nov 23 09:25:08 1991 Page -1-

External Standard Report

Data File Name : C:\HPCHEM\1\DATA\009-0101.D
Operator : PHIL KUCH
Acquired on : Sat Nov 23 09:20:48 1991
Sample Name : 7.5% MO
Run Time Bar Code:
Instrument Method: MINOIL.M
Analysis Method : MINOIL.M
Multiplier : 1
Last Recalib : 03 Oct 91 11:08 AM
ANDERSON

Instrument : HP35900C
Vial Number : 9
Injection Number: 1
Sequence Line : 1
Sample Amount : 0

ADC CHANNEL A

Ret Time	Area	Type	Width	Ref#	PERCENT	Name
2.215	18318.580	BV	0.246	1-R	6.672	MINERAL OIL

Time Reference Peak	Expected RT	Actual RT	Difference
1	2.149	2.215	3.1%

Graft Analysis Sat Nov 23 09:25:08 1991 Page -2-

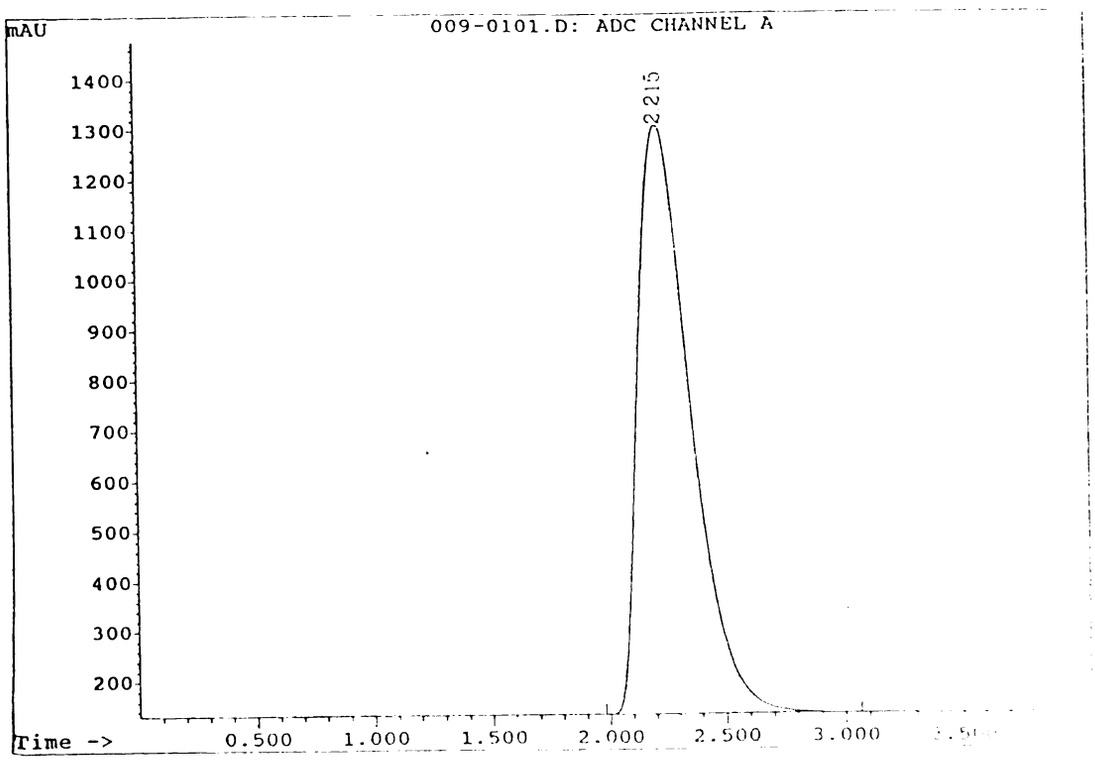

Graft Analysis Sat Nov 23 09:36:14 1991 Page -1-

External Standard Report

Data File Name : C:\HPCHEM\1\DATA\011-0101.D
Operator : PHIL KUCH
Acquired on : Sat Nov 23 09:31:54 1991
Sample Name : 10% MO
Run Time Bar Code:
Instrument Method: MINOIL.M
Analysis Method : MINOIL.M
Multiplier : 1
Last Recalib : 03 Oct 91 11:08 AM
ANDERSON

Instrument : HP35900C
Vial Number : 11
Injection Number: 1
Sequence Line : 1
Sample Amount : 0

ADC CHANNEL A

Ret Time	Area	Type	Width	Ref#	PERCENT	Name
2.218	23983.946	BV	0.262	1-R	8.633	MINERAL OIL

Time Reference Peak	Expected RT	Actual RT	Difference
1	2.149	2.218	3.2%

Graft Analysis Sat Nov 23 09:36:14 1991 Page -2-

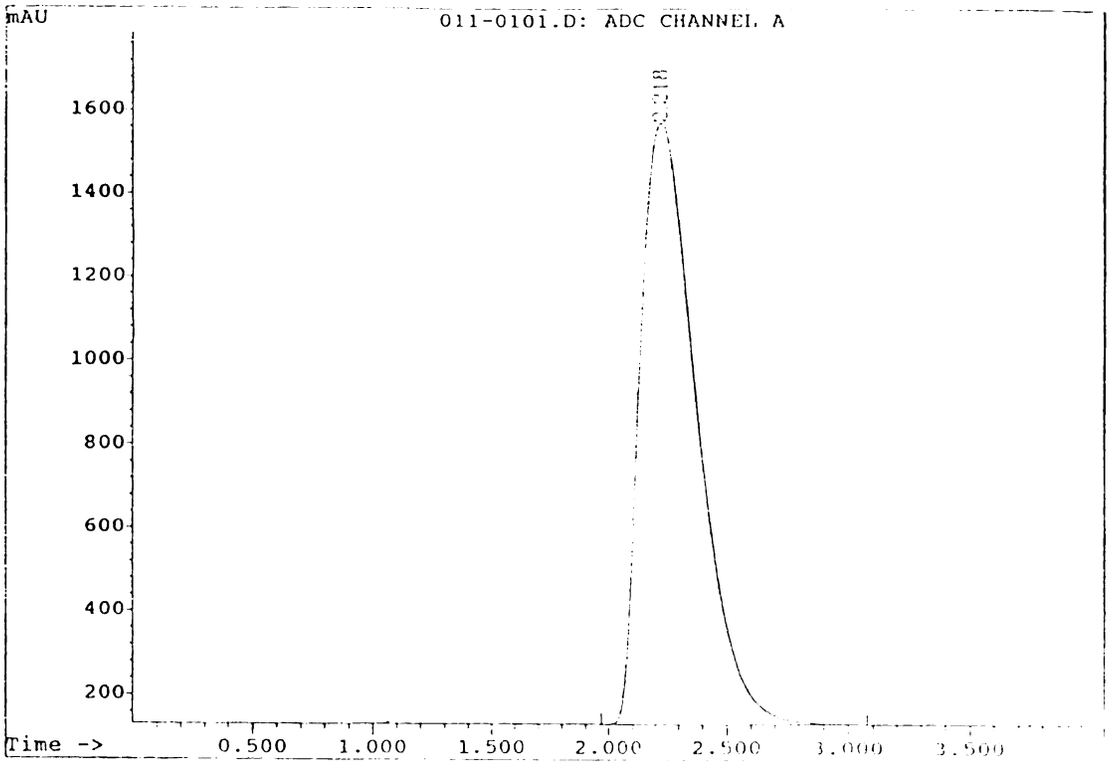

Appendix B-5. Nominal and Actual Mineral Concentrations in 128,000 MW Blends

Nominal wt%	Actual wt%	Actual vol%
0	0	0
2.5	1.92	2.3
5	2.98	3.56
7.5	2.9	3.46
10	7.84	9.26

Appendix B-6. GC Analysis of Mineral Oil in 128,000 MW Blends

External Standard Report

Data File Name : C:\HPCHEM\1\DATA\001-0101.D
Operator : PHIL KUCH
Acquired on : Sat Feb 08 09:17:27 1992
Sample Name : 0% min oil
Run Time Bar Code:
Instrument Method: MINOIL.M
Analysis Method : MINOIL.M
Multiplier : 1
Last Recalib : 03 Oct 91 11:08 AM

Instrument : HP35900C
Vial Number : 1
Injection Number: 1
Sequence Line : 1
Sample Amount : 0

ADC CHANNEL A

Ret Time	Area	Type	Width	Ref#	PERCENT	Name
2.149	* not found *			1-R		MINERAL OIL

Time Reference Peak	Expected RT	Actual RT	Difference
1	2.149	* not found *	

Could not find time reference peak:
No peak of Number 1's description at 2.149 + 0.107 - 0.107 min.
Not all time reference peaks were found

Area Percent Report

ADC CHANNEL A

Pk#	Ret Time	Area	Height	Type	Width	Area %

Total amount = 0

0%

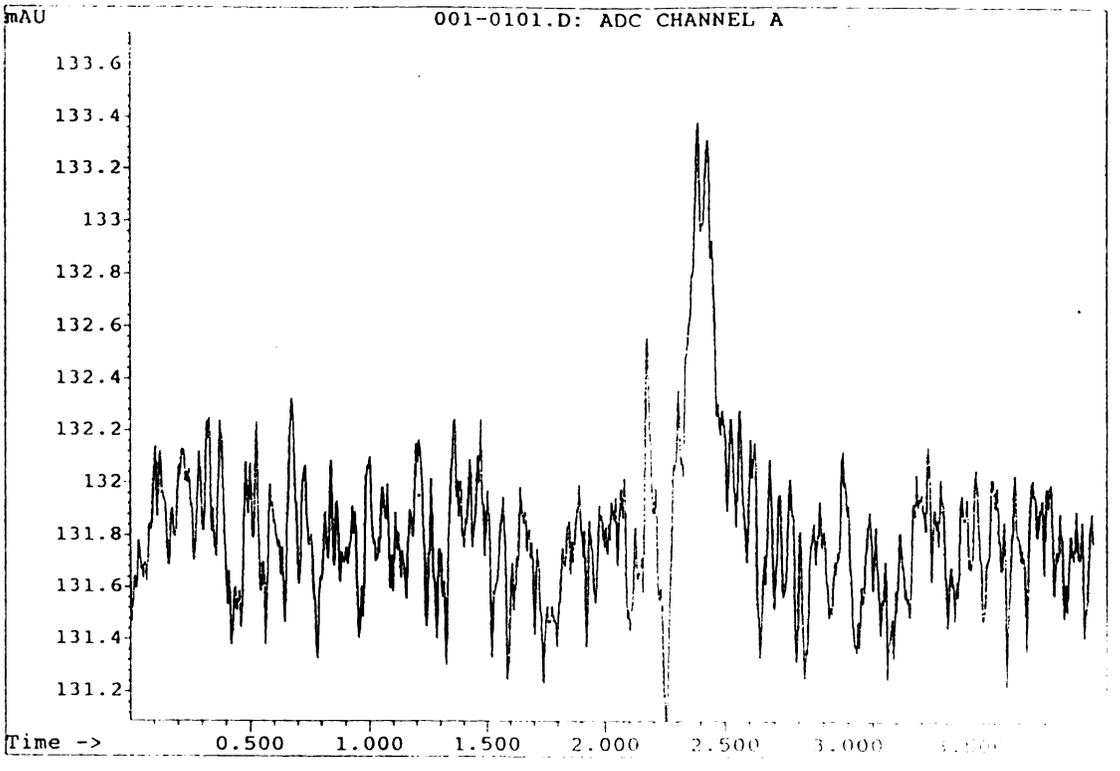

External Standard Report

Data File Name : C:\HPCHEM\1\DATA\002-0101.D
Operator : PHIL KUCH
Acquired on : Sat Feb 08 09:22:47 1992
Sample Name : 2.5% minoil
Run Time Bar Code:
Instrument Method: MINOIL.M
Analysis Method : MINOIL.M.
Multiplier : 1
Last Recalib : 03 Oct 91 11:08 AM

Instrument : HP35900C
Vial Number : 2
Injection Number: 1
Sequence Line : 1
Sample Amount : 0

ADC CHANNEL A

Ret Time	Area	Type	Width	Ref#	PERCENT	Name
2.149	* not found *			1-R		MINERAL OIL

Time Reference Peak	Expected RT	Actual RT	Difference
1	2.149	* not found *	

Could not find time reference peak:
No peak of Number 1's description at 2.149 + 0.107 - 0.107 min.
Not all time reference peaks were found

Area Percent Report

ADC CHANNEL A

Pk#	Ret Time	Area	Height	Type	Width	Area %
1	2.486	5209.336	426.836	BB	0.189	100.0000

Total amount = 5209.34

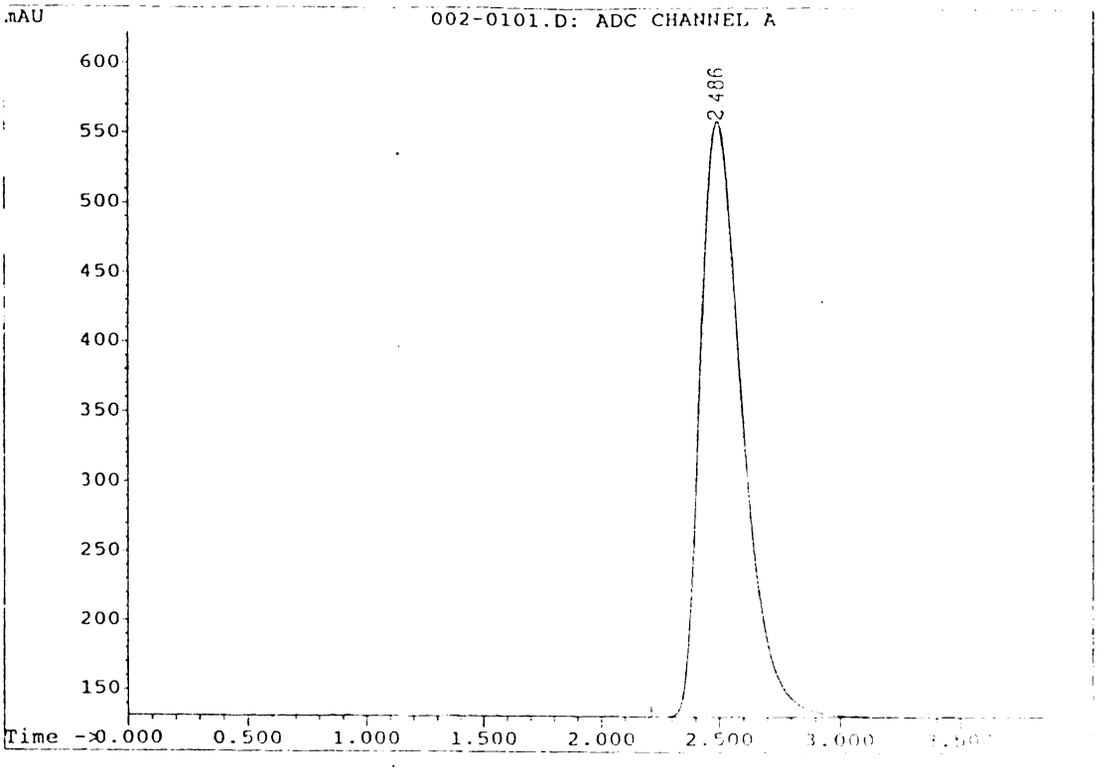

External Standard Report

Data File Name : C:\HPCHEM\1\DATA\003-0101.D
Operator : PHIL KUCH
Acquired on : Sat Feb 08 09:28:19 1992
Sample Name : 5.0% min oil
Run Time Bar Code:
Instrument Method: MINOIL.M
Analysis Method : MINOIL.M
Multiplier : 1
Last Recalib : 03 Oct 91 11:08 AM
results x2

Instrument : HP35900C
Vial Number : 3
Injection Number: 1
Sequence Line : 1
Sample Amount : 0

ADC CHANNEL A

Ret Time	Area	Type	Width	Ref#	PERCENT	Name
2.149	* not found *			1-R		MINERAL OIL

Time Reference Peak	Expected RT	Actual RT	Difference
1	2.149	* not found *	

Could not find time reference peak:
No peak of Number 1's description at 2.149 + 0.107 - 0.107 min.
Not all time reference peaks were found

Area Percent Report

ADC CHANNEL A

Pk#	Ret Time	Area	Height	Type	Width	Area %
1	2.444	3908.367	335.187	BV	0.180	100.0000

Total amount = 3908.37

1\ 149 12 = 2.98%

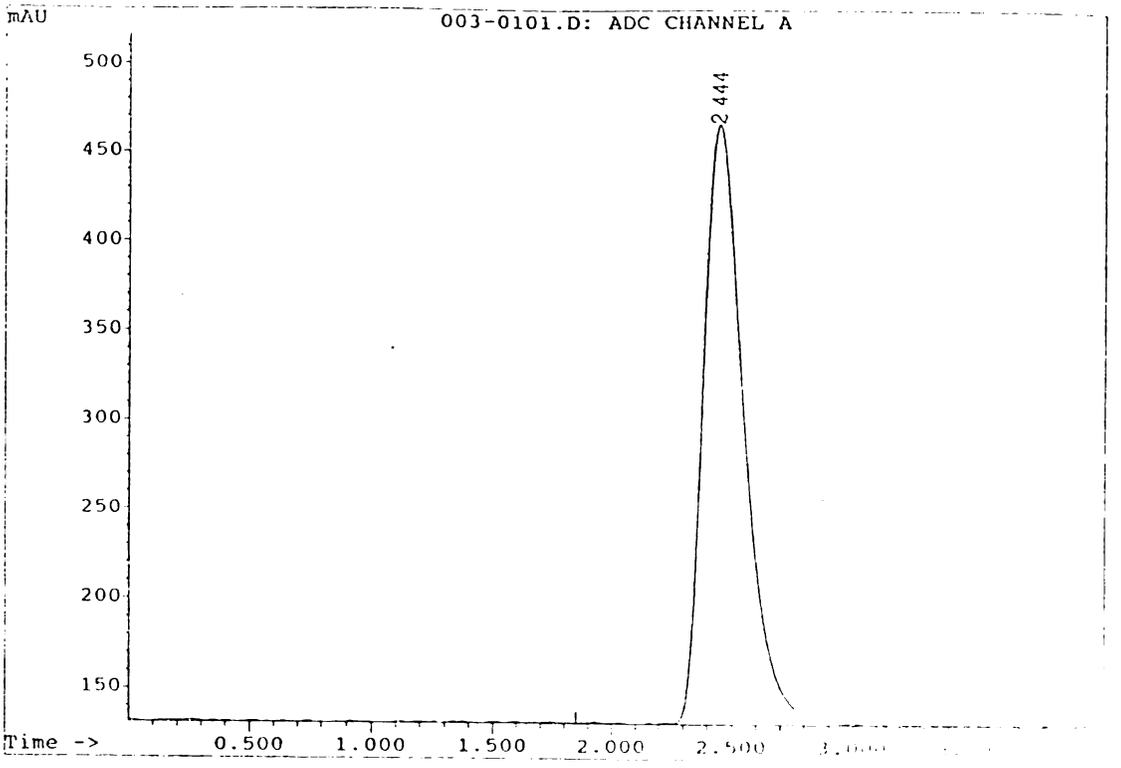

External Standard Report

Data File Name : C:\HPCHEM\1\DATA\004-0101.D
Operator : PHIL KUCH
Acquired on : Sat Feb 08 09:33:52 1992
Sample Name : 7.5% min oil
Run Time Bar Code:
Instrument Method: MINOIL.M
Analysis Method : MINOIL.M
Multiplier : 1
Last Recalib : 03 Oct 91 11:08 AM
results x2

Instrument : HP35900C
Vial Number : 4
Injection Number: 1
Sequence Line : 1
Sample Amount : 0

ADC CHANNEL A

Ret Time	Area	Type	Width	Ref#	PERCENT	Name
2.149	* not found *			1-R		MINERAL OIL

Time Reference Peak	Expected RT	Actual RT	Difference
1	2.149	* not found *	

Could not find time reference peak:
No peak of Number 1's description at 2.149 + 0.107 - 0.107 min.
Not all time reference peaks were found

Area Percent Report

ADC CHANNEL A

Pk#	Ret Time	Area	Height	Type	Width	Area %
1	2.377	3795.189	328.556	BB	0.179	100.0000

Total amount = 3795.19

1.45% x2 = 2.90%

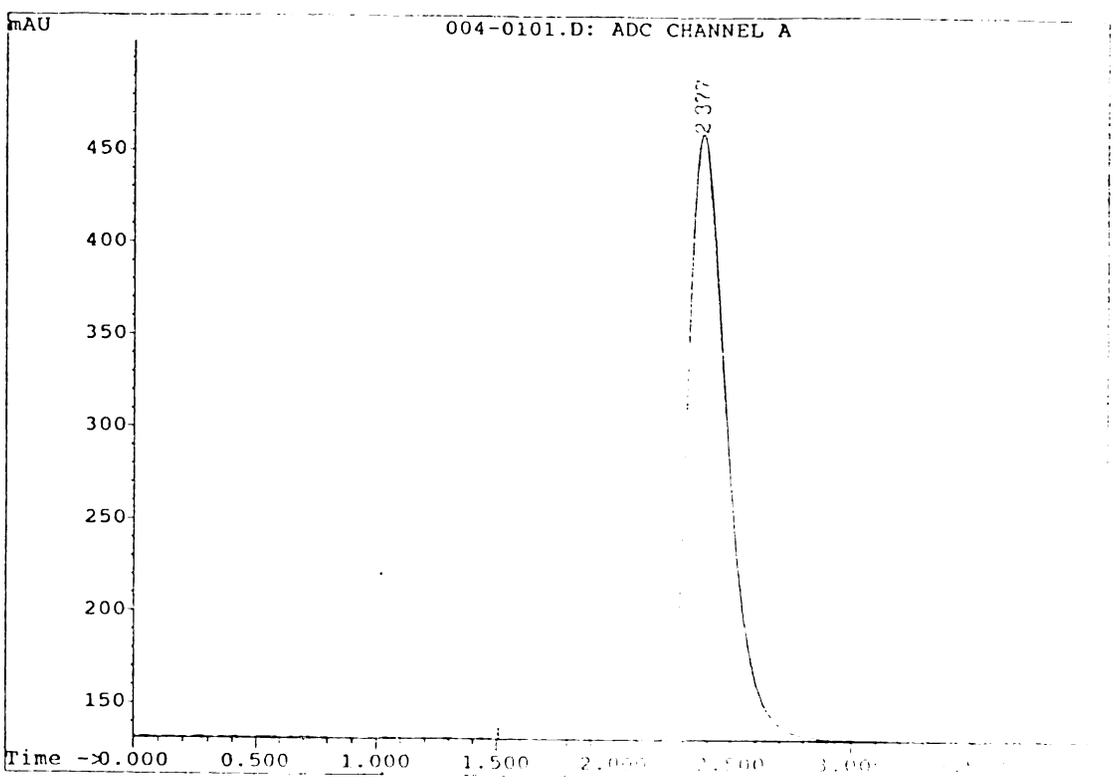

External Standard Report

Data File Name : C:\HPCHEM\1\DATA\005-0101.D
Operator : PHIL KUCH
Acquired on : Sat Feb 08 09:39:26 1992
Sample Name : 10% min oil
Run Time Bar Code:
Instrument Method: MINOIL.M
Analysis Method : MINOIL.M
Multiplier : 1
Last Recalib : 03 Oct 91 11:08 AM
results x2

Instrument : HP35900C
Vial Number : 5
Injection Number: 1
Sequence Line : 1
Sample Amount : 0

ADC CHANNEL A

Ret Time	Area	Type	Width	Ref#	PERCENT	Name
2.149	* not found *			1-R		MINERAL OIL

Time Reference Peak	Expected RT	Actual RT	Difference
1	2.149	* not found *	

Could not find time reference peak:
No peak of Number 1's description at 2.149 + 0.107 - 0.107 min.
Not all time reference peaks were found

Area Percent Report

ADC CHANNEL A

Pk#	Ret Time	Area	Height	Type	Width	Area %
1	2.514	11211.423	830.507	BB	0.211	100.0000

Total amount = 11211.4

\\ 392 x 2 = 784%

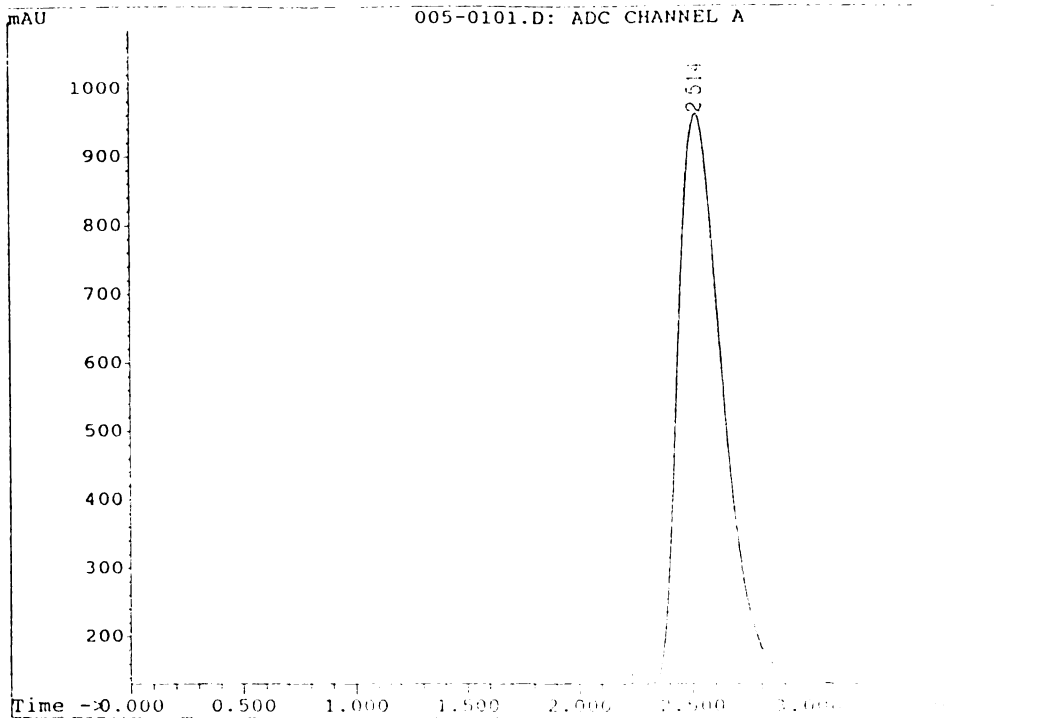

Appendix B-7. Nominal and Actual Mineral Oil Concentrations in 270,000 MW Blends

Nominal wt%	Actual wt%	Actual vol%
0	0.2	0.242
2.5	2.82	3.5
5	4.38	5.53
7.5	5.2	6.63
7.5	6.21	8
10	6.05	7.78
10	6.18	7.96

Appendix B-8. GC Analysis of Mineral Oil in 270,000 MW Blends

```
SAMPLE NAME?8

START PENDING
RUN #   484      AUG 14, 1991   11:56:33
START
```

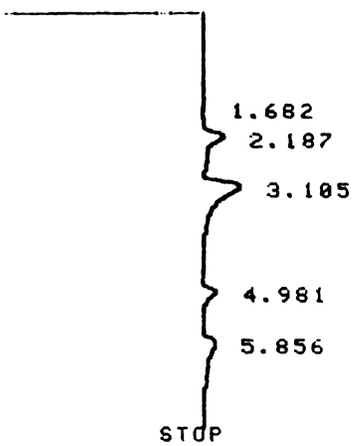


```
RUN#    484           AUG 14, 1991   11:56:33

METHOD NAME: M:MINOIL.MET

AREA%
      RT       AREA TYPE  WIDTH      AREA%
   1.682      53330   VV   .479     3.17118
   2.187     328868   VV   .282    19.55558
   3.105     794791   VP   .388    47.26088
   4.981     179769   PV   .218    10.68966
   5.856     324952   VV   .411    19.32271

TOTAL AREA=1681710
MUL FACTOR=1.0000E+00


SAMPLE:8
PEAK NUMBERS?2,4
  WT POLYMER IN MG?201.5
MINERAL OIL= 0.2
MINERAL OIL= 0.2 %
MO1= 0.24 RT1+ 2.187
MO2= 0.16 RT2=
MO2= 0.16 RT2= 4.981
```

```
SAMPLE NAME?10

START PENDING
RUN #  485      AUG 14, 1991   12:06:10
START
```

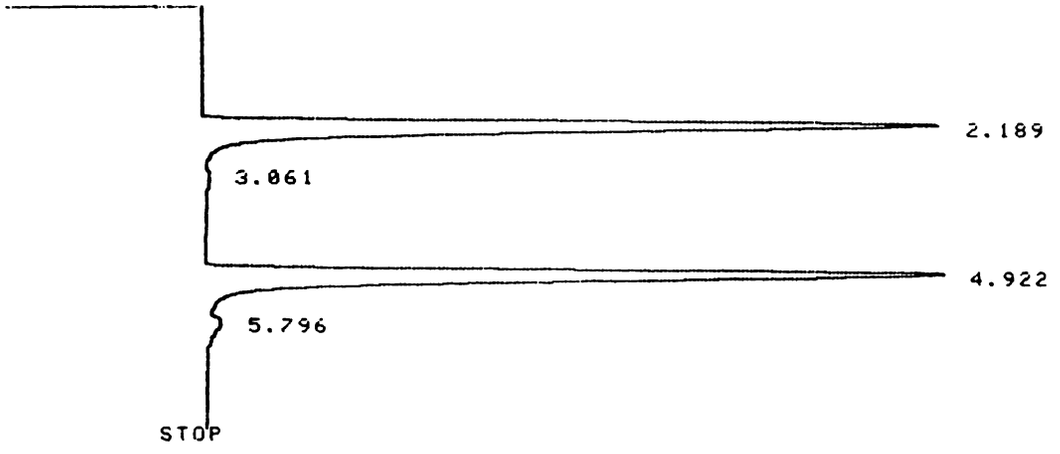


```
RUN#    485           AUG 14, 1991   12:06:10

METHOD NAME: M:MINOIL.MET

AREA%
       RT       AREA TYPE   WIDTH       AREA%
    2.189    8983520   PB    .231    48.58190
    3.061      70770   BB    .275      .38272
    4.922    9272768   PB    .237    50.14614
    5.796     164438   BP    .239      .88926

TOTAL AREA=1.8491E+07
MUL FACTOR=1.0000E+00


SAMPLE:10
PEAK NUMBERS?1,3
  WT POLYMER IN MG?201.3
MINERAL OIL= 2.82
MINERAL OIL= 2.82 %
MO1= 2.78 RT1+ 2.189
MO2= 2.85 RT2=
MO2= 2.85 RT2= 4.922
```

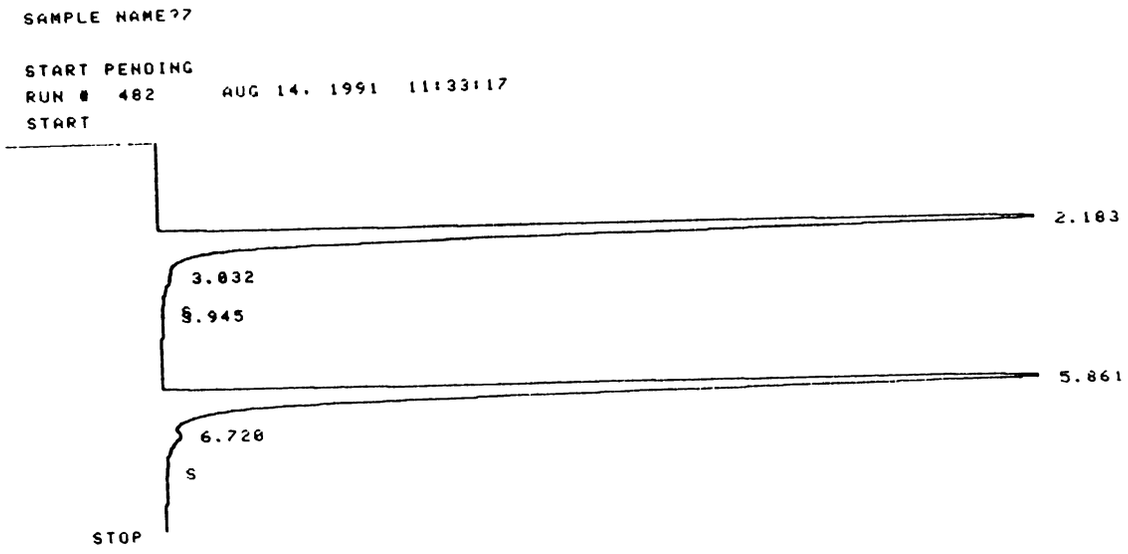

RUN# 482 AUG 14, 1991 11:33:17

METHOD NAME: M:MINOIL.MET

AREA%

RT	AREA	TYPE	WIDTH	AREA%
2.183	16322360	SPB	.265	49.43030
3.032	56579	TBB	.210	.17134
3.945	15908	BP	.225	.04818
5.861	16491288	SPB	.268	49.94187
6.720	134824	TBB	.249	.40830

TOTAL AREA=3.3021E+07
MUL FACTOR=1.0000E+00

SAMPLE:7
PEAK NUMBERS?1,4
WT POLYMER IN MG?199.0
MINERAL OIL= 4.38
MINERAL OIL= 4.38 %
MO1= 4.37 RT1= 2.183
MO2= 4.4 RT2=
MO2= 4.4 RT2= 5.861

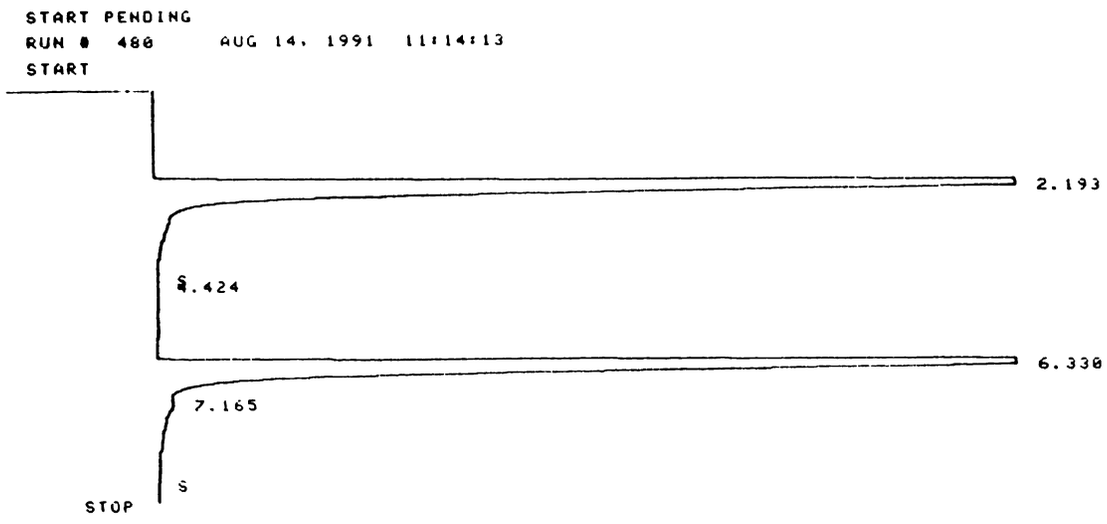

RUN# 480 AUG 14, 1991 11:14:13

METHOD NAME: M:MINOIL.MET

AREA%

RT	AREA	TYPE	WIDTH	AREA%
2.193	20890560	SPB	.297	50.06061
4.424	19801	BV	.235	.04745
6.330	20742848	SPB	.276	49.70666
7.165	77327	TBB	.209	.18530

TOTAL AREA=4.1731E+07
MUL FACTOR=1.0000E+00

SAMPLE:4
PEAK NUMBERS?1,3
WT POLYMER IN MG?200.0
MINERAL OIL= 5.2
MINERAL OIL= 5.2 %
MO1= 5.21 RT1= 2.193
MO2= 5.18 RT2=
MO2= 5.18 RT2= 6.33

```
SAMPLE NAME?15

START PENDING
RUN #  490      AUG 14, 1991  12:54:35
START
```

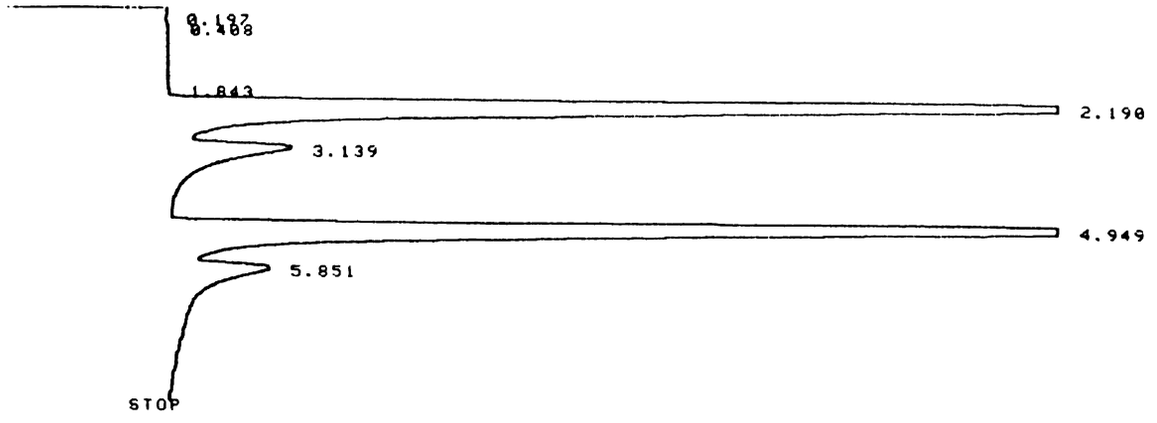

RUN# 490 AUG 14, 1991 12:54:35

METHOD NAME: M:MINOIL.MET

AREA%

RT	AREA	TYPE	WIDTH	AREA%
.197	4871	PV	.075	.00837
.408	96400	VV	.422	.16571
1.843	172863	VH	.631	.29715
2.190	25646784	SHH	.331	44.08712
3.139	2753122	TBP	.404	4.73265
4.949	27581312	ISHH	.357	47.41259
5.851	1917625	TBB	.387	3.29642

TOTAL AREA=5.8173E+07
MUL FACTOR=1.0000E+00

SAMPLE:15
PEAK NUMBERS?4,6
  WT POLYMER IN MG?200.5
MINERAL OIL= 6.21
MINERAL OIL= 6.21 %
MO1= 6.04 RT1= 2.19
MO2= 6.37 RT2=
MO2= 6.37 RT2= 4.949

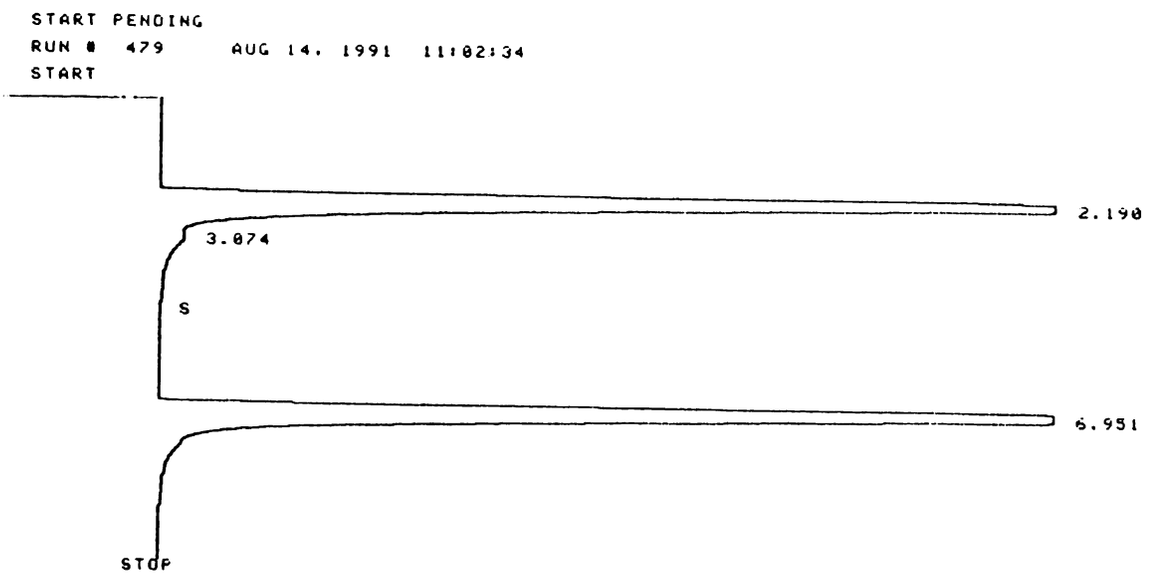

RUN# 479 AUG 14, 1991 11:02:34

METHOD NAME: M:MINOIL.MET

AREA%

RT	AREA	TYPE	WIDTH	AREA%
2.190	26473808	SBB	.321	50.13150
3.074	122591	TBB	.311	.23214
6.951	26212336	SPB	.319	49.63637

TOTAL AREA=5.2809E+07
MUL FACTOR=1.0000E+00

SAMPLE:3
PEAK NUMBERS?1,3
WT POLYMER IN MG?199.9
MINERAL OIL= 6.18
MINERAL OIL= 6.18 %
MO1= 6.2 RT1= 2.19
MO2= 6.16 RT2=
MO2= 6.16 RT2= 6.951

```
 GET MOSAM

>RUN

STARTING  AUG 14, 1991  10:45:20
MINERAL OIL ANALYSIS BY HPLC
 438 BUILDING MIDLAND
SLOPE?1.36084
INTERCEPT?13.6655


SAMPLE NAME?2

START PENDING
RUN #  478      AUG 14, 1991  10:53:41
START
```

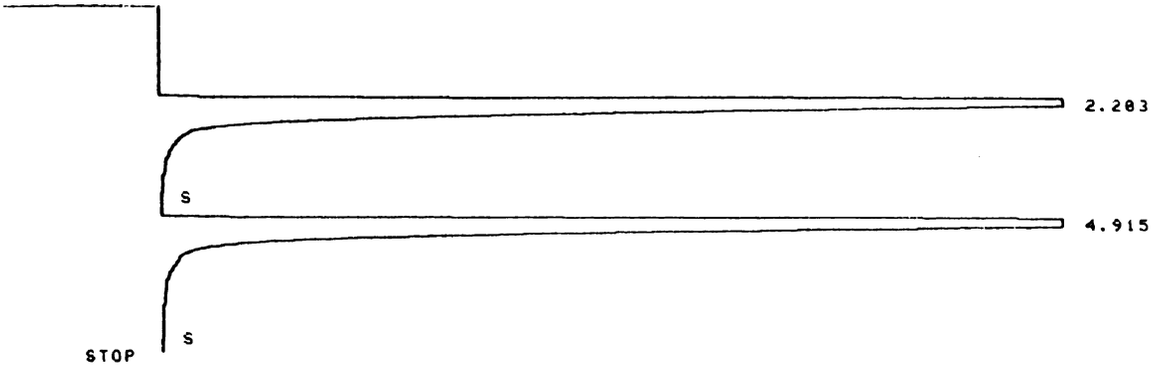


```
RUN#    478           AUG 14, 1991  10:53:41

METHOD NAME: M:MINOIL.MET

AREA%
      RT       AREA TYPE  WIDTH       AREA%
   2.203   25885296  SPB    .336    50.62106
   4.915   25250144  SPB    .313    49.37896

TOTAL AREA=5.1135E+07
MUL FACTOR=1.0000E+00


SAMPLE:2
PEAK NUMBERS?1,2
  WT POLYMER IN MG?199.8
MINERAL OIL= 6.05
MINERAL OIL= 6.05 %
MO1= 6.1 RT1= 2.203
MO2= 5.99 RT2=
MO2= 5.99 RT2= 4.915
```

APPENDIX C

GLASS TRANSITION TEMPERATURES

Appendix C-1. Glass Transition Temperatures of 40,000 MW Blends

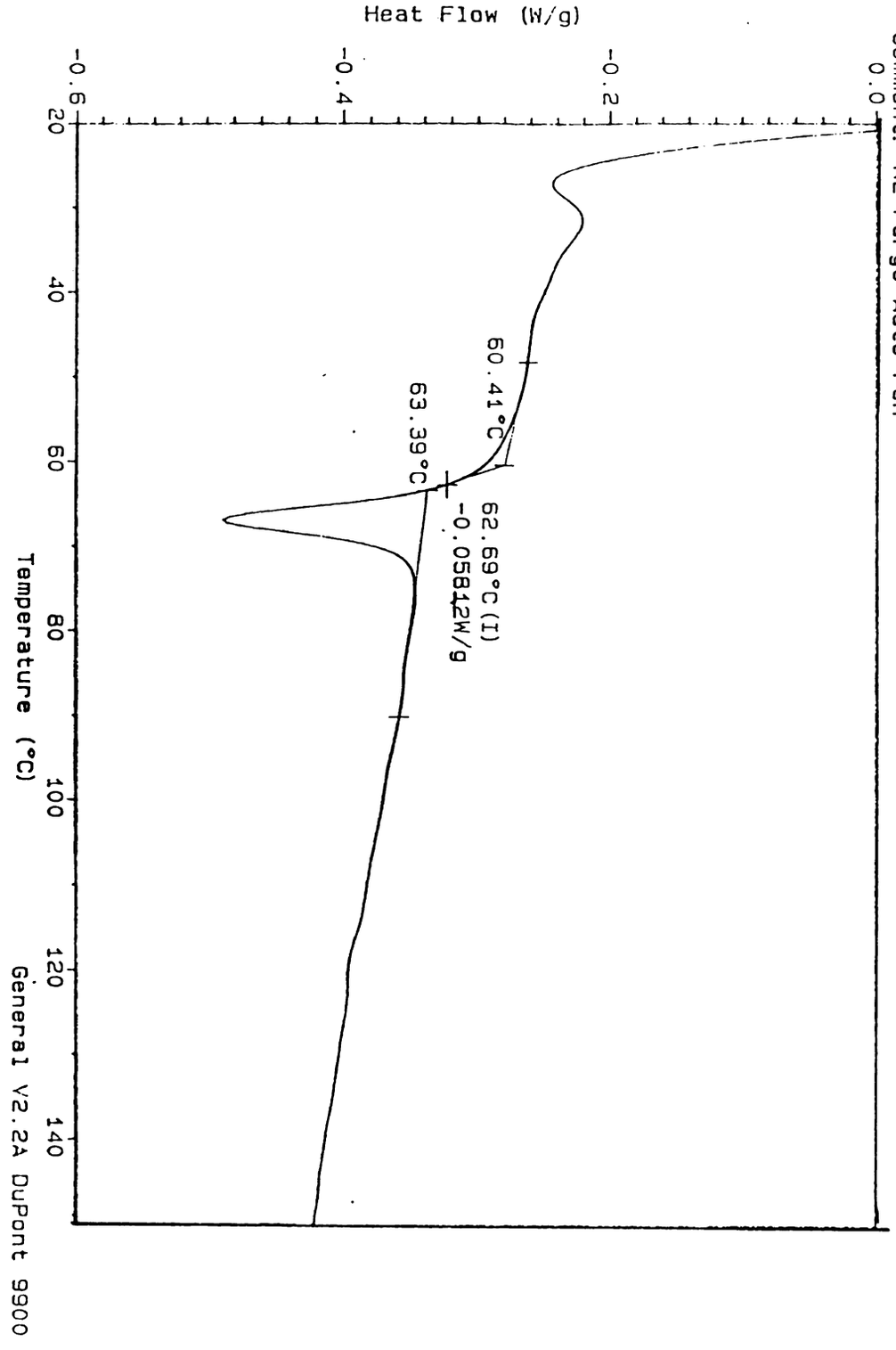
Sample: Run # 11 LMW 0% MO
Size: 10.9400 mg
Method: Amp Amb-200 @10°C/Min
Comment: N2 Purge Auto Pan
DSC
File: E:SLA072991.01
Operator: S. Anderson
Run Date: 07/29/91 11:17
Heat Flow (W/g)
-0.6
-0.4
-0.2
0.0
20
40
60
80
100
120
140
Temperature (°C)
60.41°C
63.39°C
62.69°C(I)
-0.05812W/g
General V2.2A DuPont 9900

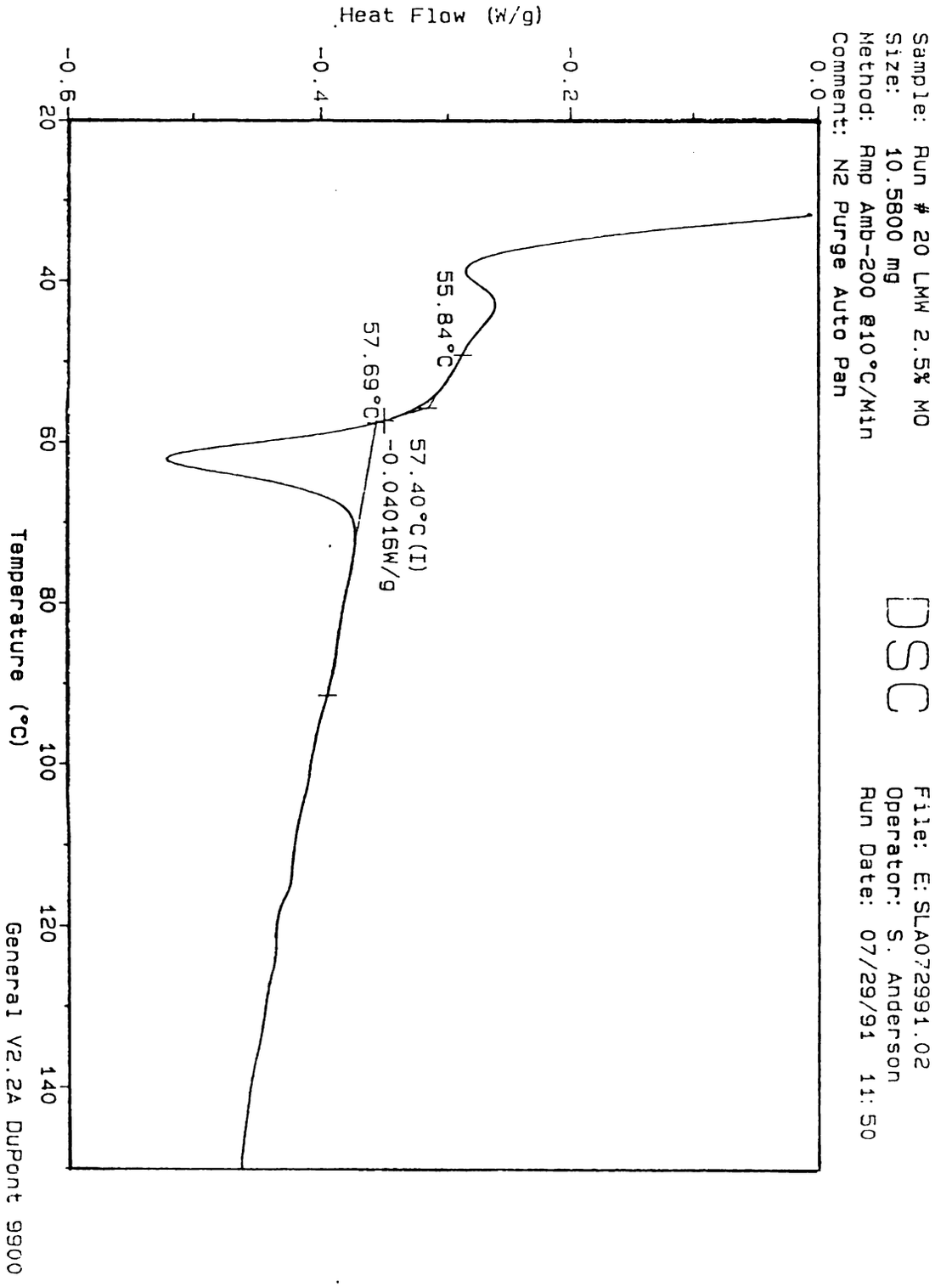
Sample: Run # 20 LMW 2.5% MO
Size: 10.5800 mg
Method: Amp Amb-200 @10°C/Min
Comment: N2 Purge Auto Pan
DSC
File: E:SLA072991.02
Operator: S. Anderson
Run Date: 07/29/91 11:50
Heat Flow (W/g)
-0.6
-0.4
-0.2
0.0
20
40
60
80
100
120
140
Temperature (°C)
55.84°C
57.69°C
57.40°C (I)
-0.04016W/g
General V2.2A DuPont 9900

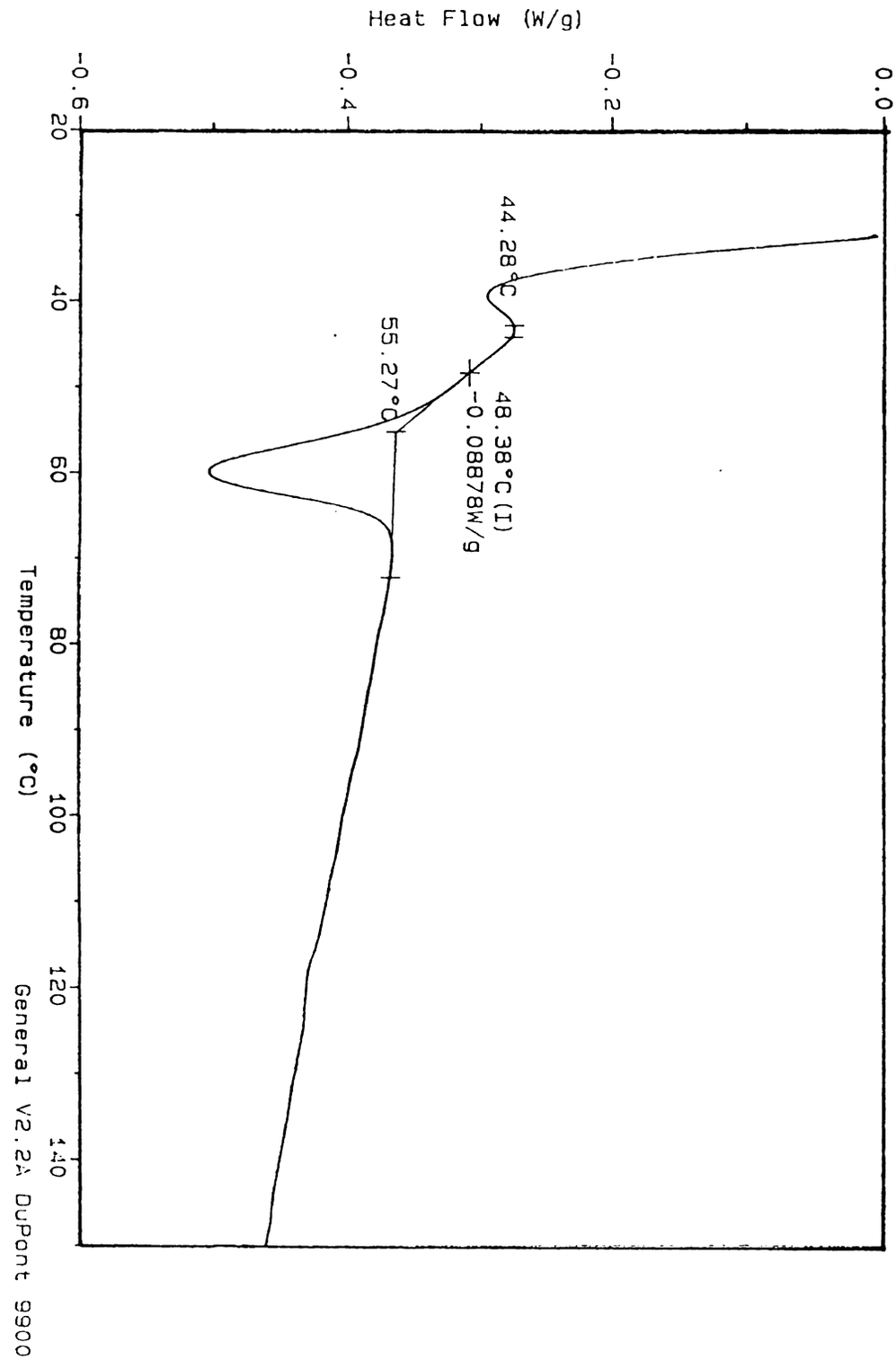
Sample: Run # 12 LMW 5.0% MO
Size: 10.3900 mg
Method: Rmp Amb-200 @10°C/Min
Comment: N2 Purge Auto Pan
DSC
File: E:SLA072991.03
Operator: S. Anderson
Run Date: 07/29/91 12:23
Heat Flow (W/g)
-0.6
-0.4
-0.2
0.0
44.28°C
55.27°C
48.38°C (I)
-0.08878W/g
20
40
60
80
100
120
140
Temperature (°C)
General V2.2A DuPont 9900

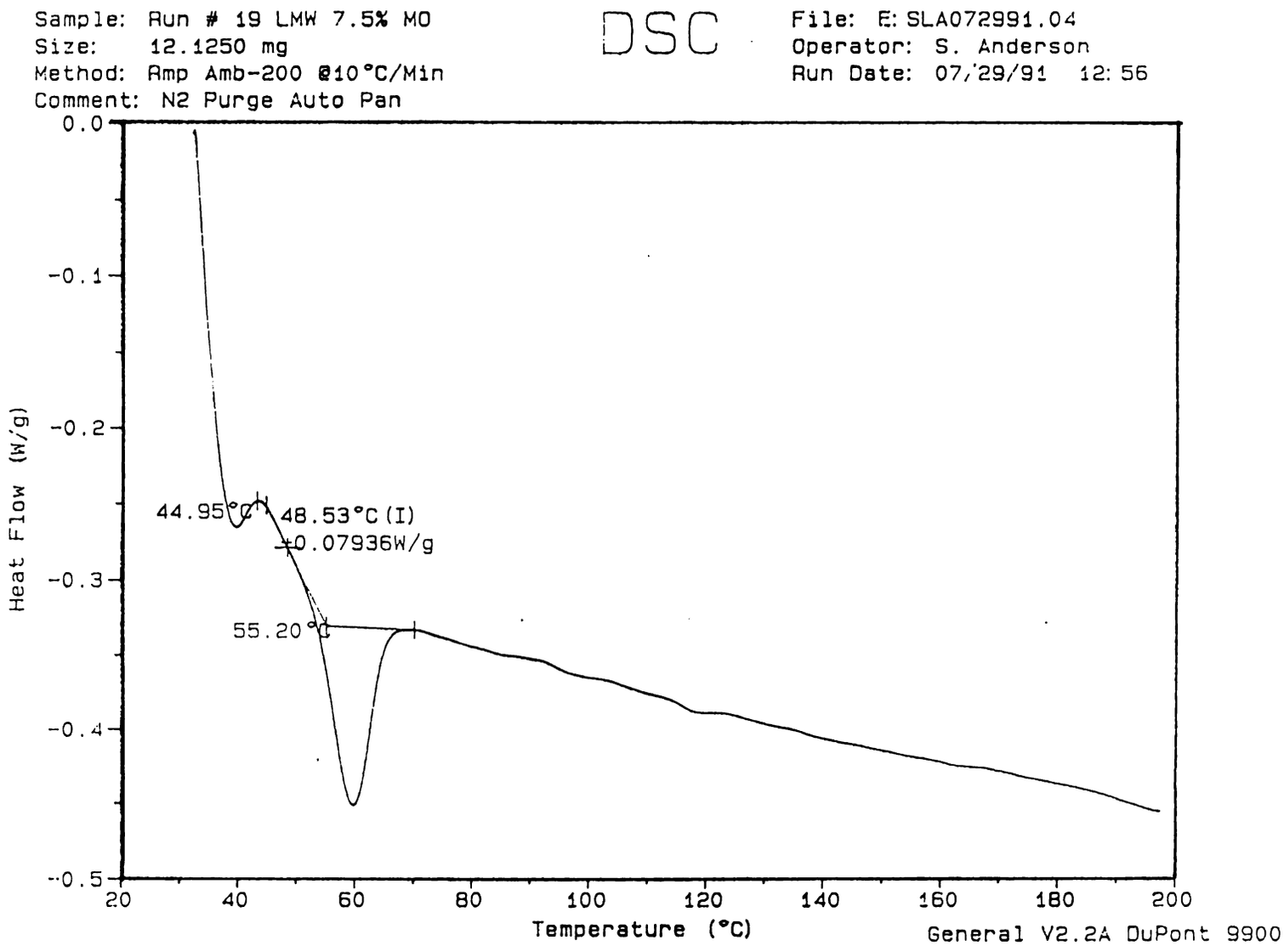
Sample: Run # 19 LMW 7.5% MO
Size: 12.1250 mg
Method: Rmp Amb-200 @10°C/Min
Comment: N2 Purge Auto Pan
DSC
File: E:SLA072991.04
Operator: S. Anderson
Run Date: 07/29/91 12:56
0.0
-0.1
-0.2
-0.3
-0.4
-0.5
Heat Flow (W/g)
44.95°C
48.53°C (I)
-0.07936W/g
55.20°C
20
40
60
80
100
120
140
160
180
200
Temperature (°C)
General V2.2A DuPont 9900

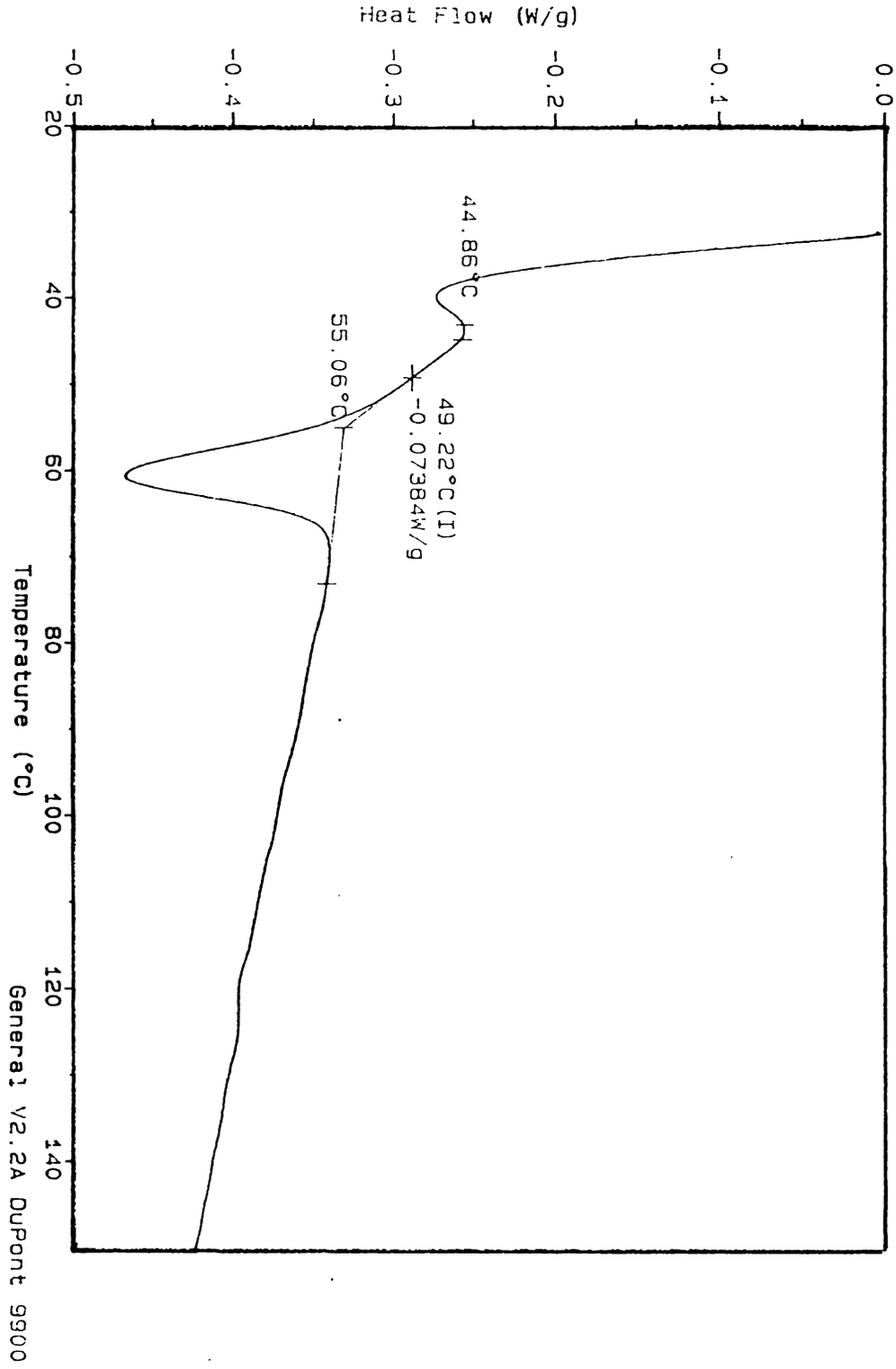
Sample: Run # 5 LMW 10.0% MO
Size: 11.2650 mg
Method: Amp Amb-200 @10°C/Min
Comment: N2 Purge Auto Pan
DSC
File: E:SLA072991.05
Operator: S. Anderson
Run Date: 07/29/91 13:29
Heat Flow (W/g)
0.0
-0.1
-0.2
-0.3
-0.4
-0.5
44.86°C
55.06°C
49.22°C(I)
-0.07384W/g
20
40
60
80
100
120
140
Temperature (°C)
General V2.2A DuPont 9900

Appendix C-2. Glass Transition Temperatures of 128,000 MW Blends

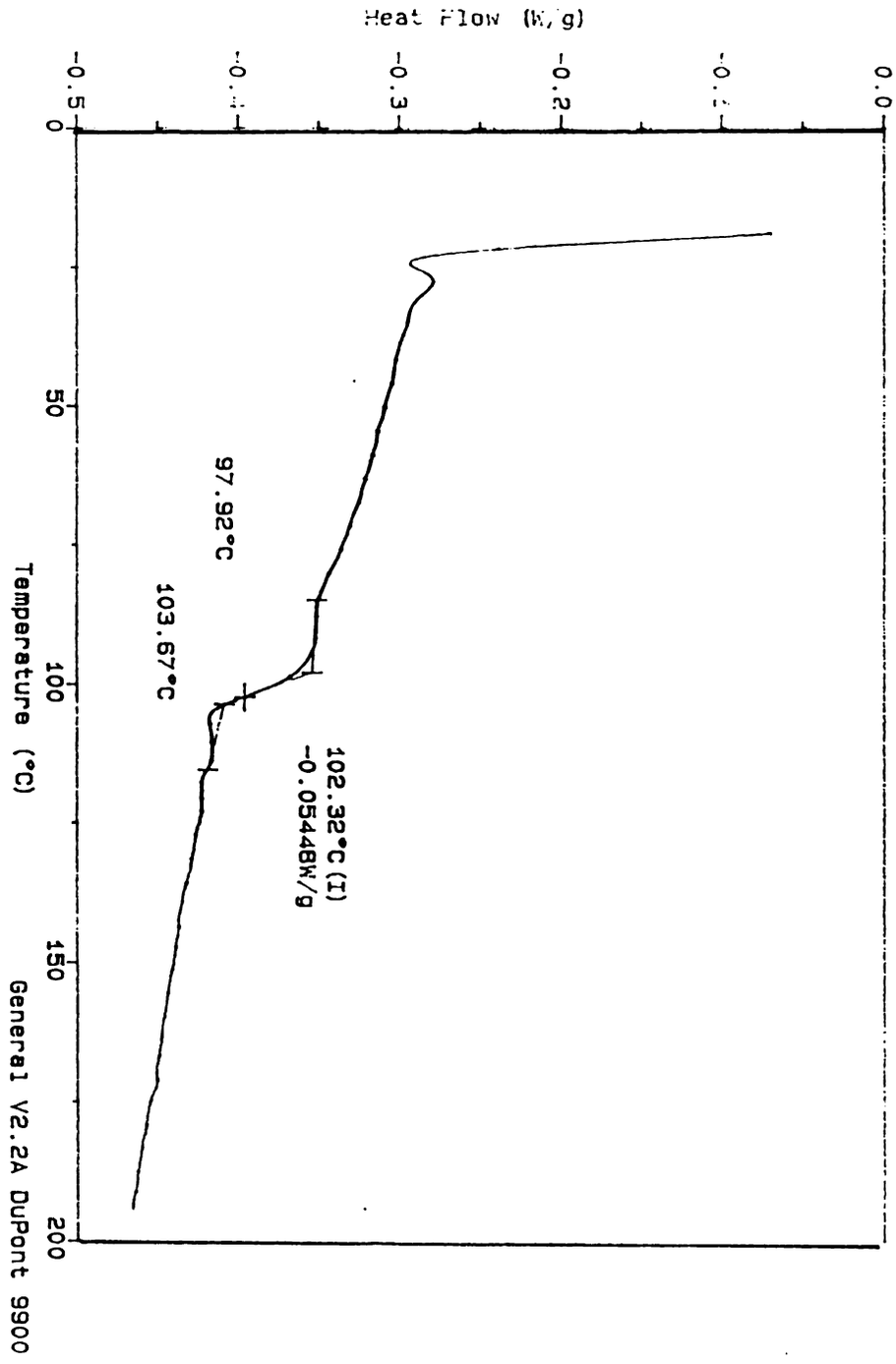
Sample: 128000MWPS 0% MO 3000 lbs
Size: 11.8820 mg
Method: Amp@10°C/Min amb - 200C
DSC
File: MMD010793.01
Operator: M.M.DULLOCK
Run Date: 01/07/93 15:28
Heat Flow (W/g)
-0.5
0
-0.4
-0.3
-0.2
-0.1
0.0
50
100
150
200
Temperature (°C)
97.92°C
103.67°C
102.32°C (I)
-0.0544W/g
General V2.2A DuPont 9900

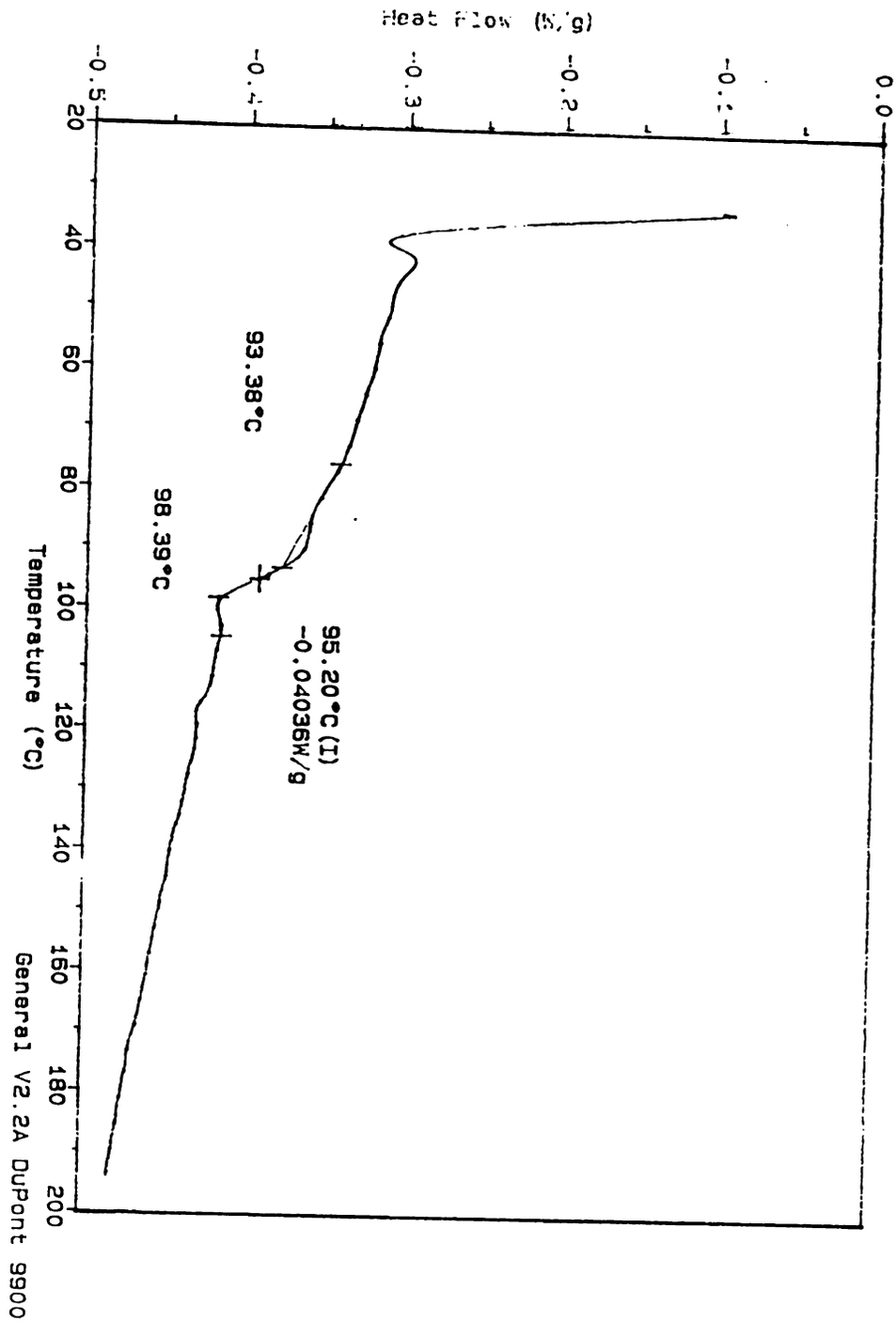
Sample: 128000MWPS 2.5% MO 3000 lbs
Size: 11.8280 mg
Method: Ramp10°C/Min amb - 200C
DSC
File: MMD010793.02
Operator: M.M.DULLOCK
Run Date: 01/07/93 15:59
Heat Flow (W/g)
0.0
-0.1
-0.2
-0.3
-0.4
-0.5
20
40
60
80
100
120
140
160
180
200
Temperature (°C)
93.38°C
98.39°C
95.20°C (I)
-0.04036W/g
General V2.2A DuPont 9900

Sample: 128000MWPS 5% MO 3000 lbs
Size: 11.9140 mg
Method: Rmp@10°C/Min amb - 200C

DSC

File: MMD010793.03
Operator: M.M. DULLOCK
Run Date: 01/07/93 16:29

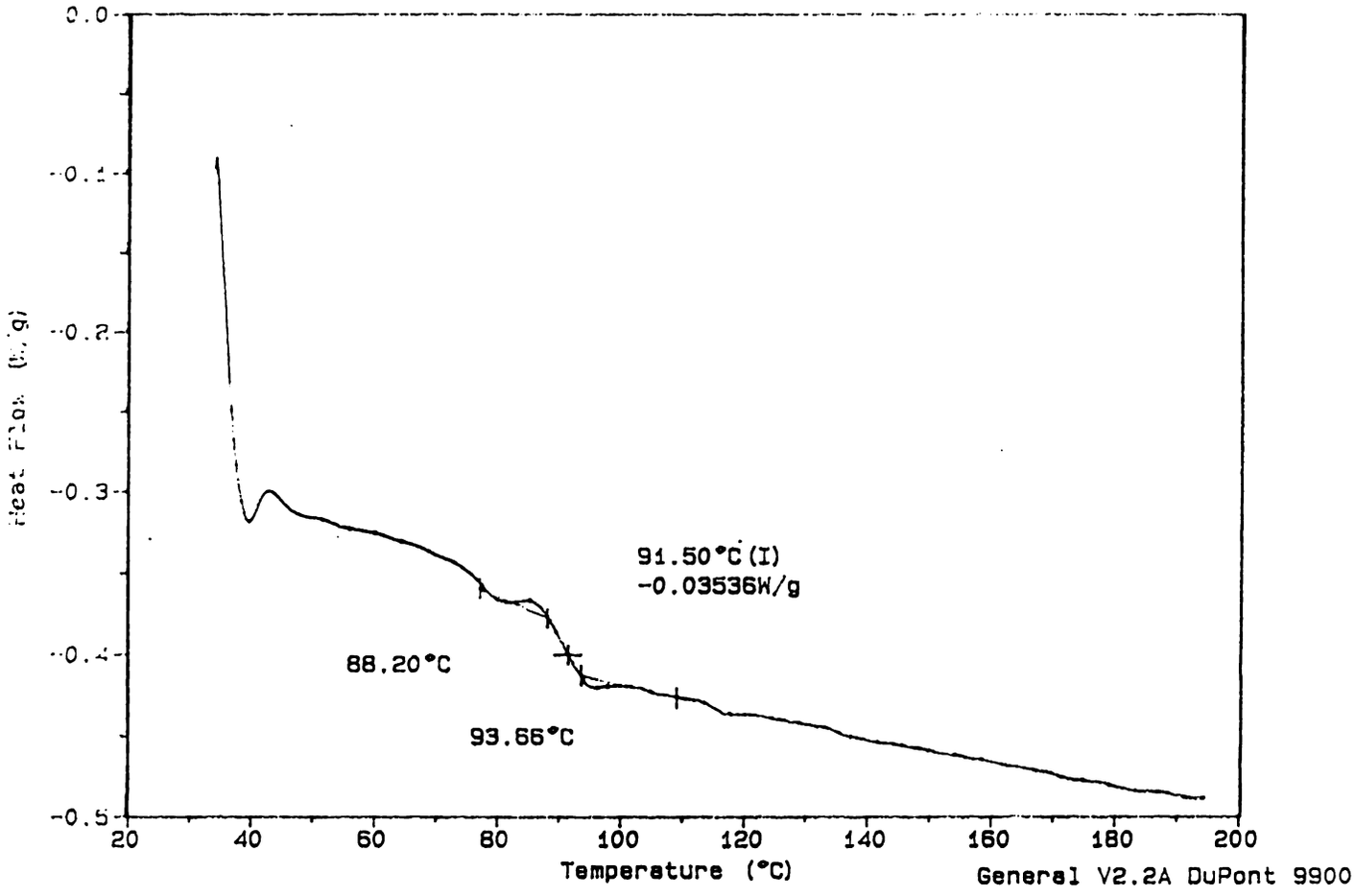

General V2.2A DuPont 9900

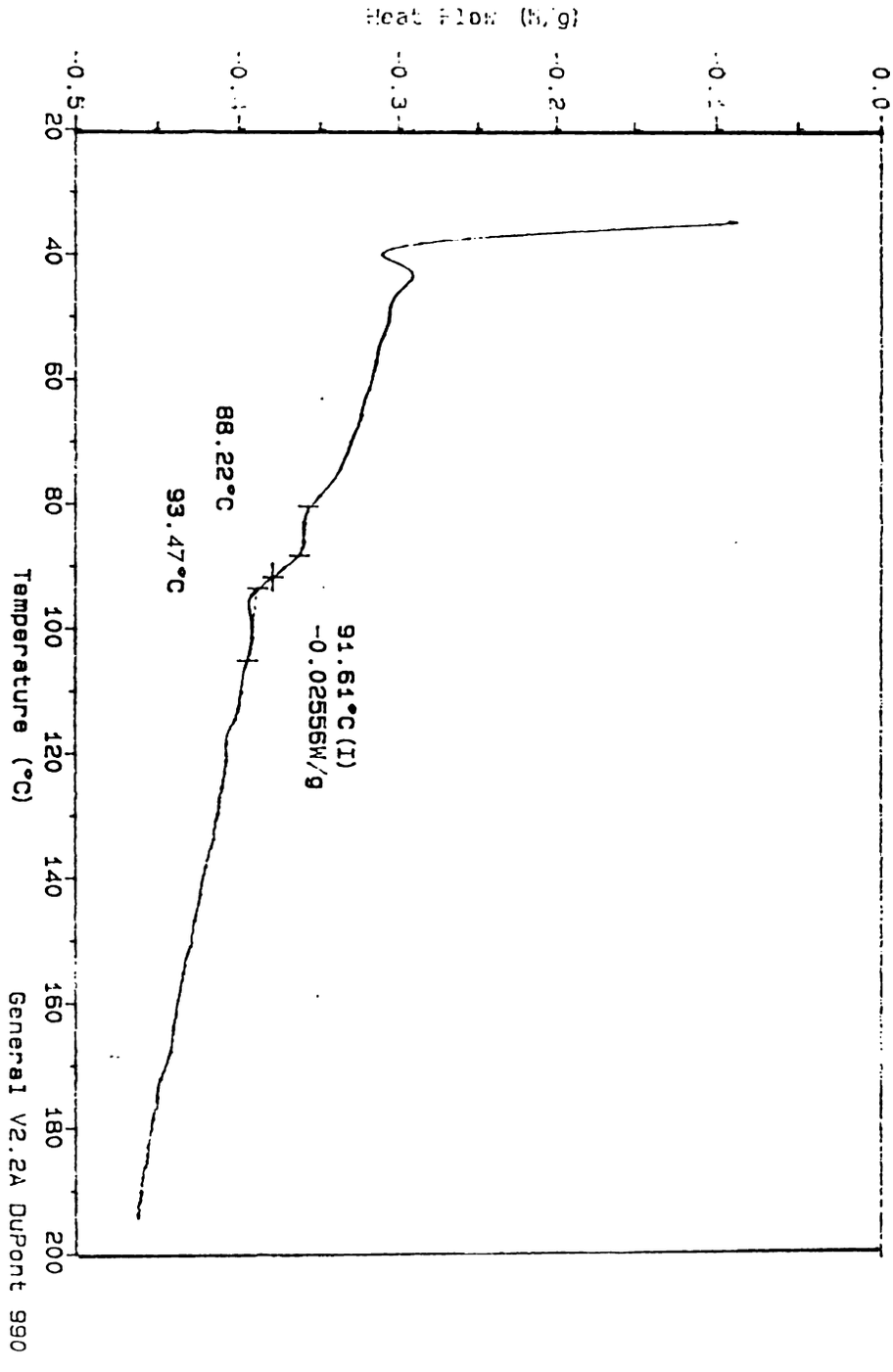
Sample: 128000MWPS 7.5% MO 3000 lbs
Size: 11.8330 mg
Method: Amp@10°C/Min amb - 200C
DSC
File: MMD010793.04
Operator: M.M. DULLOCK
Run Date: 01/07/93 17:00
Heat Flow (W/g)
0.0
-0.1
-0.2
-0.3
-0.4
-0.5
20
40
60
80
100
120
140
160
180
200
Temperature (°C)
88.22°C
93.47°C
91.61°C(I)
-0.02556W/g
General V2.2A DuPont 990

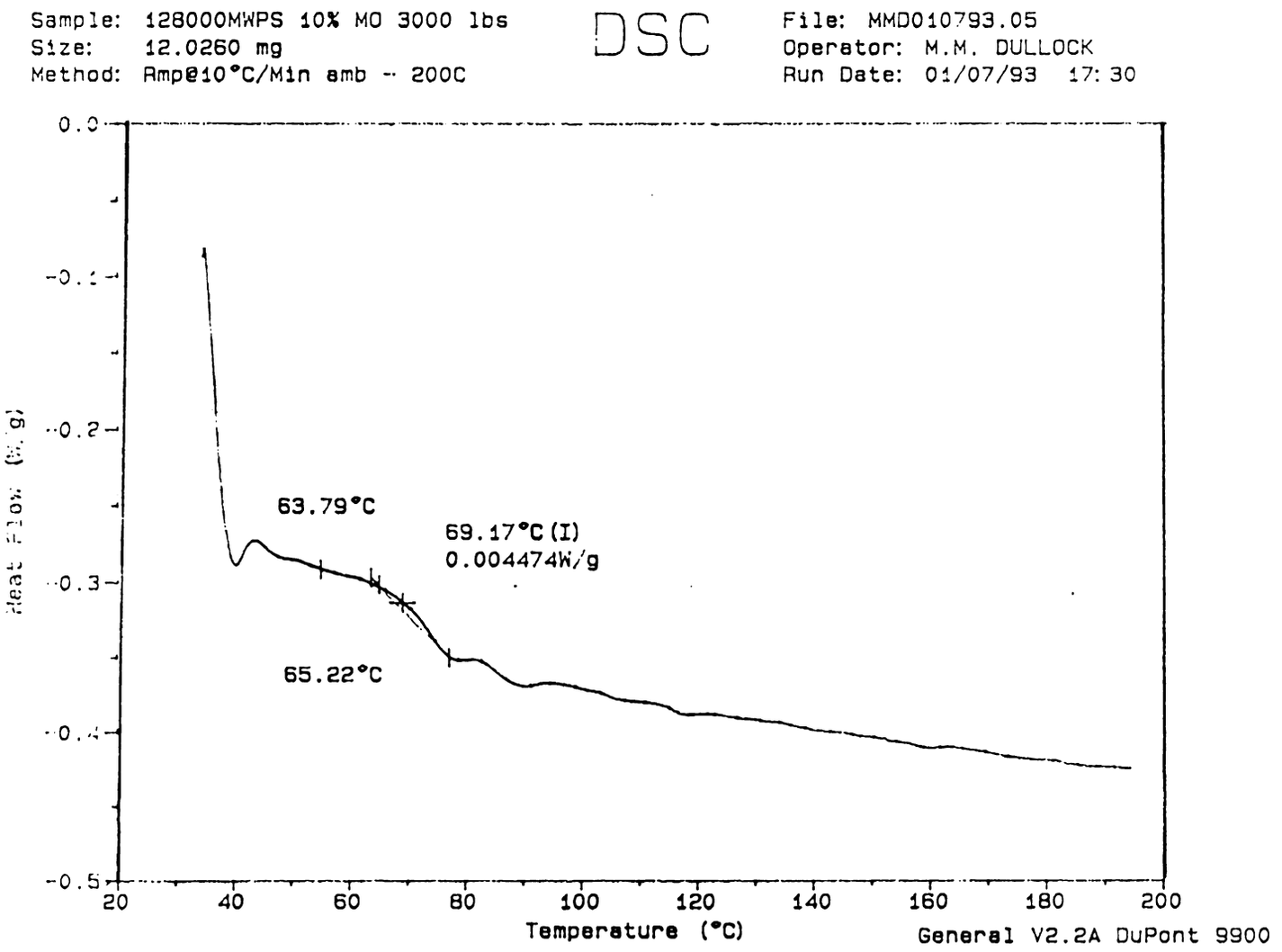
Sample: 128000MWPS 10% MO 3000 lbs
Size: 12.0260 mg
Method: Amp@10°C/Min amb - 200C
DSC
File: MMD010793.05
Operator: M.M. DULLOCK
Run Date: 01/07/93 17:30
0.0
-0.1
-0.2
-0.3
-0.4
-0.5
63.79°C
69.17°C (I)
0.004474W/g
65.22°C
20
40
60
80
100
120
140
160
180
200
Temperature (°C)
General V2.2A DuPont 9900

Appendix C-3. Glass Transition Temperatures of 270,000 MW Blends

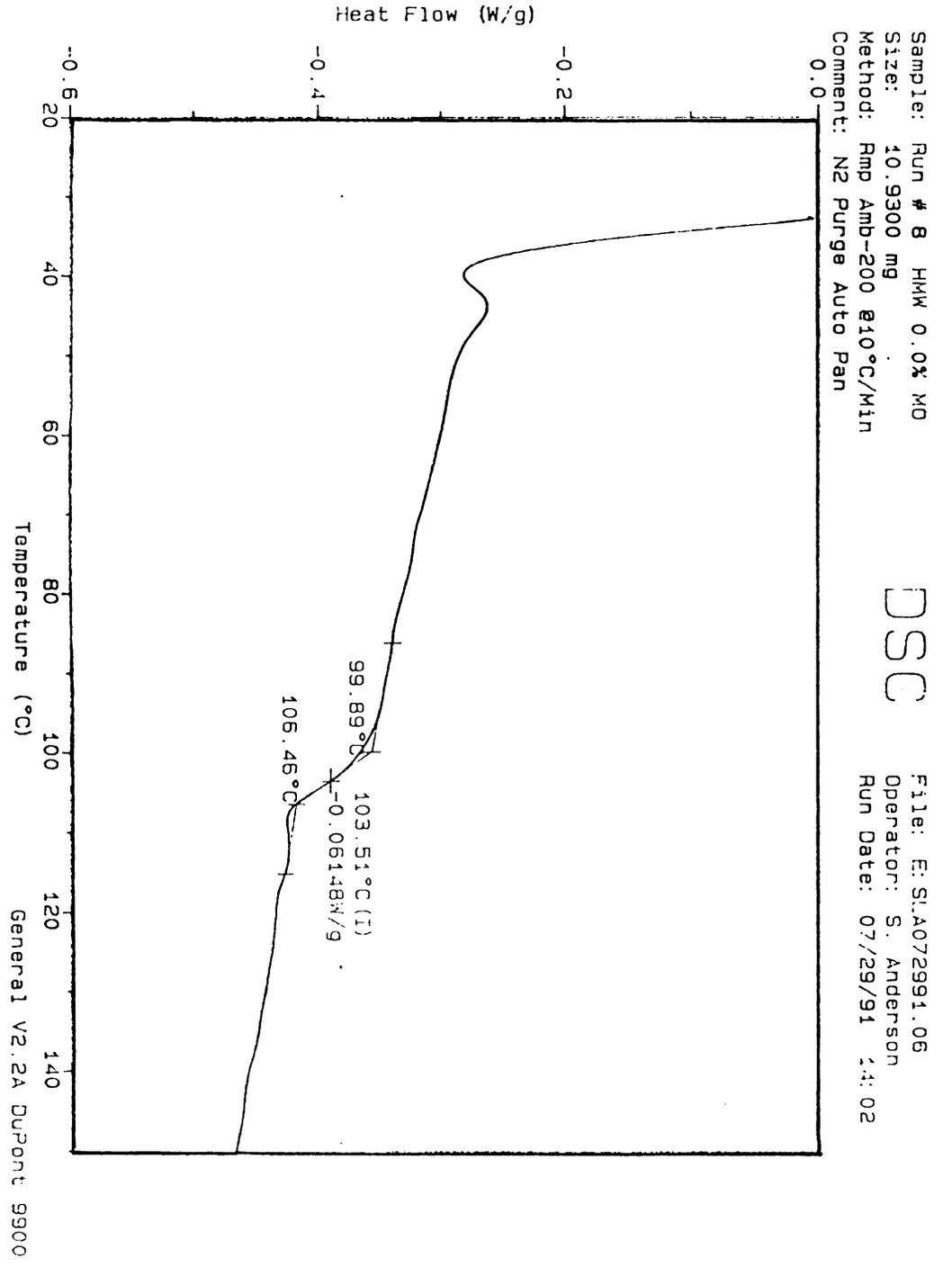
Sample: Run # 8 HMW 0.0% MO
Size: 10.9300 mg
Method: Rmp Amb-200 @10°C/Min
Comment: N2 Purge Auto Pan
DSC
File: E:\SLA072991.06
Operator: S. Anderson
Run Date: 07/29/91 14:02
Heat Flow (W/g)
-0.6
-0.4
-0.2
0.0
20
40
60
80
100
120
140
Temperature (°C)
99.89°C
103.51°C (I)
-0.06148W/g
106.46°C
General V2.2A DuPont 9900

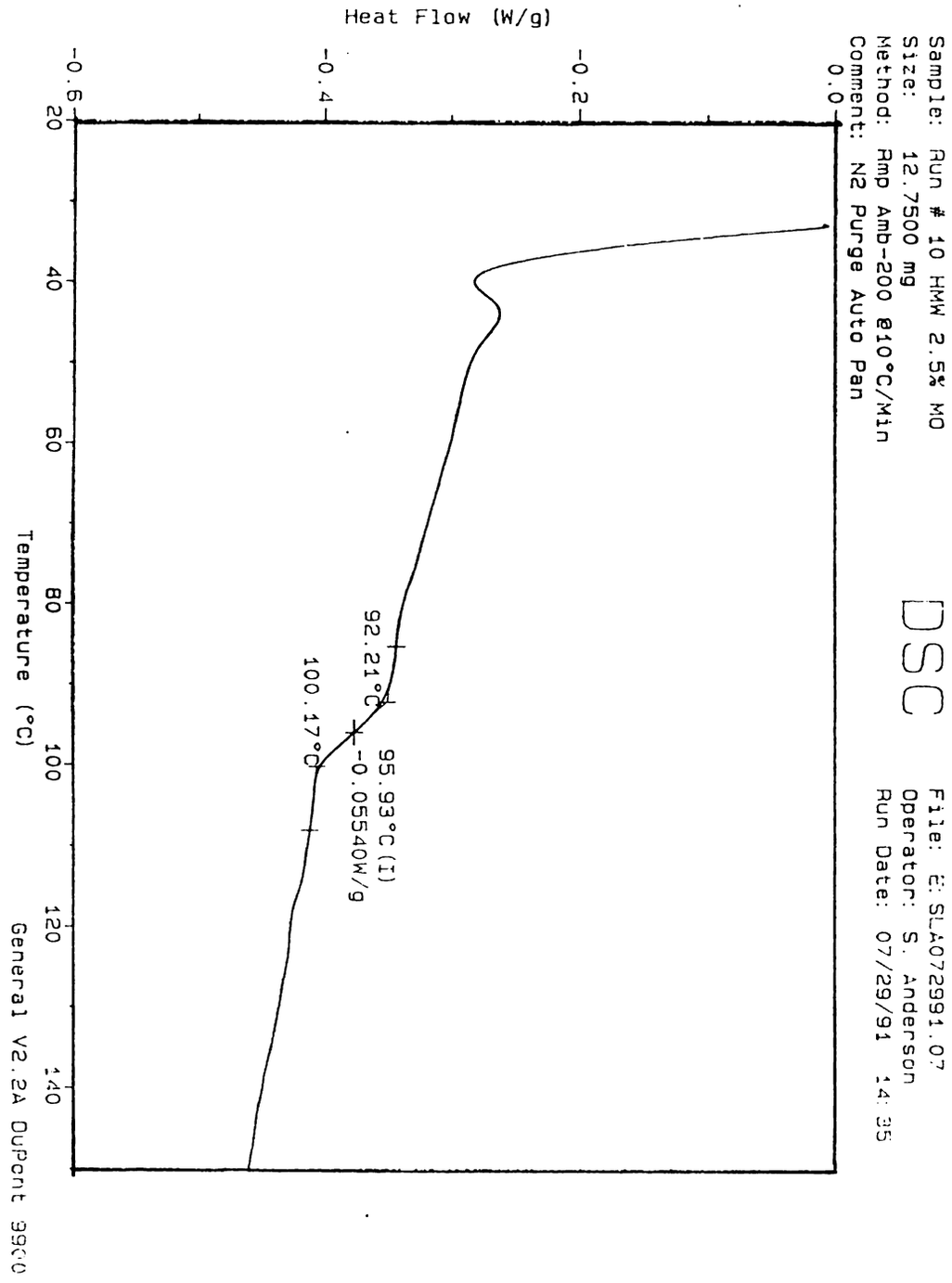
Sample: Run # 10 HMW 2.5% MO
Size: 12.7500 mg
Method: Amb-200 @10°C/Min
Comment: N2 Purge Auto Pan
DSC
File: E:\SLA072991.07
Operator: S. Anderson
Run Date: 07/29/91 14:35
Heat Flow (W/g)
-0.6
-0.4
-0.2
0.0
20
40
60
80
100
120
140
Temperature (°C)
92.21°C
100.17°C
95.93°C (I)
-0.05540W/g
General V2.2A DuPont 990

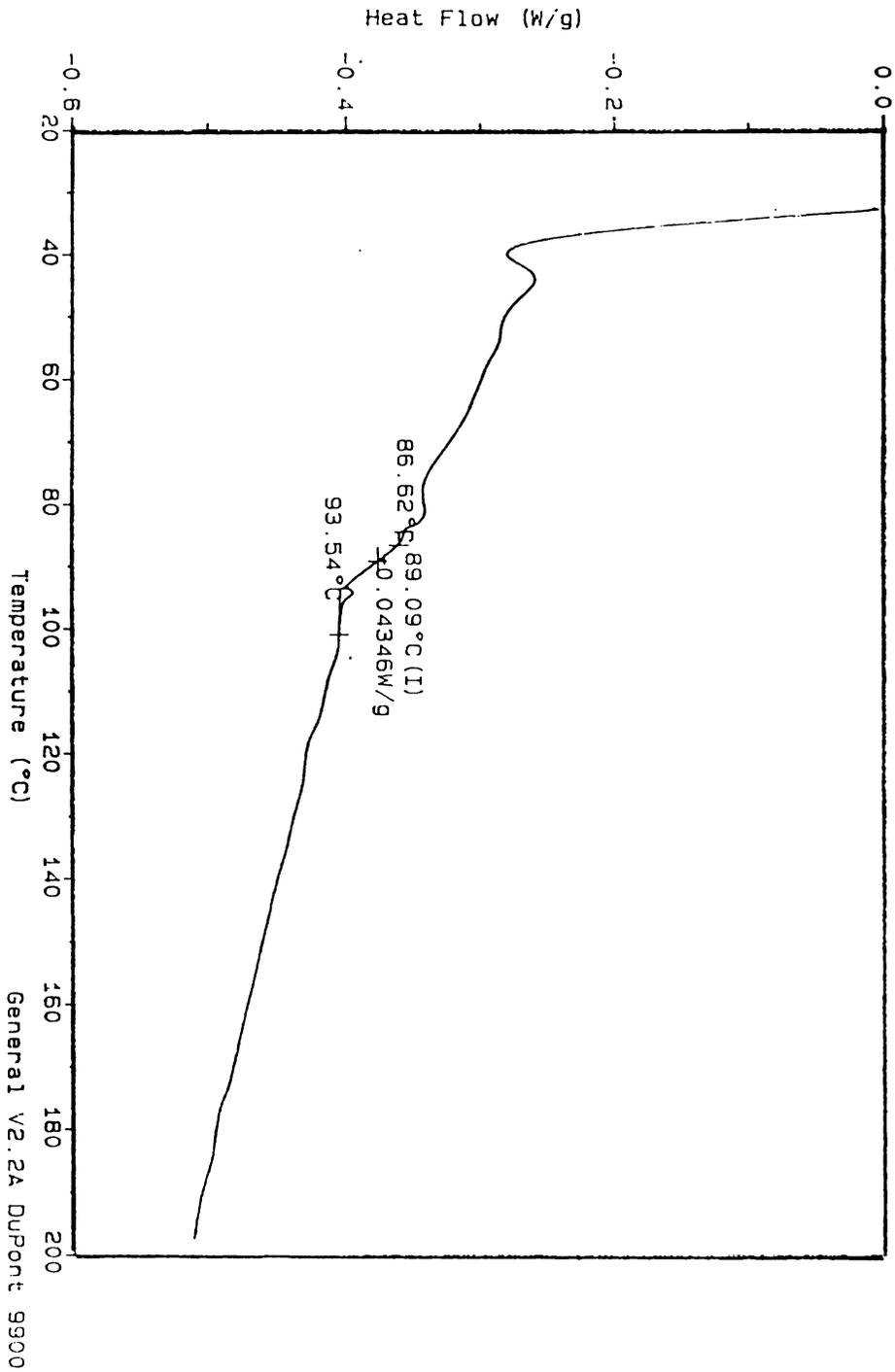
Sample: Run # 7 HMW 5.0% MO
Size: 12.3550 mg
Method: Rmp Amb-200 @10°C/Min
Comment: N2 Purge Auto Pan
DSC
File: E:SLA072991.08
Operator: S. Anderson
Run Date: 07/29/91 15:07
Heat Flow (W/g)
-0.0
-0.2
-0.4
-0.6
86.62°C
89.09°C(I)
0.04346W/g
93.54°C
20
40
60
80
100
120
140
160
180
200
Temperature (°C)
General V2.2A DuPont 9900

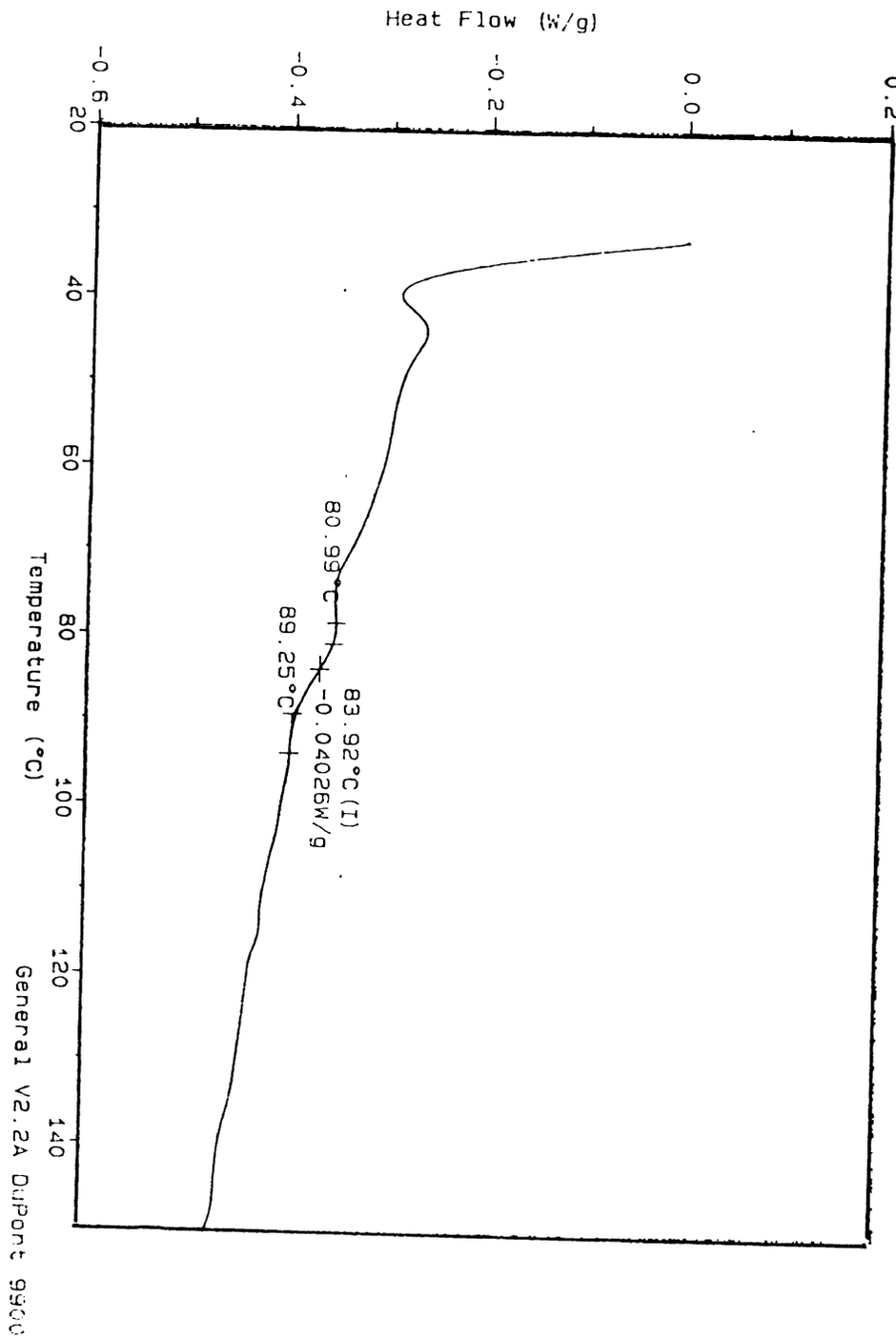
Heat Flow (W/g)
-0.6
-0.4
-0.2
0.0
0.2
20
40
60
80
100
120
140
Temperature (°C)
80.99°C
89.25°C
83.92°C (I)
-0.04026W/g
DSC
Sample: Run # 4 HMW 7.5% MO
Size: 9.3650 mg
Method: Amb-200 @10°C/Min
Comment: N2 Purge Auto Pan
File: E:SLA072991.09
Operator: S. Anderson
Run Date: 07/29/91 15:40
General V2.2A DuPont 9900

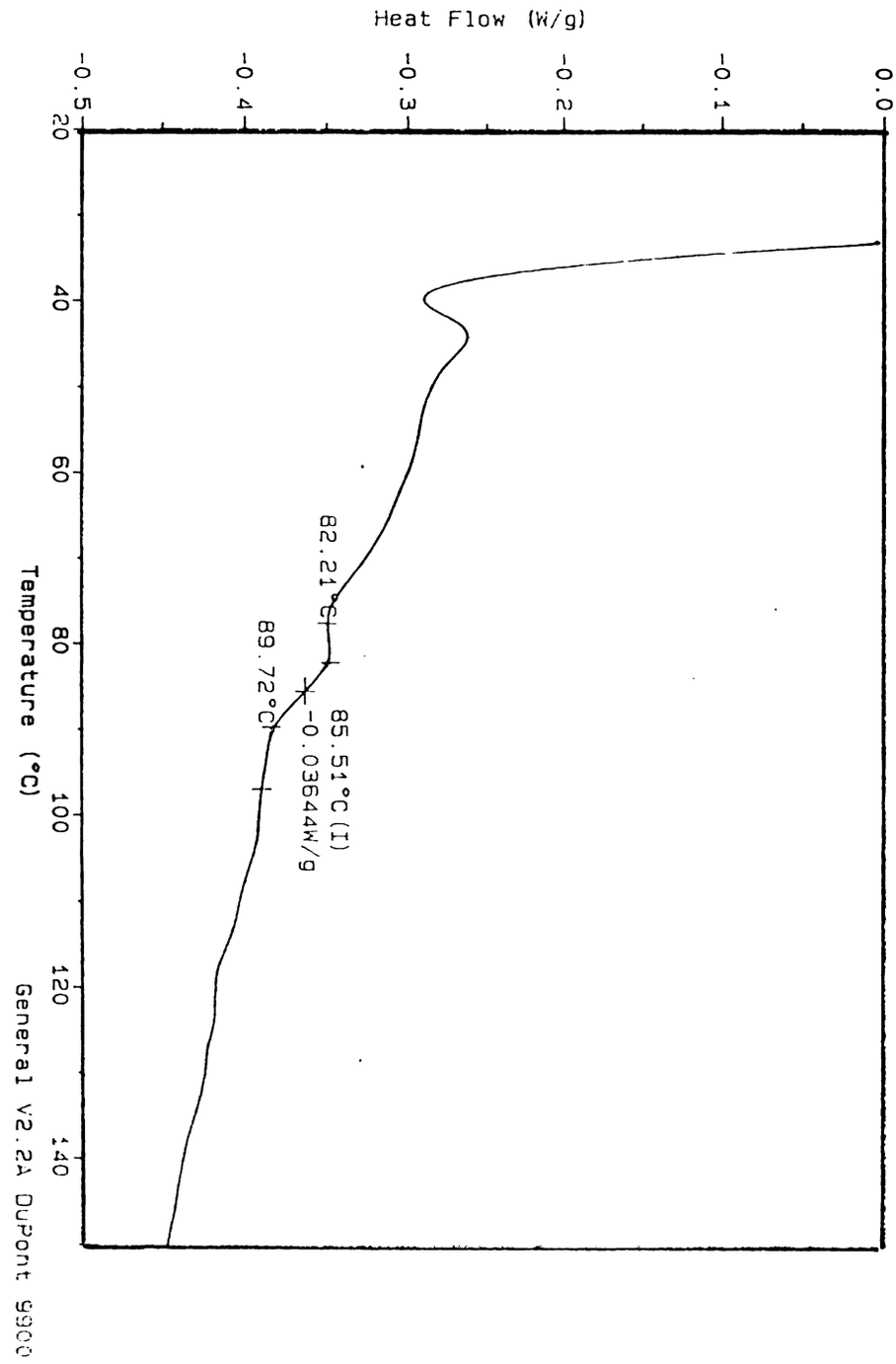
Sample: Run # 2 HMW 10.0% MO
Size: 12.3850 mg
Method: Rmp Amb-200 @10°C/Min
Comment: N2 Purge Auto Pan
DSC
File: E:SLA072991.11
Operator: S. Anderson
Run Date: 07/29/91 16:47
Heat Flow (W/g)
0.0
-0.1
-0.2
-0.3
-0.4
-0.5
82.21°C
89.72°C
85.51°C (I)
-0.03644W/g
20
40
60
80
100
120
140
Temperature (°C)
General V2.2A DuPont 9900

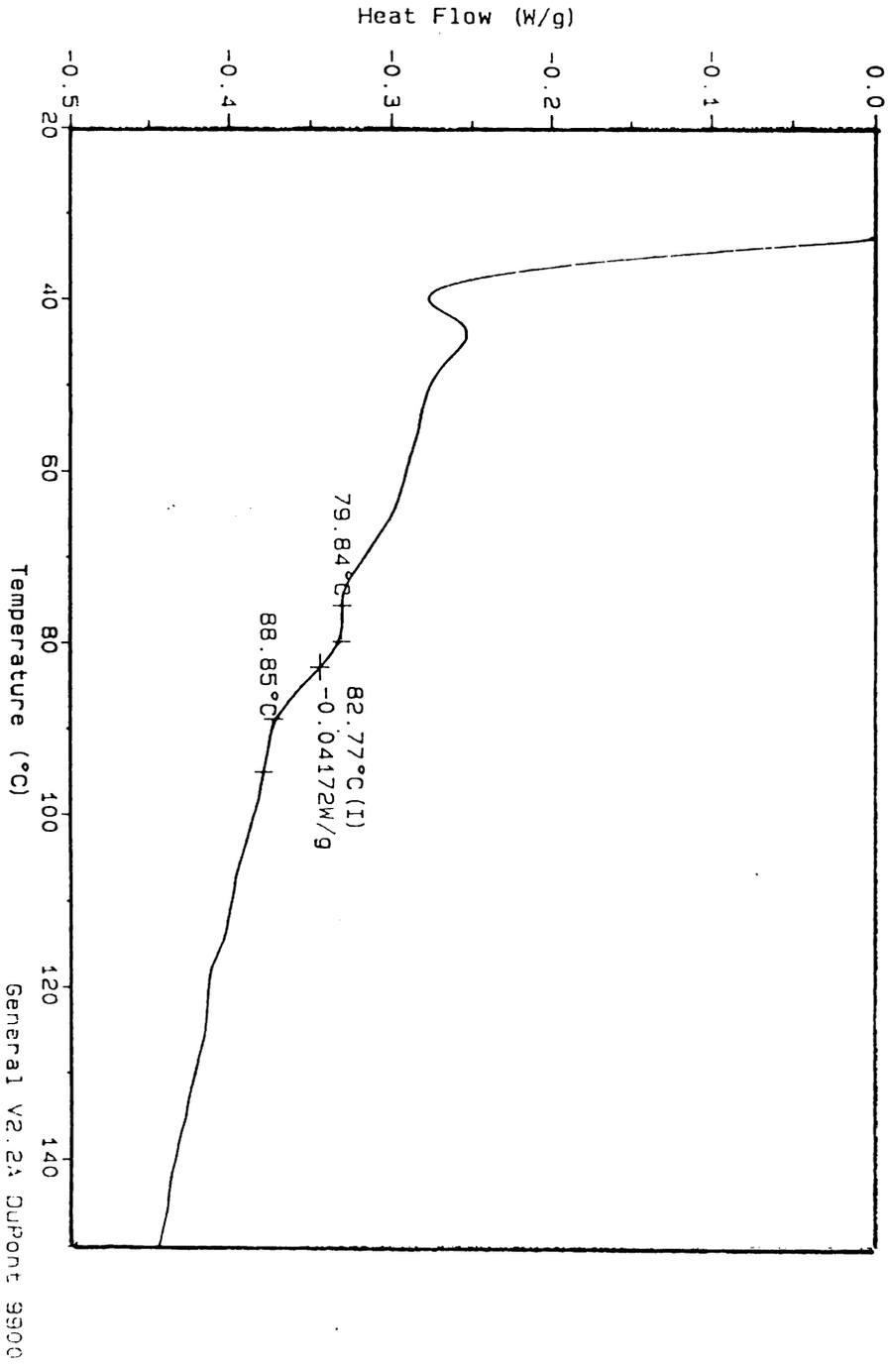
Sample: Run # 3 HMW 10.0% MO
Size: 11.2050 mg
Method: Rmp Amb-200 @10°C/Min
Comment: N2 Purge Auto Pan
DSC
File: E:SLA072991.10
Operator: S. Anderson
Run Date: 07/29/91 16:14
Heat Flow (W/g)
-0.0
-0.1
-0.2
-0.3
-0.4
-0.5
79.84°C
82.77°C (I)
-0.04172W/g
88.85°C
20
40
60
80
100
120
140
Temperature (°C)
General V2.2A DuPont 9900

APPENDIX D

FLEXURAL PROPERTIES

Appendix D-1. Flexural Properties of 40,000 MW Blends

DESIGNED THERMOPLASTICS RESEARCH 03/06/91

Test method: BLENDS STD FLEX
Sample ID: RUN #11 LMW 0% MO

Test date: Wed, Mar 06, 1991
Operator: SANDIE

Calculation inputs;

Span 1	2.00 In
Span 2	1.00 In
Brk % Drop	10 %
Brk Drop Elong	0.001 In
Brk Load Value	50.00 Lb
Yield Angle	0.00 deg
Yield % SegLen	20.00 %
Slope Tol.	99.00 %
Slope Seglen	5.00 %
Min Slope Load	1.00 Lb

Test inputs;

Initial Speed	0.05 In/Min
% Strain Limit	5.0 %
Load Limit MI	1000 Lb
Ext Limit MI	20.0 In
Time Limit	10000 Sec
Brk Sensitivity	75 %

Sample RUN #11 LMW 0% MO # 0 Ref : (None)

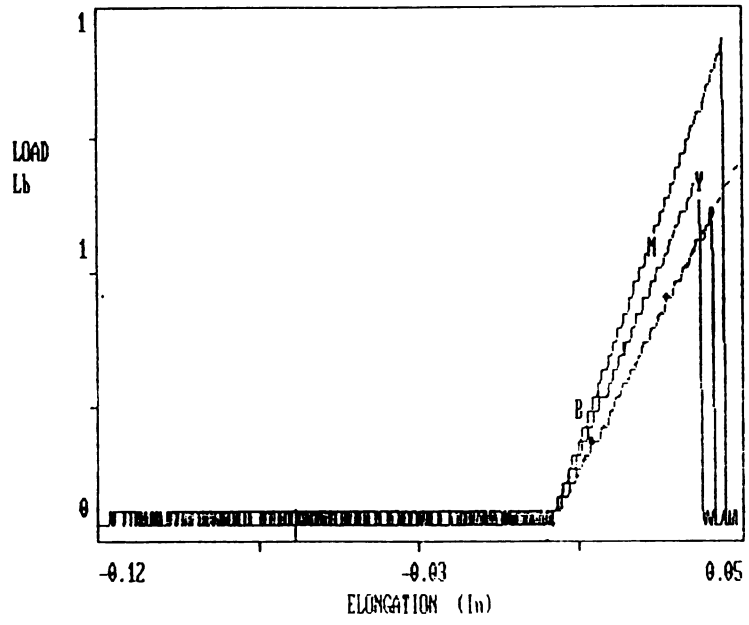

Test method: BLENDS STD FLEX
Sample ID: RUN #11 LMW 0% MO

Test date: Wed, Mar 06, 1991
Operator: SANDIE

Sample	Width (b) In	Depth (d) In	Flex Strength PSI	%Strn @ Flex St %	Modulus PSI
1	0.320	0.060	1608	0.4	416051
2	0.365	0.065	1306	0.4	354741
3	0.360	0.070	1598	0.5	343111
4					
5					
Mean	0.348	0.065	1504	0.4	371301
Std Dev	0.025	0.005	172	0.1	39189
% COV	7.081	7.692	11	14.1	11

DESIGNED THERMOPLASTICS RESEARCH 03/06/91

Test method: BLENDS STD FLEX
Sample ID: RUN #20 LMW 2.5% MO

Test date: Wed, Mar 06, 1991
Operator: SANDIE

Calculation inputs;

Span 1	2.00 In
Span 2	1.00 In
Brk % Drop	10 %
Brk Drop Elong	0.001 In
Brk Load Value	50.00 Lb
Yield Angle	0.00 deg
Yield % SegLen	20.00 %
Slope Tol.	99.00 %
Slope Seglen	5.00 %
Min Slope Load	1.00 Lb

Test inputs;

Initial Speed	0.05 In/Min
% Strain Limit	5.0 %
Load Limit HI	1000 Lb
Ext Limit HI	20.0 In
Time Limit	10000 Sec
Brk Sensitivity	75 %

Sample RUN #20 LMW 2.5% MO # 0 Ref : <None>

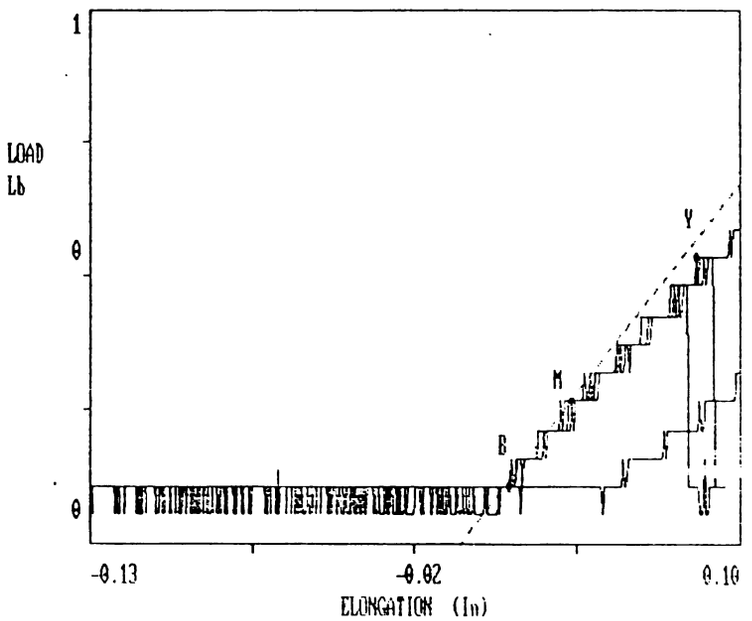

DESIGNED THERMOPLASTICS RESEARCH 03/06/91

Test method: BLENDS STD FLEX
Sample ID: RUN #20 LMW 2.5% MO

Test date: Wed, Mar 06, 1991
Operator: SANDIE

Sample	Width (b) In	Depth (d) In	Flex Strength PSI	%Strn @ Flex St %	Modulus PSI
1	0.432	0.033	1712	0.4	435901
2	0.475	0.032	1490	0.4	383771
3	0.417	0.030	1717	0.6	521011
4	0.450	0.029	2341	0.4	566651
5					
Mean	0.444	0.031	1815	0.4	476833
Std Dev	0.025	0.002	366	0.1	82371
% COV	5.628	5.889	20	19.2	17

DESIGNED THERMOPLASTICS RESEARCH 03/06/91

Test method: BLENDS STD FLEX
Sample ID: RUN #12 LMW 5% MO

Test date: Wed, Mar 06, 1991
Operator: SANDIE

Calculation inputs;

Span 1	2.00 In
Span 2	1.00 In
Brk % Drop	10 %
Brk Drop Elong	0.001 In
Brk Load Value	50.00 Lb
Yield Angle	0.00 deg
Yield % SegLen	20.00 %
Slope Tol.	99.00 %
Slope Seglen	5.00 %
Min Slope Load	1.00 Lb

Test inputs;

Initial Speed	0.05 In/Min
% Strain Limit	5.0 %
Load Limit HI	1000 Lb
Ext Limit HI	20.0 In
Time Limit	10000 Sec
Brk Sensitivity	75 %

Sample RUN #12 LMW 5% MO # 0 Ref : <None>

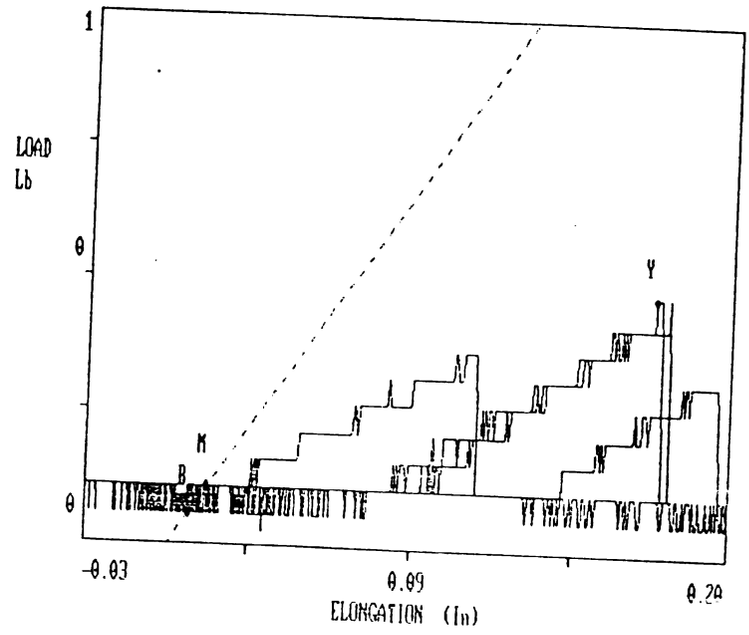

DESIGNED THERMOPLASTICS RESEARCH 03/06/91

Test method: BLENDS STD FLEX
Sample ID: RUN #12 LMW 5% MO

Test date: Wed, Mar 06, 1991
Operator: SANDIE

Sample	Width (b) In	Depth (d) In	Flex Strength PSI	%Strn @ Flex St %	Modulus PSI
1	0.384	0.031	1964	0.8	694732
2	0.330	0.030	1898	0.5	493501
3	0.386	0.026	2778	0.7	798003
4	0.350	0.033	1268	0.9	701999
5					
Mean	0.362	0.030	1977	0.7	672059
Std Dev	0.027	0.003	619	0.2	128004
% COV	7.516	9.813	31	27.3	19

DESIGNED THERMOPLASTICS RESEARCH 03/06/91

Test method: BLENDS STD FLEX
Sample ID: RUN #19 LMW 7.5% MO

Test date: Wed, Mar 06, 1991
Operator: SANDIE

Calculation inputs;

Span 1	2.00 In
Span 2	1.00 In
Brk % Drop	10 %
Brk Drop Elong	0.001 In
Brk Load Value	50.00 Lb
Yield Angle	0.00 deg
Yield % SegLen	20.00 %
Slope Tol.	99.00 %
Slope Seglen	5.00 %
Min Slope Load	1.00 Lb

Test inputs;

Initial Speed	0.05 In/Min
% Strain Limit	5.0 %
Load Limit HI	1000 Lb
Ext Limit HI	20.0 In
Time Limit	10000 Sec
Brk Sensitivity	75 %

Sample RUN #19 LMW 7.5% MO # 0 Ref : (None)

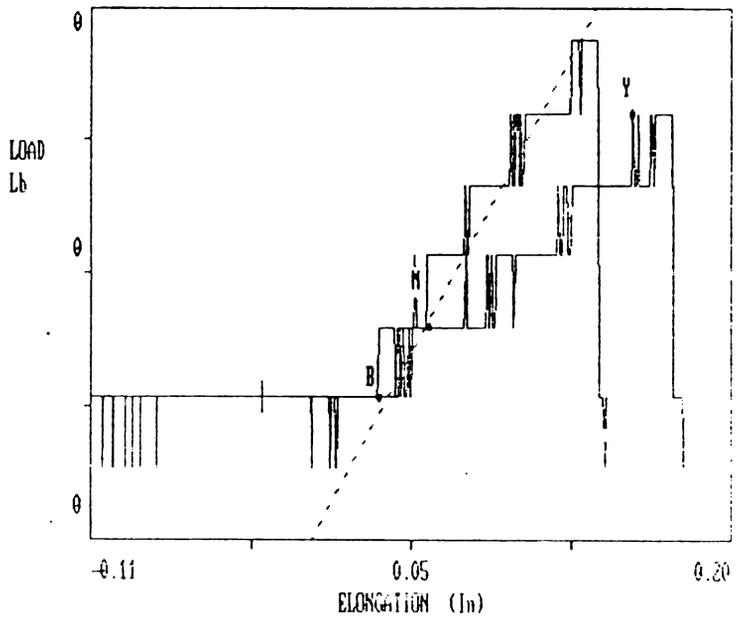

Test method: BLENDS STD FLEX
Sample ID: RUN #19 LMW 7.5% MO

Test date: Wed, Mar 06, 1991
Operator: SANDIE

Sample	Width (b) In	Depth (d) In	Flex Strength PSI	%Strn @ Flex St %	Modulus PSI
1	0.360	0.025	2148	0.6	526017
2	0.430	0.024	2276	0.4	541990
3					
4					
5					
Mean	0.395	0.025	2212	0.5	534004
Std Dev	0.049	0.001	91	0.1	11295
% COV	12.531	2.886	4	17.9	2

DESIGNED THERMOPLASTICS RESEARCH 03/06/91

Test method: BLENDS STD FLEX
Sample ID: RUN #5 LMW 10% MO

Test date: Wed, Mar 06, 1991
Operator: SANDIE

Calculation inputs;

Span 1	2.00 In
Span 2	1.00 In
Brk % Drop	10 %
Brk Drop Elong	0.001 In
Brk Load Value	50.00 Lb
Yield Angle	0.00 deg
Yield % SegLen	20.00 %
Slope Tol.	99.00 %
Slope Seglen	5.00 %
Min Slope Load	1.00 Lb

Test inputs;

Initial Speed	0.05 In/Min
% Strain Limit	5.0 %
Load Limit HI	1000 Lb
Ext Limit HI	20.0 In
Time Limit	10000 Sec
Brk Sensitivity	75 %

Sample RUN #5 LMW 10% MO # 0 Ref : (None)

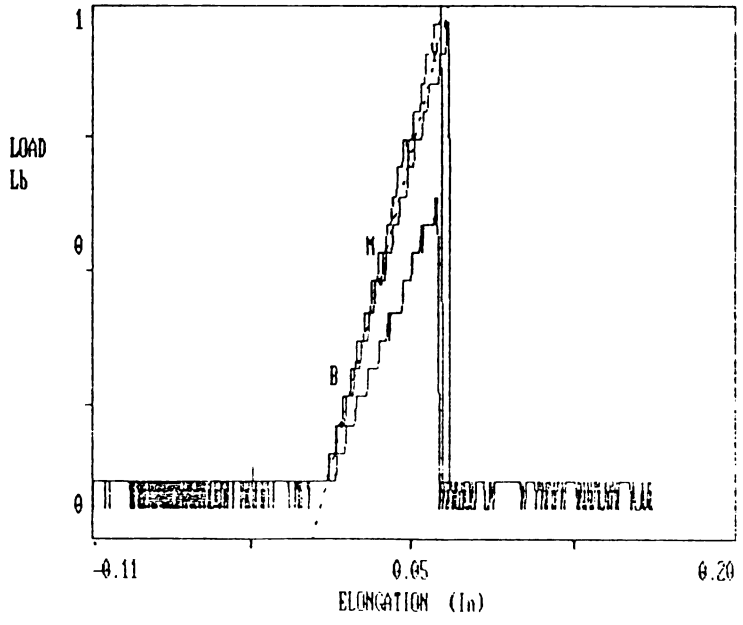

DESIGNED THERMOPLASTICS RESEARCH 03/06/91

Test method: BLENDS STD FLEX
Sample ID: RUN #5 LMW 10% MO

Test date: Wed, Mar 06, 1991
Operator: SANDIE

Sample	Width (b) In	Depth (d) In	Flex Strength PSI	%Strn @ Flex St %	Modulus PSI
1	0.440	0.047	1456	0.5	331777
2	0.430	0.047	1611	0.4	386343
3	0.400	0.045	1193	0.4	332211
4					
5					
Mean	0.427	0.046	1421	0.4	350110
Std Dev	0.025	0.001	211	0.0	31379
% COV	5.898	2.492	15	7.0	9

Appendix D-2. Flexural Properties of 270,000 MW Blends

DESIGNED THERMOPLASTICS RESEARCH . 03/06/91

Test method: BLENDS STD FLEX
Sample ID: RUN #8 HMW 0% MO

Test date: Wed, Mar 06, 1991
Operator: SANDIE

Calculation inputs;

Span 1	2.00 In
Span 2	1.00 In
Brk % Drop	10 %
Brk Drop Elong	0.001 In
Brk Load Value	50.00 Lb
Yield Angle	0.00 deg
Yield % SegLen	20.00 %
Slope Tol.	99.00 %
Slope Seglen	5.00 %
Min Slope Load	1.00 Lb

Test inputs;

Initial Speed	0.05 In/Min
% Strain Limit	5.0 %
Load Limit HI	1000 Lb
Ext Limit HI	20.0 In
Time Limit	10000 Sec
Brk Sensitivity	75 %

Sample RUN #8 HMW 0% MO # 0 Ref : <None>

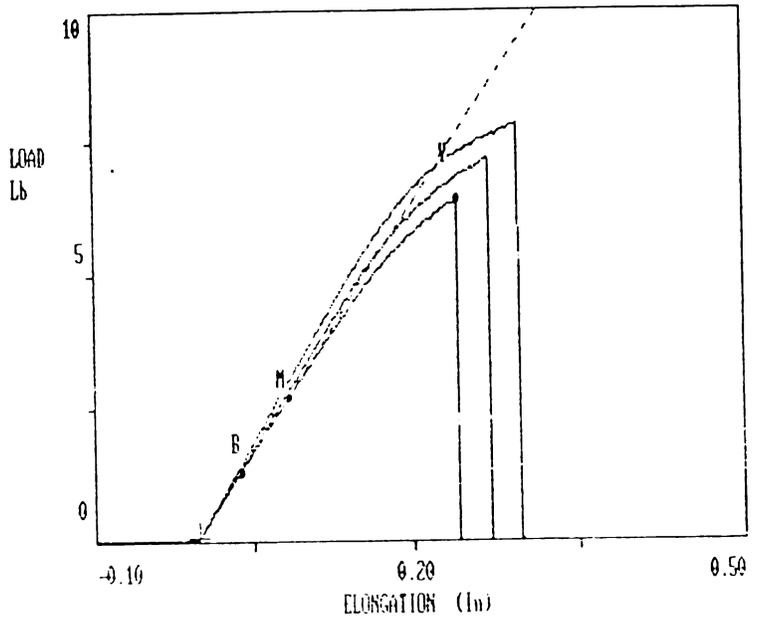

Test method: BLENDS STD FLEX
Sample ID: RUN #8 HMW 0% MO

Test date: Wed, Mar 06, 1991
Operator: SANDIE

Sample	Width (b) In	Depth (d) In	Flex Strength PSI	%Strn @ Flex St %	Modulus PSI
1	0.370	0.070	10705	2.6	498512
2	0.375	0.070	12886	3.1	550146
3	0.365	0.070	12158	2.8	528898
4					
5					
Mean	0.370	0.070	11916	2.8	525852
Std Dev	0.005	0.000	1110	0.3	25951
% COV	1.351	0.000	9	10.1	5

DESIGNED THERMOPLASTICS RESEARCH 03/06/91

Test method: BLENDS STD FLEX
Sample ID: RUN #10 HMW 2.5% MO

Test date: Wed, Mar 06, 1991
Operator: SANDIE

Calculation inputs;

Span 1	2.00 In
Span 2	1.00 In
Brk % Drop	10 %
Brk Drop Elong	0.001 In
Brk Load Value	50.00 Lb
Yield Angle	0.00 deg
Yield % SegLen	20.00 %
Slope Tol.	99.00 %
Slope Seglen	5.00 %
Min Slope Load	1.00 Lb

Test inputs;

Initial Speed	0.05 In/Min
% Strain Limit	5.0 %
Load Limit HI	1000 Lb
Ext Limit HI	20.0 In
Time Limit	10000 Sec
Brk Sensitivity	75 %

Sample RUN #10 HMW 2.5% MO # 0 Ref : (None)

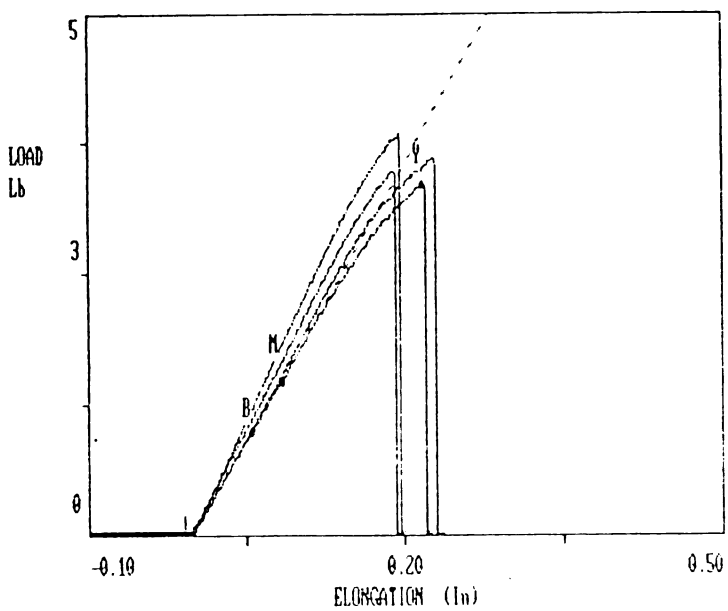

Test method: BLENDS STD FLEX
Sample ID: RUN #10 HMW 2.5% MO

Test date: Wed, Mar 06, 1991
Operator: SANDIE

Sample	Width (b) In	Depth (d) In	Flex Strength PSI	%Strn @ Flex St %	Modulus PSI
1	0.300	0.062	8799	2.0	499032
2	0.320	0.066	8320	1.9	477882
3	0.300	0.062	9148	1.8	563211
4	0.287	0.064	9249	2.2	490476
5					
Mean	0.302	0.064	8879	2.0	507650
Std Dev	0.014	0.002	420	0.2	38045
% COV	4.515	3.016	5	8.6	7

DESIGNED THERMOPLASTICS RESEARCH 03/06/91

Test method: BLENDS STD FLEX
Sample ID: RUN #7 HMW 5% MO

Test date: Wed, Mar 06, 1991
Operator: SANDIE

Calculation inputs;

Span 1	2.00 In
Span 2	1.00 In
Brk % Drop	10 %
Brk Drop Elong	0.001 In
Brk Load Value	50.00 Lb
Yield Angle	0.00 deg
Yield % SegLen	20.00 %
Slope Tol.	99.00 %
Slope Seglen	5.00 %
Min Slope Load	1.00 Lb

Test inputs;

Initial Speed	0.05 In/Min
% Strain Limit	5.0 %
Load Limit MI	1000 Lb
Ext Limit MI	20.0 In
Time Limit	10000 Sec
Brk Sensitivity	75 %

Sample RUN #7 HMW 5% MO # 0 Ref : (None)

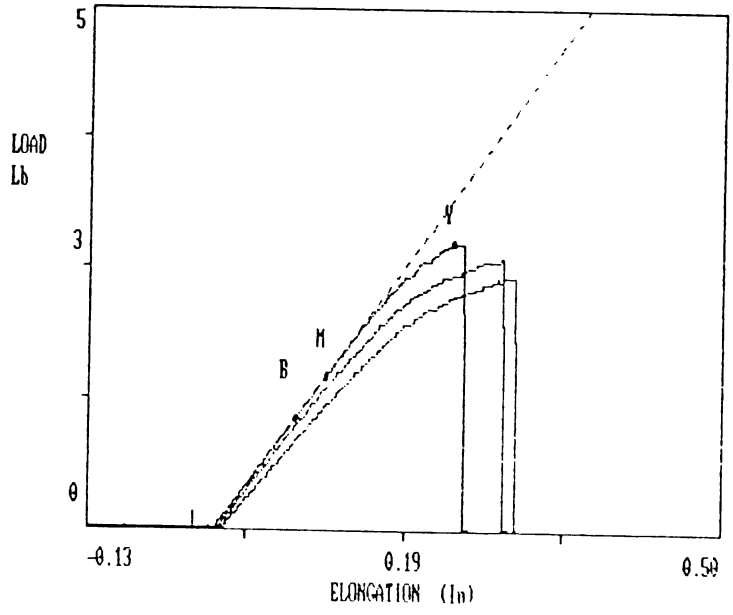

DESIGNED THERMOPLASTICS RESEARCH 03/06/91

Test method: BLENDS STD FLEX
Sample ID: RUN #7 HMW 5% MO

Test date: Wed, Mar 06, 1991
Operator: SANDIE

Sample	Width (b) In	Depth (d) In	Flex Strength PSI	%Strn @ Flex St %	Modulus PSI
1	0.315	0.054	9031	1.9	550211
2	0.287	0.054	8757	2.3	486384
3	0.300	0.053	9366	2.2	566741
4					
5					
Mean	0.301	0.054	9051	2.2	534445
Std Dev	0.014	0.001	305	0.2	42435
% COV	4.660	1.076	3	10.7	8

DESIGNED THERMOPLASTICS RESEARCH 03/06/91

Test method: BLENDS STD FLEX
Sample ID: RUN #4 HMW 7.5% MO

Test date: Wed, Mar 06, 1991
Operator: SANDIE

Calculation inputs;

Span 1	2.00 In
Span 2	1.00 In
Brk % Drop	10 %
Brk Drop Elong	0.001 In
Brk Load Value	50.00 Lb
Yield Angle	0.00 deg
Yield % SegLen	20.00 %
Slope Tol.	99.00 %
Slope Seglen	5.00 %
Min Slope Load	1.00 Lb

Test inputs;

Initial Speed	0.05 In/Min
% Strain Limit	5.0 %
Load Limit HI	1000 Lb
Ext Limit HI	20.0 In
Time Limit	10000 Sec
Brk Sensitivity	75 %

Sample RUN #4 HMW 7.5% MO # 0 Ref : (None)

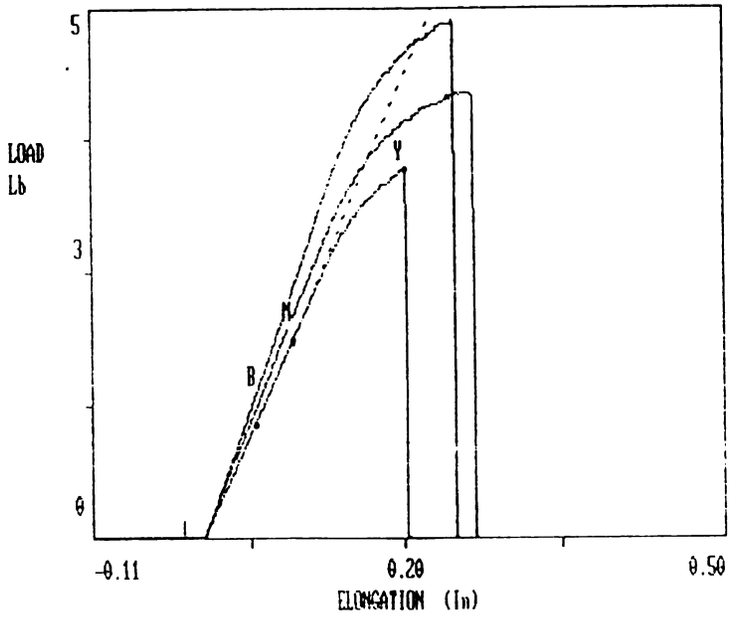

Test method: BLENDS STD FLEX
Sample ID: RUN #4 HMW 7.5% MO

Test date: Wed, Mar 06, 1991
Operator: SANDIE

Sample	Width (b) In	Depth (d) In	Flex Strength PSI	%Strn @ Flex St %	Modulus PSI
1	0.270	0.069	8144	2.1	501980
2	0.384	0.069	8061	2.5	442257
3	0.325	0.071	7716	2.6	430950
4					
5					
Mean	0.326	0.070	7974	2.4	458396
Std Dev	0.057	0.001	226	0.3	38166
% COV	17.470	1.657	3	12.8	8

DESIGNED THERMOPLASTICS RESEARCH 03/06/91

Test method: BLENDS STD FLEX
Sample ID: RUN #3 HMW 10% MO

Test date: Wed, Mar 06, 1991
Operator: SANDIE

Calculation inputs;

Span 1	2.00 In
Span 2	1.00 In
Brk % Drop	10 %
Brk Drop Elong	0.001 In
Brk Load Value	50.00 Lb
Yield Angle	0.00 deg
Yield % SegLen	20.00 %
Slope Tol.	99.00 %
Slope Seglen	5.00 %
Min Slope Load	1.00 Lb

Test inputs;

Initial Speed	0.05 In/Min
% Strain Limit	5.0 %
Load Limit HI	1000 Lb
Ext Limit HI	20.0 In
Time Limit	10000 Sec
Brk Sensitivity	75 %

Sample RUN #3 HMW 10% MO # 0 Ref : <None>

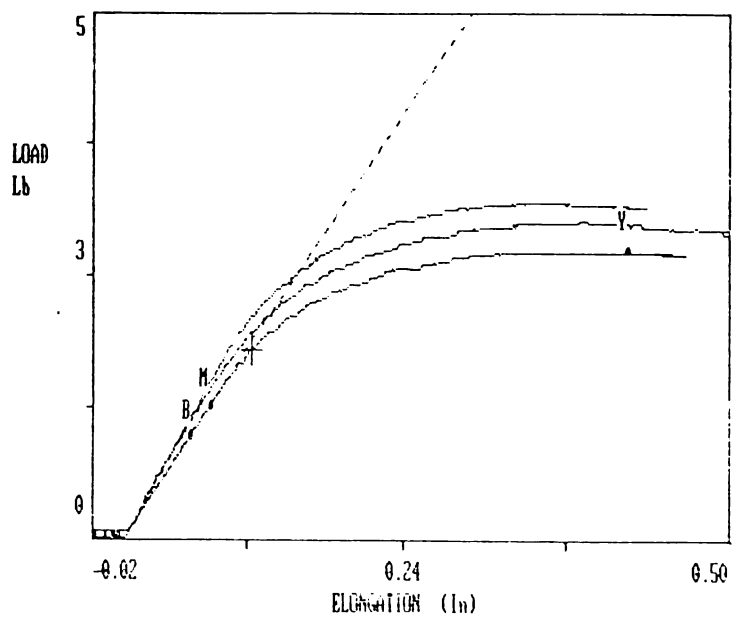

Test method: BLENDS STD FLEX
Sample ID: RUN #3 HMW 10% MO

Test date: Wed, Mar 06, 1991
Operator: SANDIE

Sample	Width (b) In	Depth (d) In	Flex Strength PSI	%Strn @ Flex St %	Modulus PSI
1	0.294	0.068	6102	4.3	370651
2	0.320	0.069	5973	3.9	368544
3	0.350	0.063	6957	3.1	457247
4					
5					
Mean	0.321	0.067	6344	3.8	398814
Std Dev	0.028	0.003	535	0.6	50615
% COV	8.721	4.822	8	14.4	13

APPENDIX E

TORQUE DATA

Appendix E-1. Torque Data for 40,000 MW Blends

Torque 40 MW

	0% MO		0% MO		6% MO		6% MO		6% MO		8% MO		8% Mo		8% MO	
	Torque (m-g)	Torque (Nm)	Temp(C)	Torque (m-g)	Torque (Nm)	Temp (C)	Torque (m-g)	Torque (Nm)	Temp (C)	Torque (m-g)	Torque (Nm)	Temp
1	16.000	0.157	146.000	12.000	0.118	176.000	11.000	0.108	183.000	11.000	0.108	166
2	20.000	0.196	144.000	14.000	0.137	173.000	11.000	0.108	180.000	12.000	0.118	165
3	29.000	0.284	143.000	13.000	0.128	170.000	14.000	0.137	178.000	10.000	0.098	162
4	39.000	0.383	141.000	18.000	0.177	167.000	16.000	0.157	174.000	15.000	0.147	158
5	41.000	0.402	139.000	18.000	0.177	164.000	15.000	0.147	170.000	14.000	0.137	156
6	56.000	0.549	138.000	22.000	0.216	162.000	18.000	0.177	167.000	17.000	0.167	154
7	62.000	0.608	137.000	25.000	0.245	160.000	20.000	0.196	165.000	20.000	0.196	152
8	69.000	0.677	136.000	25.000	0.245	157.000	17.000	0.167	162.000	17.000	0.167	149
9	77.000	0.755	135.000	25.000	0.245	155.000	22.000	0.216	160.000	22.000	0.216	147
10	101.000	0.891	134.000	31.000	0.304	152.000	23.000	0.226	157.000	20.000	0.196	147
11	120.000	1.177	132.000	34.000	0.334	150.000	25.000	0.245	154.000	25.000	0.245	144
12	122.000	1.197	131.000	35.000	0.343	148.000	28.000	0.275	152.000	28.000	0.255	143
13	141.000	1.383	131.000	39.000	0.383	148.000	31.000	0.304	150.000	31.000	0.304	144
14	160.000	1.570	131.000	40.000	0.392	144.000	36.000	0.353	148.000	34.000	0.334	142
15	182.000	1.785	129.000	46.000	0.451	141.000	38.000	0.373	145.000	34.000	0.334	141
16	207.000	2.031	128.000	52.000	0.510	140.000	36.000	0.353	143.000	35.000	0.343	141
17	228.000	2.237	127.000	61.000	0.598	138.000	46.000	0.451	141.000	41.000	0.402	140
18	251.000	2.462	127.000	63.000	0.618	136.000	46.000	0.451	139.000	37.000	0.363	139
19	279.000	2.737	126.000	70.000	0.687	134.000	50.000	0.490	137.000	40.000	0.392	138
20	302.000	2.963	125.000	78.000	0.765	132.000	59.000	0.579	135.000	44.000	0.432	138
21	338.000	3.316	124.000	82.000	0.804	131.000	67.000	0.657	133.000	48.000	0.471	138
22	340.000	3.335	123.000	92.000	0.903	129.000	76.000	0.746	131.000	54.000	0.530	137
23			122.000	100.000	0.981	127.000	79.000	0.775	130.000	55.000	0.540	135
24				111.000	1.089	126.000	90.000	0.883	128.000	54.000	0.530	135
25				123.500	1.207	125.000	98.000	0.961	126.000	57.000	0.559	133
26				129.000	1.265	124.000	107.000	1.050	125.000	65.000	0.638	133
27				141.000	1.383	123.000	117.000	1.148	124.000	69.000	0.677	133
28							122.000	1.197	124.000	70.000	0.687	133
29										75.000	0.736	132
30										79.000	0.775	131
31										82.000	0.804	130
32										85.000	0.834	129
33										88.000	0.863	129
34										91.000	0.893	129
35										95.000	0.932	128
36										96.000	0.942	128
37										100.000	0.981	129
38										107.000	1.050	128
39										109.000	1.069	127
40										114.000	1.118	126
41										117.000	1.148	126
42										121.000	1.187	125
43												

Appendix E-2. Torque Data for 128,000 MW Blends

TORQUE 128 MW DATA

	0% MO		0% MO		2% MO		2% MO		4% MO		4% MO		8% MO		8% MO	
	Torque (m-g)	Torque (Nm)	Temp (C)	Torque (m-g)	Torque (m-g)	Temp (C)	Torque (m-g)	Torque (Nm)	Temp (C)	Torque (m-g)	Torque (Nm)	Temp (C)
1																
2	227.000	2.227	200.000	339.000	3.326	202.000	299.000	2.933	202.000	99.000	0.971	300
3	244.000	2.394	196.000	365.000	3.581	199.000	312.000	3.061	199.000	102.000	1.001	000
4	266.000	2.609	193.000	391.000	3.836	195.000	339.000	3.326	197.000	109.000	1.069	000
5	287.000	2.815	189.000	414.000	4.061	192.000	358.000	3.512	194.000	111.000	1.089	000
6	312.000	3.061	185.000	443.000	4.346	189.000	382.000	3.747	192.000	125.000	1.226	000
7	338.000	3.316	182.000	480.000	4.709	186.000	408.000	3.983	189.000	130.000	1.275	000
8	368.000	3.590	178.000	519.000	5.091	183.000	436.000	4.277	186.000	143.000	1.403	000
9	398.000	3.885	175.000	555.000	5.445	180.000	458.000	4.473	184.000	152.000	1.491	000
10	423.000	4.150	172.000	593.000	5.817	177.000	489.000	4.797	181.000	165.000	1.619	000
11	455.000	4.464	169.000	633.000	6.210	174.000	520.000	5.101	178.000	177.000	1.736	000
12	484.000	4.748	166.000	665.000	6.524	171.000	555.000	5.445	176.000	191.000	1.874	000
13	519.000	5.091	163.000	706.000	6.926	169.000	592.000	5.808	173.000	208.000	2.040	000
14	560.000	5.494	160.000	743.000	7.289	167.000	633.000	6.210	172.000	225.000	2.207	000
15	593.000	5.817	158.000	785.000	7.701	165.000	671.000	6.583	170.000	241.000	2.364	000
16	620.000	6.082	157.000	816.000	8.005	162.000	708.000	6.945	167.000	254.000	2.492	000
17	646.000	6.337	157.000	843.000	8.270	161.000	755.000	7.407	165.000	275.000	2.698	000
18	677.000	6.641	157.000	870.000	8.535	160.000	795.000	7.799	163.000	286.000	2.806	000
19	707.000	6.936	157.000	901.000	8.839	160.000	832.000	8.162	161.000			
20	733.000	7.191	156.000	938.000	9.182	160.000	861.000	8.843	160.000			
21				953.000	9.349	158.000	913.000	8.957	159.000			
22				975.000	9.565	158.000	948.000	9.300	158.000			
23				1000.000	9.810	157.000	988.000	9.673	158.000			
24							1004.000	9.849	158.000			

Appendix E-3. Torque Data for 270,000 MW Blends

Torque 270 mw data

	0% MO	0% Mo	0% MO	5% MO	5% MO	5% MO	8% MO	8% MO	8% MO
	Torque (m-g)	Torque (Nm)	Temp (C)	Torque (m-g)	Torque (Nm)	Temp (C)	Torque (m-g)	Torque (Nm)	Temp (C)
1									
2	1130.000	11.085	208.000	946.000	9.280	203.000	809.000	7.936	196.000
3	1137.000	11.154	205.000	966.000	9.476	201.000	844.000	8.280	193.000
4	1163.000	11.409	203.000	991.000	9.722	198.000	887.000	8.701	190.000
5	1189.000	11.664	199.000	1015.000	9.957	195.000	921.000	9.035	187.000
6	1210.000	11.870	196.000	1038.000	10.183	192.000	944.000	9.261	184.000
7	1235.000	12.115	194.000	1074.000	10.536	189.000	983.000	9.447	182.000
8	1263.000	12.390	191.000	1095.000	10.742	188.000	977.000	9.584	181.000
9	1280.000	12.557	188.000	1131.000	11.095	183.000	991.000	9.722	180.000
10	1317.000	12.920	185.000	1164.000	11.419	180.000			
11	1354.000	13.283	183.000	1191.000	11.684	178.000			
12	1382.000	13.557	180.000	1223.000	11.998	176.000			
13	1411.000	13.842	177.000	1258.000	12.341	173.000			
14	1446.000	14.185	175.000	1290.000	12.655	171.000			
15	1481.000	14.529	173.000	1318.000	12.930	169.000			
16	1515.000	14.862	171.000	1351.000	13.253	167.000			
17	1553.000	15.235	169.000	1389.000	13.628	165.000			
18	1593.000	15.627	166.000	1408.000	13.812	162.000			
19	1636.000	16.049	164.000	1445.000	14.175	161.000			
20	1693.000	16.608	162.000	1486.000	14.578	159.000			
21	1744.000	17.109	160.000	1520.000	14.911	157.000			
22	1790.000	17.560	158.000	1553.000	15.235	155.000			
23	1823.000	17.884	156.000	1586.000	15.559	153.000			
24	1872.000	18.364	154.000	1619.000	15.882	151.000			
25	1930.000	18.933	153.000	1675.000	16.432	150.000			
26	1992.000	19.542	151.000	1737.000	17.040	148.000			
27	2044.000	20.052	149.000	1812.000	17.778	147.000			
28				1891.000	18.551	145.000			
29				1967.000	19.296	144.000			
30				2009.000	19.708	142.000			
31				2070.000	20.307	140.000			

APPENDIX F

POSITRON ANNIHILATION SPECTROSCOPY

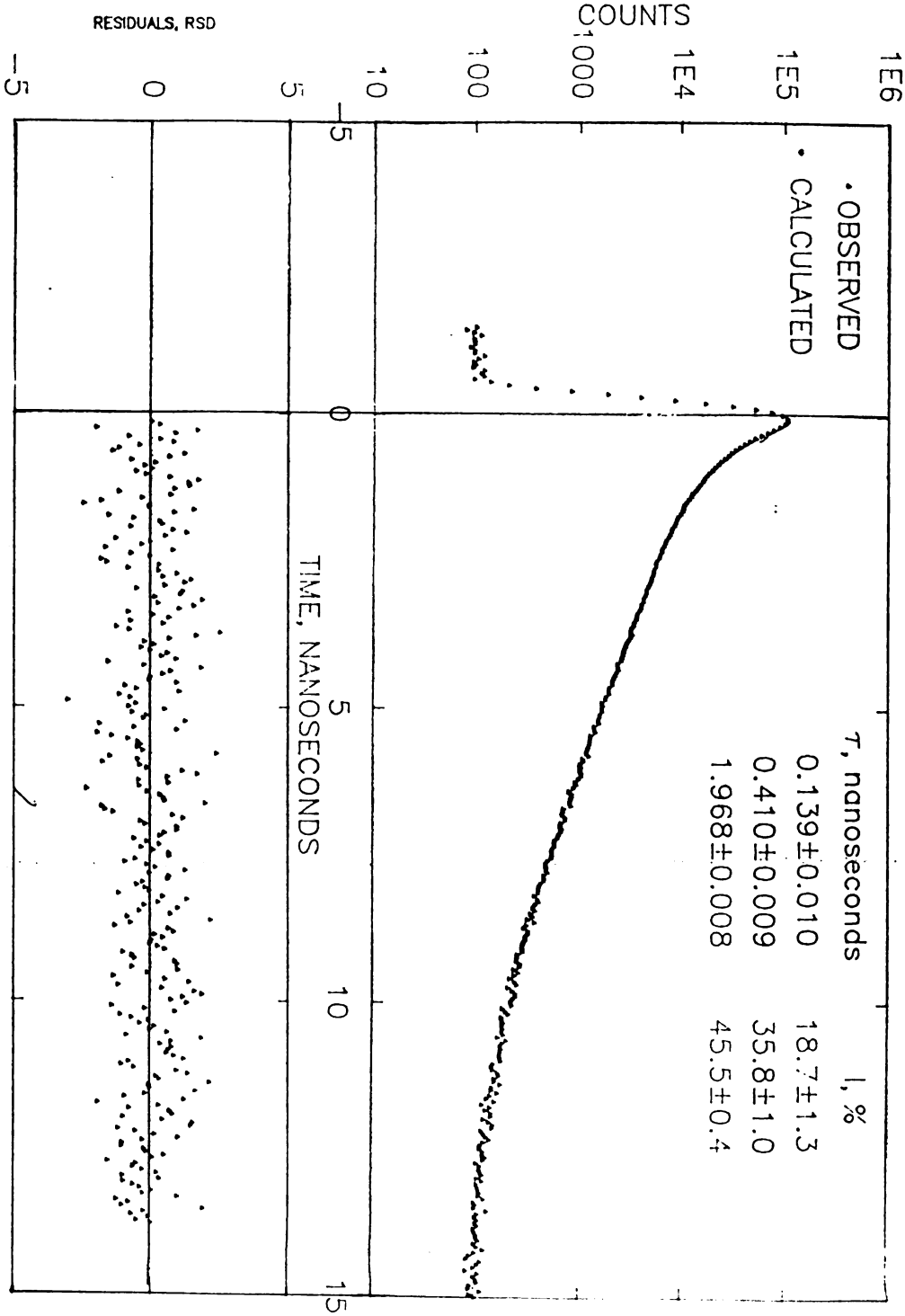
100001 polystyrene heat treated 0% mineral oil
COUNTS
1E6
1E5
1E4
1000
100
10
• OBSERVED
• CALCULATED
τ, nanoseconds
I, %
0.139±0.010
18.7±1.3
0.410±0.009
35.8±1.0
1.968±0.008
45.5±0.4
RESIDUALS, RSD
5
0
−5
TIME, NANOSECONDS
0
5
10
15

Appendix F-2. PAS Data for 40,000 MW Blends

10-30-1991

****
LMW PS 0% MINERAL OIL - HAAKE EXTRUDER 100001.DAT
****

TIME SCALE = 0.0500 NSEC/CHANNEL

PROMPT CURVE

FWHM(NSEC)	0.195	0.297
INTENSITIES($)	55.400	44.600
SHIFT(NSEC)	0.000	0.026

SPECTRUM ANALYSIS STARTS IN CH. 33 AND ENDS IN CH. 307

NUMBER OF TERMS = 3 NUMBER OF LIFETIME CONSTRAINTS = 0

NUMBER OF CONSTRAINTS FOR RELATIVE INTENSITIES = 0

FREE BACKGROUND FREE TIME-ZERO

NO SOURCE CORRECTION

VARIANCE OF THE FIT = 1.048
ITS DISTRIBUTION SHOULD BE APPROXIMATELY NORMAL (1,0.087)
EXCESS PROBABILITY = 28.77 PCT

LIFETIMES IN NSEC	0.143	0.412	1.969
STANDARD DEVIATIONS	0.008	0.009	0.008
RELATIVE INTENSITIES IN PCT	19.14	35.60	45.26
STANDARD DEVIATIONS	1.15	0.96	0.27
BACKGROUND	89.99		
STANDARD DEVIATION	1.72		
TIME-ZERO CHANNEL NUMBER	30.942		
STANDARD DEVIATION	0.070		

AREA CHECK AREA FROM FIT = 0.17816E+07
AREA FROM TABLE = 0.18679E+07

11- 5-1991

****
LMW PS 2.5% MINERAL OIL 500001.DAT
****

TIME SCALE = 0.0500 NSEC/CHANNEL

PROMPT CURVE
FWHM(NSEC) 0.195 0.297
INTENSITIES($) 55.400 44.600
SHIFT(NSEC) 0.000 0.026
SPECTRUM ANALYSIS STARTS IN CH. 33 AND ENDS IN CH. 307

NUMBER OF TERMS = 3 NUMBER OF LIFETIME CONSTRAINTS = 0

NUMBER OF CONSTRAINTS FOR RELATIVE INTENSITIES = 0

FREE BACKGROUND FREE TIME-ZERO

NO SOURCE CORRECTION

VARIANCE OF THE FIT = 1.325
ITS DISTRIBUTION SHOULD BE APPROXIMATELY NORMAL (1,0.087)
EXCESS PROBABILITY = 0.01 PCT

LIFETIMES IN NSEC	0.170	0.428	1.982
STANDARD DEVIATIONS	0.007	0.011	0.008
RELATIVE INTENSITIES IN PCT	22.56	33.74	43.69
STANDARD DEVIATIONS	1.44	1.27	0.24

BACKGROUND 109.30
STANDARD DEVIATION 1.95

TIME-ZERO CHANNEL NUMBER 31.679
STANDARD DEVIATION 0.033

AREA CHECK AREA FROM FIT = 0.21725E+07
AREA FROM TABLE = 0.22496E+07

10-30-1991

```
********************
LMW PS 5% MINERAL OIL  400001.DAT
**************************************************

TIME SCALE = 0.0500 NSEC/CHANNEL

PROMPT CURVE
FWHM(NSEC)         0.195  0.297
INTENSITIES($)    55.400 44.600
SHIFT(NSEC)        0.000  0.026
SPECTRUM ANALYSIS STARTS IN CH.  33 AND ENDS IN CH. 307

NUMBER OF TERMS = 3      NUMBER OF LIFETIME CONSTRAINTS = 0

NUMBER OF CONSTRAINTS FOR RELATIVE INTENSITIES = 0

FREE BACKGROUND          FREE TIME-ZERO

NO SOURCE CORRECTION


VARIANCE OF THE FIT =     1.120
ITS DISTRIBUTION SHOULD BE APPROXIMATELY NORMAL (1,0.087)
EXCESS PROBABILITY =    8.26 PCT


LIFETIMES IN NSEC              0.151   0.414   1.983
STANDARD DEVIATIONS            0.007   0.007   0.008

RELATIVE INTENSITIES IN PCT   19.05   40.16   40.79
STANDARD DEVIATIONS            1.10    0.95    0.21

BACKGROUND                   119.87
STANDARD DEVIATION             1.98


TIME-ZERO    CHANNEL NUMBER   31.324
STANDARD DEVIATION             0.044


AREA CHECK     AREA FROM FIT   = 0.23419E+07
               AREA FROM TABLE = 0.24112E+07
```

11-10-1991

****
LMW PS 7.5% MINERAL OIL 600001.DAT
****

TIME SCALE = 0.0500 NSEC/CHANNEL

PROMPT CURVE

FWHM(NSEC)	0.195	0.297
INTENSITIES($)	55.400	44.600
SHIFT(NSEC)	0.000	0.026

SPECTRUM ANALYSIS STARTS IN CH. 33 AND ENDS IN CH. 307

NUMBER OF TERMS = 3 NUMBER OF LIFETIME CONSTRAINTS = 0

NUMBER OF CONSTRAINTS FOR RELATIVE INTENSITIES = 0

FREE BACKGROUND FREE TIME-ZERO

NO SOURCE CORRECTION

VARIANCE OF THE FIT = 1.216
ITS DISTRIBUTION SHOULD BE APPROXIMATELY NORMAL (1,0.087)
EXCESS PROBABILITY = 0.62 PCT

LIFETIMES IN NSEC	0.153	0.415	1.997
STANDARD DEVIATIONS	0.008	0.010	0.008
RELATIVE INTENSITIES IN PCT	20.09	35.26	44.65
STANDARD DEVIATIONS	1.35	1.15	0.27

BACKGROUND	92.09
STANDARD DEVIATION	1.78

TIME-ZERO CHANNEL NUMBER	31.002
STANDARD DEVIATION	0.064

AREA CHECK AREA FROM FIT = 0.17807E+07
AREA FROM TABLE = 0.18553E+07

10-30-1991

****
LMW PS 10% MINERAL OIL - RUN #13 300001.DAT
****

TIME SCALE = 0.0500 NSEC/CHANNEL

PROMPT CURVE

FWHM(NSEC)	0.195	0.297
INTENSITIES($)	55.400	44.600
SHIFT(NSEC)	0.000	0.026

SPECTRUM ANALYSIS STARTS IN CH. 33 AND ENDS IN CH. 307

NUMBER OF TERMS = 3 NUMBER OF LIFETIME CONSTRAINTS = 0

NUMBER OF CONSTRAINTS FOR RELATIVE INTENSITIES = 0

FREE BACKGROUND FREE TIME-ZERO

NO SOURCE CORRECTION

VARIANCE OF THE FIT = 1.182
ITS DISTRIBUTION SHOULD BE APPROXIMATELY NORMAL (1,0.087)
EXCESS PROBABILITY = 1.77 PCT

LIFETIMES IN NSEC	0.154	0.423	2.030
STANDARD DEVIATIONS	0.007	0.009	0.008
RELATIVE INTENSITIES IN PCT	20.18	36.90	42.92
STANDARD DEVIATIONS	1.16	1.00	0.23

BACKGROUND	104.66
STANDARD DEVIATION	1.97

TIME-ZERO CHANNEL NUMBER	31.416
STANDARD DEVIATION	0.043

AREA CHECK AREA FROM FIT = 0.20753E+07
AREA FROM TABLE = 0.21378E+07

Appendix F-3. PAS Data for 128,000 MW Blends

THIS IS DATA SET 128K0A1
THE ACQUISITION DATE AND TIME WAS 06FEB92 AT 1329
THE REAL TIME WAS 3 HOURS, 0 MINUTES, AND 0 SECONDS.
THE LIVE TIME WAS 2 HOURS, 59 MINUTES, AND 17 SECONDS.

2- 6-1992

****
128,000 MW PS 0% MINERAL OIL (MOLDED @ 3000 LBS)
****

TIME SCALE = 0.0500 NSEC/CHANNEL

PROMPT CURVE

FWHM(NSEC)	0.195	0.297
INTENSITIES($)	55.400	44.600
SHIFT(NSEC)	0.000	0.026

SPECTRUM ANALYSIS STARTS IN CH. 33 AND ENDS IN CH. 309

NUMBER OF TERMS = 3 NUMBER OF LIFETIME CONSTRAINTS = 0

NUMBER OF CONSTRAINTS FOR RELATIVE INTENSITIES = 0

FREE BACKGROUND FREE TIME-ZERO

NO SOURCE CORRECTION

VARIANCE OF THE FIT = 1.183
ITS DISTRIBUTION SHOULD BE APPROXIMATELY NORMAL (1,0.086)
EXCESS PROBABILITY = 1.71 PCT

LIFETIMES IN NSEC	0.141	0.400	2.075
STANDARD DEVIATIONS	0.005	0.006	0.007
RELATIVE INTENSITIES IN PCT	18.60	36.82	44.58
STANDARD DEVIATIONS	0.84	0.74	0.17

BACKGROUND	345.42
STANDARD DEVIATION	3.07
TIME-ZERO CHANNEL NUMBER	32.657
STANDARD DEVIATION	0.020

AREA CHECK AREA FROM FIT = 0.28722E+07
AREA FROM TABLE = 0.29249E+07

THIS IS DATA SET 128K2A1
THE ACQUISITION DATE AND TIME WAS 06FEB92 AT 0946
THE REAL TIME WAS 3 HOURS, 0 MINUTES, AND 0 SECONDS.
THE LIVE TIME WAS 2 HOURS, 59 MINUTES, AND 20 SECONDS.

2- 6-1992

****
128,000 MW PS 2.5% MINERAL OIL (MOLDED @ 3000 LBS)
****

TIME SCALE = 0.0500 NSEC/CHANNEL

PROMPT CURVE

FWHM(NSEC)	0.195	0.297
INTENSITIES($)	55.400	44.600
SHIFT(NSEC)	0.000	0.026

SPECTRUM ANALYSIS STARTS IN CH. 33 AND ENDS IN CH. 309

NUMBER OF TERMS = 3 NUMBER OF LIFETIME CONSTRAINTS = 0

NUMBER OF CONSTRAINTS FOR RELATIVE INTENSITIES = 0

FREE BACKGROUND FREE TIME-ZERO

NO SOURCE CORRECTION

VARIANCE OF THE FIT = 1.101
ITS DISTRIBUTION SHOULD BE APPROXIMATELY NORMAL (1,0.086)
EXCESS PROBABILITY = 12.08 PCT

LIFETIMES IN NSEC	0.153	0.419	2.086
STANDARD DEVIATIONS	0.005	0.007	0.008
RELATIVE INTENSITIES IN PCT	20.24	36.36	43.39
STANDARD DEVIATIONS	0.93	0.81	0.18

BACKGROUND	318.18
STANDARD DEVIATION	3.02
TIME-ZERO CHANNEL NUMBER	33.001
STANDARD DEVIATION	0.016

AREA CHECK AREA FROM FIT = 0.26964E+07
AREA FROM TABLE = 0.27379E+07

THIS IS DATA SET 128K5A1
THE ACQUISITION DATE AND TIME WAS 07FEB92 AT 1046
THE REAL TIME WAS 3 HOURS, 0 MINUTES, AND 0 SECONDS.
THE LIVE TIME WAS 2 HOURS, 59 MINUTES, AND 13 SECONDS.

2- 7-1992

****
128,000 MW PS 5% MINERAL OIL (MOLDED @ 3000 LBS)
****

TIME SCALE = 0.0500 NSEC/CHANNEL

PROMPT CURVE

FWHM(NSEC)	0.195	0.297
INTENSITIES($)	55.400	44.600
SHIFT(NSEC)	0.000	0.026

SPECTRUM ANALYSIS STARTS IN CH. 33 AND ENDS IN CH. 309

NUMBER OF TERMS = 3 NUMBER OF LIFETIME CONSTRAINTS = 0

NUMBER OF CONSTRAINTS FOR RELATIVE INTENSITIES = 0

FREE BACKGROUND FREE TIME-ZERO

NO SOURCE CORRECTION

VARIANCE OF THE FIT = 1.176
ITS DISTRIBUTION SHOULD BE APPROXIMATELY NORMAL (1,0.086)
EXCESS PROBABILITY = 2.05 PCT

LIFETIMES IN NSEC	0.153	0.427	2.099
STANDARD DEVIATIONS	0.004	0.007	0.008
RELATIVE INTENSITIES IN PCT	21.24	36.04	42.72
STANDARD DEVIATIONS	0.83	0.71	0.18

BACKGROUND	364.04
STANDARD DEVIATION	3.27

TIME-ZERO CHANNEL NUMBER	32.737
STANDARD DEVIATION	0.017

AREA CHECK AREA FROM FIT = 0.30995E+07
AREA FROM TABLE = 0.31553E+07

THIS IS DATA SET 128K7A1
THE ACQUISITION DATE AND TIME WAS 07FEB92 AT 1412
THE REAL TIME WAS 3 HOURS, 0 MINUTES, AND 0 SECONDS.
THE LIVE TIME WAS 2 HOURS, 59 MINUTES, AND 16 SECONDS.

2- 7-1992

****
128,000 MW PS 7.5% MINERAL OIL (MOLDED @ 3000 LBS)
****

TIME SCALE = 0.0500 NSEC/CHANNEL

PROMPT CURVE

FWHM(NSEC)	0.195	0.297
INTENSITIES($)	55.400	44.600
SHIFT(NSEC)	0.000	0.026

SPECTRUM ANALYSIS STARTS IN CH. 33 AND ENDS IN CH. 309

NUMBER OF TERMS = 3 NUMBER OF LIFETIME CONSTRAINTS = 0

NUMBER OF CONSTRAINTS FOR RELATIVE INTENSITIES = 0

FREE BACKGROUND FREE TIME-ZERO

NO SOURCE CORRECTION

VARIANCE OF THE FIT = 1.259
ITS DISTRIBUTION SHOULD BE APPROXIMATELY NORMAL (1,0.086)
EXCESS PROBABILITY = 0.13 PCT

LIFETIMES IN NSEC	0.152	0.416	2.086
STANDARD DEVIATIONS	0.005	0.007	0.008
RELATIVE INTENSITIES IN PCT	19.83	37.59	42.58
STANDARD DEVIATIONS	0.91	0.79	0.17

BACKGROUND	347.18
STANDARD DEVIATION	3.13

TIME-ZERO CHANNEL NUMBER	32.802
STANDARD DEVIATION	0.017

AREA CHECK AREA FROM FIT = 0.29287E+07
AREA FROM TABLE = 0.29774E+07

THIS IS DATA SET 128K1A1
THE ACQUISITION DATE AND TIME WAS 06FEB92 AT 1640
THE REAL TIME WAS 3 HOURS, 0 MINUTES, AND 1 SECONDS.
THE LIVE TIME WAS 2 HOURS, 59 MINUTES, AND 13 SECONDS.

2- 6-1992

****
128,000 MW PS 10% MINERAL OIL (MOLDED @ 3000 LBS)
****

TIME SCALE = 0.0500 NSEC/CHANNEL

PROMPT CURVE

FWHM(NSEC)	0.195	0.297
INTENSITIES($)	55.400	44.600
SHIFT(NSEC)	0.000	0.026

SPECTRUM ANALYSIS STARTS IN CH. 33 AND ENDS IN CH. 309

NUMBER OF TERMS = 3 NUMBER OF LIFETIME CONSTRAINTS = 0

NUMBER OF CONSTRAINTS FOR RELATIVE INTENSITIES = 0

FREE BACKGROUND FREE TIME-ZERO

NO SOURCE CORRECTION

VARIANCE OF THE FIT = 1.218
ITS DISTRIBUTION SHOULD BE APPROXIMATELY NORMAL (1,0.086)
EXCESS PROBABILITY = 0.57 PCT

LIFETIMES IN NSEC	0.153	0.419	2.098
STANDARD DEVIATIONS	0.004	0.007	0.008
RELATIVE INTENSITIES IN PCT	21.23	36.01	42.76
STANDARD DEVIATIONS	0.86	0.76	0.17

BACKGROUND	372.64
STANDARD DEVIATION	3.28
TIME-ZERO CHANNEL NUMBER	33.030
STANDARD DEVIATION	0.015

AREA CHECK AREA FROM FIT = 0.31071E+07
AREA FROM TABLE = 0.31528E+07

Appendix F-4. PAS Data for 270,000 MW Blends

1-15-1992

```
**********
HMW PS 0% MINERAL OIL H00001.DAT
**************************************************

TIME SCALE = 0.0500 NSEC/CHANNEL

PROMPT CURVE
FWHM(NSEC)        0.195  0.297
INTENSITIES($)   55.400 44.600
SHIFT(NSEC)       0.000  0.026
SPECTRUM ANALYSIS STARTS IN CH.  33 AND ENDS IN CH. 307

NUMBER OF TERMS = 3      NUMBER OF LIFETIME CONSTRAINTS = 0

NUMBER OF CONSTRAINTS FOR RELATIVE INTENSITIES = 0

FREE BACKGROUND          FREE TIME-ZERO

NO SOURCE CORRECTION


VARIANCE OF THE FIT =     1.264
ITS DISTRIBUTION SHOULD BE APPROXIMATELY NORMAL (1,0.087)
EXCESS PROBABILITY =    0.12 PCT


LIFETIMES IN NSEC              0.156   0.416   2.069
STANDARD DEVIATIONS            0.006   0.009   0.007

RELATIVE INTENSITIES IN PCT   20.76   34.49   44.75
STANDARD DEVIATIONS            1.13    0.99    0.20

BACKGROUND                   124.77
STANDARD DEVIATION             2.25


TIME-ZERO    CHANNEL NUMBER   31.568
STANDARD DEVIATION             0.036


AREA CHECK     AREA FROM FIT   = 0.24898E+07
               AREA FROM TABLE = 0.25546E+07
```

THIS IS DATA SET H251
THE ACQUISITION DATE AND TIME WAS 14JAN92 AT 0938
THE REAL TIME WAS 3 HOURS, 0 MINUTES, AND 0 SECONDS.
THE LIVE TIME WAS 2 HOURS, 59 MINUTES, AND 33 SECONDS.

1-14-1992

****
HMW PS 2.5% MINERAL OIL
****

TIME SCALE = 0.0500 NSEC/CHANNEL

PROMPT CURVE

FWHM(NSEC)	0.195	0.297
INTENSITIES($)	55.400	44.600
SHIFT(NSEC)	0.000	0.026

SPECTRUM ANALYSIS STARTS IN CH. 33 AND ENDS IN CH. 309

NUMBER OF TERMS = 3 NUMBER OF LIFETIME CONSTRAINTS = 0

NUMBER OF CONSTRAINTS FOR RELATIVE INTENSITIES = 0

FREE BACKGROUND FREE TIME-ZERO

NO SOURCE CORRECTION

VARIANCE OF THE FIT = 1.094
ITS DISTRIBUTION SHOULD BE APPROXIMATELY NORMAL (1,0.086)
EXCESS PROBABILITY = 13.68 PCT

LIFETIMES IN NSEC	0.155	0.406	2.060
STANDARD DEVIATIONS	0.008	0.010	0.010
RELATIVE INTENSITIES IN PCT	18.57	36.33	45.09
STANDARD DEVIATIONS	1.40	1.24	0.23

BACKGROUND	230.09
STANDARD DEVIATION	2.47
TIME-ZERO CHANNEL NUMBER	32.318
STANDARD DEVIATION	0.029

AREA CHECK AREA FROM FIT = 0.17490E+07
AREA FROM TABLE = 0.17894E+07

THIS IS DATA SET H051
THE ACQUISITION DATE AND TIME WAS 14JAN92 AT 1615
THE REAL TIME WAS 3 HOURS, 0 MINUTES, AND 0 SECONDS.
THE LIVE TIME WAS 2 HOURS, 59 MINUTES, AND 25 SECONDS.

1-14-1992

****
HMW PS 5% MINERAL OIL
****

TIME SCALE = 0.0500 NSEC/CHANNEL

PROMPT CURVE

FWHM(NSEC)	0.195	0.297
INTENSITIES($)	55.400	44.600
SHIFT(NSEC)	0.000	0.026

SPECTRUM ANALYSIS STARTS IN CH. 33 AND ENDS IN CH. 309

NUMBER OF TERMS = 3 NUMBER OF LIFETIME CONSTRAINTS = 0

NUMBER OF CONSTRAINTS FOR RELATIVE INTENSITIES = 0

FREE BACKGROUND FREE TIME-ZERO

NO SOURCE CORRECTION

VARIANCE OF THE FIT = 1.276
ITS DISTRIBUTION SHOULD BE APPROXIMATELY NORMAL (1,0.086)
EXCESS PROBABILITY = 0.07 PCT

LIFETIMES IN NSEC	0.162	0.416	2.067
STANDARD DEVIATIONS	0.007	0.010	0.009
RELATIVE INTENSITIES IN PCT	20.35	34.69	44.96
STANDARD DEVIATIONS	1.32	1.17	0.22

BACKGROUND	295.60
STANDARD DEVIATION	2.83
TIME-ZERO CHANNEL NUMBER	32.127
STANDARD DEVIATION	0.027

AREA CHECK AREA FROM FIT = 0.22685E+07
AREA FROM TABLE = 0.23240E+07

THIS IS DATA SET H751
THE ACQUISITION DATE AND TIME WAS 15JAN92 AT 0822
THE REAL TIME WAS 3 HOURS, 0 MINUTES, AND 0 SECONDS.
THE LIVE TIME WAS 2 HOURS, 59 MINUTES, AND 28 SECONDS.

1-15-1992

****
HMW PS 7.5% MINERAL OIL
****

TIME SCALE = 0.0500 NSEC/CHANNEL

PROMPT CURVE

FWHM(NSEC)	0.195	0.297
INTENSITIES($)	55.400	44.600
SHIFT(NSEC)	0.000	0.026

SPECTRUM ANALYSIS STARTS IN CH. 33 AND ENDS IN CH. 309

NUMBER OF TERMS = 3 NUMBER OF LIFETIME CONSTRAINTS = 0

NUMBER OF CONSTRAINTS FOR RELATIVE INTENSITIES = 0

FREE BACKGROUND FREE TIME-ZERO

NO SOURCE CORRECTION

VARIANCE OF THE FIT = 1.036
ITS DISTRIBUTION SHOULD BE APPROXIMATELY NORMAL (1,0.086)
EXCESS PROBABILITY = 33.92 PCT

LIFETIMES IN NSEC	0.137	0.403	2.060
STANDARD DEVIATIONS	0.007	0.008	0.009
RELATIVE INTENSITIES IN PCT	17.64	37.32	45.04
STANDARD DEVIATIONS	0.96	0.82	0.21

BACKGROUND	273.68
STANDARD DEVIATION	2.65
TIME-ZERO CHANNEL NUMBER	31.694
STANDARD DEVIATION	0.042

AREA CHECK AREA FROM FIT = 0.20783E+07
AREA FROM TABLE = 0.21488E+07

THIS IS DATA SET H101
THE ACQUISITION DATE AND TIME WAS 15JAN92 AT 1449
THE REAL TIME WAS 3 HOURS, 0 MINUTES, AND 0 SECONDS.
THE LIVE TIME WAS 2 HOURS, 59 MINUTES, AND 26 SECONDS.

1-15-1992

****
HMW PS 10% MINERAL OIL
****

TIME SCALE = 0.0500 NSEC/CHANNEL

PROMPT CURVE

FWHM(NSEC)	0.195	0.297
INTENSITIES($)	55.400	44.600
SHIFT(NSEC)	0.000	0.026

SPECTRUM ANALYSIS STARTS IN CH. 33 AND ENDS IN CH. 309

NUMBER OF TERMS = 3 NUMBER OF LIFETIME CONSTRAINTS = 0

NUMBER OF CONSTRAINTS FOR RELATIVE INTENSITIES = 0

FREE BACKGROUND FREE TIME-ZERO

NO SOURCE CORRECTION

VARIANCE OF THE FIT = 1.352
ITS DISTRIBUTION SHOULD BE APPROXIMATELY NORMAL (1,0.086)
EXCESS PROBABILITY = 0.00 PCT

LIFETIMES IN NSEC	0.143	0.400	2.065
STANDARD DEVIATIONS	0.007	0.008	0.008
RELATIVE INTENSITIES IN PCT	17.89	37.27	44.84
STANDARD DEVIATIONS	1.08	0.94	0.21

BACKGROUND	294.59
STANDARD DEVIATION	2.76
TIME-ZERO CHANNEL NUMBER	31.726
STANDARD DEVIATION	0.038

AREA CHECK AREA FROM FIT = 0.22141E+07
AREA FROM TABLE = 0.22772E+07

APPENDIX G

NUCLEAR MAGNETIC RESONANCE

Appendix G-1. Data and Decay Curves for 6% Mineral Oil Blend $T_{1\rho}$ C Analysis

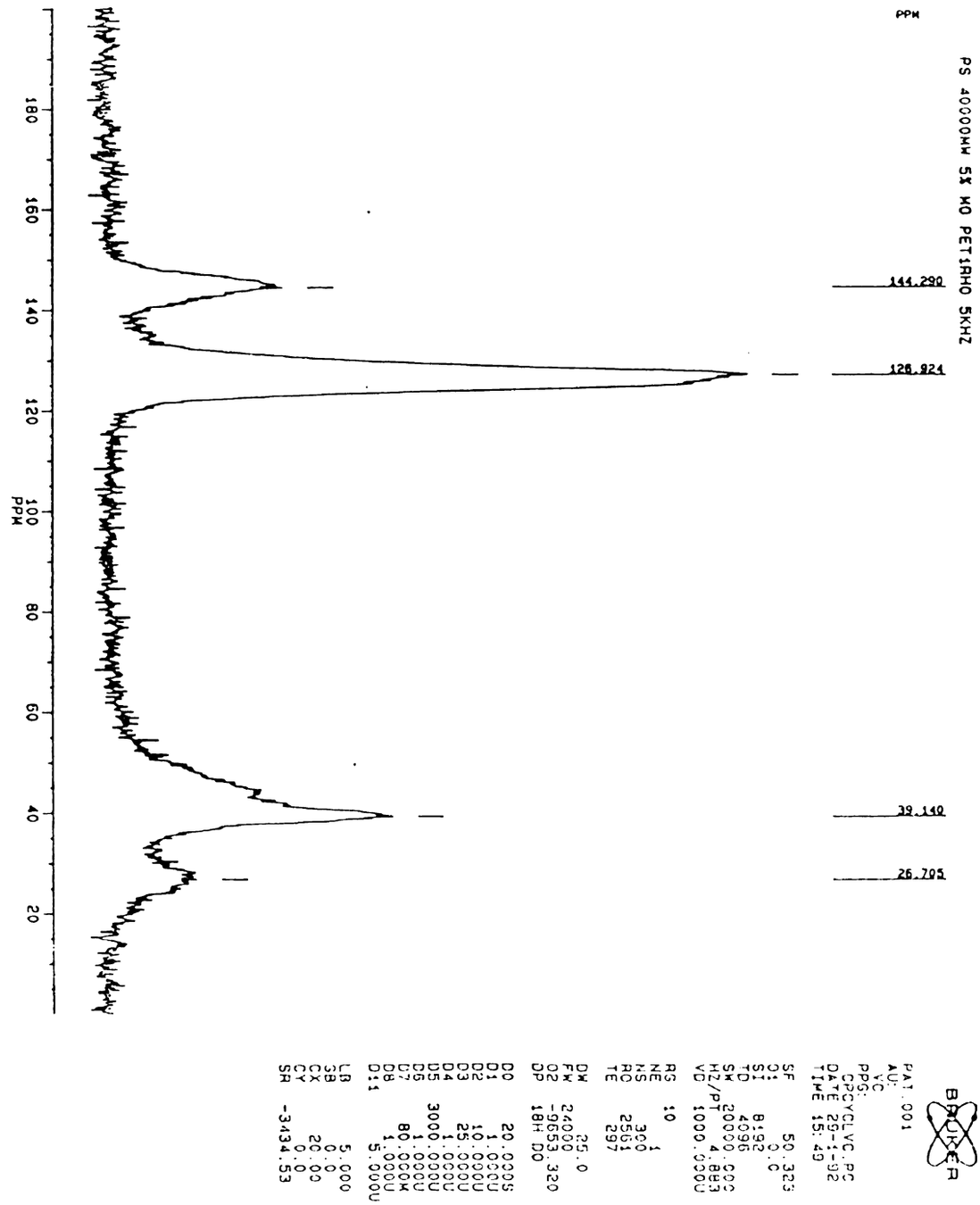
PS 40000HW 5% MO PET1RHO 5KHZ
PPM
144.290
126.924
39.140
26.705
180
160
140
120
100
80
60
40
20
PPM
BRUKER
PAT 001
AU:
VC
PPG:
CPCYCLVC.PC
DATE 29-1-92
TIME 15:49
SF 50.323
O1 0.0
SI 8192
TD 4096
SW 20000.000
SW/PT 4.883
VD 1000.000U
RG 10
NE 1
NS 300
AQ 2561
TE 297
DW 25.0
FW 24000
O2 -9653.320
DP 18H DO
D0 20.000S
D1 1.000U
D2 10.000U
D3 25.000U
D4 1.000U
D5 3000.000U
D6 1.000U
D7 80.000M
D8 1.000U
D11 5.000U
LB 5.000
SB 0.0
CX 20.00
CY 0.0
SR -3434.53

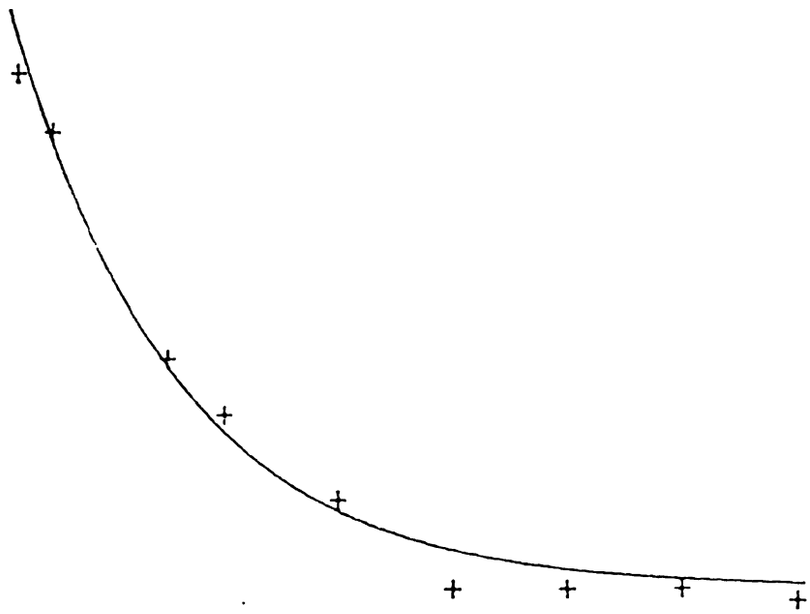

T2 7.116M

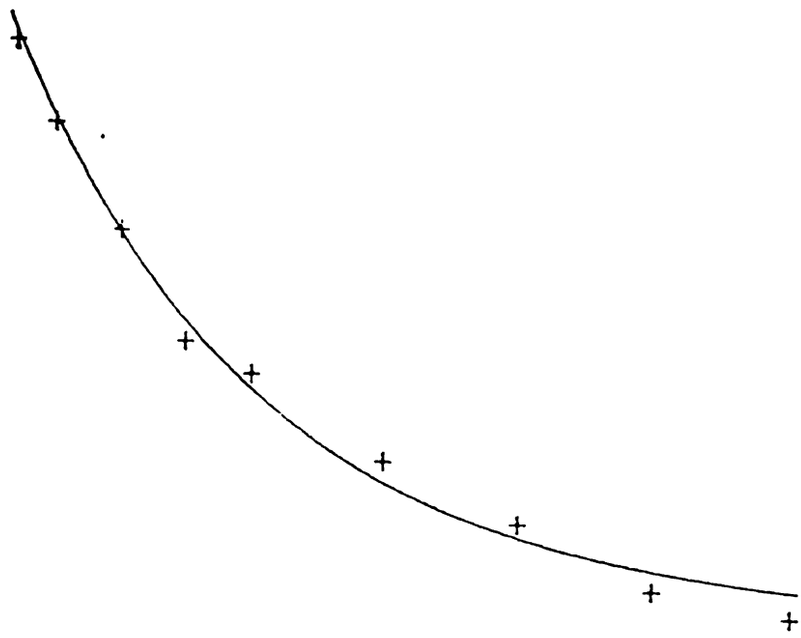

T2 9.413M

10 INTENSITIES FIT IN 2 ITERATIONS

CURSOR	FREQ	PPM	$T_{1\rho}$	STD DEV	
1266	7305.387	145.1699	9.631M	0.030982	
TAU	CURSOR	FREQ	PPM	INTEGRAL	INTENSITY
1000.000U	1264	7315.153	145.364	4.09	18.801
2500.000U	1265	7310.27	145.267	7.733	15.496
5.000M	1261	7329.801	145.655	2.258	12.092
7.500M	1264	7315.153	145.364	.579	8.568
10.000M	1267	7300.505	145.073	.856	7.297
15.000M	1264	7315.153	145.364	1.084	4.828
20.000M	1265	7310.27	145.267	.019	1.351
25.000M	1266	7305.387	145.170	.039	1.934
30.000M	1267	7300.505	145.073	-.018	1.239
35.000M	1266	7305.387	145.170	.090	1.297

10 INTENSITIES FIT IN 2 ITERATIONS

CURSOR	FREQ	PPM	$T_{1\rho}$	STD DEV	
1448	6416.715	127.5106	8.619	.014447	
TAU	CURSOR	FREQ	PPM	INTEGRAL	INTENSITY
1000.000U	1449	6411.833	127.414	11.597	75.326
2500.000U	1443	6441.130	127.996	52.295	67.518
5.000M	1448	6416.715	127.511	7.325	49.162
7.500M	1447	6436.247	127.608	2.568	36.120
10.000M	1444	6402.067	127.899	12.838	27.564
15.000M	1451	6416.715	127.220	2.117	14.863
20.000M	1448	7310.27	127.511	.930	7.642
25.000M	1447	6421.598	127.608	.704	4.444
30.000M	1447	6421.598	127.608	.093	2.586
35.000M	1448	6416.715	127.511	.092	2.060

9 INTENSITIES FIT IN 5 ITERATIONS

CURSOR	FREQ	PPM	T_2	STD DEV	
2341	2056.364	40.8633	7.116M	0.040803	
TAU	CURSOR	FREQ	PPM	INTEGRAL	INTENSITY
1000.000U	2341	2056.364	40.863	9.135	31.275
2500.000U	2346	2031.950	40.378	21.114	27.725
5.000M					
7.500M	2344	2041.715	40.572	1.261	13.907
10.000M	2345	2036.833	40.475	1.545	10.531
15.000M	2342	2051.481	40.766	1.135	5.355
20.000M					
25.000M					
30.000M					
35.000M	2341	2056.364	40.863	-.012	-.763

Appendix G-2. Data and Decay Curves for 6% Mineral Oil Blend Contact Time Experiments to Determine $T_{1\rho}H$ and T_{CH}

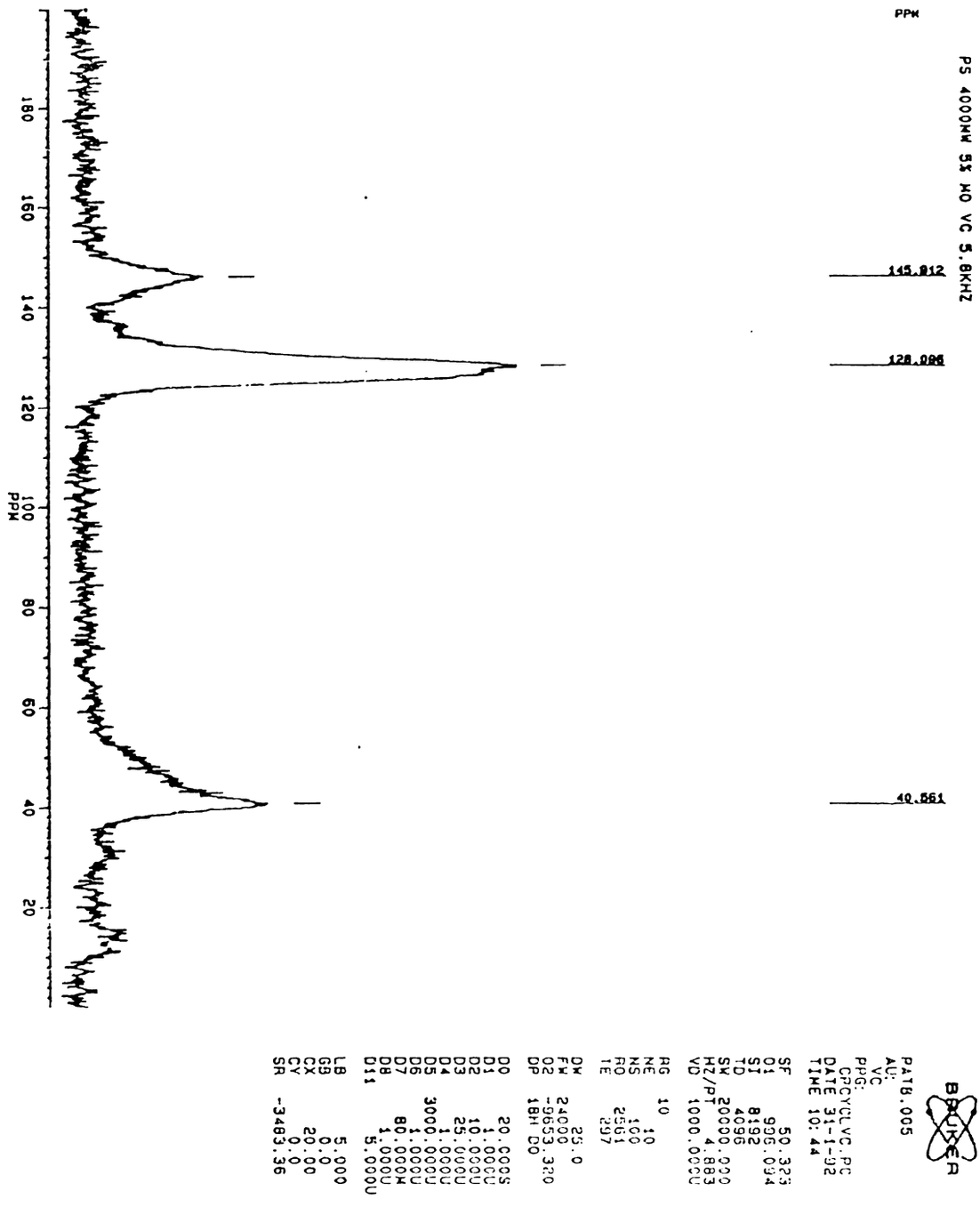
PS 4000HW 5% MO VC 5.8KHZ
PPM
145.812
128.096
40.561
180
160
140
120
100
80
60
40
20
PPM
PATH.005
AU:
VC
PPG:
C2CYCLVC.PC
DATE 31-1-92
TIME 10:44
SF 50.323
O1 936.054
SI 8192
TD 40960
SW 20000.000
HZ/PT 4.883
VD 1000.000U
RG 10
NE 10
NS 100
RO 2501
IE 297
DW 25.0
FW 24000
O2 -9653.320
DP 18H DD
D0 20.000S
D1 1.000DU
D2 10.000U
D3 25.000U
D4 1.000DU
D5 3000.000U
D6 1.000DU
D7 80.000M
D8 1.000U
D11 5.000U
LB 5.000
GB 0.0
CX 20.00
CY 0.0
SR -3483.36
BRUKER

T.CONV =
1.00E-5

TAU	CURSOR	FREQ	PPM	INTEGRAL	INTENSITY
100.000U	1462	7335.898	145.776	.360	7.446
250.000U	1463	7331.015	145.679	1.143	17.948
500.000U	1465	7321.249	145.485	3.073	20.754
750.000U	1465	7321.249	145.485	2.897	24.221
1000.000U	1465	7321.249	145.485	1.275	25.015
2000.000U	1464	7326.132	145.582	3.556	25.188
4.000M	1462	7335.898	145.776	.986	19.668
6.000M	1466	7316.366	145.388	3.525	20.797
8.000M	1461	7340.780	145.873	1.655	14.838
10.000M	1464	7326.132	145.582	.818	8.666

TAU	CURSOR	FREQ	PPM	INTEGRAL	INTENSITY
100.000U	1645	6442.3434	128.020	41.282	80.844
250.000U	1645	6442.343	128.020	27.468	89.703
500.000U	1646	6437.46	127.923	41.392	97.414
750.000U	1649	6422.812	127.632	61.652	103.947
1000.000U	1645	6442.343	128.020	64.649	104.751
2000.000U	1645	6442.343	128.020	44.830	100.284
4.000M	1643	6452.108	128.214	35.981	81.253
6.000M	1645	6442.343	128.020	5.710	62.340
8.000M	1643	6452.108	128.214	8.535	46.987
10.000M	1645	6442.343	128.020	10.881	40.192

TAU	CURSOR	FREQ	PPM	INTEGRAL	INTENSITY
100.000U	2544	2052.694	40.790	3.981	30.985
250.000U	2547	2038.046	40.499	8.863	39.273
500.000U	2546	2042.929	40.596	13.578	40.951
750.000U	2549	2028.28	40.305	24.221	42.678
1000.000U	2547	2038.046	40.499	4.642	42.570
2000.000U	2548	2033.163	40.402	2.690	37.327
4.000M	2545	2047.812	40.693	6.338	28.708
6.000M	2545	2047.812	40.693	1.849	20.904
8.000M	2547	2038.046	40.499	.910	18.014
10.000M	2546	2042.929	40.596	1.433	15.655

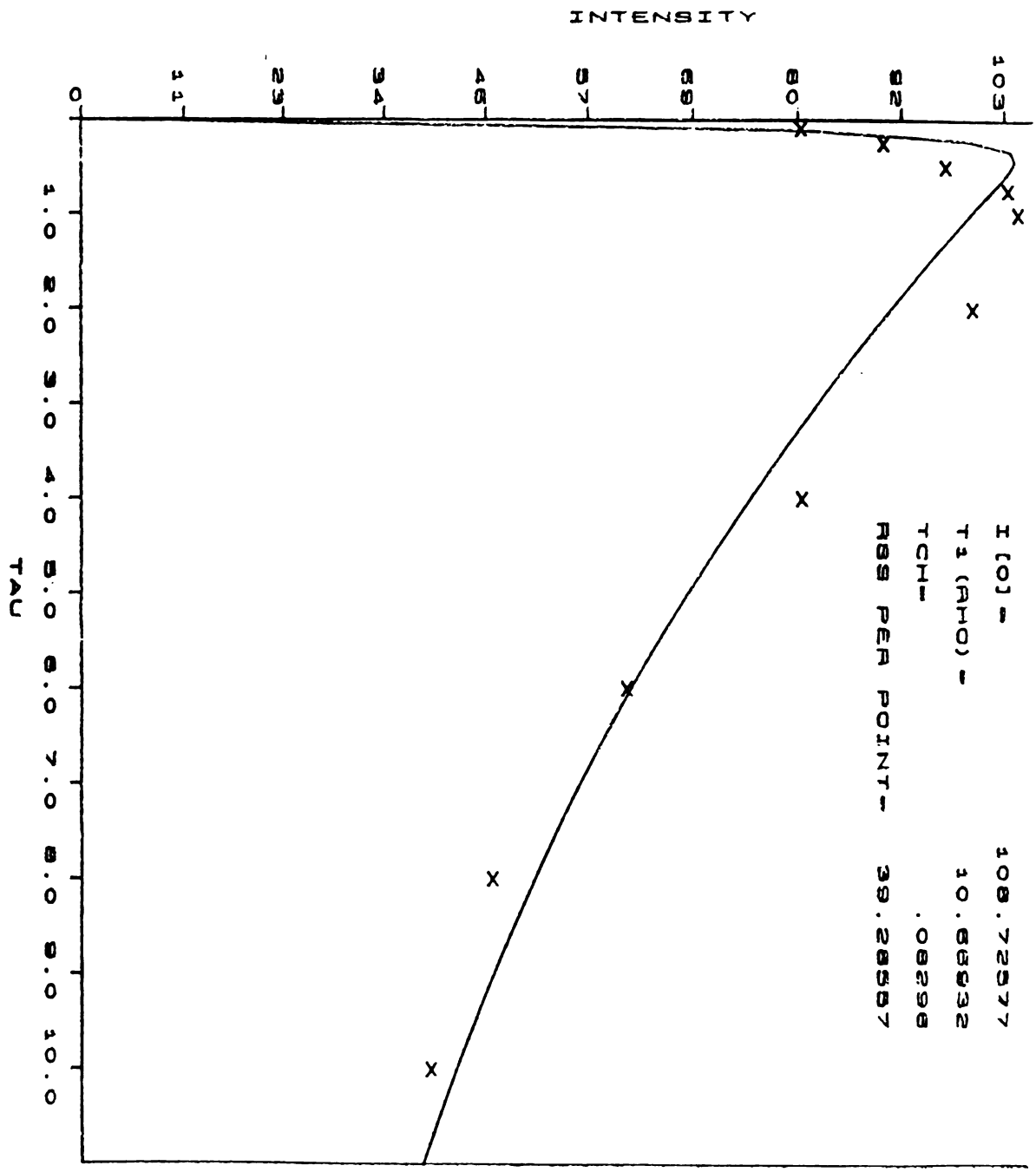
INTENSITY
0
11
23
34
46
57
69
80
92
103
TAU
1.0
2.0
3.0
4.0
5.0
6.0
7.0
8.0
9.0
10.0
I [O] =
108.72577
T1 (RHO) =
10.66632
TCH=
.08298
RSS PER POINT=
39.28587

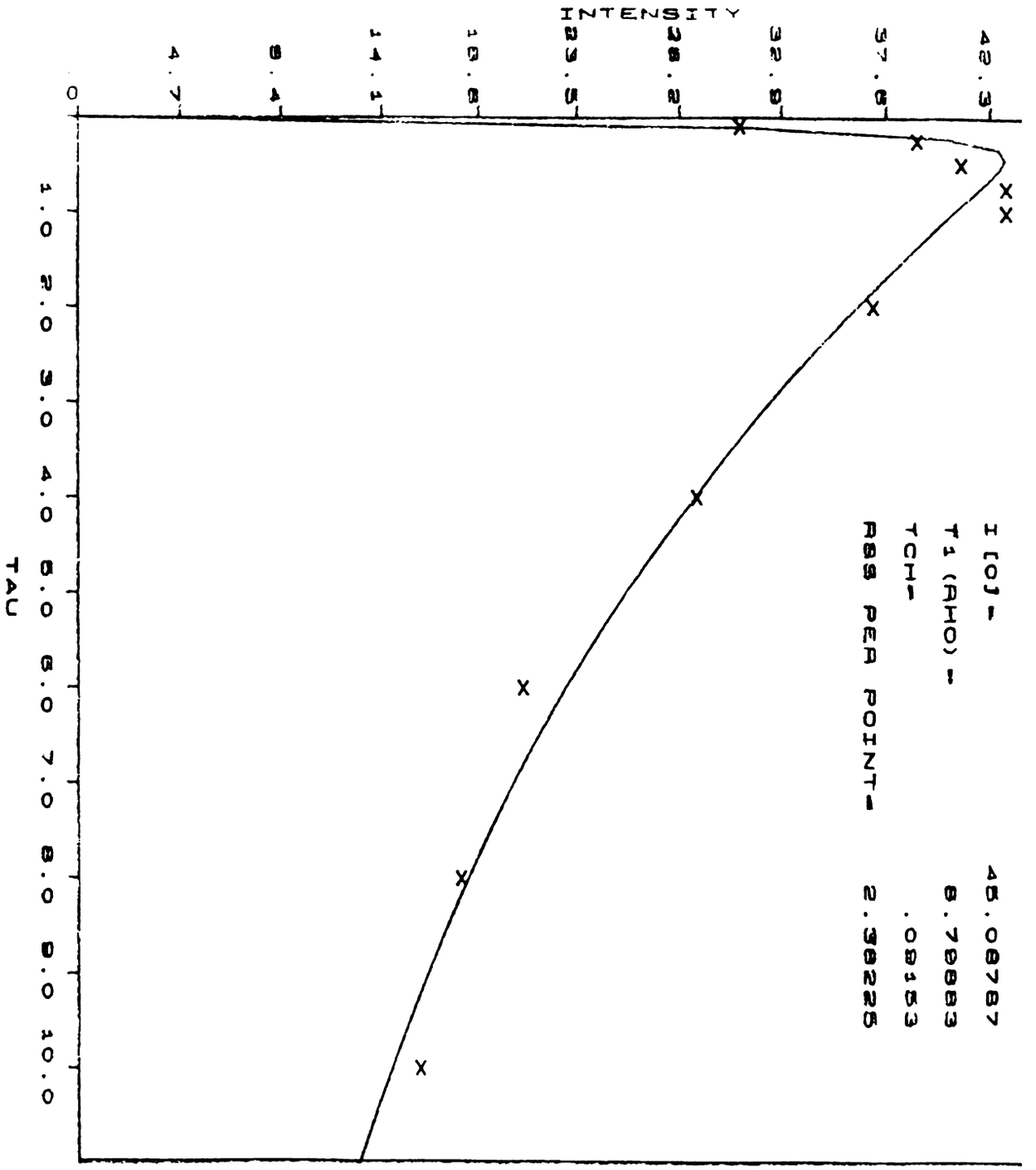
INTENSITY
0
4.7
8.4
14.1
19.8
25.5
26.2
32.9
37.6
42.3
TAU
1.0
2.0
3.0
4.0
5.0
6.0
7.0
8.0
9.0
10.0
I [0] =
45.08787
T1 (RHO) =
8.78883
TCH=
.08153
RSS PER POINT=
2.38225

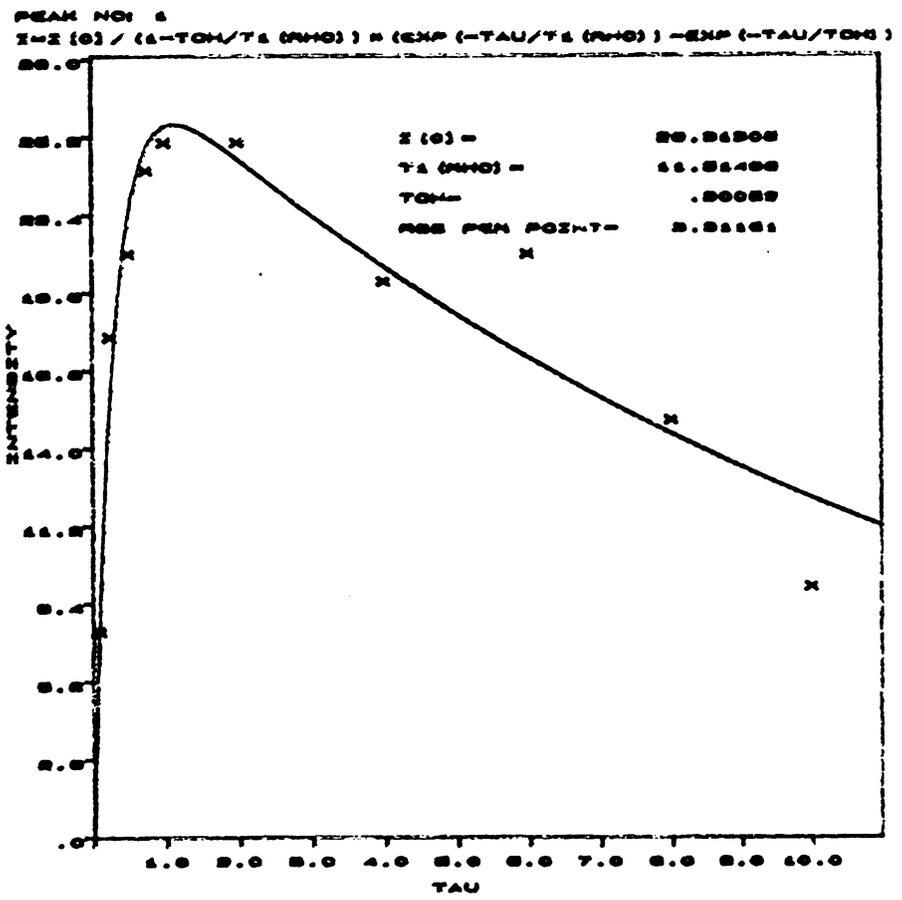
PEAK NO: 6
I=I (0) / (1-TOM/T1 (RHO)) * (EXP (-TAU/T1 (RHO)) -EXP (-TAU/TOM))
I (0) =
T1 (RHO) =
TOM=
RMS PER POINT=
INTENSITY
TAU

SIMFIT VERSION 880601.1 DATE:4/2/92
SIMFIT FUNCTION I=I[0]/(1-TCH/T1(RHO))*(EXP(-TAU/T1(RHO))-EXP(-TAU/TCH))
DATA SOURCE=KEYBOARD
PEAK NUMBER = 1
NUMBER OF DATA POINTS USED = 10

#	TAU	I[OBS]	I[CALC]	DIFF
1	.100000	7.4000	7.9776	-.5776
2	.250000	18.0000	15.7947	2.2053
3	.500000	21.0000	22.3297	-1.3297
4	.750000	24.0000	24.8419	-.8419
5	1.000000	25.0000	25.6105	-.6105
6	2.000000	25.0000	24.3991	.6009
7	4.000000	20.0000	20.5403	-.5403
8	6.000000	21.0000	17.2654	3.7346
9	8.000000	15.0000	14.5126	.4874
10	10.000000	9.0000	12.1987	-3.1987

SIMFIT VERSION:880601.1 DATE 4/2/92
SIMFIT FUNCTION I=I[0]/(1-TCH/T1(RHO))*(EXP(-TAU/T1(RHO))-EXP(-TAU/TCH))
DATA SOURCE = KEYBOARD
PEAK NUMBER = 1
NUMBER OF DATA POINTS USED = 10
NUMBER OF COMPONENTS = 1
NUMBER OF ITERATIONS = 163
RSS PER POINT = 3.31161
ESTIMATED ERROR OF FUNCTION = .68781
CALCULATED PARAMETERS:
I[0] = 28.313055
T1(RHO) = 11.514959
TCH = .300518

SIMFIT VERSION 880601.1 DATE:4/2/92
SIMFIT FUNCTION I=I[0]/(1-TCH/T1(RHO))*(EXP(-TAU/T1(RHO))-EXP(-TAU/TCH))
DATA SOURCE=KEYBOARD
PEAK NUMBER = 2
NUMBER OF DATA POINTS USED = 10

#	TAU	I[OBS]	I[CALC]	DIFF
1	.100000	80.8000	75.7312	5.0688
2	.250000	90.0000	101.6585	-11.6585
3	.500000	97.0000	104.2967	-7.2967
4	.750000	103.9000	102.1265	1.7735
5	1.000000	105.0000	99.7734	5.2266
6	2.000000	100.0000	90.8474	9.1526
7	4.000000	81.0000	75.3186	5.6814
8	6.000000	62.0000	62.4443	-.4443
9	8.000000	47.0000	51.7705	-4.7705
10	10.000000	40.0000	42.9213	-2.9213

SIMFIT VERSION:880601.1 DATE 4/2/92
SIMFIT FUNCTION I=I[0]/(1-TCH/T1(RHO))*(EXP(-TAU/T1(RHO))-EXP(-TAU/TCH))
DATA SOURCE = KEYBOARD

```
PEAK NUMBER = 2
NUMBER OF DATA POINTS USED = 10
NUMBER OF COMPONENTS = 1
NUMBER OF ITERATIONS = 80
RSS PER POINT = 39.28558
ESTIMATED ERROR OF FUNCTION = 2.36901
CALCULATED PARAMETERS:
I[0] = 108.725772
T1(RHO) = 10.669321
TCH = .082955

SIMFIT VERSION 880601.1 DATE:4/2/92
SIMFIT FUNCTION I=I[0]/(1-TCH/T1(RHO))*(EXP(-TAU/T1(RHO))-EXP(-TAU/TCH))
DATA SOURCE=KEYBOARD
PEAK NUMBER = 3
NUMBER OF DATA POINTS USED = 10
```

#	TAU	I[OBS]	I[CALC]	DIFF
1	.100000	31.0000	29.7668	1.2332
2	.250000	39.0000	41.3178	-2.3178
3	.500000	41.0000	42.8516	-1.8516
4	.750000	43.0000	41.8265	1.11735
5	1.000000	43.0000	40.6663	2.3337
6	2.000000	37.0000	36.2982	.7018
7	4.000000	29.0000	28.9180	.0820
8	6.000000	21.0000	23.0384	-2.0384
9	8.000000	18.0000	18.3542	-.35452
10	10.000000	16.0000	14.6224	1.3776

```
SIMFIT VERSION:880601.1 DATE 4/2/92
SIMFIT FUNCTION I=I[0]/(1-TCH/T1(RHO))*(EXP(-TAU/T1(RHO))-EXP(-TAU/TCH))
DATA SOURCE = KEYBOARD
PEAK NUMBER = 3
NUMBER OF DATA POINTS USED = 10
NUMBER OF COMPONENTS = 1
NUMBER OF ITERATIONS = 55
RSS PER POINT = 2.38225
ESTIMATED ERROR OF FUNCTION = ..58337
CALCULATED PARAMETERS:
I[0] = 45.087868
T1(RHO) = 8.798826
TCH = .091532
```

Appendix G-3. ^{1}H NMR Spectra of 40,000 MW Blends

PS 40,000 MW 0% MO

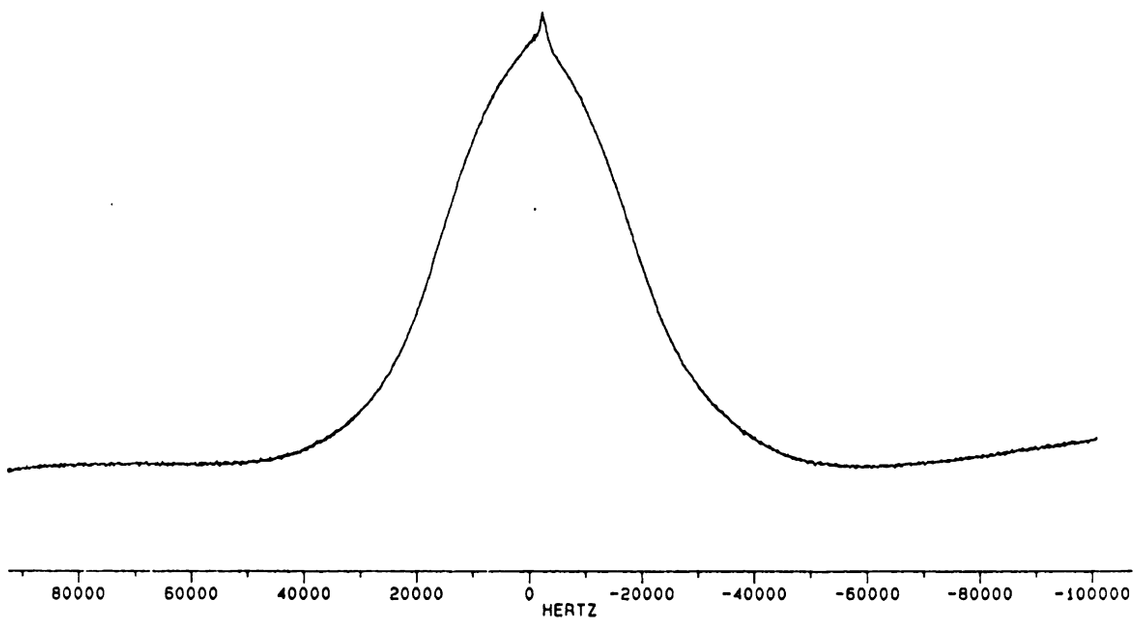

BRUKER

```
M02.PS
AU:
 VC
PPG:
 ONEPULSE.PC
DATE 27-7-80
TIME 14:04

SF     200.140
O1  -21469.727
SI    4096
TD    4096
SW 200000.000
HZ/PT  97.656
VD   1000.000U

RG   30
NE      13
NS     348
AQ    2561
TE     297

DW       2.5
FW 500000
O2  -11508.789
DP   18H DO

D0       8.000S
D1       6.000U
D2      10.000U
D3      10.000U
D4      50.000U
D5    3000.000U
D6       1.000U
D7      80.000M
D8       1.000U
D11      5.000U

LB      20.000
GB       0.0
CX      20.00
CY       0.0
SR  -20590.82
```

PS 4000MW 2.5% MO

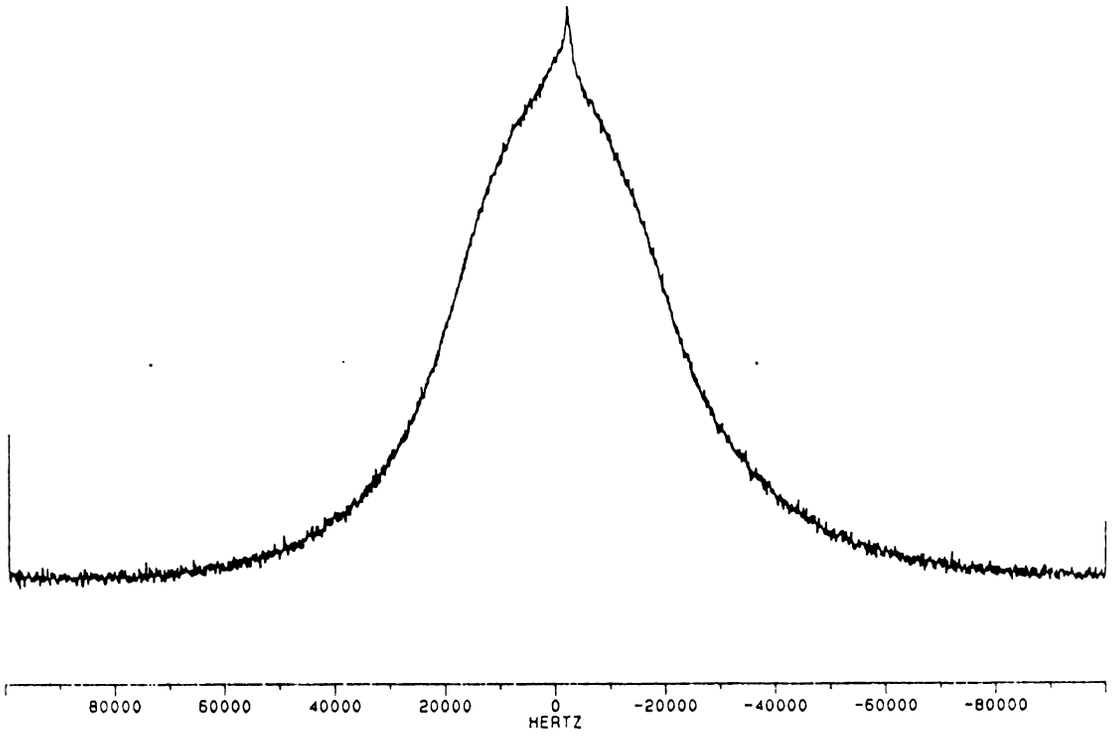

BRUKER

```
MO.PS
AU:
 VC
PPG:
 ONEPULSE.PC
DATE 27-7-80
TIME 11:56

SF     200.140
O1 -21469.727
SI     4096
TD     4096
SW 200000.000
HZ/PT   97.656
VD   1000.000U

RG   30
NE      13
NS      88
RO    2561
TE     297

DW       2.5
FW 500000
O2 -11508.789
DP   18H D0

D0       8.000S
D1       6.000U
D2      10.000U
D3      10.000U
D4      50.000U
D5    3000.000U
D6       1.000U
D7      80.000M
D8       1.000U
D11      5.000U

LB      20.000
GB       0.0
CX      20.00
CY       0.0
SR  -20590.82
```

PS 40000MW 5% MO

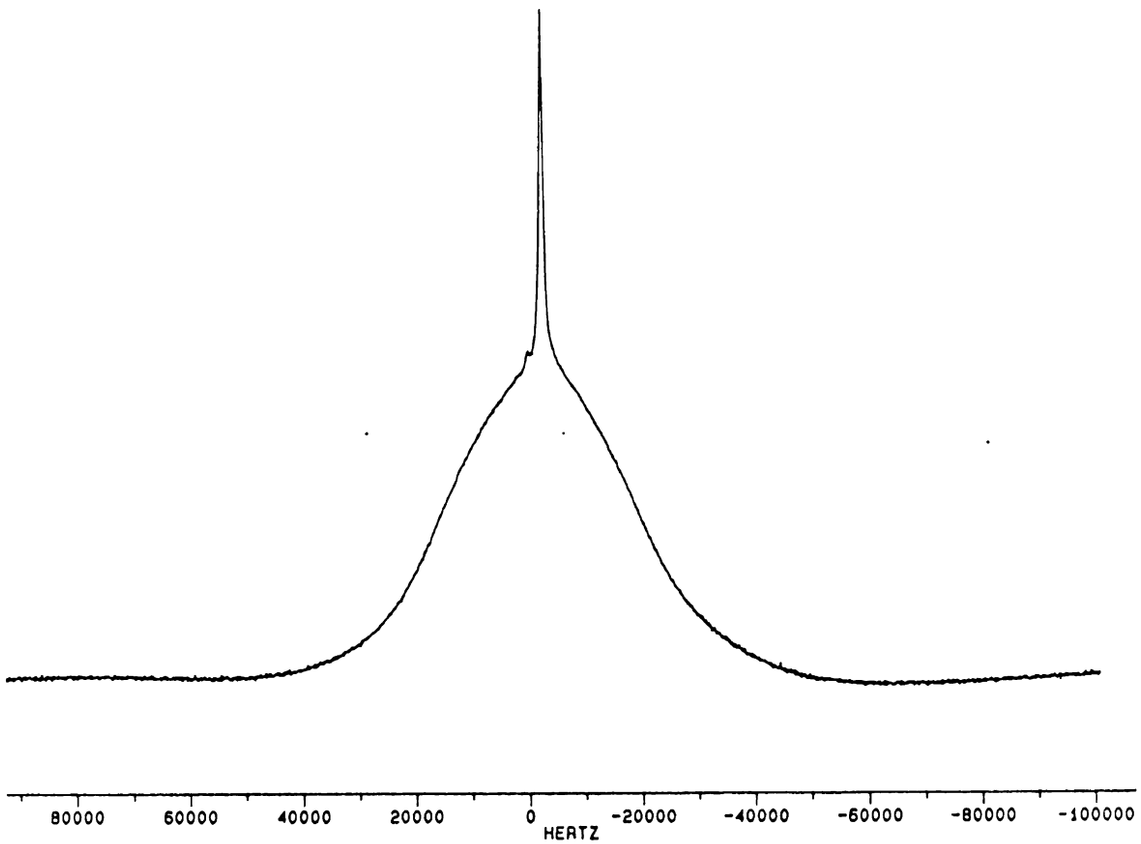

BRUKER

MO1.PS
AU:
VC
PPG:
ONEPULSE.PC
DATE 27-7-80
TIME 13:15

SF 200.140
O1 -21469.727
SI 4096
TD 4096
SW 200000.000
HZ/PT 97.656
VD 1000.000

RG 30
NE 13
NS 104
RO 2561
TE 297

DW 2.5
FW 500000
O2 -11508.789
DP 18H DO

D0 8.000S
D1 6.000U
D2 10.000U
D3 10.000U
D4 50.000U
D5 3000.000U
D6 1.000U
D7 80.000M
D8 1.000U
D11 5.000U

LB 20.000
GB 0.0
CX 20.00
CY 0.0
SA -20590.82

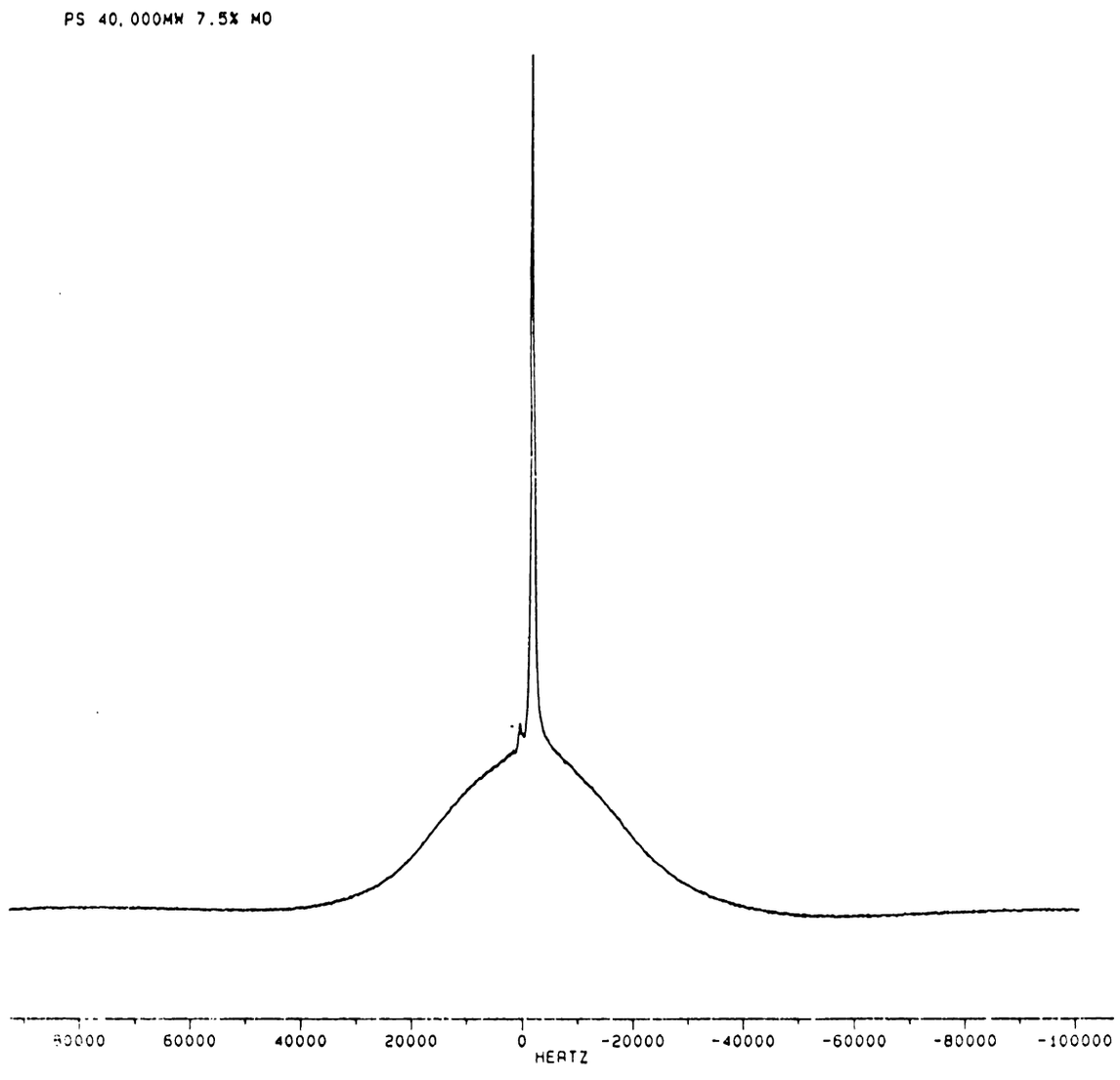

BRUKER

M03.PS
AU:
VC
PPG:
ONEPULSE.PC
DATE 27-7-80
TIME 14:29

SF 200.140
O1 -21469.727
SI 4096
TD 4096
SW 200000.000
HZ/PT 97.656
VC 1000.000U

RG 30
NE 13
NS 140
RD 2561
TE 297

DW 2.5
FW 500000
O2 -11508.789
DP 18H DO

D0 8.000S
D1 6.000U
D2 10.000U
D3 10.000U
D4 50.000U
D5 3000.000U
D6 1.000U
D7 80.000M
D8 1.000U
D11 5.000U

LB 20.000
GB 0.0
CX 20.00
CY 0.0
SR -20590.82